AD-A019 111

THE GENERALIZED TRAJECTORY SIMULATION SYSTEM. VOLUME V. WEIGHT ESTIMATION MODELS FOR SIZING APPLICATIONS

Charles C. DeBilzan

Aerospace Corporation

Prepared for:

Space and Missile Systems Organization
Air Force Rocket Propulsion Laboratory

21 November 1975

REPORT SAMSO-TR-75-255, VOL V

GENERALIZED TRAJECTORY SIMULATION

Volume V: Weight Estimation Models for Sizing Applications

TRAJECTORY ANALYSIS PROGRAMMING DEPARTMENT
Information Processing Division
Engineering Science Operations
The Aerospace Corporation
El Segundo, Calif. 90245

21 November 1975

Final Report

APPROVED FOR PUBLIC RELEASE;
DISTRIBUTION UNLIMITED

Prepared for

AIR FORCE ROCKET PROPULSION LABORATORY
AIR FORCE SYSTEMS COMMAND
Edwards Air Force Base, Calif. 93523

and THE AEROSPACE CORPORATION

SPACE AND MISSILE SYSTEMS ORGANIZATION
AIR FORCE SYSTEMS COMMAND
Los Angeles Air Force Station
P.O. Box 92960, Worldway Postal Center
Los Angeles, Calif. 90009

This report was prepared by The Aerospace Corporation, El Segundo, California, under Contract F04701-75-C-0076 with the Space and Missile Systems Organization (AFSC), P.O. Box 92960, Worldway Postal Center, Los Angeles, California 90009. The work was sponsored by the Air Force Rocket Propulsion Laboratory (AFSC), Edwards AFB, California 93523, with Capt. Francis Lymburner as project officer. This report has been reviewed by the Information Office (OI) and is releasable to the National Technical Information Service (NTIS). At NTIS, it will be available to the general public, including foreign nationals.

Approved by

A.R. Sims

A.R. Sims, Director
Mathematics and Programming Subdivision
Information Processing Division
Engineering Science Operations

This technical report has been reviewed and is approved for publication.

FOR THE COMMANDER

Gerhard E. Aichinger
Technical Advisor
Contracts Management Office

for Gerhard E. Aichinger

Frank J. Bane
Chief, Contracts Management Office

UNCLASSIFIED

SECURITY CLASSIFICATION OF THIS PAGE (When Data Entered)

REPORT DOCUMENTATION PAGE

READ INSTRUCTIONS BEFORE COMPLETING FORM

1. REPORT NUMBER: Report SAMSO-TR-75-255, Vol V
2. GOVT ACCESSION NO.
3. RECIPIENT'S CATALOG NUMBER

4. TITLE (and Subtitle): The Generalized Trajectory Simulation System, Volume V: Weight Estimation Models for Sizing Applications

5. TYPE OF REPORT & PERIOD COVERED: Final Report 7-1-74 to 6-30-75

6. PERFORMING ORG. REPORT NUMBER: TR-0076(6666)-1, Vol. V

7. AUTHOR(s): Trajectory Analysis Programming Department
Information Processing Division
Engineering Science Operations

8. CONTRACT OR GRANT NUMBER(s): F04701-74-C-0075
F04701-75-C-0076

9. PERFORMING ORGANIZATION NAME AND ADDRESS: The Aerospace Corporation
El Segundo, California 90245

10. PROGRAM ELEMENT, PROJECT, TASK AREA & WORK UNIT NUMBERS

11. CONTROLLING OFFICE NAME AND ADDRESS: Space and Missile Systems Organization
Air Force Systems Command
Los Angeles, California 90045

12. REPORT DATE: 21 November 1975

13. NUMBER OF PAGES: 498

14. MONITORING AGENCY NAME & ADDRESS (if different from Controlling Office): Air Force Rocket Propulsion Laboratory
Air Force Systems Command
Edwards Air Force Base, California 93523

15. SECURITY CLASS. (of this report): Unclassified

15a. DECLASSIFICATION/DOWNGRADING SCHEDULE

16. DISTRIBUTION STATEMENT (of this Report): Approved for public release; distribution unlimited.

DDC
REGISTERED
JAN 12 1976
D

17. DISTRIBUTION STATEMENT (of the abstract entered in Block 20, if different from Report)

18. SUPPLEMENTARY NOTES

19. KEY WORDS (Continue on reverse side if necessary and identify by block number)

Sizing
Solid rocket motor sizing
Sizing solid rocket motors
Vehicle/mission sizing
Mission/vehicle sizing
Vehicle/trajectory sizing
Trajectory/vehicle sizing
Boost vehicle sizing
Weight estimation
Weight prediction
Weight scaling
Parametric weight scaling

20. ABSTRACT (Continue on reverse side if necessary and identify by block number)

The Generalized Trajectory Simulation (GTS) system provides a vehicle design and trajectory simulation capability. GTS is written in FORTRAN compatible with CDC 7000/6000 series computer systems. User-oriented input data specifications, computational efficiency, diverse program applicability, and convenient program modifications have been primary considerations in the design of the GTS system. The trajectory simulation capability can accommodate diverse types of vehicle configurations, flight profiles, and mission

DD FORM 1473 (FACSIMILE)

UNCLASSIFIED

SECURITY CLASSIFICATION OF THIS PAGE (When Data Entered)

19. KEY WORDS (Continued)

20. ABSTRACT (Continued)

objectives. Additionally, the GTS system contains an extensive vehicle sizing capability and a state-of-the-art optimization capability.

This volume documents the GTS library of weight estimation models which provide a vehicle sizing capability for space and missile vehicles that utilize solid propellant rocket motors. Liquid propelled vehicles can also be accommodated within the sizing procedure; however, they require the development of specialized weight estimation models to represent particular characteristics of the desireu liquid propellant system.

Primary applications include preliminary design studies, booster sub-system trade-off studies, and growth studies of existing systems, including the analysis of advanced propellant technology or new launch concepts.

PREFACE

This volume, the fifth of five volumes that describe the Generalized Trajectory Simulation System (GTS), documents the GTS library of weight estimation models utilized for sizing applications. The remaining volumes are:

> Volume I: <u>GTS Overview.</u> This document provides the user with an overview of GTS, including a summary of the major operational capabilities and structural design of the GTS system.
>
> Volume II: <u>GTS Usage Guide.</u> This volume serves as a general usage guide to GTS and includes a set of example problems, a comprehensive description of the Generalized Trajectory Language, and a discussion of the trajectory simulation control. In addition, this volume contains a master reference list for all volumes and supplementary information to aid the user in defining his problem.
>
> Volume III: <u>GTS Flight Dynamic Models.</u> This report concerns the GTS library of flight mechanics and flight dynamics models utilized for trajectory simulations.
>
> Volume IV: <u>GTS Numerical Operators.</u> This publication deals with the GTS library of numerical operators, including integration, optimization, and interpolation operators.

This report was prepared by Charles C. DeBilzan. The author acknowledges the beneficial contributions and suggestions made by A. D. Hemenover, F. R. Henry, J. R. McLaughlin, D. S. Meder, J. Milligan, W. T. Milloway, W. E. Pickett, and J. L. Searcy.

Preceding page blank

CONTENTS

CONTENTS (Cont.)

CONTENTS (Cont.)

FIGURES

FIGURES (cont.)

FIGURES (cont.)

1. INTRODUCTION

1.0.1 Program Description

The solid rocket motor weight estimation models presented within this volume, combined with a general purpose optimization scheme (Vol. IV) and trajectory simulation capability (Vol. III), form a generalized vehicle sizing program for solid rockets. The program, normally utilized in preliminary design level studies, estimates performance sensitive component weights which will determine a propulsion system configuration consistent with realistic vehicle geometry, performance and mission constraints. Specifically, it sizes each major rocket component, bases weight predictions on past and present experience, recognizes actual hardware and system constraints, and permits the inclusion of technology changes. It is valid for propulsion system weights between 3000 and 2,000,000 lbs. and does not require the generation of reference designs prior to generating results. It should be noted that the program does not replace the design, weight, and performance processes associated with hard point design studies. However, it has proven a valuable tool when sufficient data, funding, or time is not available for such a design effort.

1.0.2 Program Applications

The propulsion system configuration generated by this program has served as a reference vehicle design for:

- booster subsystem trade-off studies;
- preliminary design of major new missile weapon and space system concepts;
- growth studies of existing boost and post-boost vehicles;
- determining the effects of advanced propellent technology on missile systems;
- determining effects of new launch concepts on missile systems.

1.1 SUMMARY OF WEIGHT ESTIMATION METHODOLOGY

This section summarizes the principal methods used for derivation of the weight prediction equations and gives some general comments on the accuracy to be expected. For a detailed exposition of the methodology for specific applications, and the derivation of many of the weight prediction equations used, see reference 8.[1]

There are three principal methods of weight analysis associated with the development of the weight estimation models within this volume. The first two listed below, actual and hard point design, served as the data base for the development of the weight scaling equations used by this program.

1. Actual weight analysis--determination of the measurements and weights of existing rockets.

2. Hard point design analysis--development of detailed mathematical models of the geometry and physics of a specific proposed rocket system.

3. Preliminary design analysis using weight scaling--development of simple mathematical models using weight scaling equations derived by analysis of the physical and statistical properties of existing rockets. The resulting design, using estimated weights, serves as a reference vehicle which may require further perturbation for analysis of a specific rocket system. The primary scaling methods used are:

    - theoretical weight scaling
    - statistical weight scaling
    - parametric weight scaling

1.1.1 Theoretical Weight Scaling

Theoretical weight scaling equations are developed by generating a simple mathematical model of the physics and geometry, which includes only elements common to a wide range of rockets.

The scaling equation is an analytical equation expressed in terms of design parameters which are either performance sensitive or basic quantities of the subsystem being modeled.

1. Kimble, J. E. "Parametric Weight Scaling Equations for Solid Propellent Launch Vehicles," TR-669(6560)-2, The Aerospace Corp., El Segundo, Calif., April 1966 (U).

Preceding page blank

The principal advantage of theoretical scaling is that the analytical approach assists in determining the significant design parameters and, since the fundamental physics and geometry are being modeled, weight trends due to design parameter perturbations can be predicted with confidence. However, due to the simple universal models employed, the absolute weights predicted may be considerably different than the actual subsystem weight.

The principal steps in developing a theoretical weight scaling model are:

1. Collect data. The data may include weights and design parameters of both existing rockets and hard point designs.

2. Derive a theoretical equation for the weight of the subsystem using physical properties. Select significant design parameters and re-express the weight equation as a function of these design parameters.

3. Compare the theoretical equation results with the data.

4. Repeat steps 2 and 3 until the comparison is satisfactory.

1.1.2 Statistical Weight Scaling

Statistical weight scaling equations are developed by generating a mathematical model using statistical analysis of existing rockets.

The scaling equation and scaling parameters are both statistical in nature, chosen to give a "best fit" to the data.

When compared with the data from which they are derived, statistical equations yield better estimates of absolute component weights than the theoretical scaling equations described above. Further, for complex subsystems where a simple theoretical model may not be feasible, statistical scaling may be required. However, since both the equation and parameters do not reflect the physics of the subsystems being modeled, weight trends due to perturbation of design parameters cannot be predicted with confidence.

The principal steps in developing a statistical weight scaling model are:

1. Collect data. The data may include weights and design parameters of both existing rockets and hard point designs.

2. Determine both the form of the weight estimation function and the statistical parameters by analysis of the mathematical properties of the data.

3. Determine coefficient and exponent values which result in a "best fit" curve.

4. Perform correlation analysis.

5. Repeat steps 2 through 4 until errors are acceptable.

1.1.3 Parametric Weight Scaling

Parametric weight scaling equations are developed by generating a mathematical model which combines both statistical weight scaling and theoretical weight scaling techniques.

The scaling equation is statistical in form, using elements of the theoretical equation as statistical parameters. As with theoretical weight scaling, design parameters are either performance sensitive or basic quantities of the subsystem being modeled.

Parametric weight scaling attempts to combine the advantages of both theoretical and statistical scaling methods. The analytical approach yields insight into selection of significant design parameters and is a basis for good weight trend predictions, whereas the statistical fitting yields realistic absolute weights by accounting for weight contributions not predicted by the theoretical equation. Whenever possible, the weight models documented within this volume use parametric weight scaling for predicting rocket component weights.

The principal steps in developing a parametric weight scaling model are:

1. Collect data. The data may include weights and design parameters of both existing rockets and hard point designs.

2. Derive a theoretical equation for the weight of the subsystem using physical properties. Select significant design parameters and re-express the weight equation as a function of these design parameters.

3. Compare the theoretical equation results with the data. Particular emphasis is placed on weight trend results since the statistical fitting in the following steps will account for bias in the absolute weights predicted.

4. Repeat steps 2 and 3 until the comparison is satisfactory.

5. Determine the form of the weight estimation function to be used for the statistical analysis. Rearrange the theoretical equation such that the elements serve as statistical parameters.

6. Determine coefficient and exponent values which result in a "best fit" curve.

7. Perform correlation analysis.

8. Repeat steps 2 through 7 until errors are acceptable.

1.1.4 Accuracy of Weight Scaling Results

For studies coordinated with competent weight prediction personnel, the following general statements may be made for the accuracy of the results using the weight estimation models presented within this volume.

1. Weight predictions do not include the effects of design philosophy, program funding, or technological advances difficult to evaluate or forecast.

2. The subsystems can be manufactured with the predicted weight.

3. Weight trends resulting from design parameter perturbations can be predicted with higher confidence than absolute weights. Weights of complex subsystems will have reduced accuracy.

4. The stage structure factor (ratio of stage burnout weight to stage gross weight) will be within 15%.

5. Statistical weight scaling models cannot be used for subsystem tradeoff studies.

6. The geometrical configuration produced is of secondary importance and requires considerable interpretation for correlation with geometrical configurations produced by a "hard point design" analysis.

1.2 USE OF GTS FUNCTION GENERATORS TO SOLVE THE SIZING PROBLEM

Two principal components of the GTS system are a "model library" and a set of "program control executive models" (referred to as "function generators"), which select and control the execution of the subset of library models required for solution of a particular problem. Specifically, three subsets of the model library are pertinent for sizing applications: optimization numerical operator models (which are documented in Volume IV), weight estimation models (which are documented within this volume), and trajectory simulation models (which are documented in Volume III). In addition, to control these models, three function generators are required: OPTSYS, for control of the optimization numerical operator models; SIZE, for control of the weight estimation models; and TRAJCEM, for control of the trajectory simulation models.

This section will illustrate the general techniques utilized for solving sizing problems using the appropriate function generators and models. For specific model requirements, refer to the pertinent GTS volume, and for a detailed discussion of the input language, including the precise method and syntax required to implement the function generators and models, see Volume II.

1.2.1 Statement of the Sizing Problem

In general, the sizing problem is to estimate the "best" rocket weight breakdown which will result in a propulsion system configuration which is consistent with realistic vehicle geometry, performance, and mission constraints.

The problem may be stated as three distinct, but not normally independent, subproblems:

1. The optimization subproblem. Determine the variable values which extremize the objective function subject to a set of equality and inequality constraints or determine the values of N variables which satisfy N equality constraints.

2. The weight estimation subproblem. Given a set of variable values, determine the vehicle geometry, propulsion, and weights.

3. The trajectory simulation subproblem. Given a set of variable values and vehicle parameters, determine the trajectory profile.

It must be noted that this problem statement completely separates the determination of variable values, constraint solving, and objective function maximization or minimization from the evaluation of the vehicle and trajectory quantities. This is not only required for a valid solution to the theoretical problem, it will be shown within the following sections that this method of breaking down the problem renders itself to natural, flexible, and efficient methods of solution using GTS function generators and GTS models.

1.2.2 Pertinent Function Generators

A GTS function generator is the principal executive subprogram which controls the execution of the set of models required to solve a class of problems. The function generator will, in turn, call a lower level executive model (usually via a "definition" model type) to solve a specific problem within the class.

That is, a function generator is used to solve a particular type of problem.

A problem, which has been partitioned into distinct, functional, subproblems, may be solved by linking function generators, each type of subproblem solved by a specific function generator.

The pertinent function generators for sizing applications are OPTSYS, SIZE, and TRAJCEM.

OPTSYS - Optimization System Program Control Executive Model.

For sizing applications, OPTSYS normally executes UOPTIM or UBEST (or USCHN for special problem applications involving only trajectory quantities) via the optimization problem definition model type PROBDEF. Both UOPTIM and UBEST are general purpose optimization schemes designed for solving problems incorporating an objective function and a very large number of variables, equality constraints and inequality constraints. USCHN is a special purpose optimization scheme designed for efficiently solving search problems by satisfying equality constraints.

SIZE - Weight Estimation Program Control Executive Model.

For the current set of available weight estimation models, SIZE executes VHDM1, a vehicle definition model which controls the evaluation of the geometry, propulsion, and weight equations for a sequentially staged vehicle.

TRAJCEM - Trajectory Program Control Executive Model.

TRAJCEM executes TRJDM1, the trajectory definition model which controls the trajectory simulation. (TRJDM1 is a default model and is normally not of concern to the program user.)

1.2.3 Interaction of Function Generators

As mentioned above, the sizing problem may be set up as three distinct (but dependent) subproblems, each subproblem solved by a particular function generator (i.e., OPTSYS is responsible for determining variable values, solving constraints, etc., SIZE is responsible for evaluating the weight estimation equations, and TRAJCEM is responsible for evaluating the trajectory equations). To solve the real problem, the function generators must be linked together by the program user in a manner which insures that the major dependencies are satisfied correctly. For example, generally, a valid optimization problem may have only a single objective function. If a multi-case setup is being utilized where the vehicle parameters are optimized within the first case by extremizing a particular objective function. then the resulting vehicle is flown in the second case extremizing a second objective function, it is the responsibility of the program user to insure that the "two" optimization problems are not dependent.

Due to the nature of the sizing problem, the engineering design cycle for an application will frequently involve repeated computer runs using alternate function generator linkages. The repeated runs may be required to investigate a specific subsystem prior to sizing the total vehicle and mission, the alternate linkages may be required for the initial subsystem analysis or to minimize computer charges. The latter becomes especially important for applications where many vehicles are being sized. This section will illustrate the various function generator linkages useful for sizing applications.

1. Evaluate Vehicle Configuration and Simulate Trajectory (no optimization).

Figure 1 illustrates two examples where SIZE and TRAJCEM are used in a "stand alone" mode without optimization. The first example illustrated is a two case job. The first case executes SIZE directly, which in turn calls a vehicle definition model (e.g., VHDM1) to evaluate the vehicle geometry, weight and propulsion quantities. The second case, which is optional, executes TRAJCEM, which simulates the trajectory using the vehicle parameters determined in case I. The second example illustrated is a single case job. TRAJCEM is executed directly and SIZE is executed from a trajectory initialization model type when vehicle parameters are required as input to the trajectory models.

Since there is no optimization and associated constraint solving, the above function generator linkages are not frequently used. The program user must furnish input data values which will satisfy the vehicle geometry constraints. Generally, these values, especially for the grain geometry, are not known apriori.

2. Optimize Vehicle Configuration, Then Optimize Trajectory.

Figure 2 illustrates a two case setup which optimizes the vehicle configuration and trajectory separately. The first case executes OPTSYS which estimates vehicle variable values and, when a function evaluation is required for constraint solving or extremizing the objective function, calls SIZE. After the vehicle optimization problem is solved, the second case is executed if desired. OPTSYS estimates variable values and, when a function evaluation is required, TRAJCEM uses the optimization determined trajectory variable values, together with the vehicle parameters determined within the first case to simulate the trajectory.

In practice, this function generator setup is used frequently. However, since the "two" optimization problems solved may not be independent, it must be used with extreme caution. The solution should be verified by rerunning the final job with the function generator setup illustrated in Figure 3 and described below.

3. Optimize Vehicle Configuration and Trajectory.

Figure 3 illustrates a single case function generator setup which optimizes the combined vehicle configuration and trajectory. OPTSYS estimates vehicle and trajectory variables and, when a function evaluation is required, TRAJCEM is executed from OPTSYS. TRAJCEM in turn calls SIZE out of a trajectory initialization model type when vehicle data is required.

Since the optimization dependencies are always valid, this is the preferred setup for sizing applications. No distinction is made between vehicle and trajectory quantities since both sets of equations are evaluated simultaneously with respect to the optimization. The only disadvantage is that for some problems, many trajectories will be needlessly generated for solving the set of vehicle constraints which are independent of the trajectory. Normally, it is not recommended that the user attempt to determine dependencies of this nature and economize by splitting the optimization problem into two parts. The dependencies are very subtle and results are usually not valid. However, some important, frequently used, basic sizing applications may be formulated such that the vehicle optimization problem is independent of the trajectory optimization problem.

Example 1

Case I	**EXECUTE SIZE** Evaluate vehicle weight, geometry, and propulsion equations.
	↓
Case II (Optional)	**EXECUTE TRAJCEM** Simulate trajectory using stage weights, thrust, etc., determined in Case I, as input data to the trajectory models.

Example 2

Case I	**EXECUTE TRAJCEM** Simulate trajectory by calling SIZE directly (via a trajectory initialization model type) when stage weights, thrust, etc., are required as input data to the trajectory models.	⟷	**SIZE** Evaluate vehicle weight, geometry, and propulsion equations when requested by TRAJCEM.

Fig. 1.2.3-1 Typical Function Generator Interaction. Determine Vehicle Configuration and Simulate Trajectory. (No Optimization)

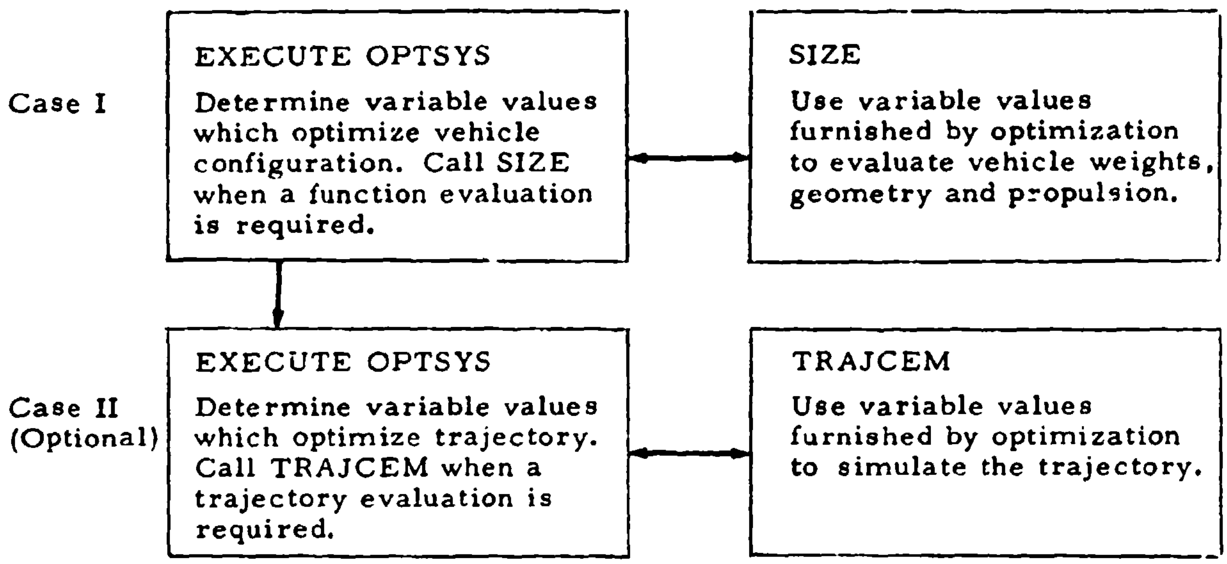

Fig. 1.2.3-2 Typical Function Generator Interaction. Optimize Vehicle Configuration, Then Optimize Trajectory. (Optimization Problems Must Be Uncoupled.)

Case I

EXECUTE OPTSYS	TRAJCEM	SIZE
Determine variable values which optimize the system. Call TRAJCEM when a function evaluation is required.	Simulate trajectory by calling SIZE directly (via a trajectory initialization model type) when stage weights, thrust, etc., are required as input data to the trajectory models.	Evaluate vehicle, weights, geometry, and propulsion equations when requested by TRAJCEM.

Fig. 1.2.3-3 Typical Function Generator Interaction. Optimize System by Combining Vehicle and Trajectory. (Optimization Problem May Have Interdependent Vehicle and Trajectory Quantities.)

1.3 CLASSIFICATION AND PURPOSE OF WEIGHT ESTIMATION MODELS.

The weight estimation models within this volume are organized functionally into three major classifications:

vehicle definition models

weight models

geometry, internal ballistics, and propulsion models

Except for the vehicle definition models, which are presented first, the individual model writeups are ordered alphabetically within this document starting with Section 10.

1.3.1 Vehicle Definition Models

The vehicle definition model is an executive model (called by the SIZE function generator) which controls the execution of the individual models required to evaluate a specific application. The documentation for each vehicle definition model (Section 10) lists the applicable model types and serves as a guide for selecting models when setting up a new data deck.

1.3.2 Weight Models

There are two types of weight models--scaling models and synthesis models.

Scaling models predict subsystem weights using weight scaling equations which are a function of design parameters selected when the weight scaling equations were developed. Whenever possible, parametric weight scaling is utilized. However, because of subsystem complexity, insufficient data, etc., statistical weight scaling and theoretical weight scaling are used for some component weights. Typical design parameters include:

length to diameter ratios

volumetric loading efficiency

propellent weight

burn time

nozzle expansion ratio

chamber pressure

specific impulse

Preceding page blank

Synthesis models are used to combine subsystem weights, evaluated by scaling models or other synthesis models, to form composite subsystems.

In addition to component weights peculiar to the subsystem being modeled, each weight model outputs a general expended component weight breakdown (for performance evaluation) of the following form:

$$W = W_{PP} + W_X + W_{NX}$$

$$W_X = W_{XI} + W_{XT}$$

where

W	is the total subsystem weight.
W_{PP}	is the primary propellent weight component associated with the subsystem.
W_X	is the total expended weight component associated with the subsystem.
W_{NX}	is the total non-expended weight component associated with the subsystem.
W_{XI}	is the expended (non-thrust producing) weight component associated with W_X.
W_{XT}	is the expended (thrust producing) weight component associated with W_X.

1.3.3 Geometry, Internal Ballistic and Propulsion Models

The SOLE purpose of the geometry, internal ballistic, and weight models is to determine the design parameter values required by the weight scaling models. Note that what constitutes a "design parameter" is specified by the weight model, NOT the geometry, internal ballistics or propulsion model.

The geometrical configuration produced is of secondary importance and requires considerable interpretation for correlation with geometrical configurations produced by a "hard point design" analysis.

2. NOMENCLATURE CONVENTIONS

The following conventions have been established to facilitate symbol identification within the weight estimation models. It must be emphasized that these are conventions, not rigid rules, and that exceptions will occur.

Except for ratios and factors:

the symbol	$P_{SS_{XXX}}$
corresponds to the mnemonic	PSSXXX

where

P	designates the primary attribute of the quantity
SS	designates the secondary attribute of the quantity
XXX	designates an identifier which makes the quantity unique (up to three characters)

For ratios:

the symbol	R_{PPSSSS}
corresponds to the mnemonic	RPPSSSS

where

R	designates a ratio quantity
the first P	designates the numerator primary attribute
the second P	designates the denominator primary attribute (if different from first P)
the first SS	designates the numerator secondary attribute
the second SS	designates the denominator secondary attribute (if different from first SS)

For factors:

the symbol	K_{PSSXXX}
corresponds to the mnemonic	KPSSXXX

where

K	designates a factor quantity
PSSXXX	designates the left hand member of the equation containing the factor

Examples of primary attributes are:

P =	A	Plane area (in^2)
	B	Burn rate (in/sec)
	C	Constant (N. D.)
	D	Diameter (in)
	I	Impulse
	K	Factor, coefficient or bias
	L	Length (measured parallel to centerline) (in)
	N	Number of (N. D.)
	P	Pressure (psia)
	Q	Associative quantity
	R	Ratio (N. D.)
	S	Surface area (in^2)
	T	Thickness (in), time (sec), temperature
	V	Volume (in^3)
	W	Weight (lb)
	Y	Centroid (in)

Examples of secondary attributes are:

SS =	CH	Chamber
	CS	Case
	GN	Grain
	IN	Insulation
	IT	Interstage
	JT	Joint
	MT	Motor
	NZ	Nozzle
	PA	Payload
	PL	Payload section
	PP	Primary propellent
	PS	Propulsion system
	PT	Port
	SG	Stage
	SH	Shroud
	SK	Skirt
	SL	Slot
	SS	Substage
	ST	Structure
	TH	Throat
	TT	Thrust termination
	TV	Thrust vector

Examples of identifiers which make a quantity unique:

XXX =	A	Aft
	F	Forward
	CL or C	Closure
	CH	Closure hole
	CY or Y	Cylinder
	H	Hole
	I	Inside
	O	Outside

Some examples using the conventions:

DCSO	D_{CS_O}	Outside case diameter
DCSI	D_{CS_I}	Inside case diameter
WNZ	W_{NZ}	Total nozzle weight
LNZ	L_{NZ}	Total nozzle length
LNZCV	$L_{NZ_{CV}}$	Length of convergent portion of nozzle
LNZDV	$L_{NZ_{DV}}$	Length of divergent portion of nozzle
ANZTH	$A_{NZ_{TH}}$	Nozzle throat area
ANZEXT	$A_{NZ_{EXT}}$	Nozzle exit area
ANZENT	$A_{NZ_{ENT}}$	Nozzle entrance area
DNZTH	$D_{NZ_{TH}}$	Nozzle throat diameter
DNZEXT	$D_{NZ_{EXT}}$	Nozzle exit diameter
DNZENT	$D_{NZ_{ENT}}$	Nozzle entrance diameter

LNZB	L_{NZ_B}	Buried nozzle length
KLNZB	K_{LNZB}	Buried nozzle factor
RLDGNCY	R_{LDGNCY}	Cylindrical grain length to diameter ratio

10.1

MODEL TYPE: VEHDEF (VEHicle DEFinition)

MODEL NAME: VHDM1 (Sequential stages with payload)

DESCRIPTION:

VHDM1 (VeHicle Definition Model number 1) is an executive model which defines a rocket configuration consisting of a single propulsion system (i.e., boost vehicle), with sequential stages, and a single payload section (i.e., post-boost vehicle). The rocket is comprised of the following major components, each of which has a separate data block for input of its models and associated data (see figure 1).

The "vehicle" is comprised of a single "propulsion system" and a single "payload section". The "vehicle" data is input within the same data block as the vehicle definition model. In addition to the vehicle definition model type, VEHDEF, the following model types are applicable.

VEHG	Vehicle geometry
VEHW	Vehicle weight

The "propulsion system" (i.e., boost vehicle) is comprised of up to ten sequential "stages". Data is input using the data block specified by DBPS(1) (see Intra-Model Input). The following model types are applicable.

PROSYSG	Propulsion system geometry
PROSYSW	Propulsion system weight

A "stage" is comprised of a single "substage" and a single "interstage". "Stage" data is input using the data block specified by DBSG(i), i = 1, 10, where i is the stage number. Stages are numbered consecutively, from the bottom to the top, starting with any integer less than, or equal to, 10. The following model types are applicable.

STAGEG	Stage geometry
STAGEW	Stage weight

DESCRIPTION (Cont.):

A "substage" is comprised of the motor and nozzle associated with a "stage". "Substage" data is input using the data block specified by DBSS(i), i = 1, 10, where i is the stage number. The following model types are applicable.

CASEG	Case geometry
CASEW	Case weight
GRAING	Grain geometry
IBGAS	Internal ballistics, gas
IBFLOW	Internal ballistics, flow
IBPERF	Internal ballistics, performance
INSULG	Internal insulation geometry
INSULW	Internal insulation weight
MISCMTW	Miscellaneous motor weight
MOTORG	Motor geometry
MOTORW	Motor weight
NOZZLEG	Nozzle geometry
NOZZLEW	Nozzle weight
PROPELW	Propellent weight
PROPUL	Propulsion characteristics
SUBSTGG	Substage geometry
SUBSTGW	Substage weight
TVCG	Thrust vector control geometry
TVCW	Thrust vector control weight
TTERMG	Thrust termination geometry
TTERMW	Thrust termination weight

An "interstage" is comprised of the structure to join either "substages" or a "substage" and the "payload" (i.e., payload adapter). The "interstage" associated with a "stage" is on top of (forward of) the "substage" associated with that "stage". "Interstage" data is input using the data block specified by DBIT(i), i = 1, 10. The following model types are applicable.

DESCRIPTION (Cont.):

INTINSW	Interstage external insulation weight
INTSTGG	Interstage geometry
INTSTGW	Interstage weight
INTSTRW	Interstage structure weight

The "payload section" (i.e., post-boost vehicle) is comprised of a single payload. "Payload section" data is input using the data block specified by DBPL(1). The following model types are applicable.

PAYSECG	Payload section geometry
PAYSECW	Payload section weight
SHROUDW	Shroud weight

"Payload" data is input using the data block specified by DBPA(1). The following model types are applicable.

PAYLODG	Payload geometry
PAYLODW	Payload weight

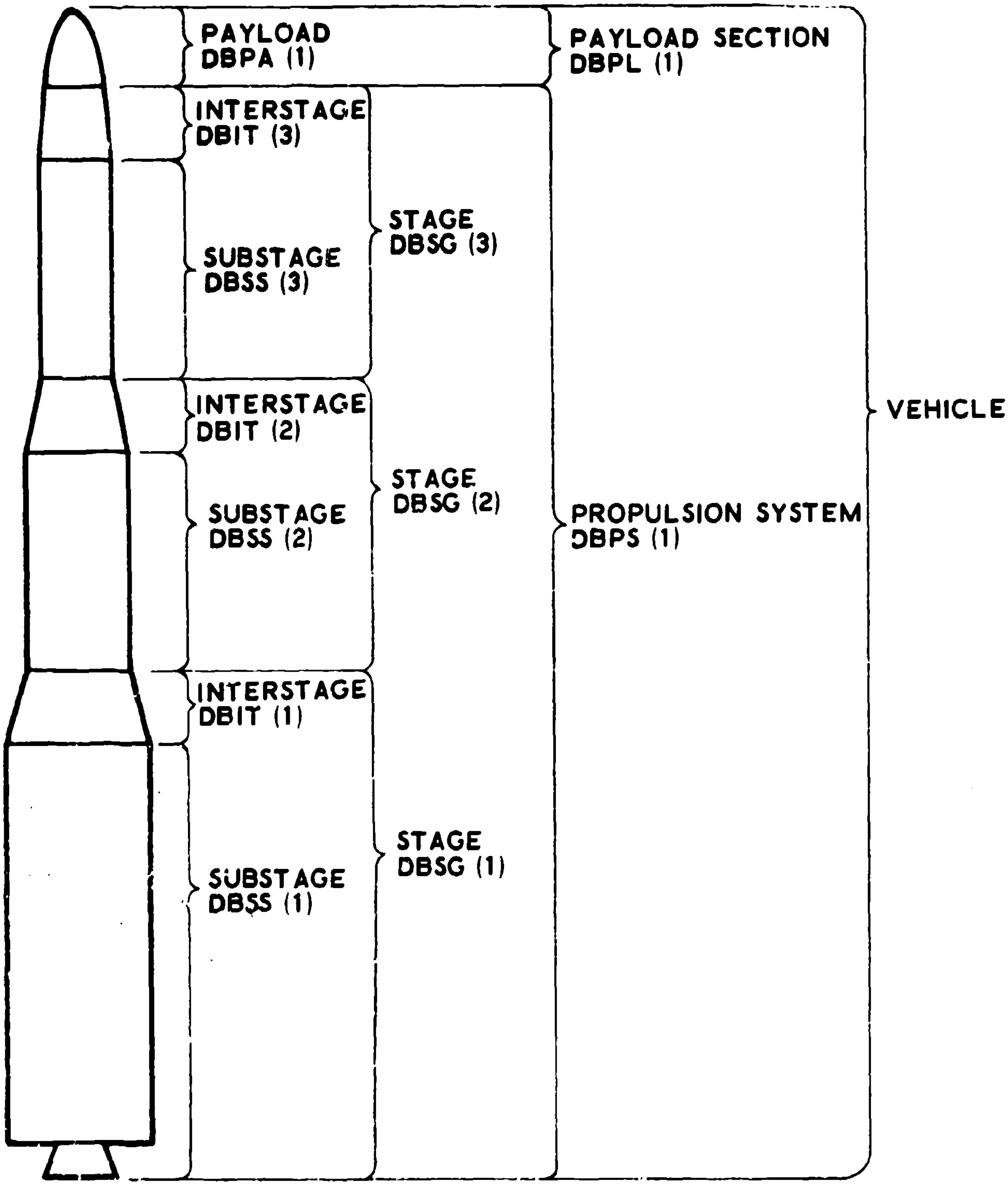

Fig. 10.1-1 Major Components and Data Block Designation for a Typical Three Stage Rocket

INPUT DATA, INTRA-MODEL:

The following data is input directly to this model by the program user.

Mnemonic	Symbol	Description; Ext. (Int.) Units
DBIT(i)	DBIT(i)	Name of data block containing interstage data for the interstage associated with the i-th stage. i = 1, 10 where i is the stage number. The data block name is arbitrary (i.e., user defined), except that it cannot be a previously mentioned user-defined symbol or an existing GTS symbol. e.g., DBIT(1) = [INTSTG1]; N. D.
DBPA(1)	DBPA(1)	Name of data block containing payload data. The data block name is arbitrary (i.e., user defined), except that it cannot be a previously mentioned user-defined symbol or an existing GTS symbol. e.g., DBPA(1) = [PAYLOD]; N. D.
DBPL(1)	DBPL(1)	Name of data block containing payload section (i.e., post-boost vehicle) data. The data block name is arbitrary (i.e., user defined), except that it cannot be a previously mentioned user-defined symbol or an existing GTS symbol. e.g., DBPL(1) = [PAYSEC]; N. D.
DBPS(1)	DBPS(1)	Name of data block containing propulsion system (i.e., boost vehicle) data. The data block name is arbitrary (i.e., user defined), except that it cannot be a previously mentioned user-defined symbol or an existing GTS symbol. e.g., DBPS(1) = [PROSYS]; N. D.

INPUT DATA, INTRA-MODEL (Cont.):

Mnemonic	Symbol	Description; Ext. (Int.) Units
DBSG(i)	DBSG(i)	Name of data block containing stage data for the i-th stage. i = 1, 10 where i is the stage number. Note that stages are numbered consecutively, from the bottom to the top, starting with any integer less than, or equal to, 10. The data block name is arbitrary (i.e., user defined), except that it cannot be a previously mentioned user-defined symbol or an existing GTS symbol. e.g., DBSG(1) = [STAGE1]; N. D.
DBSS(i)	DBSS(i)	Name of data block containing substage data for the substage associated with the i-th stage, i = 1, 10 where i is the stage number. The data block name is arbitrary (i.e., user defined), except that it cannot be a previously mentioned user-defined symbol or an existing GTS symbol. e.g., DBSS(1) = [SUBSTG1] ; N. D.

INPUT DATA, INTER-MODEL:

This model requires as input certain data which is usually output from a model of the specified model type. If the user has not specified such a source for this data, then it must be input directly with the intra-model input.

Mnemonic	Symbol	Description; Ext. (Int.) Units	Model Type
None			

OUTPUT DATA:

The following data is output from this model. It is available for use as inter-model input to other models and to print, plot, and optimization routines.

Mnemonic	Symbol	Description; Ext. (Int.) Units

None

20.1

MODEL TYPE: CASEG (CASE Geometry)

MODEL NAME: CSGM1 (Metal case)

DESCRIPTION:

CSGM1 (CaSe Geometry Model number 1) determines the pertinent geometry for a solid rocket motor metal case subject to internal pressure. This model does not account for buckling or aerodynamic loads.

As illustrated by Figure 1, the basic case geometry is comprised of a cylindrical section with forward and aft closure sections. The inside and outside surfaces of a closure section form concentric hemi-ellipsoids having coincident equatorial planes and, normally, unequal head ratios. The closures may have cylindrical holes, centered on the hemi-ellipsoid axis of revolution, for modeling geometry associated with the igniter, submerged nozzles and TVC systems. Generally, the geometry may be degenerated for simulating spherical motors, etc.

It should be noted that since the model does not include raceways or external protrusions associated with segmented cases, the outside case diameter is not necessarily the maximum diameter of the motor. If such protrusions exist, they would be evaluated by the models specified for the MOTORG (motor geometry) or SUBSTGG (substage geometry) model types.

PROCEDURE:

Prior to entering CSGM1, the models specified by the IBGAS and NOZZLEG model types have determined the average chamber pressure and buried nozzle diameter.

Upon the first entrance to CSGM1, the thickness, closure lengths, diameters, head ratios, and closure hole geometry associated with a metal motor case are evaluated.

The models specified for the INSULG and GRAING model types then evaluate the remaining principal motor component geometry, the insulation and the grain.

After determining the grain geometry, CSGM1 is re-entered (second entrance) and quantities associated with the total case length are evaluated.

EQUATIONS, FIRST ENTRANCE:

Case thickness, cylindrical section.

$$T_{CS_{CY}} = \left[\frac{C_1 K_{FS} P_{MEO} D_{CS_O}}{2 K_{UTS}} \right] K_{CS_1} + K_{CS_2} \qquad (1)$$

Case thickness, center of aft closure.

$$T_{CS_{CLA}} = \left(C_2 T_{CS_{CY}} \right) K_{CS_3} + K_{CS_4} \qquad (2)$$

Case thickness, center of forward closure.

$$T_{CS_{CLF}} = \left(C_3 T_{CS_{CY}} \right) K_{CS_5} + K_{CS_6} \qquad (3)$$

Case inside diameter.

$$D_{CS_I} = D_{CS_O} - 2 T_{CS_{CY}} \qquad (4)$$

Outside equatorial diameter for case closures.

$$D_{CS_{CLO}} = D_{CS_O} \qquad (5)$$

Inside equatorial diameter for case closures.

$$D_{CS_{CLI}} = D_{CS_I} \qquad (6)$$

Outside length of aft case closure.

$$L_{CS_{CLAO}} = \frac{R_{DCSCAO}}{2} D_{CS_{CLO}} \qquad (7)$$

Inside length of aft case closure.

$$L_{CS_{CLAI}} = L_{CS_{CLAO}} - T_{CS_{CLA}} \qquad (8)$$

EQUATIONS, FIRST ENTRANCE (Cont.):

Inside head ratio of aft closure.

$$R_{DCSCAI} = 2 \frac{L_{CS_{CLAI}}}{D_{CS_{CLI}}} \tag{9}$$

Outside length of forward closure.

$$L_{CS_{CLFO}} = \frac{R_{DCSCFO} \, D_{CS_{CLO}}}{2} \tag{10}$$

Inside length of forward closure.

$$L_{CS_{CLFI}} = L_{CS_{CLFO}} - T_{CS_{CLF}} \tag{11}$$

Inside head ratio of forward closure.

$$R_{DCSCFI} = \frac{2 \, L_{CS_{CLFI}}}{D_{CS_{CLI}}} \tag{12}$$

Diameter of hole in aft outside case closure surface.

$$D_{CS_{HAO}} = K_{CS_7} \, D_{NZ_B} + K_{CS_8} \tag{13}$$

Diameter of hole in aft inside case closure surface.

$$D_{CS_{HAI}} = D_{CS_{HAO}} \tag{14}$$

Diameter of hole in forward outside case closure surface.

$$D_{CS_{HFO}} = K_{CS_9} \, D_{CS_{CLO}} + K_{CS_{10}} \tag{15}$$

Diameter of hole in forward inside case closure surface.

$$D_{CS_{HFI}} = D_{CS_{HFO}} \tag{16}$$

EQUATIONS, FIRST ENTRANCE (Cont.):

Diameter ratio. Aft outside case hole diameter to outside case closure diameter.

$$R_{DCSHAO} = \frac{D_{CS_{HAO}}}{D_{CS_{CLO}}} \tag{17}$$

Outside length of aft case closure, adjusted for hole.

$$L_{CS_{CHAO}} = L_{CS_{CLAO}} \sqrt{1 - R^2_{DCSHAO}} \tag{18}$$

Diameter ratio. Aft inside case hole diameter to inside case closure diameter.

$$R_{DCSHAI} = \frac{D_{CS_{HAI}}}{D_{CS_{CLI}}} \tag{19}$$

Inside length of aft case closure, adjusted for hole.

$$L_{CS_{CHAI}} = L_{CS_{CLAI}} \sqrt{1 - R^2_{DCSHAI}} \tag{20}$$

Diameter ratio. Forward outside case hole diameter to outside case closure diameter.

$$R_{DCSHFO} = \frac{D_{CS_{HFO}}}{D_{CS_{CLO}}} \tag{21}$$

Outside length of forward case closure, adjusted for hole.

$$L_{CS_{CHFO}} = L_{CS_{CLFO}} \sqrt{1 - R^2_{DCSHFO}} \tag{22}$$

Diameter ratio, forward inside case hole diameter to inside case closure diameter.

$$R_{DCSHFI} = \frac{D_{CS_{HFI}}}{D_{CS_{CLI}}} \tag{23}$$

EQUATIONS, FIRST ENTRANCE (Cont.):

Inside length of forward case closure, adjusted for hole.

$$L_{CS_{CHFI}} = L_{CS_{CLFI}} \sqrt{1 - R^2_{DCSHFI}} \tag{24}$$

Length of hole in aft case closure.

$$L_{CS_{HA}} = L_{CS_{CHAO}} - L_{CS_{CHAI}} \tag{25}$$

Length of hole in forward case closure.

$$L_{CS_{HF}} = L_{CS_{CHFO}} - L_{CS_{CHFI}} \tag{26}$$

Case cross sectional area.

$$A_{CS} = \left(\frac{\pi}{4}\right) D^2_{CS_O} \tag{27}$$

Head ratio for use of models which define a single head ratio for forward and aft closures.

$$R_{DCSCHO} = R_{DCSCAO} \tag{27-a}$$

Associative quantities. The following quantities are intended solely for optional utilization by the program user. Their primary usage within this model is for forming constraint quantities.

$$Q_{DI1} = K_{QDI1} D_{CS_I} \tag{28}$$

$$Q_{DI2} = K_{QDI2} D_{CS_I} \tag{29}$$

$$Q_{DI3} = K_{QDI3} D_{CS_I} \tag{30}$$

$$Q_{DO1} = K_{QDO1} D_{CS_O} \tag{31}$$

EQUATIONS, FIRST ENTRANCE (Cont.):

$$Q_{DO2} = K_{QDO2} D_{CS_O} \tag{32}$$

$$Q_{DO3} = K_{QDO3} D_{CS_O} \tag{33}$$

EQUATIONS, SECOND ENTRANCE:

Length of cylindrical case section.

$$L_{CS_{CY}} = L_{GN_{CY}} \tag{34}$$

Total case length.

$$L_{CS} = L_{CS_{CY}} + L_{CS_{CHAO}} + L_{CS_{CHFO}} \tag{35}$$

Cylindrical case length to diameter ratio.

$$R_{LDCSCY} = \frac{L_{CS_{CY}}}{D_{CS_O}} \tag{36}$$

Total case length to diameter ratio.

$$R_{LDCS} = \frac{L_{CS}}{D_{CS_O}} \tag{37}$$

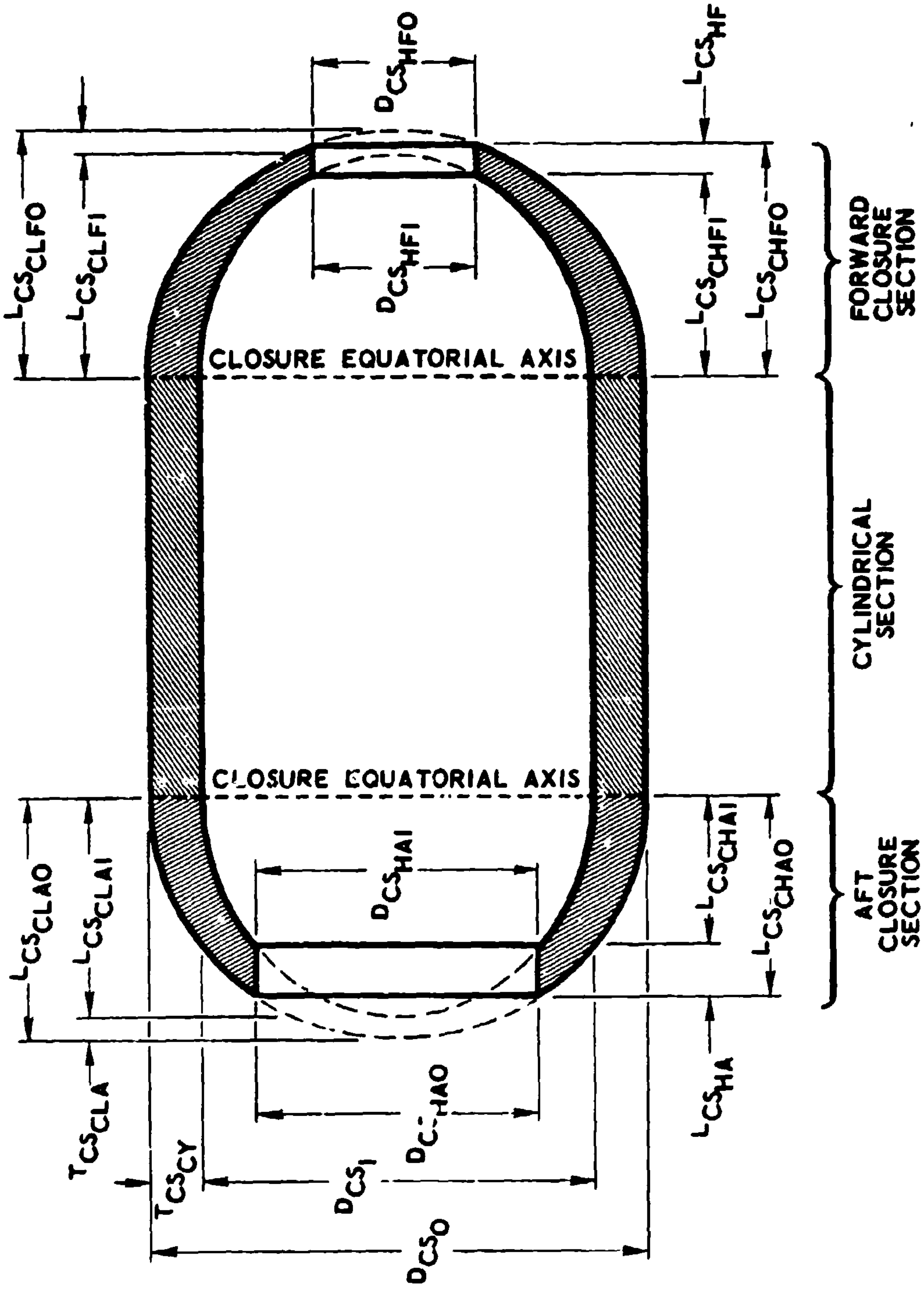

Fig. 20.1-1 Metal Case Geometry

INPUT DATA, INTRA-MODEL:

The following data is input directly to this model by the program user. If a value is not input, the preset value is used.

Mnemonic	Symbol	Description; Ext. (Int.) Units	Preset
CCSG1	C_1	Constant for TCSCY computation; N. D.	1.05
CCSG2	C_2	Proportionality constant relating the case thickness at the center of the aft closure to the case thickness of the cylindrical section; N. D.	0.5
CCSG3	C_3	Proportionality constant relating the case thickness at the center of the forward closure to the case thickness of the cylindrical section; N. D.	0.5
DCSO	D_{CS_O}	Motor case outside diameter. Outside diameter of pressure vessel cylindrical case section. Does not include raceways, protrusions, etc.; in Fig. 1	0
KCS1	K_{CS_1}	Coefficient for TCSCY computation; N. D.	1
KCS2	K_{CS_2}	Bias for TCSCY computation; in	0
KCS3	K_{CS_3}	Coefficient for TCSCLA computation; N. D.	1
KCS4	K_{CS_4}	Bias for TCSCLA computation; in	0

INPUT DATA, INTRA-MODEL (Cont.):

Mnemonic	Symbol	Description; Ext. (Int.) Units	Preset
KCS5	K_{CS_5}	Coefficient for TCSCLF computation; N. D.	1
KCS6	K_{CS_6}	Bias for TCSCLF computation; in	0
KCS7	K_{CS_7}	Coefficient for DCSHAO computation; N. D.	1
KCS8	K_{CS_8}	Bias for DCSHAO computation; in	0
KCS9	K_{CS_9}	Coefficient for DCSHFO computation; N. D.	1
KCS10	$K_{CS_{10}}$	Bias for DCSHFO computation; in	0
KCSFS	K_{FS}	Case factor of safety. Ratio of minimum burst pressure to maximum expected operating pressure; N. D.	1
KCSUTS	K_{UTS}	Ultimate tensile strength for metal case material; lb/in^2	0
KQDCSI1	K_{QDI1}	Associative quantity coefficient for QDCSI1 computation; N. D.	0
KQDCSI2	K_{QDI2}	Associative quantity coefficient for QDCSI2 computation; N. D.	0

INPUT DATA, INTRA-MODEL (Cont.):

Mnemonic	Symbol	Description; Ext. (Int.) Units	Preset
KQDCSI3	K_{QDI3}	Associative quantity coefficient for QDCSI3 computation; N. D.	0
KQDCSO1	K_{QDO1}	Associative quantity coefficient for QDCSO1 computation; N. D.	0
KQDCSO2	K_{QDO2}	Associative quantity coefficient for QDCSO2 computation; N. D.	0
KQDCSO3	K_{QDO3}	Associative quantity coefficient for QDCSO3 computation; N. D.	0
RDCSCAO	R_{DCSCAO}	Head ratio of the ellipsoid associated with the aft outside case closure surface. Ratio of twice the closure length to the closure diameter, i.e., the aft outside case closure surface is an oblate spheroid. The head ratio is the ratio of the axis of revolution (minor axis) to the equatorial diameter (major axis); N. D.	1
RDCSCFO	R_{DCSCFO}	Head ratio of the ellipsoid associated with the forward outside case closure surface. Ratio of twice the closure length to the closure diameter, i.e., the forward outside case closure surface is an oblate spheroid. The head ratio is the ratio of the axis of revolution (minor axis) to the equatorial diameter (major axis); N. D.	1

INPUT DATA, INTER-MODEL:

This model requires as input certain data which is usually output from a model of the specified model type. If the user has not specified such a source for this data, then it must be input directly with the intra-model input.

Mnemonic	Symbol	Description; Ext. (Int.) Units	Model Type
DNZB	D_{NZ_B}	Buried nozzle diameter; in	NOZZLEG
PCHMEO	P_{MEO}	Maximum expected operating chamber pressure; psia	IBGAS
LGNCY	$L_{GN_{CY}}$	Length of cylindrical grain section. Includes all adjustments for submerged nozzle, displaced propellent, cutouts, etc.; in	GRAING

OUTPUT DATA:

The following data is output from this model. It is available for use as inter-model input to other models and to print, plot, and optimization routines.

Mnemonic	Symbol	Description; Ext. (Int.) Units		
ACS	A_{CS}	Motor case cross sectional area. Area of pressure vessel cylindrical case section. Does not include raceways, protrusions, etc.; in^2		Eq. 27
DCSCLI	$D_{CS_{CLI}}$	Equatorial diameter of the ellipsoids formed by the inside surfaces of the forward and aft case closure sections; in	Fig. 1	Eq. 6
DCSCLO	$D_{CS_{CLO}}$	Equatorial diameter of the ellipsoids formed by the outside surfaces of the forward and aft case closure section; in	Fig. 1	Eq. 5

OUTPUT DATA (Cont.):

Mnemonic	Symbol	Description; Ext. (Int.) Units		
DCSHAI	$D_{CS_{HAI}}$	Diameter of circular hole, for the nozzle, centered on the axis of revolution of the hemi-ellipsoid formed by the inside surface of the aft case closure;		
		in	Fig. 1	Eq. 14
DCSHAO	$D_{CS_{HAO}}$	Diameter of circular hole, for the nozzle, centered on the axis of revolution of the hemi-ellipsoid formed by the outside surface of the aft case closure;		
		in	Fig. 1	Eq. 13
DCSHFI	$D_{CS_{HFI}}$	Diameter of circular hole, for the igniter, centered on the axis of revolution of the hemi-ellipsoid formed by the inside surface of the forward case closure;		
		in	Fig. 1	Eq. 16
DCSHFO	$D_{CS_{HFO}}$	Diameter of circular hole, for the igniter, centered on the axis of revolution of the hemi-ellipsoid formed by the outside surface of the forward case closure;		
		in	Fig. 1	Eq. 15
DCSI	D_{CS_I}	Case inside diameter, cylindrical section;		
		in	Fig. 1	Eq. 4
LCS	L_{CS}	Total case length. Distance between the forward base of the hemi-ellipsoid frustum associated with the forward outside closure surface to the aft base of the hemi-ellipsoid frustum associated with the aft outside closure surface. Includes all adjustments to grain;		
		in	Fig. 1	Eq. 35
LCSCHAI	$L_{CS_{CHAI}}$	Length of hemi-ellipsoidal frustum which forms the inside surface of the aft case closure. Includes adjustment for nozzle hole;		
		in	Fig. 1	Eq. 20

OUTPUT DATA (Cont.):

Mnemonic	Symbol	Description; Ext. (Int.) Units		
LCSCHAO	$L_{CS_{CHAO}}$	Length of hemi-ellipsoidal frustum which forms the outside surface of the aft case closure. Includes adjustment for nozzle hole;		
		in	Fig. 1	Eq. 18
LCSCHFI	$L_{CS_{CHFI}}$	Length of hemi-ellipsoidal frustum which forms the inside surface of the forward case closure. Includes adjustment for igniter hole;		
		in	Fig. 1	Eq. 24
LCSCHFO	$L_{CS_{CHFO}}$	Length of hemi-ellipsoidal frustum which forms the outside surface of the forward case closure. Includes adjustment for igniter hole;		
		in	Fig. 1	Eq. 22
LCSCLAI	$L_{CS_{CLAI}}$	Length of the axis of revolution of the hemi-ellipsoid formed by the inside surface of the aft case closure section;		
		in	Fig. 1	Eq. 8
LCSCLAO	$L_{CS_{CLAO}}$	Length of the axis of revolution of the hemi-ellipsoid formed by the outside surface of the aft case closure section;		
		in	Fig. 1	Eq. 7
LCSCLFI	$L_{CS_{CLFI}}$	Length of the axis of revolution of the hemi-ellipsoid formed by the inside surface of the forward case closure section;		
		in	Fig. 1	Eq. 11
LCSCLFO	$L_{CS_{CLFO}}$	Length of the axis of revolution of the hemi-ellipsoid formed by the outside surface of the forward case closure section;		
		in	Fig. 1	Eq. 10
LCSCY	$L_{CS_{CY}}$	Length of cylindrical case section. Includes all adjustments to grain;		
		in	Fig. 1	Eq. 34

OUTPUT DATA (Cont.):

Mnemonic	Symbol	Description; Ext. (Int.) Units
LCSHA	$L_{CS_{HA}}$	Length of the cylindrical hole, for the nozzle, in the aft case closure; in Fig. 1 Eq. 25
LCSHF	$L_{CS_{HF}}$	Length of the cylindrical hole, for the igniter, in the forward case closure; in Fig. 1 Eq. 26
QDCSI1	Q_{DI1}	Associative quantity, inside case diameter (see DCSI); in Eq. 28
QDCSI2	Q_{DI2}	Associative quantity, inside case diameter (see DCSI); in Eq. 29
QDCSI3	Q_{DI3}	Associative quantity, inside case diameter (see DCSI); in Eq. 30
QDCSO1	Q_{DO1}	Associative quantity, outside case diameter (see DCSO); in Eq. 31
QDCSO2	Q_{DO2}	Associative quantity, outside case diameter (see DCSO); in Eq. 32
QDCSO3	Q_{DO3}	Associative quantity, outside case diameter (see DCSO); in Eq. 33
RDCSCAI	R_{DCSCAI}	Head ratio of the ellipsoid associated with the aft inside case closure surface. Ratio of twice the closure length to the closure diameter, i.e., the aft inside case closure surface is an oblate spheroid. The head ratio is the ratio of the axis of revolution (minor axis) to the equatorial diameter (major axis); N. D. Eq. 9

OUTPUT DATA (Cont.):

Mnemonic	Symbol	Description; Ext. (Int.) Units	
RDCSCFI	R_{DCSCFI}	Head ratio of the ellipsoid associated with the forward inside case closure surface. Ratio of twice the closure length to the closure diameter, i.e., the forward inside case closure surface is an oblate spheroid. The head ratio is the ratio of the axis of revolution (minor axis) to the equatorial diameter (major axis);	
		N. D.	Eq. 12
RDCSHAI	R_{DCSHAI}	Diameter ratio, hole diameter to equatorial diameter, inside surface of aft case closure;	
		N. D.	Eq. 19
RDCSHAO	R_{DCSHAO}	Diameter ratio, hole diameter to equatorial diameter, outside surface of aft case closure;	
		N. D.	Eq. 17
RDCSHFI	R_{DCSHFI}	Diameter ratio, hole diameter to equatorial diameter, inside surface of forward case closure;	
		N. D.	Eq. 23
RDCSHFO	R_{DCSHFO}	Diameter ratio, hole diameter to equatorial diameter, outside surface of forward case closure;	
		N. D.	Eq. 21
RDCSCHO	R_{DCSCHO}	Head ratio for usage by models which define a single head ratio for forward and aft closures;	
		N. D.	Eq. 27-a
RLDCS	R_{LDCS}	Length to diameter ratio, total case;	
		N. D.	Eq. 37
RLDCSCY	R_{LDCSCY}	Length to diameter ratio, cylindrical case section;	
		N. D.	Eq. 36

OUTPUT DATA (Cont.):

Mnemonic	Symbol	Description; Ext. (Int.) Units		
TCSCLA	$T_{CS_{CLA}}$	Case thickness at center of aft case closure. Distance between the aft inside and outside hemi-ellipsoid surfaces, measured on the axis of revolution;		
		in	Fig. 1	Eq. 2
TCSCLF	$T_{CS_{CLF}}$	Case thickness at center of forward case closure. Distance between the forward inside and outside hemi-ellipsoid surfaces, measured on the axis of revolution;		
		in	Fig. 1	Eq. 3
TCSCY	$T_{CS_{CY}}$	Case thickness, cylindrical section;		
		in	Fig. 1	Eq. 1

PRINT BLOCK KEY:

Nominally, only those lines with an asterisk to the left of the line number will be printed. By input, any of the lines given below may be printed or suppressed (see the section on output models for the details).

			CASEG	CSGM1	CASE GEOMETRY	
CCSG1	CCSG2	CCSG3	*1			
ACS	DCSCLI	DCSCLO	*3	DCSHAI	DCSHAO	DCSHFI
DCSHFO	DCSI	DCSO	*4			
KCS1	KCS2	KCS3	*5	KCS4	KCS5	KCS6
KCS7	KCS8	KCS9	*6	KCS10		
KCSFS	KCSUTS	KQDCSI1	*9	KQDCSI2	KQDCSI3	KQDCSO1
KQDCSO2	KQDCSO3	LCS	*10	LCSHA	LCSHF	LCSCHAI
LCSCHAO	LCSCHFI	LCSCHFO	*11	LCSCLAI	LCSCLAO	LCSCLFI
LCSCLFO	LCSCY	QDCSI1	*12	QDCSI2	QDCSI3	QDCSO1
QDCSO2	QDCSO3	RDCSCAI	*13	RDCSCAO	RDCSCFI	RDCSCFO
RDCSCHO	RDCSHAI	RDCSHAO	*14	RDCSHFI	RDCSHFO	RLDCS
RLDCSCY	TCSCLA	TCSCLF	*15	TCSCY		

20.2

MODEL TYPE: CASEG (CASE Geometry)

MODEL NAME: CSGM2 (Glass case)

DESCRIPTION:

CSGM2 (CaSe Geometry Model number 2) determines the pertinent geometry for a solid rocket motor fiberglass case subject to internal pressure. This model does not account for buckling or aerodynamic loads.

As illustrated by Figure 1, the basic case geometry is comprised of a cylindrical section with forward and aft closure sections. The inside and outside surfaces of a closure section form concentric hemi-ellipsoids having coincident equatorial planes and, normally, unequal head ratios. The closures may have cylindrical holes, centered on the hemi-ellipsoid axis of revolution, for modeling geometry associated with the igniter, submerged nozzles and TVC systems. Generally, the geometry may be degenerated for simulating spherical motors, etc.

It should be noted that, since the model does not include raceways or external protrusions associated with segmented cases, the outside case diameter is not necessarily the maximum diameter of the motor. If such protrusions exist, they would be evaluated by the models specified for the MOTORG (motor geometry) or SUBSTGG (substage geometry) model types.

PROCEDURE:

Prior to entering CSGM2, the models specified by the IBGAS and NOZZLEG model types have determined the average chamber pressure and buried nozzle diameter.

Upon the first entrance to CSGM2, the thickness, closure lengths, diameters, head ratios, and closure hole geometry associated with a fiberglass motor case are evaluated.

The models specified for the INSULG and GRAING model types then evalu the remaining principal motor component geometry, the insulation and the grain.

After determining the grain geometry, CSGM2 is re-entered (second entrance) and quantities associated with the total case length are evaluated.

EQUATIONS, FIRST ENTRANCE:

Case thickness, cylindrical section.

$$T_{CS_{CY}} = \left[\frac{C_4 K_{FS} P_{MEO} \left(D_{CS_O}\right)^{C_5}}{2 K_{UTS}}\right] K_{CS_{11}} + K_{CS_{12}} \tag{1}$$

Case thickness, center of aft closure.

$$T_{CS_{CLA}} = \left(C_6 T_{CS_{CY}}\right) K_{CS_{13}} + K_{CS_{14}} \tag{2}$$

Case thickness, center of forward closure.

$$T_{CS_{CLF}} = \left(C_7 T_{CS_{CY}}\right) K_{CS_{15}} + K_{CS_{16}} \tag{3}$$

Case inside diameter.

$$D_{CS_I} = D_{CS_O} - 2 T_{CS_{CY}} \tag{4}$$

Outside equatorial diameter for case closures.

$$D_{CS_{CLO}} = D_{CS_O} \tag{5}$$

Inside equatorial diameter for case closures

$$D_{CS_{CLI}} = D_{CS_I} \tag{6}$$

Outside length of aft case closure.

$$L_{CS_{CLAO}} = \frac{R_{DCSCAO}}{2} D_{CS_{CLO}} \tag{7}$$

Inside length of aft case closure.

$$L_{CS_{CLAI}} = L_{CS_{CLAO}} - T_{CS_{CLA}} \tag{8}$$

EQUATIONS, FIRST ENTRANCE (Cont.):

Inside head ratio of aft closure.

$$R_{DCSCAI} = 2 \frac{L_{CS_{CLAI}}}{D_{CS_{CLI}}} \tag{9}$$

Outside length of forward closure.

$$L_{CS_{CLFO}} = \frac{R_{DCSCFO} \, D_{CS_{CLO}}}{2} \tag{10}$$

Inside length of forward closure.

$$L_{CS_{CLFI}} = L_{CS_{CLFO}} - T_{CS_{CLF}} \tag{11}$$

Inside head ratio of forward closure.

$$R_{DCSCFI} = \frac{2 \, L_{CS_{CLFI}}}{D_{CS_{CLI}}} \tag{12}$$

Diameter of hole in aft outside case closure surface.

$$D_{CS_{HAO}} = K_{CS_{17}} \, D_{NZ_B} + K_{CS_{18}} \tag{13}$$

Diameter of hole in aft inside case closure surface.

$$D_{CS_{HAI}} = D_{CS_{HAO}} \tag{14}$$

Diameter of hole in forward outside case closure surface.

$$D_{CS_{HFO}} = K_{CS_{19}} \, D_{CS_{CLO}} + K_{CS_{20}} \tag{15}$$

Diameter of hole in forward inside case closure surface.

$$D_{CS_{HFI}} = D_{CS_{HFO}} \tag{16}$$

EQUATIONS, FIRST ENTRANCE (Cont.):

Diameter ratio. Aft outside case hole diameter to outside case closure diameter.

$$R_{DCSHAO} = \frac{D_{CS_{HAO}}}{D_{CS_{CLO}}} \tag{17}$$

Outside length of aft case closure, adjusted for hole.

$$L_{CS_{CHAO}} = L_{CS_{CLAO}} \sqrt{1 - R^2_{DCSHAO}} \tag{18}$$

Diameter ratio. Aft inside case hole diameter to inside case closure diameter.

$$R_{DCSHAI} = \frac{D_{CS_{HAI}}}{D_{CS_{CLI}}} \tag{19}$$

Inside length of aft case closure, adjusted for hole.

$$L_{CS_{CHAI}} = L_{CS_{CLAI}} \sqrt{1 - R^2_{DCSHAI}} \tag{20}$$

Diameter ratio. Forward outside case hole diameter to outside case closure diameter.

$$R_{DCSHFO} = \frac{D_{CS_{HFO}}}{D_{CS_{CLO}}} \tag{21}$$

Outside length of forward case closure, adjusted for hole.

$$L_{CS_{CHFO}} = L_{CS_{CLFO}} \sqrt{1 - R^2_{DCSHFO}} \tag{22}$$

EQUATIONS, FIRST ENTRANCE (Cont.):

Diameter ratio, forward inside case hole diameter to inside case closure diameter.

$$R_{DCSHFI} = \frac{D_{CS_{HFI}}}{D_{CS_{CLI}}} \tag{23}$$

Inside length of forward case closure, adjusted for hole.

$$L_{CS_{CHFI}} = L_{CS_{CLFI}} \sqrt{1 - R^2_{DCSHFI}} \tag{24}$$

Length of hole in aft case closure.

$$L_{CS_{HA}} = L_{CS_{CHAO}} - L_{CS_{CHAI}} \tag{25}$$

Length of hole in forward case closure.

$$L_{CS_{HF}} = L_{CS_{CHFO}} - L_{CS_{CHFI}} \tag{26}$$

Case cross sectional area.

$$A_{CS} = \left(\frac{\pi}{4}\right) D^2_{CS_O} \tag{27}$$

Head ratio for usage by models which define a single head ratio for the forward and aft closures.

$$R_{DCSCHO} = R_{DCSCAO} \tag{27-a}$$

Associative quantities. The following quantities are intended solely for optional utilization by the program user. Their primary usage within this model is for forming constraint quantities.

$$Q_{DI1} = K_{QDI1} D_{CS_I} \tag{28}$$

$$Q_{DI2} = K_{QDI2} D_{CS_I} \tag{29}$$

$$Q_{DI3} = K_{QDI3} D_{CS_I} \tag{30}$$

EQUATIONS, FIRST ENTRANCE (Cont.):

$$Q_{DO1} = K_{QDO1} D_{CS_O} \tag{31}$$

$$Q_{DO2} = K_{QDO2} D_{CS_O} \tag{32}$$

$$Q_{DO3} = K_{QDO3} D_{CS_O} \tag{33}$$

EQUATIONS, SECOND ENTRANCE:

Length of cylindrical case section.

$$L_{CS_{CY}} = L_{GN_{CY}} \tag{34}$$

Total case length.

$$L_{CS} = L_{CS_{CY}} + L_{CS_{CHAO}} + L_{CS_{CHFO}} \tag{35}$$

Cylindrical case length to diameter ratio.

$$R_{LDCSCY} = \frac{L_{CS_{CY}}}{D_{CS_O}} \tag{36}$$

Total case length to diameter ratio.

$$R_{LDCS} = \frac{L_{CS}}{D_{CS_O}} \tag{37}$$

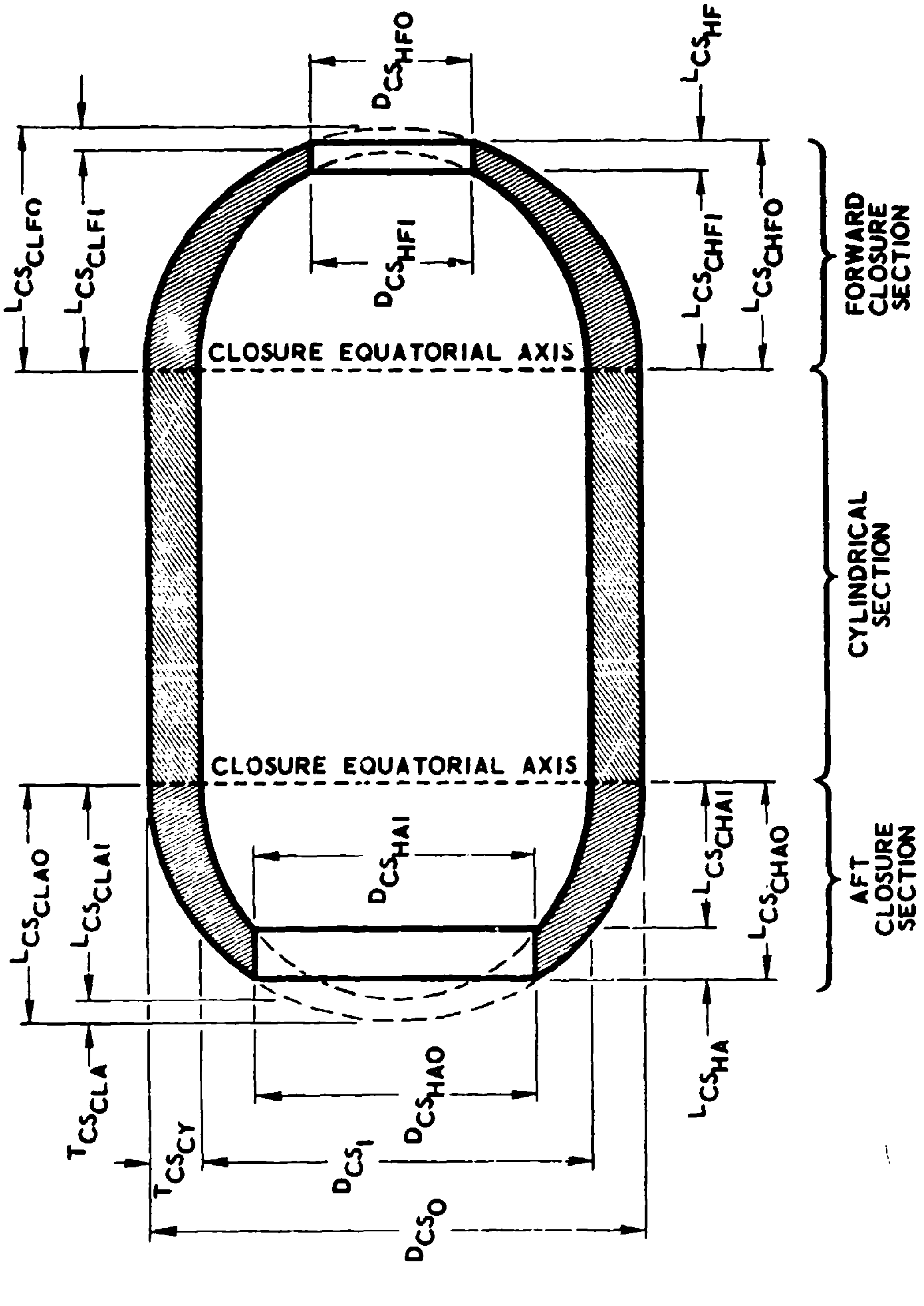

Fig. 20.2-1 Fiberglass Case Geometry

INPUT DATA, INTRA-MODEL:

The following data is input directly to this model by the program user. If a value is not input, the preset value is used.

Mnemonic	Symbol	Description; Ext. (Int.) Units	Preset
CCSG4	C_4	Constant for TCSCY computation; N. D.	1.18
CCSG5	C_5	Constant for TCSCY computation; N. D.	1.16
CCSG6	C_6	Proportionality constant relating the case thickness at the center of the aft closure to the case thickness of the cylindrical section; N. D.	0.5
CCSG7	C_7	Proportionality constant relating the case thickness at the center of the forward closure to the case thickness of the cylindrical section; N. D.	0.5
DCSO	D_{CS_O}	Motor case outside diameter. Outside diameter of pressure vessel cylindrical case section. Does not include raceways, protrusions, etc.; in Fig. 1	0
KCS11	$K_{CS_{11}}$	Coefficient for TCSCY computation; N. D.	1
KCS12	$K_{CS_{12}}$	Bias for TCSCY computation; in	0
KCS13	$K_{CS_{13}}$	Coefficient for TCSCLA computation; N. D.	1
KCS14	$K_{CS_{14}}$	Bias for TCSCLA computation; in	0

INPUT DATA, INTRA-MODEL (Cont.):

Mnemonic	Symbol	Description; Ext. (Int.) Units	Preset
KCS15	$K_{CS_{15}}$	Coefficient for TCSCLF computation; N. D.	1
KCS16	$K_{CS_{16}}$	Bias for TCSCLF computation; in	0
KCS17	$K_{CS_{17}}$	Coefficient for DCSHAO computation; N. D.	1
KCS18	$K_{CS_{18}}$	Bias for DCSHAO computation; in	0
KCS19	$K_{CS_{19}}$	Coefficient for DCSHFO computation; N. D.	1
KCS20	$K_{CS_{20}}$	Bias for DCSHFO computation; in	0
KCSFS	K_{FS}	Case factor of safety. Ratio of minimum burst pressure to maximum expected operating pressure; N. D.	1
KCSUTS	K_{UTS}	Ultimate tensile strength for fiberglass filament case material; lb/in^2	0
KQDCSI1	K_{QDI1}	Associative quantity coefficient for QDCSI1 computation; N. D.	0
KQDCSI2	K_{QDI2}	Associative quantity coefficient for QDCSI2 computation; N. D.	0

INPUT DATA, INTRA-MODEL (Cont.):

Mnemonic	Symbol	Description; Ext. (Int.) Units	Preset
KQDCSI3	K_{QDI3}	Associative quantity coefficient for QDCSI3 computation; N. D.	0
KQDCSO1	K_{QDO1}	Associative quantity coefficient for QDCSO1 computation; N. D.	0
KQDCSO2	K_{QDO2}	Associative quantity coefficient for QDCSO2 computation; N. D.	0
KQDCSO3	K_{QDO3}	Associative quantity coefficient for QDCSO3 computation; N. D.	0
RDCSCAO	R_{DCSCAO}	Head ratio of the ellipsoid associated with the aft outside case closure surface. Ratio of twice the closure length to the closure diameter, i.e., the aft outside case closure surface is an oblate spheroid. The head ratio is the ratio of the axis of revolution (minor axis) to the equatorial diameter (major axis); N. D.	1
RDCSCFO	R_{DCSCFO}	Head ratio of the ellipsoid associated with the forward outside case closure surface. Ratio of twice the closure length to the closure diameter, i.e., the forward outside case closure surface is an oblate spheroid. The head ratio is the ratio of the axis of revolution (minor axis) to the equatorial diameter (major axis); N. D.	1

INPUT DATA, INTER-MODEL:

This model requires as input certain data which is usually output from a model of the specified model type. If the user has not specified such a source for this data, then it must be input directly with the intra-model input.

Mnemonic	Symbol	Description; Ext. (Int.) Units	Model Type
DNZB	D_{NZ_B}	Buried nozzle diameter; in	NOZZLEG
PCHMEO	P_{MEO}	Maximum expected operating chamber pressure; psia	IBGAS
LGNCY	$L_{GN_{CY}}$	Length of cylindrical grain section. Includes all adjustments for submerged nozzle, displaced propellent, cutouts, etc.; in	GRAING

OUTPUT DATA:

The following data is output from this model. It is available for use as inter-model input to other models and to print, plot, and optimization routines.

Mnemonic	Symbol	Description; Ext. (Int.) Units		
ACS	A_{CS}	Motor case cross sectional area. Area of pressure vessel cylindrical case section. Does not include raceways, protrusions, etc.; in^2		Eq. 27
DCSCLI	$D_{CS_{CLI}}$	Equatorial diameter of the ellipsoids formed by the inside surfaces of the forward and aft case closure sections; in	Fig. 1	Eq. 6
DCSCLO	$D_{CS_{CLO}}$	Equatorial diameter of the ellipsoids formed by the outside surfaces of the forward and aft case closure sections; in	Fig. 1	Eq. 5

OUTPUT DATA (Cont.):

Mnemonic	Symbol	Description; Ext. (Int.) Units		
DCSHAI	$D_{CS_{HAI}}$	Diameter of circular hole, for the nozzle, centered on the axis of revolution of the hemi-ellipsoid formed by the inside surface of the aft case closure;		
		in	Fig. 1	Eq. 14
DCSHAO	$D_{CS_{HAO}}$	Diameter of circular hole, for the nozzle, centered on the axis of revolution of the hemi-ellipsoid formed by the outside surface of the aft case closure;		
		in	Fig. 1	Eq. 13
DCSHFI	$D_{CS_{HFI}}$	Diameter of circular hole, for the igniter, centered on the axis of revolution of the hemi-ellipsoid formed by the inside surface of the forward case closure;		
		in	Fig. 1	Eq. 16
DCSHFO	$D_{CS_{HFO}}$	Diameter of circular hole, for the igniter, centered on the axis of revolution of the hemi-ellipsoid formed by the outside surface of the forward case closure;		
		in	Fig. 1	Eq. 15
DCSI	D_{CS_I}	Case inside diameter, cylindrical section;		
		in	Fig. 1	Eq. 4
LCS	L_{CS}	Total case length. Distance between the forward base of the hemi-ellipsoid frustum associated with the forward outside closure surface to the aft base of the hemi-ellipsoid frustum associated with the aft outside closure surface. Includes all adjustments to grain;		
		in	Fig. 1	Eq. 35
LCSCHAI	$L_{CS_{CHAI}}$	Length of hemi-ellipsoidal frustum which forms the inside surface of the aft case closure. Includes adjustment for nozzle hole;		
		in	Fig. 1	Eq. 20

OUTPUT DATA (Cont.):

Mnemonic	Symbol	Description; Ext. (Int.) Units		
LCSCHAO	$L_{CS_{CHAO}}$	Length of hemi-ellipsoidal frustum which forms the outside surface of the aft case closure. Includes adjustment for nozzle hole;		
		in	Fig. 1	Eq. 18
LCSCHFI	$L_{CS_{CHFI}}$	Length of hemi-ellipsoidal frustum which forms the inside surface of the forward case closure. Includes adjustment for igniter hole;		
		in	Fig. 1	Eq. 24
LCSCHFO	$L_{CS_{CHFO}}$	Length of hemi-ellipsoidal frustum which forms the outside surface of the forward case closure. Includes adjustment for igniter hole;		
		in	Fig. 1	Eq. 22
LCSCLAI	$L_{CS_{CLAI}}$	Length of the axis of revolution of the hemi-ellipsoid formed by the inside surface of the aft case closure section;		
		in	Fig. 1	Eq. 8
LCSCLAO	$L_{CS_{CLAO}}$	Length of the axis of revolution of the hemi-ellipsoid formed by the outside surface of the aft case closure section;		
		in	Fig. 1	Eq. 7
LCSCLFI	$L_{CS_{CLFI}}$	Length of the axis of revolution of the hemi-ellipsoid formed by the inside surface of the forward case closure section;		
		in	Fig. 1	Eq. 11
LCSCLFO	$L_{CS_{CLFO}}$	Length of the axis of revolution of the hemi-ellipsoid formed by the outside surface of the forward case closure section;		
		in	Fig. 1	Eq. 10
LCSCY	$L_{CS_{CY}}$	Length of cylindrical case section. Includes all adjustments to grain;		
		in	Fig. 1	Eq. 34

OUTPUT DATA (Cont.):

Mnemonic	Symbol	Description; Ext. (Int.) Units		
LCSHA	$L_{CS_{HA}}$	Length of the cylindrical hole, for the nozzle, in the aft case closure;		
		in	Fig. 1	Eq. 25
LCSHF	$L_{CS_{HF}}$	Length of the cylindrical hole, for the igniter, in the forward case closure;		
		in	Fig. 1	Eq. 26
QDCSI1	Q_{DI1}	Associative quantity, inside case diameter (see DCSI);		
		in		Eq. 28
QDCSI2	Q_{DI2}	Associative quantity, inside case diameter (see DCSI);		
		in		Eq. 29
QDCSI3	Q_{DI3}	Associative quantity, inside case diameter (see DCSI);		
		in		Eq. 30
QDCSO1	Q_{DO1}	Associative quantity, outside case diameter (see DCSO);		
		in		Eq. 31
QDCSO2	Q_{DO2}	Associative quantity, outside case diameter (see DCSO);		
		in		Eq. 32
QDCSO3	Q_{DO3}	Associative quantity, outside case diameter (see DCSO);		
		in		Eq. 33
RDCSCAI	R_{DCSCAI}	Head ratio of the ellipsoid associated with the aft inside case closure surface. Ratio of twice the closure length to the closure diameter, i.e., the aft inside case closure surface is an oblate spheroid. The head ratio is the ratio of the axis of revolution (minor axis) to the equatorial diameter (major axis);		
		N. D.		Eq. 9

OUTPUT DATA (Cont.):

Mnemonic	Symbol	Description; Ext. (Int.) Units	
RDCSCFI	R_{DCSCFI}	Head ratio of the ellipsoid associated with the forward inside case closure surface. Ratio of twice the closure length to the closure diameter, i.e., the forward inside case closure surface is an oblate spheroid. The head ratio is the ratio of the axis of revolution (minor axis) to the equatorial diameter (major axis);	
		N. D.	Eq. 12
RDCSHAI	R_{DCSHAI}	Diameter ratio, hole diameter to equatorial diameter, inside surface of aft case closure;	
		N. D.	Eq. 19
RDCSHAO	R_{DCSHAO}	Diameter ratio, hole diameter to equatorial diameter, outside surface of aft case closure;	
		N. D.	Eq. 17
RDCSHFI	R_{DCSHFI}	Diameter ratio, hole diameter to equatorial diameter, inside surface of forward case closure;	
		N. D.	Eq. 23
RDCSHFO	R_{DCSHFO}	Diameter ratio, hole diameter to equatorial diameter, outside surface of forward case closure;	
		N. D.	Eq. 21
RDCSCHO	R_{DCSCHO}	Head ratio for usage by models which define a single head ratio for forward and aft closures;	
		N. D.	Eq. 27-a
RLDCS	R_{LDCS}	Length to diameter ratio, total case;	
		N. D.	Eq. 37
RLDCSCY	R_{LDCSCY}	Length to diameter ratio, cylindrical case section;	
		N. D.	Eq. 36

OUTPUT DATA (Cont.):

Mnemonic	Symbol	Description; Ext. (Int.) Units		
TCSCLA	$T_{CS_{CLA}}$	Case thickness at center of aft case closure. Distance between the aft inside and outside hemi-ellipsoid surfaces, measured on the axis of revolution;		
		in	Fig. 1	Eq. 2
TCSCLF	$T_{CS_{CLF}}$	Case thickness at center of forward case closure. Distance between the forward inside and outside hemi-ellipsoid surfaces, measured on the axis of revolution;		
		in	Fig. 1	Eq. 3
TCSCY	$T_{CS_{CY}}$	Case thickness, cylindrical section;		
		in	Fig. 1	Eq. 1

PRINT BLOCK KEY:

Nominally, only those lines with an asterisk to the left of the line number will be printed. By input, any of the lines given below may be printed or suppressed (see the section on output models for the details).

			CASEG	CSGM2	CASE GEOMETRY	
CCSG4	CCSG5	CCSG6	*2	CCSG7		
ACS	DCSCLI	DCSCLO	*3	DCSHAI	DCSHAO	DCSHFI
DCSHFO	DCSI	DCSO	*4			
KCS11	KCS12	KCS13	*7	KCS14	KCS15	KCS16
KCS17	KCS13	KCS19	*8	KCS20		
KCSFS	KCSUTS	KQDCSI1	*9	KQDCSI2	KQDCSI3	KQDCSO1
KQDCSO2	KQDCSO3	LCS	*10	LCSHA	LCSHF	LCSCHAI
LCSCHAO	LCSCHFI	LCSCHFO	*11	LCSCLAI	LCSCLAO	LCSCLFI
LCSCLFO	LCSCY	QDCSI1	*12	QDCSI2	QDCSI3	QDCSO1
QDCSO2	QDCSO3	RDCSCAI	*13	RDCSCAO	RDCSCFI	RDCSCFO
RDCSCHO	RDCSHAI	RDCSHAO	*14	RDCSHFI	RDCSHFO	RLDCS
RLDCSCY	TCSCLA	TCSCLF	*15	TCSCY		

30.1

MODEL TYPE: CASEW (CASE Weight)

MODEL NAME: CSWM1 (Metal Case, Parametric Scaling)

DESCRIPTION:

CSWM1 (CaSe Weight Model number 1) utilizes parametric weight scaling equations to determine the weight of a solid rocket motor, unjointed or jointed, metal case. See references 8 and 34 for a description of the equations and scaling coefficient rationale.

The model is applicable for performance parameters within the following limits (see Input Data, Inter-Model).

$$500 < \text{PCHMEO} < 1950 \text{ psia}$$

$$0.6 < \text{RDCSCHO} < 1.0$$

$$0.25 < \text{RLDGNCY} < 8.0$$

$$3000 < \text{WPPMT} < 2,000,000 \text{ lb.}$$

PROCEDURE:

Prior to entering CSWM1, the models specified by the PROPELW and IBGAS model types have evaluated the propellent and gas properties. The models specified by the CASEG, GRAING and MOTORG have evaluated the motor geometry.

The CSWM1 model is then executed and the motor case weight is evaluated using parametric weight scaling equations. In addition, the case weight is broken down into expended and non-expended components.

These expended and non-expended case weight components will later be used by the model specified for the MOTORW model type to determine the motor weights and mass fractions.

EQUATIONS:

Total case weight, no joints.

$$K_1 = \frac{R_{LDGNCY} + C_1 \left[\left(\left| R_{DCSCHO} - C_2 \right| \right)^{C_3} + C_4 \right]}{\left(\frac{R_{DCSCHO}}{C_3} \right) + C_5 \, R_{LDGNCY}} \qquad (1)$$

$$W_{CS_{NOJT}} = K_{WCSNOJ} \left\{ \frac{C_{CSG1} \, W_{PP_{MT}} \, P_{MEO} \, K_{FS} \, \rho_{CS} \, K_1}{K_{UTS} \, \rho_{PP_{MT}} \, \eta_{MT}} + \frac{C_6 \, \rho_{CS} \, R_{DCSCHO} \, D^2_{CS_O}}{W_{PP_{MT}}^{C_7}} \sqrt{\frac{K_{FS} \, W_{PP_{MT}}}{K_{UTS}}} \right\}$$

Case weight penalty per joint.

$$W_{JT_{CSU}} = K_{WJTCSU} \left\{ \frac{K_{FS} \, P_{MEO} \, D^2_{CS_O}}{K_{UTS}} \right\} C_{14} \qquad (2)$$

Total joint weight penalty.

$$W_{JT_{CS}} = N_{JT_{CS}} \, W_{JTU} \qquad (3)$$

Total case weight.

$$W_{CS} = K_{WCS} \left(W_{CS_{NOJT}} + W_{JT_{CS}} \right) \qquad (4)$$

Total non-expended case weight component.

$$W_{CS_{NX}} = K_{WCSNX} \, W_{CS} \qquad (5)$$

Total expended case weight component.

$$W_{CS_X} = 0 \qquad (6)$$

EQUATIONS (Cont.):

Expended (non-thrust producing) case weight component.

$$W_{CS_{XI}} = 0 \tag{7}$$

Expended (thrust producing) case weight component.

$$W_{CS_{XT}} = 0 \tag{8}$$

INPUT DATA, INTRA-MODEL:

The following data is input to this model directly by the program user. If a value is not input, the preset value is used.

Mnemonic	Symbol	Description; Ext. (Int.) Units	Preset
CCSW1	C_1	Scaling constant for WCS computation; N. D.	0.5
CCSW2	C_2	Scaling constant for WCS computation; N. D.	0.77
CCSW3	C_3	Scaling constant for WCS computation; N. D.	1.3
CCSW4	C_4	Scaling constant for WCS computation; N. D.	0.856
CCSW5	C_5	Scaling constant for WCS computation; N. D.	0.5
CCSW6	C_6	Scaling constant for WCS computation; N. D.	9.0712
CCSW7	C_7	Scaling constant for WCS computation; N. D.	0.20288

INPUT DATA, INTRA-MODEL (Cont.):

Mnemonic	Symbol	Description; Ext. (Int.) Units	Preset
CCSW14	C_{14}	Scaling constant for WJTCSU computation; N. D.	7.7
NJTCS	$N_{JT_{CS}}$	Number of joints in motor case; N. D.	0
KWCS	K_{WCS}	Proportionality factor for total case weight, includes joint penalty; N. D.	1
KWCSNOJ	K_{WCSNOJ}	Proportionality factor for total case weight, does not include joint penalty; N. D.	1
KWCSNX	K_{WCSNX}	Proportionality factor for case non-expended weight, includes joint penalty; N. D.	1
KWJTCSU	K_{WJTCSU}	Proportionality factor for the weight of a joint; N. D.	1
RHOCS	ρ_{CS}	Density of metal case material; lb/in^3	0

INPUT DATA, INTER-MODEL:

This model requires as input certain data which is usually output from a model of the specified model type. If the user has not specified such a source for this data, then it must be input directly with the intra-model input.

Mnemonic	Symbol	Description; Ext. (Int.) Units	Model Type
CCSG1	C_{CSG1}	Constant for case thickness computation; N. D.	CASEG

INPUT DATA, INTER-MODEL (Cont.):

Mnemonic	Symbol	Description; Ext. (Int.) Units	Model Type
DCSO	D_{CS_O}	Motor case outside diameter; in	CASEG
KCSFS	K_{FS}	Case factor of safety; N. D.	CASEG
KCSUTS	K_{UTS}	Ultimate tensile strength for metal case material; lb/in^2	CASEG
PCHMEO	P_{MEO}	Maximum expected operating chamber pressure; psia	IBGAS
RDCSCHO	R_{DCSCHO}	Case closure outside surface head ratio; N. D.	CASEG
RLDGNCY	R_{LDGNCY}	Ratio, cylindrical grain length to grain diameter. Includes all adjustments to grain; N. D.	GRAING
RHOPPMT	$\rho_{PP_{MT}}$	Propellent density; lb/in^3	PROPEL
RVPPMT	η_{MT}	Motor volumetric loading efficiency; N. D.	MOTORG
WPPMT	$W_{PP_{MT}}$	Propellent weight; lb	PROPELW

OUTPUT DATA:

The following data is output from this model. It is available for use as inter-model input to other models and to print, plot, and optimization routines.

Mnemonic	Symbol	Description; Ext. (Int.) Units	
WCS	W_{CS}	Total case weight, includes joint penalty; lb	Eq. 4

OUTPUT DATA (Cont.):

Mnemonic	Symbol	Description; Ext. (Int.) Units	
WCSNOJT	$W_{CS_{NOJT}}$	Total case weight, no joints; lb	Eq. 1
WCSNX	$W_{CS_{NX}}$	Total non-expended case weight, includes joint penalty; lb	Eq. 5
WCSX	W_{CS_X}	Total expended case weight; lb	Eq. 6
WCSXI	$W_{CS_{XI}}$	Expended (non-thrust producing) case weight component; lb	Eq. 7
WCSXT	$W_{CS_{XT}}$	Expended (thrust producing) case weight component; lb	Eq. 8
WJTCS	$W_{JT_{CS}}$	Total joint weight penalty; lb	Eq. 3
WJTCSU	$W_{JT_{CSU}}$	Case weight penalty per joint; lb	Eq. 2

PRINT BLOCK KEY:

Nominally, only those lines with an asterisk to the left of the line number will be printed. By input, any of the lines given below may be printed or suppressed (see the section on output models for the details).

			CASEW	CSWM1	CASE WEIGHT	
WCS	WCSNX	WCSX	*1	WCSXI	WCSXT	
CCSW1	CCSW2	CCSW3	*2	CCSW4	CCSW5	CCSW6
CCSW7	CCSW12		*3			
NJTCS	KWCS	KWCSNOJ	*5	KWCSNX	KWJTCSU	RHOCS
WCSNOJT	WJTCS	WJTCSU	*6			

30.2

MODEL TYPE: CASEW (CASE Weight)

MODEL NAME: CSWM2 (Glass Case, Parametric scaling)

DESCRIPTION:

CSWM2 (CaSe Weight Model number 2) utilizes parametric weight scaling equations to evaluate the weight of a solid rocket motor (unjointed or jointed) fiberglass motor case.

The basic assumptions used to develop the equations were as follows:

1. Bosses are made from aluminum with a minimum ultimate tensile strength of 70 ksi.

2. Bolts used for the attachment of the igniter and nozzle to the bosses are heat treated 170 ksi (minimum).

3. Forward and aft boss diameters are 20% and 50% of the case diameter, respectively.

4. Equal margins of safety are maintained at all points on the composite shell.

The most important point for the engineer preparing input data is that KCSUTS is a representative strength for the fiber under consideration. For example, KCSUTS would be 350,000 psi for type S-901 (S-944) fibers.

See references 41-42 for a description of the unjointed case weight equation. The joint penalty is described in reference 44.

This model is applicable for performance parameters within the following limits (see Input Data, Inter-Model).

$$600 < \text{PCHMEO} < 1950 \text{ psia}$$

$$3000 < \text{WPPMT} < 2{,}000{,}000 \text{ lb.}$$

PROCEDURE:

Prior to entering CSWM2, the models specified by the PROPEL and IBGAS model types have evaluated the propellent and gas properties. The models specified by the CASEG, GRAING and MOTORG have evaluated the motor geometry.

The CSWM2 model is then executed and the motor case weight is evaluated using parametric weight scaling equations. In addition, the case weight is broken down into expended and non-expended components.

These expended and non-expended case weight components will later be used by the model specified for the MOTORW model type to determine the motor weights and mass fractions.

EQUATIONS:

Total case weight, no joints.

$$K_1 = \frac{\rho_{CS} K_{FS} P_{MEO} \left(D_{CS_O}\right)^{C_8}}{K_{UTS}} \left[\frac{C_9 W_{PP_{MT}}}{\rho_{PP_{MT}} \eta_{PP_{MT}}} + C_{10} L_{MT_{SKA}} D^2_{CS_O}\right] \qquad (1)$$

$$K_2 = C_{11} D^3_{CS_O} \left(1. + C_{12} P_{MEO} K_{FS}\right)$$

$$W_{CS_{NOJT}} = K_{WCSNOJ} \left(K_1 + K_2\right)$$

Case weight penalty per joint.

$$W_{JT_{CSU}} = K_{WJTCSU} \left\{\frac{K_{FS} P_{MEO} D^2_{CS_O}}{K_{UTS}}\right\} C_{13} \qquad (2)$$

Total joint weight penalty.

$$W_{JT_{CS}} = N_{JT} W_{JT_{CSU}} \qquad (3)$$

Total case weight.

$$W_{CS} = K_{WCS} \left(W_{CS_{NOJT}} + W_{JT_{CS}}\right) \qquad (4)$$

EQUATIONS (Cont.):

Total non-expended case weight component.

$$W_{CS_{NX}} = K_{WCSNX} W_{CS} \quad (5)$$

Total expended case weight component.

$$W_{CS_X} = 0 \quad (6)$$

Expended (non-thrusting producing) case weight component.

$$W_{CS_{XI}} = 0 \quad (7)$$

Expended (thrust producing) case weight component.

$$W_{CS_{XT}} = 0 \quad (8)$$

INPUT DATA, INTRA-MODEL:

The following data is input to this model directly by the program user. If a value is not input, the preset value is used.

Mnemonic	Symbol	Description; Ext. (Int.) Units	Preset
CCSW8	C_8	Scaling constant for WCSNOJT computation; N. D.	0.16
CCSW9	C_9	Scaling constant for WCSNOJT computation; N. D.	2.62
CCSW10	C_{10}	Scaling constant for WCSNOJT computation; N. D.	6.09
CCSW11	C_{11}	Scaling constant for WCSNOJT computation; N. D.	0.000016
CCSW12	C_{12}	Scaling constant for WCSNOJT computation; N. D.	0.01

INPUT DATA, INTRA-MODEL (Cont.):

Mnemonic	Symbol	Description; Ext. (Int.) Units	Preset
CCSW13	C_{13}	Scaling constant for WJTCSU computation; N. D.	7.7
NJTCS	$N_{JT_{CS}}$	Number of joints in motor case; N. D.	0
KWCS	K_{WCS}	Proportionality factor for total case weight, includes joint penalty; N. D.	1
KWCSNOJ	K_{WCSNOJ}	Proportionality factor for case weight, does not include joint penalty; N. D.	1
KWCSNX	K_{WCSNX}	Proportionality factor for case non-expended weight component, includes joint penalty; N. D.	1
KWJTCSU	K_{WJTCSU}	Proportionality factor for the weight of a joint; N. D.	1
RHOCS	ρ_{CS}	Density of composite glass case material; lb/in^3	0

INPUT DATA, INTER-MODEL:

This model requires as input certain data which is usually output from a model of the specified model type. If the user has not specified such a source for this data, then it must be input directly with the intra-model input.

Mnemonic	Symbol	Description; Ext. (Int.) Units	Model Type
DCSO	D_{CS_O}	Outside case diameter; in	CASEG

INPUT DATA, INTER-MODEL (Cont.):

Mnemonic	Symbol	Description; Ext. (Int.) Units	Model Type
KCSFS	K_{FS}	Case factor of safety; N. D.	CASEG
KCSUTS	K_{UTS}	Ultimate tensile strength for fiberglass filament case material; lb/in^2	CASEG
LMTSKA	$L_{MT_{SKA}}$	Aft motor skirt length. The model assumes that the fore and aft skirts have equal lengths; in	MOTORG
PCHMEO	P_{MEO}	Maximum expected operating chamber pressure; psia	IBGAS
RHOPPMT	$\rho_{PP_{MT}}$	Propellent density; lb/in^3	PROPELW
RVPPMT	$\eta_{PP_{MT}}$	Motor volumetric loading efficiency; N. D.	MOTORG
WPPMT	$W_{PP_{MT}}$	Propellent weight; lb	PROPELW

OUTPUT DATA:

The following data is output by this model. It is available for use as inter-model input to other models and to print, plot, and optimization routines.

Mnemonic	Symbol	Description; Ext. (Int.) Units	
WCS	W_{CS}	Total case weight, includes joint penalty; lb	Eq. 4
WCSNOJT	$W_{CS_{NOJT}}$	Total case weight, no joints; lb	Eq. 1

OUTPUT DATA (Cont.):

Mnemonic	Symbol	Description; Ext. (Int.) Units	
WCSNX	$W_{CS_{NX}}$	Total non-expended case weight component. Includes joint penalty;	
		lb	Eq. 5
WCSX	W_{CS_X}	Total expended case weight component;	
		lb	Eq. 6
WCSXI	$W_{CS_{XI}}$	Expended (non-thrust producing) case weight component;	
		lb	Eq. 7
WCSXT	$W_{CS_{XT}}$	Expended (thrust producing) case weight component;	
		lb	Eq. 8
WJTCS	$W_{JT_{CS}}$	Total joint weight penalty;	
		lb	Eq. 3
WJTCSU	$W_{JT_{CSU}}$	Case weight penalty per joint;	
		lb	Eq. 2

PRINT BLOCK KEY:

Nominally, only those lines with an asterisk to the left of the line number will be printed. By input, any of the lines given below may be printed or suppressed (see the section on output models for the details).

			CASEW	CSWM2	CASE WEIGHT	
WCS	WCSNX	WCSX	*1	WCSXI	WCSXT	
CCSW8	CCSW9	CCSW10	*4	CCSW11	CCSW12	CCSW13
NJTCS	KWCS	KWCSNOJ	*5	KWCSNX	KWJTCSU	RHOCS
WCSNOJT	WJTCS	WJTCSU	*6			

40.1

MODEL TYPE: GRAING (GRAIN Geometry)

MODEL NAME: GNGM1 (cylindrical central perforate)

DESCRIPTION:

GNGM1 (GraiN Geometry Model number 1) evaluates the pertinent geometry for a solid rocket propellent grain to be enclosed within a motor case having a cylindrical section with hemi-ellipsoidal closures and a single nozzle. The port is a cylindrical central perforate with provision for lateral slot cutouts, lateral motor joint cutouts, and a cone frustum section to accommodate a submerged nozzle. Provision is also made for a cylindrical grain length penalty for the propellent displacement due to internal insulation in the forward and aft hemi-ellipsoid closures.

Reference 52, "Some Useful Theorems Associated With Hemi-Ellipsoids" is the basis for the derivation of the equations.

PROCEDURE:

Prior to entering GNGM1, the models specified by the NOZZLEG and CASEG model types have determined the nozzle and case geometry. The model specified by the INSULG model type has determined (first entrance) the pertinent internal insulation quantities required for interfacing between the case and grain.

Upon the first entrance to GNGM1, the basic grain geometry is determined and then adjusted for nozzle submergence. The propellent surface area is computed and the model specified by the IBFLOW model type is executed to determine the slot length penalty.

GNGM1 is then entered for the second time and the grain is adjusted to account for the slot and joint volumes. Using this corrected grain geometry, the model specified for the INSULG model type (second entrance) evaluates the internal insulation geometry within the grain envelope.

Upon the third entrance to GNGM1, the cylindrical grain length is adjusted to include the propellent displaced by the internal insulation, and the remaining grain geometry quantities are evaluated.

PROCEDURE (Cont.):

After completing the grain geometry, the model specified for the INSULG model type is entered for the third time and the internal insulation geometry is completed.

A block diagram illustrating the inter-model coupling with the grain geometry is included in the documentation of the model specified for the INSULG model type.

NOTATION CONVENTIONS:

The following notation conventions are used within this model whenever possible.

First character

A	Plane area. (in^2)
D	Diameter, measured normal to centerline. (in)
K	Coefficient or bias.
L	Length, measured parallel to centerline. (in)
Q	Associative quantity.
R	Ratio. Next character(s) will be L or D to indicate diameter or length ratio. (N. D.)
S	Surface area. (in^2)
T	Thickness. (in)
V	Volume. (in^3)

Next two characters.

GN	Grain
PT	Port

Next character(s)

A	Aft
C or CL	Closure
CH	Insulation liner closure hole
CY or Y	Cylinder
E	Ellipsoid
F	Forward
H	Insulation liner hole
PD	Propellent displaced
PP	Propellent
NS	Nozzle submergence
NZ	Nozzle

EQUATIONS, FIRST ENTRANCE:

GENERAL GRAIN AND BASIC PORT COMPUTATIONS:

Diameter of cylindrical grain section. (Figures 2, 6)

$$D_{GN} = D_{IL_1} \tag{1}$$

Diameter of basic cylindrical port section. (Figures 2, 3, 4, 6)

$$D_{PT} = K_{DPT_1} D_{GN} + K_{DPT_2} \tag{2}$$

Cross-sectional area of basic cylindrical port section. (Figure 6)

$$A_{PT} = \left(\frac{\pi}{4}\right) D_{PT}^2 \tag{3}$$

Area ratio, basic cylindrical port section area to nozzle throat area.

$$R_{APTTH} = \frac{A_{PT}}{A_{NZ_{TH}}} \tag{4}$$

Propellent web thickness for cylindrical grain and basic cylindrical port sections. (Figures 2, 3, 6)

$$T_{PP_{WEB}} = \left(\frac{D_{GN} - D_{PT}}{2}\right) \tag{5}$$

Propellent web cross-sectional area for cylindrical grain and basic cylindrical port sections. (Figure 6)

$$A_{PP_{WEB}} = \left(\frac{\pi}{4}\right) \left(D_{GN}^2 - D_{PT}^2\right) \tag{6}$$

BASIC CLOSURE SECTIONS (FORWARD AND AFT):

Equatorial diameter of grain closures. (Figures 2, 3, 4)

$$D_{GN_{CL}} = D_{GN} \tag{7}$$

EQUATIONS, FIRST ENTRANCE (Cont.):

BASIC CLOSURE SECTIONS (FORWARD AND AFT)(Cont.):

Diameter ratio, basic cylindrical port section diameter to grain closure equatorial diameter.

$$R_{DPTCL} = \frac{D_{PT}}{D_{GN_{CL}}} \tag{8}$$

BASIC FORWARD CLOSURE SECTION:

Head ratio of ellipsoid associated with the forward grain closure section.

$$R_{DGNCLF} = R_{DILCFI} \tag{9}$$

Length of hemi-ellipsoid associated with the forward grain closure section. (Figures 2, 3)

$$L_{GN_{CLF}} = L_{IL_{CLFI}} \tag{10}$$

Volume of hemi-ellipsoid associated with the forward grain closure section. (Figure 3)

$$V_{GN_{CLF}} = \left(\frac{\pi}{6}\right) L_{GN_{CLF}} D^2_{GN_{CL}} \tag{11}$$

Length of cylindrical portion of basic port within the hemi-ellipsoid associated with the forward grain closure section. (Figure 3)

$$L_{PT_{YCLF}} = L_{GN_{CLF}} \sqrt{1 - R^2_{DPTCL}} \tag{12}$$

Volume of cylindrical portion of basic port within the hemi-ellipsoid associated with the forward grain closure section. (Figure 3)

$$V_{PT_{YCLF}} = \left(\frac{\pi}{4}\right) L_{PT_{YCLF}} D^2_{PT} \tag{13}$$

EQUATIONS, FIRST ENTRANCE (Cont.):

BASIC FORWARD CLOSURE SECTION (Cont.):

Length ratio. Length of cylindrical portion of basic port within the hemi-ellipsoid to the length of the hemi-ellipsoid, forward grain closure section.

$$R_{LPTCYF} = \frac{L_{PT_{YCLF}}}{L_{GN_{CLF}}} \tag{14}$$

Volume of ellipsoidal cap at base of cylindrical portion of basic port section, within the hemi-ellipsoid associated with the forward grain closure section. (Figure 3)

$$V_{PT_{ECLF}} = \left(\frac{V_{GN_{CLF}}}{2}\right)\left(2 - 3\,R_{LPTCYF} + R^3_{LPTCYF}\right) \tag{15}$$

Volume of basic port within the hemi-ellipsoid associated with the forward grain closure section. (Figure 3)

$$V_{PT_{CLF}} = V_{PT_{ECLF}} + V_{PT_{YCLF}} \tag{16}$$

Volume of propellent associated with the hemi-ellipsoid of the forward grain closure section. Note that this volume is an intermediate quantity and does not include corrections for insulation wedges, igniter, etc. (Figure 3)

$$V_{PP_{CLF}} = V_{GN_{CLF}} - V_{PT_{CLF}} \tag{17}$$

Length of hemi-ellipsoid frustum associated with the forward grain closure section. (Figures 2, 3)

$$L_{GN_{CHF}} = L_{IL_{CHFI}} \tag{18}$$

Diameter of forward base of hemi-ellipsoid frustum associated with the forward grain closure section. (Figures 2, 3)

$$D_{GN_{HF}} = D_{IL_{HFI}} \tag{19}$$

EQUATIONS, FIRST ENTRANCE (Cont.):

BASIC FORWARD CLOSURE SECTION (Cont.):

Length ratio. Length of hemi-ellipsoidal frustum to length of hemi-ellipsoid, forward grain closure section.

$$R_{LGNCHF} = \frac{L_{GN_{CHF}}}{L_{GN_{CLF}}} \tag{20}$$

Volume of hemi-ellipsoid frustum associated with the forward grain closure section. (Figure 3)

$$V_{GN_{CHF}} = \left(\frac{V_{GN_{CLF}}}{2}\right)\left(3\,R_{LGNCHF} - R^3_{LGNCHF}\right) \tag{21}$$

BASIC AFT CLOSURE SECTION:

Head ratio of ellipsoid associated with the aft grain closure section.

$$R_{DGNCLA} = R_{DILCAI} \tag{22}$$

Length of hemi-ellipsoid associated with the aft grain closure section. (Figures 2, 4)

$$L_{GN_{CLA}} = L_{IL_{CLAI}} \tag{23}$$

Volume of hemi-ellipsoid associated with the aft grain closure section. (Figure 5)

$$V_{GN_{CLA}} = \left(\frac{\pi}{6}\right) L_{GN_{CLA}}\, D^2_{GN_{CL}} \tag{24}$$

Length of cylindrical portion of basic port within the hemi-ellipsoid associated with the aft grain closure section. (Figure 4)

$$L_{PT_{YCLA}} = L_{GN_{CLA}} \sqrt{1 - R^2_{DPTCL}} \tag{25}$$

EQUATIONS, FIRST ENTRANCE (Cont.):

BASIC AFT CLOSURE SECTION (Cont.):

Volume of cylindrical portion of basic port within the hemi-ellipsoid associated with the aft grain closure section. (Figure 5)

$$V_{PT_{YCLA}} = \left(\frac{\pi}{4}\right) L_{PT_{YCLA}} D_{PT}^{2} \tag{26}$$

Length ratio. Length of cylindrical portion of basic port within the hemi-ellipsoid to the length of the hemi-ellipsoid, aft grain closure section.

$$R_{LPTCYA} = \frac{L_{PT_{YCLA}}}{L_{GN_{CLA}}} \tag{27}$$

Volume of ellipsoidal cap at base of cylindrical portion of basic port section within the hemi-ellipsoid associated with the aft grain closure section. (Figure 5)

$$V_{PT_{ECLA}} = \left(\frac{V_{GN_{CLA}}}{2}\right) \left(2 - 3\,R_{LPTCYA} + R_{LPTCYA}^{3}\right) \tag{28}$$

Volume of basic port within the hemi-ellipsoid associated with the aft grain closure section. (Figure 5)

$$V_{PT_{CLA}} = V_{PT_{ECLA}} + V_{PT_{YCLA}} \tag{29}$$

Volume of propellent associated with the hemi-ellipsoid of the aft grain closure section. Note that this volume is an intermediate quantity and does not include corrections for nozzle submergence, insulation wedges, etc. (Figure 5)

$$V_{PP_{CLA}} = V_{GN_{CLA}} - V_{PT_{CLA}} \tag{30}$$

Length of hemi-ellipsoid frustum associated with the aft grain closure section. (Figures 2, 4)

$$L_{GN_{CHA}} = L_{IL_{CHAI}} \tag{31}$$

EQUATIONS, FIRST ENTRANCE (Cont.):

BASIC AFT CLOSURE SECTION (Cont.):

Diameter of aft base of hemi-ellipsoid frustum associated with the aft grain closure section. (Figures 2, 4)

$$D_{GN_{HA}} = D_{IL_{HAI}} \tag{32}$$

Length ratio. Length of hemi-ellipsoid frustum to length of hemi-ellipsoid, aft grain closure section.

$$R_{LGNCHA} = \frac{L_{GN_{CHA}}}{L_{GN_{CLA}}} \tag{33}$$

Volume of hemi-ellipsoid frustum associated with the aft grain closure section. (Figure 5)

$$V_{GN_{CHA}} = \left(\frac{V_{GN_{CLA}}}{2}\right)\left(3\,R_{LGNCHA} - R^3_{LGNCHA}\right) \tag{34}$$

BASIC CYLINDRICAL GRAIN SECTION:

Volume of propellent within basic cylindrical grain section. Does not include displaced propellent corrections for nozzle submergence or internal insulation.

$$V_{PP_{CY1}} = V_{PP_{MT}} - V_{PP_{CLF}} - V_{PP_{CLA}} \tag{35}$$

Length of basic cylindrical grain section. Does not include length penalties for nozzle submergence, slots, joints, or internal insulation. (Figure 2)

$$L_{GN_{CY1}} = \frac{V_{PP_{CY1}}}{A_{PP_{WEB}}} \tag{36}$$

Length of diameter ratio, basic cylindrical grain section. Does not include penalties for nozzle submergence, slots, joints, or internal insulation.

$$R_{LDGNY1} = \frac{L_{GN_{CY1}}}{D_{GN}} \tag{37}$$

EQUATIONS, FIRST ENTRANCE (Cont.):

BASIC CYLINDRICAL PORT SECTION:

Total length of cylindrical portion of basic port. Does not include adjustments for nozzle submergence, slots, joints or internal insulation.

$$L_{PT_{CY1}} = L_{GN_{CY1}} + L_{PT_{YCLA}} + L_{PT_{YCLF}} \tag{38}$$

CORRECTIONS TO BASIC GRAIN FOR NOZZLE SUBMERGENCE:

Distance nozzle is submerged in port. (Figure 4)

$$L_{PT_{NS}} = L_{NZ_B} - L_{1L_{HA}} - L_{CS_{HA}} \tag{39}$$

Distance nozzle is submerged in cylindrical grain section. (Figure 4)

$$L_{GN_{NSCY}} = L_{PT_{NS}} - L_{GN_{CHA}} \tag{40}$$

Diameter ratio, port cone frustum section aft base diameter to grain closure equatorial diameter.

$$R_{DCFACL} = \frac{D_{PT_{CFA}}}{D_{GN_{CL}}} \tag{41}$$

Length of portion of port cone frustum section within aft grain closure section. (Figures 2, 4)

$$L_{PT_{CFCA}} = L_{GN_{CLA}} \sqrt{1 - R^2_{DCFACL}} \tag{42}$$

Submerged nozzle inlet allowance. (Figure 4)

$$L_{PT_{NZI}} = L_{PT_{CFHA}} - L_{PT_{NS}} \tag{43}$$

Length of portion of port cone frustum section within cylindrical grain section. (Figures 2, 4)

$$L_{PT_{CFCY}} = L_{GN_{NSCY}} + L_{PT_{NZI}} \tag{44}$$

EQUATIONS, FIRST ENTRANCE (Cont.):

CORRECTIONS TO BASIC GRAIN FOR NOZZLE SUBMERGENCE (Cont.):

Total length of port cone frustum section. (Figures 2, 4, 6)

$$L_{PT_{CF}} = L_{PT_{CFCY}} + L_{PT_{CFCA}} \tag{45}$$

Half-angle of port cone frustum section. (Figure 2)

$$\theta_{CF} = \arctan\left(\frac{D_{PT_{CFA}} - D_{PT_{CFF}}}{2\,L_{PT_{CF}}}\right) \tag{46}$$

Slant height of port cone frustum section. (Figure 4)

$$L_{PT_{CFS}} = \left(\frac{1}{2}\right)\sqrt{4\,L^2_{PT_{CF}} + \left(D_{PT_{CFA}} - D_{PT_{CFF}}\right)^2} \tag{47}$$

Total volume of port cone frustum section. (Figure 5)

$$V_{PT_{CF}} = \left(\frac{\pi}{12}\right) L_{PT_{CF}} \left(D^2_{PT_{CFA}} + D^2_{PT_{CFF}} + D_{PT_{CFA}}\,D_{PT_{CFF}}\right) \tag{48}$$

Length ratio, length of portion of port cone frustum section within aft grain closure section to length of aft grain closure section. (Figure 4)

$$R_{LCFCA} = \frac{L_{PT_{CFCA}}}{L_{GN_{CLA}}} \tag{49}$$

Volume of ellipsoidal cap at aft base of port cone frustum section within aft grain closure section. (Figure 5)

$$V_{PT_{ECFA}} = \left(\frac{V_{GN_{CLA}}}{2}\right)\left(2 - 3\,R_{LCFCA} + R^3_{LCFCA}\right) \tag{50}$$

Volume of basic port portion of port cone frustum section within cylindrical grain section. (Figure 5)

$$V_{PT_{CFCY}} = \left(\frac{\pi}{4}\right) L_{PT_{CFCY}}\,D^2_{PT} \tag{51}$$

EQUATIONS, FIRST ENTRANCE (Cont.):

CORRECTIONS TO BASIC GRAIN FOR NOZZLE SUBMERGENCE (Cont.):

Volume of basic port section associated with nozzle submergence. (Figure 5)

$$V_{PT_{CYCF}} = V_{PT_{CFCY}} + V_{PT_{CLA}} \tag{52}$$

Volume of propellent displaced due to nozzle submergence. (Figure 5)

$$V_{PP_{PDNS}} = V_{PT_{CF}} + V_{PT_{ECFA}} - V_{PT_{CYCF}} \tag{53}$$

Cylindrical grain length penalty required for propellent displaced by nozzle submergence. (Figure 2)

$$L_{GN_{PDNS}} = K_{GN_1} \left(\frac{V_{PP_{PDNS}}}{A_{PP_{WEB}}} \right) + K_{GN_2} \tag{54}$$

Adjusted length of cylindrical grain section, includes nozzle submergence penalty. (Figure 2)

$$L_{GN_{CY2}} = L_{GN_{CY1}} + L_{GN_{PDNS}} \tag{55}$$

Length to diameter ratio, cylindrical grain section. Includes nozzle submergence penalty.

$$R_{LDGNY2} = \frac{L_{GN_{CY2}}}{D_{GN}} \tag{56}$$

Adjusted length of cylindrical port section. Includes nozzle submergence penalty. (Figure 6)

$$L_{PT_{CY2}} = L_{PT_{CY1}} - L_{PT_{YCLA}} - L_{PT_{CFCY}} + L_{GN_{PDNS}} \tag{57}$$

PROPELLENT BURNING SURFACE:

Port surface area component, lateral cylindrical port propellent surface area. (Figure 6)

$$S_{PT_{CY2}} = \pi D_{PT} L_{PT_{CY2}} \tag{58}$$

EQUATIONS, FIRST ENTRANCE (Cont.):

PROPELLENT BURNING SURFACE (Cont.):

Port surface area component, lateral cone frustum port propellent surface area. (Figure 6)

$$S_{PT_{CFS}} = \left(\frac{\pi}{2}\right) L_{PT_{CFS}} \left(D_{PT_{CFF}} + D_{PT_{CFA}}\right) \tag{59}$$

Port surface area component, forward base of port cone frustum propellent surface area. (Figure 6)

$$S_{PT_{CFB}} = \left(\frac{\pi}{4}\right) \left(D^2_{PT_{CFF}} - D^2_{PT}\right) \tag{60}$$

Propellent surface area associated with the port. Includes submerged nozzle corrections.

$$S_{PT_2} = S_{PT_{CY2}} + S_{PT_{CFS}} + S_{PT_{CFB}} \tag{61}$$

Initial propellent burning surface area, excluding slots. (Figure 6)

$$S_{BS_{PT}} = S_{PT_2} \tag{62}$$

EQUATIONS, SECOND ENTRANCE:

CORRECTIONS TO GRAIN FOR SLOTS AND JOINTS:

Cylindrical grain section length penalty for slots. (Figure 2)

$$L_{GN_{SL}} = K_{GN_3} L_{SL_{GN}} + K_{GN_4} \tag{63}$$

Adjusted length of cylindrical grain section, includes nozzle submergence and slot penalties. (Figure 2)

$$L_{GN_{CY3}} = L_{GN_{CY2}} + L_{GN_{SL}} \tag{64}$$

EQUATIONS, SECOND ENTRANCE (Cont.):

CORRECTIONS TO GRAIN FOR SLOTS AND JOINTS (Cont.):

Length to diameter ratio, cylindrical grain section. Includes nozzle submergence and slot penalties.

$$R_{LDGNY3} = \frac{L_{GN_{CY3}}}{D_{GN}} \tag{65}$$

Adjusted length of cylindrical grain section, includes nozzle submergence, slot and joint penalties. (Figure 2)

$$L_{GN_{CY4}} = L_{GN_{CY3}} + L_{JT_{CUT}} \tag{66}$$

Length to diameter ratio, cylindrical grain section. Includes nozzle submergence, slot and joint penalties.

$$R_{LDGNY4} = \frac{L_{GN_{CY4}}}{D_{GN}} \tag{67}$$

EQUATIONS, THIRD ENTRANCE:

CORRECTIONS TO GRAIN FOR INTERNAL INSULATION:

Cylindrical grain length penalty for propellent displaced by internal insulation. (Figure 2)

$$L_{GN_{PDIN}} = K_{GN_5}\left(\frac{V_{IN_{PD}}}{A_{PP_{WEB}}}\right) + K_{GN_6} \tag{68}$$

Adjusted length of cylindrical grain section, includes nozzle submergence, slot, joint, and internal insulation penalties. (Figure 2)

$$L_{GN_{CY5}} = L_{GN_{CY4}} + L_{GN_{PDIN}} \tag{69}$$

Length to diameter ratio, cylindrical grain section. Includes nozzle submergence, slot, joints, and internal insulation penalties.

$$R_{LDGNY5} = \frac{L_{GN_{CY5}}}{D_{GN}} \tag{70}$$

EQUATIONS, THIRD ENTRANCE (Cont.):

TOTAL GRAIN GEOMETRY:

Length of cylindrical grain section. Includes nozzle submergence, slot, joint and internal insulation penalties. (Figure 2)

$$L_{GN_{CY}} = K_{GN_7} L_{GN_{CY5}} + K_{GN_8} \quad (71)$$

Length to diameter ratio, cylindrical grain section. Includes nozzle submergence, slot, joint and internal insulation penalties.

$$R_{LDGNCY} = \frac{L_{GN_{CY}}}{D_{GN}} \quad (72)$$

Volume of cylindrical grain section. Includes port, submerged nozzle penalty, slots, joints and internal insulation except liner.

$$V_{GN_{CY}} = \left(\frac{\pi}{4}\right) L_{GN_{CY}} D_{GN}^2 \quad (73)$$

Volume of grain envelope. Includes port, submerged nozzle penalty, slots, joints and all internal insulation except liner. Note that the grain closures are hemi-ellipsoid frustums, not hemi-ellipsoids.

$$V_{GN} = V_{GN_{CY}} + V_{GN_{CHF}} + V_{GN_{CHA}} \quad (74)$$

Length of grain envelope. Includes nozzle submergence, slot, joint and internal insulation penalties. (Figure 2)

$$L_{GN} = L_{GN_{CY}} + L_{GN_{CHF}} + L_{GN_{CHA}} \quad (75)$$

ASSOCIATIVE QUANTITIES:

The following associative quantities are intended solely for optional utilization by the program user. Their primary usage is for optional inter-model coupling and for forming constraint quantities.

$$Q_{DCFA1} = K_{QDCFA1} D_{PT_{CFA}} \quad (76)$$

EQUATIONS, THIRD ENTRANCE (Cont.):

ASSOCIATIVE QUANTITIES (Cont.):

$$Q_{DCFA2} = K_{QDCFA2} \, D_{PT_{CFA}} \tag{77}$$

$$Q_{DCFA3} = K_{QDCFA3} \, D_{PT_{CFA}} \tag{78}$$

$$Q_{DCFF1} = K_{QDCFF1} \, D_{PT_{CFF}} \tag{79}$$

$$Q_{DCFF2} = K_{QDCFF2} \, D_{PT_{CFF}} \tag{80}$$

$$Q_{DCFF3} = K_{QDCFF3} \, D_{PT_{CFF}} \tag{81}$$

$$Q_{DGN1} = K_{QDGN1} \, D_{GN} \tag{82}$$

$$Q_{DGN2} = K_{QDGN2} \, D_{GN} \tag{83}$$

$$Q_{DGN3} = K_{QDGN3} \, D_{GN} \tag{84}$$

$$Q_{DPT1} = K_{QDPT1} \, D_{PT} \tag{85}$$

$$Q_{DPT2} = K_{QDPT2} \, D_{PT} \tag{86}$$

$$Q_{DPT3} = K_{QDPT3} \, D_{PT} \tag{87}$$

$$Q_{RAPTH1} = K_{QRAPH1} \, R_{APTTH} \tag{88}$$

$$Q_{RAPTH2} = K_{QRAPH2} \, R_{APTTH} \tag{89}$$

$$Q_{RAPTH3} = K_{QRAPH3} \, R_{APTTH} \tag{90}$$

OPTIMIZATION CONSIDERATIONS:

Generally, the nature of the problem which would require usage of this model would also require that the following variables and constraints be set up by the program user.

Variables.

Suggested nominal values for initial estimates of the variable values and bounds are included for each optimization variable listed below. These values are only guidelines, applicable to a very wide class of problems, and values corresponding to the specific application (quantities within parenthesis) should be used if they are easily available.

KDPT1 — Port fraction. The following values will insure that a propellent web is always defined.

Upper bound: 0.9
Lower bound: 0.1
Initial estimate: 0.2

DPTCFF — Diameter of forward base of port cone frustum section. (Figures 2, 4)

Upper bound: 500. (approximate case diameter)
Lower bound: 5.
Initial estimate: approximate port diameter

DPTCFA — Diameter of aft base of port cone frustum section. (Figures 2, 4)

Upper bound: 500. (approximate case diameter)
Lower bound: 5.
Initial estimate: approximate port diameter

LPTCFHA — Distance from forward base of port cone frustum section to aft base of grain envelope. (Figure 2)

Upper bound: approximate length of case
Lower bound: zero
Initial estimate: approximate length nozzle is buried within case

Constraints.

The following set of inequality constraints are formulated such that the motor volumetric loading efficiency (see MOTORG model type) will be maximum if a minimum vehicle length (fixed diameter) objective function is being utilized. For other objective functions, some of these constraints may require implementation as equality constraints.

OPTIMIZATION CONSIDERATIONS (Cont.):

Constraints 91 through 96 are required for "shaping" the port cone frustum grain cutout utilized for submerged nozzle geometry. It should be noted that these constraints should always be set up, even if the nozzle is not submerged.

The forward base diameter of the port cone frustum section is greater than, or equal to, the port diameter. (Figures 2, 4)

$$D_{PT_{CFF}} \geq D_{PT} \tag{91}$$

The aft base diameter of the port cone frustum section is less than, or equal to, the grain diameter. (Figures 2, 4)

$$D_{PT_{CFA}} \leq D_{GN} \tag{92}$$

The aft base diameter of the port cone frustum section is greater than, or equal to, the forward base diameter of the port cone frustum section. (Figures 2, 4)

$$D_{PT_{CFA}} \geq D_{PT_{CFF}} \tag{93}$$

The aft base diameter of the port cone frustum section is greater than, or equal to, the diameter of the hole in the aft closure required for the nozzle. (Figures 2, 4)

$$D_{PT_{CFA}} \geq D_{GN_{HA}} \tag{94}$$

Nozzle inlet allowance. Sufficient space must be provided forward of the nozzle inlet to allow flow from the port cone frustum section to the nozzle entrance. QDNZENT and QDNZTH are associative quantities which must be set up, by the program user, in the nozzle geometry model. (Figure 4)

$$L_{PT_{NZI}} \geq \text{QDNZENT} \tag{95}$$

$$D_{PT_{CFF}} \geq \text{QDNZTH} \tag{96}$$

The cylindrical grain section length must be greater than, or equal to, zero for valid closure geometry. (Figure 2)

$$L_{GN_{CY}} \geq 0 \tag{97}$$

OPTIMIZATION CONSIDERATIONS (Cont.):

The nozzle entrance must be within the port. (Figure 4)

$$L_{PT_{CFHA}} \leq L_{GN} \tag{98}$$

$$L_{PT_{NS}} \geq 0 \tag{99}$$

Considerations of structural integrity of the grain and acceptable internal ballistics limit feasible values of the port fraction.

$$K_{DPT1} \geq 0.2 \tag{100}$$

To avoid unacceptable nozzle erosion, a lower bound in placed upon the ratio of the cylindrical port section cross section area to the nozzle throat area. (Note that this constraint corresponds to a lower limit of port fraction.)

$$RAPTTH \geq 1.15 \tag{101}$$

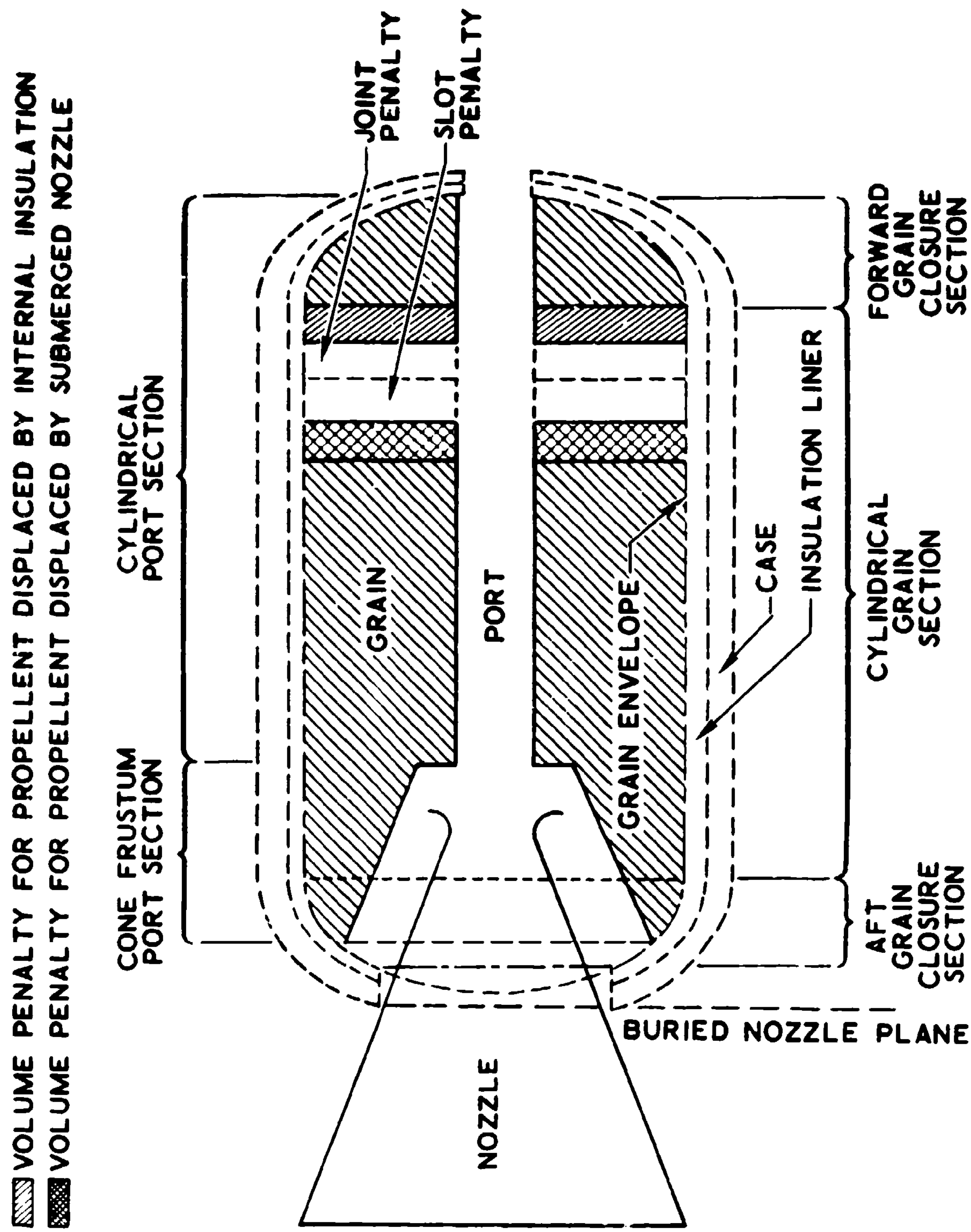

Fig. 40.1-1 Basic Grain Geometry Components

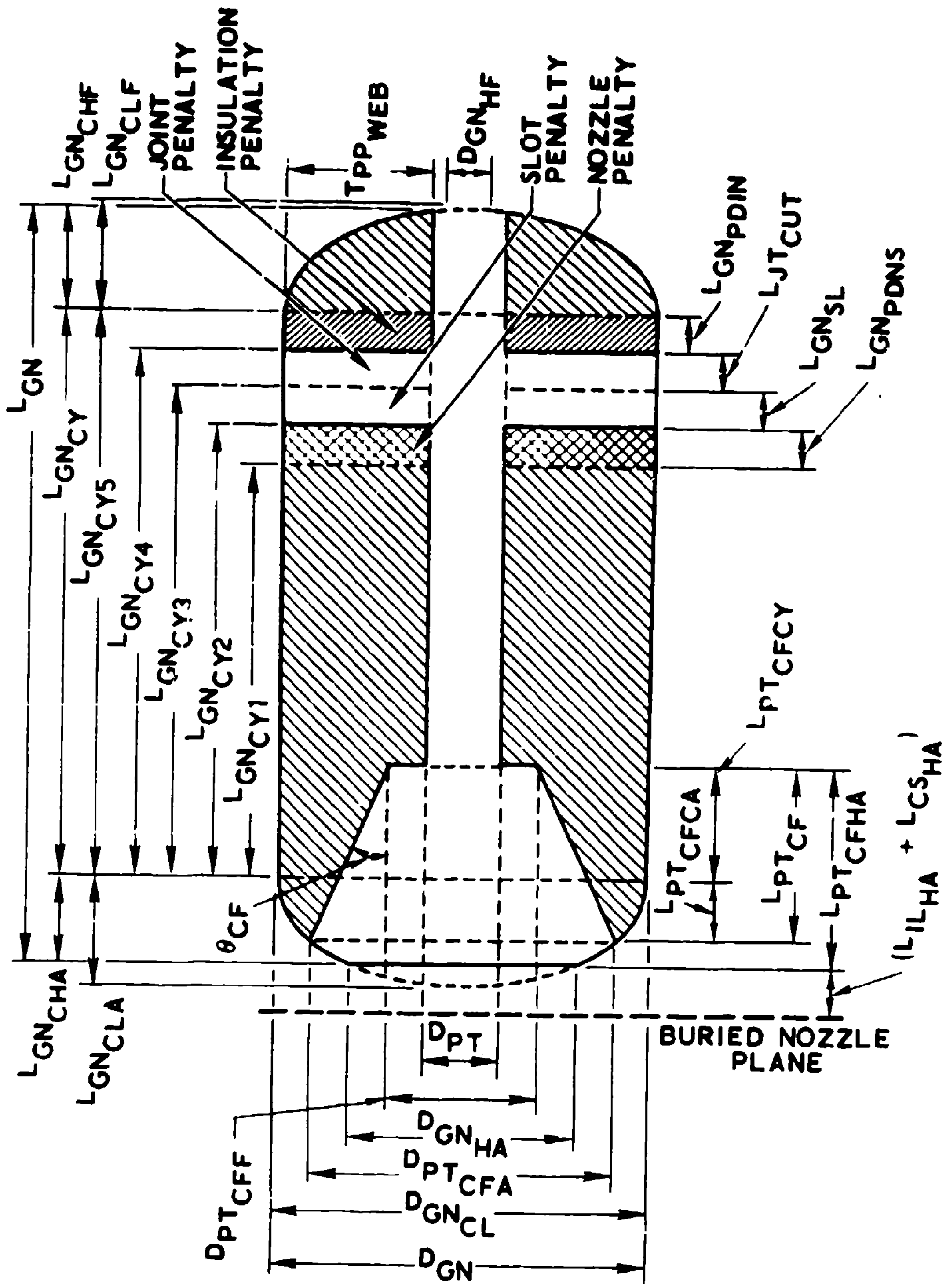

Fig. 40.1-2 Total Grain Geometry

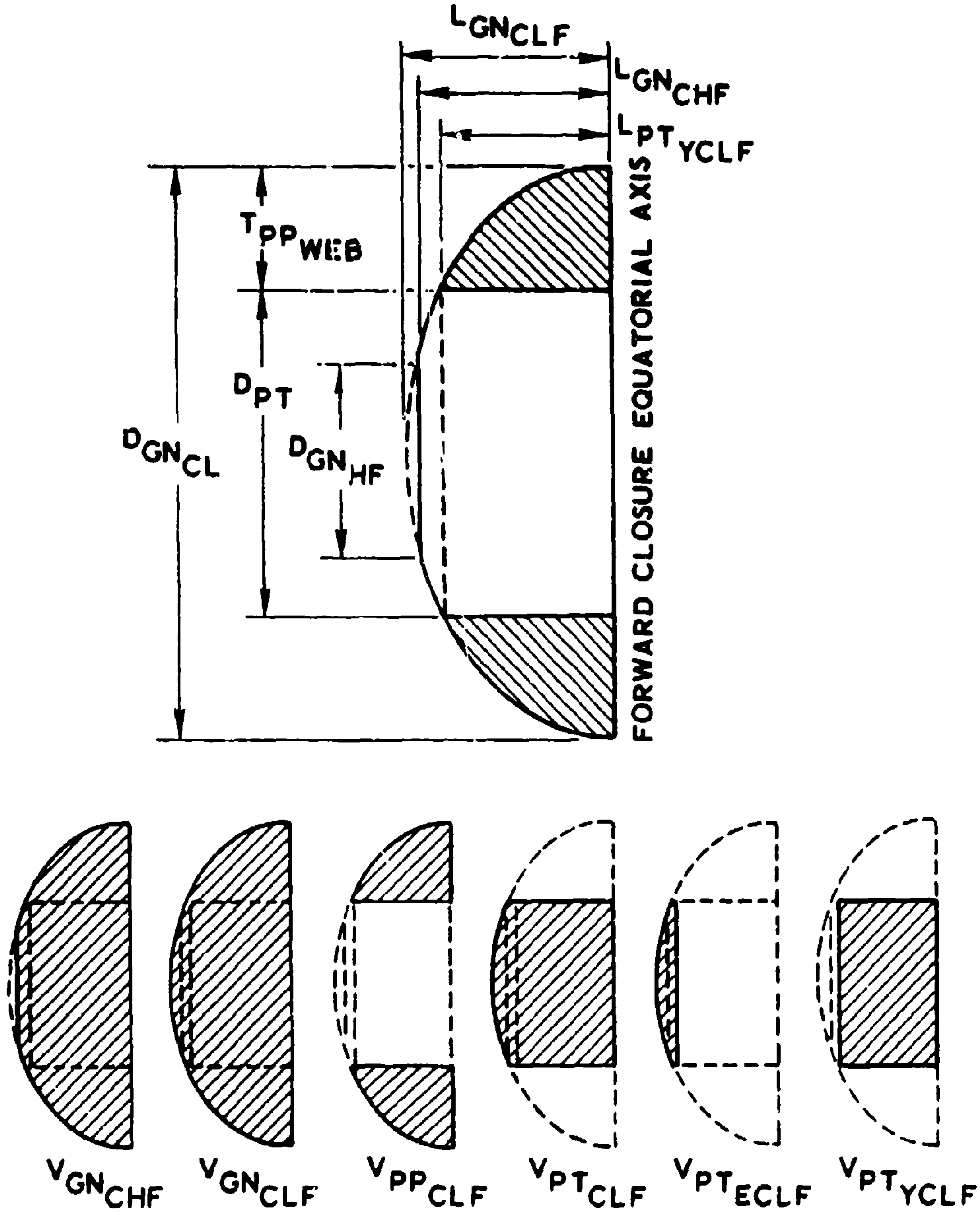

Fig. 40.1-3 Forward Grain Closure Geometry

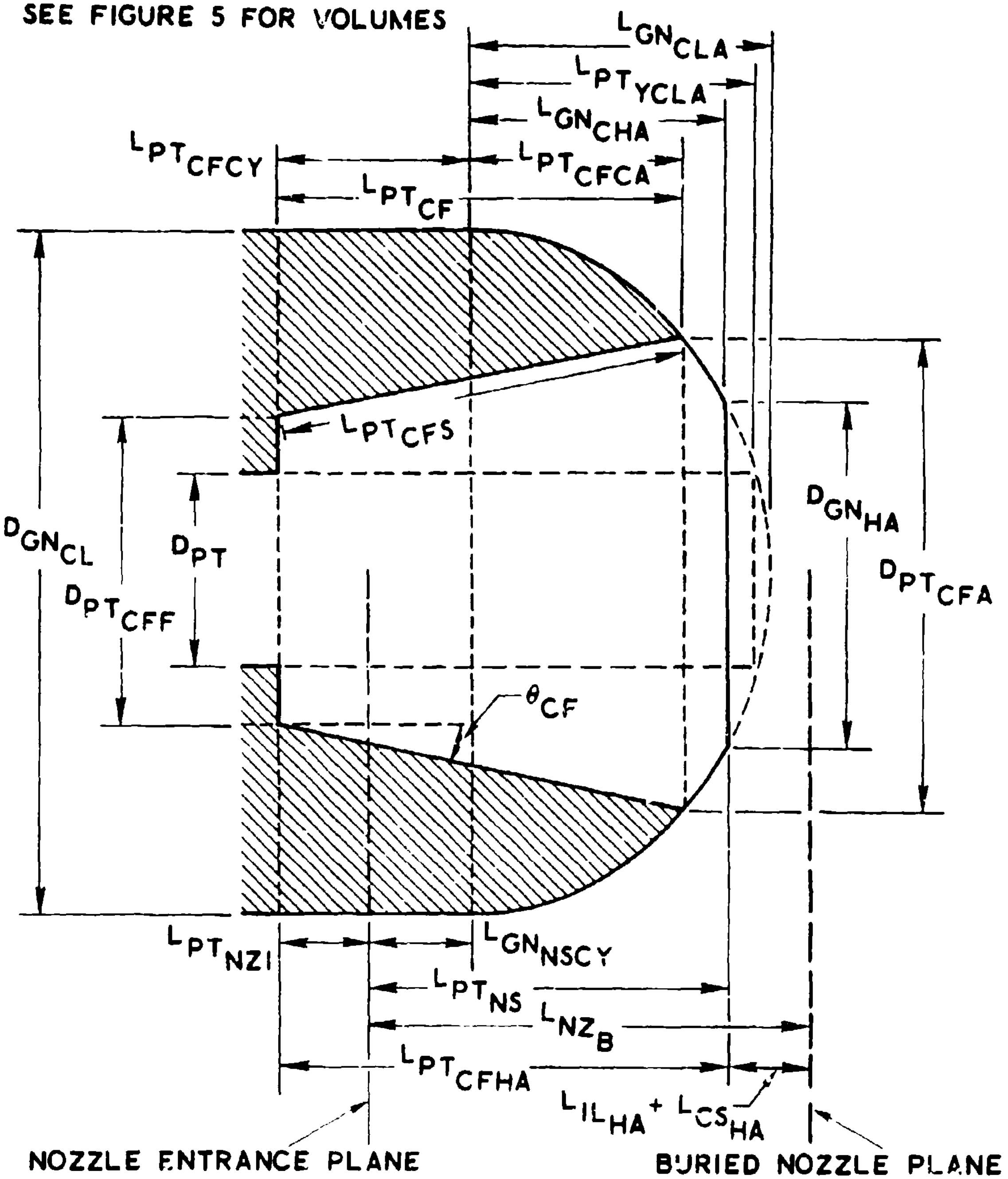

Fig. 40.1-4 Aft Grain Closure and Nozzle Submergence Geometry

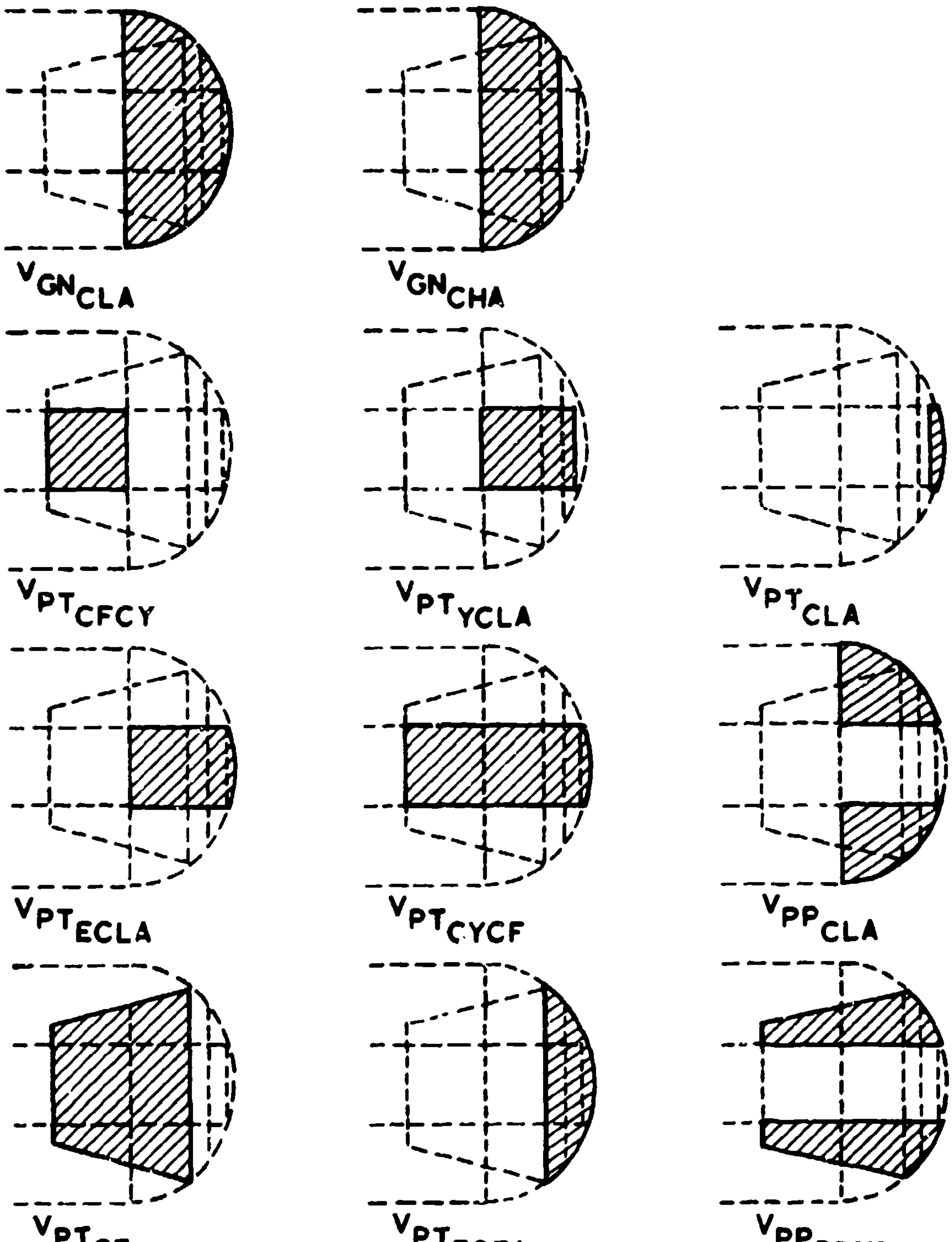

Fig. 40.1-5 Aft Grain Closure and Nozzle Submergence Volumes

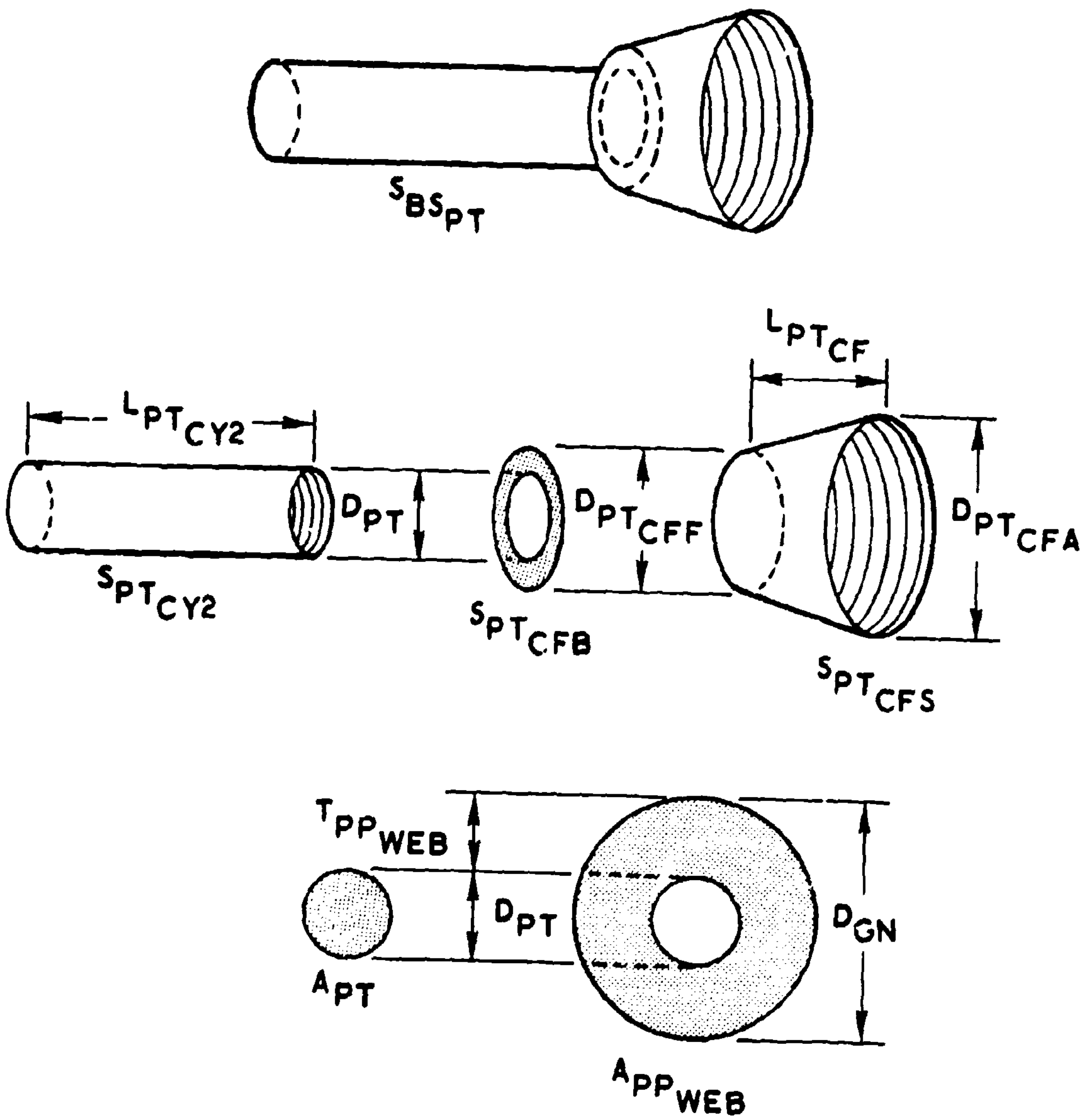

Fig. 40.1-6 Surface and Cross-sectional Areas

INPUT DATA, INTRA-MODEL:

The following data is input directly to this model by the program user. If a value is not input, the preset value is used.

Due to the nature of this model, many of the following required user inputs will be optimization variables. See the "Optimization Considerations" section.

Mnemonic	Symbol	Description; Ext. (Int.) Units		Preset
DPTCFA	$D_{PT_{CFA}}$	Diameter of aft base of port cone frustum section;		
		in	Figs. 2, 4, 6	0
DPTCFF	$D_{PT_{CFF}}$	Diameter of forward base of port cone frustum section;		
		in	Figs. 2, 4, 6	0
KDPT1	K_{DPT_1}	Coefficient relating the diameter of the cylindrical section of the port to the diameter of the cylindrical grain section. See DPT computation, equation 2.		
		N. D.		0
KDPT2	K_{DPT_2}	Bias for DPT computation;		
		in		0
LJTCUT	$L_{JT_{CUT}}$	Total length of cutout, within the cylindrical grain section, for joints. Does not include slot lengths if a slot is being utilized as a joint;		
		in	Fig. 2	0
LPTCFHA	$L_{PT_{CFHA}}$	Distance from forward base of the port cone frustum section to the aft base of the hemi-ellipsoid frustum associated with the aft grain closure section;		
		in	Figs. 2, 4	0

INPUT DATA, INTRA-MODEL (Cont.):

The following coefficient and bias quantities are made available for input. However, in normal applications, the preset values are used for most, if not all, of these quantities. Note that these coefficient quantities are preset (1) and the bias quantities are preset (0).

Mnemonic	Symbol	Description; Ext. (Int.) Units	Preset
KGN1	K_{GN_1}	Coefficient for LGNPDNS computation; N. D.	1
KGN2	K_{GN_2}	Bias for LGNPDNS computation; in	0
KGN3	K_{GN_3}	Coefficient for LGNSL computation; N. D.	1
KGN4	K_{GN_4}	Bias for LGNSL computation; in	0
KGN5	K_{GN_5}	Coefficient for LGNPDIN computation; N. D.	1
KGN6	K_{GN_6}	Bias for LGNPDIN computation; in	0
KGN7	K_{GN_7}	Coefficient for LGNCY computation; N. D.	1
KGN8	K_{GN_8}	Bias for LGNCY computation; in	0

The following associative quantity coefficients are intended solely for optional utilization by the program user. Their primary usage is for optional inter-model coupling and for forming constraint quantities. Note that all associative quantity coefficients are preset (0).

KQDCFA1	K_{QDCFA1}	Associative quantity coefficient for QDCFA1 computation; N. D.	0

INPUT DATA, INTRA-MODEL (Cont.):

Mnemonic	Symbol	Description; Ext. (Int.) Units	Preset
KQDCFA2	K_{QDCFA2}	Associative quantity coefficient for QDCFA2 computation; N. D.	0
KQDCFA3	K_{QDCFA3}	Associative quantity coefficient for QDCFA3 computation; N. D.	0
KQDCFF1	K_{QDCFF1}	Associative quantity coefficient for QDCFF1 computation; N. D.	0
KQDCFF2	K_{QDCFF2}	Associative quantity coefficient for QDCFF2 computation; N.D.	0
KQDCFF3	K_{QDCFF3}	Associative quantity coefficient for QDCFF3 computation; N. D.	0
KQDGN1	K_{QDGN1}	Associative quantity coefficient for QDGN1 computation; N. D.	0
KQDGN2	K_{QDGN2}	Associative quantity coefficient for QDGN2 computation; N. D.	0
KQDGN3	K_{QDGN3}	Associative quantity coefficient for QDGN3 computation; N. D.	0
KQDPT1	K_{QDPT1}	Associative quantity coefficient for QDPT1 computation; N. D.	0
KQDPT2	K_{QDPT2}	Associative quantity coefficient for QDPT2 computation; N. D.	0

INPUT DATA, INTRA-MODEL (Cont.):

Mnemonic	Symbol	Description; Ext. (Int.) Units	Preset
KQDPT3	K_{QDPT3}	Associative quantity coefficient for QDPT3 computation; N. D.	0
KQRAPH1	K_{QRAPH1}	Associative quantity coefficient for QRAPTH3 computation; N. D.	0
KQRAPH2	K_{QRAPH2}	Associative quantity coefficient for QRAPTH2 computation; N. D.	0
KQRAPH3	K_{QRAPH3}	Associative quantity coefficient for QRAPTH3 computation; N. D.	0

INPUT DATA, INTER-MODEL:

This model requires as input certain data which is usually output from a model of the specified model type. If the user has not specified such a source for this data, then it must be input directly with the intra-model input.

Mnemonic	Symbol	Description; Ext. (Int.) Units	Model Type
ANZTH	$A_{NZ_{TH}}$	Nozzle throat area; in^2	NOZZLEG
DILHAI	$D_{IL_{HAI}}$	Diameter of circular hole, for the nozzle, within the inside surface of the insulation liner associated with the aft closure section; in	INSULG
DILHFI	$D_{IL_{HFI}}$	Diameter of circular hole, for the igniter, within the inside surface of the insulation liner associated with the forward closure section; in	INSULG

INPUT DATA, INTER-MODEL (Cont.):

Mnemonic	Symbol	Description; Ext. (Int.) Units		Model Type
DILI	D_{IL_I}	Inside diameter of the insulation liner within the case cylindrical section;		
		in		INSULG
LCSHA	$L_{CS_{HA}}$	Length of hole, for the nozzle, within the case associated with the aft case closure section;		
		in	Figs. 2, 4	CASEG
LILCHAI	$L_{IL_{CHAI}}$	Length of hemi-ellipsoid frustum associated with the inside surface of the insulation liner within the aft case closure;		
		in		INSULG
LILCHFI	$L_{IL_{CHFI}}$	Length of hemi-ellipsoid frustum associated with the inside surface of the insulation liner within the forward case closure section;		
		in		INSULG
LILCLAI	$L_{IL_{CLAI}}$	Length of the hemi-ellipsoid associated with the inside surface of the insulation liner within the aft case closure section;		
		in		INSULG
LILCLFI	$L_{IL_{CLFI}}$	Length of the hemi-ellipsoid associated with the inside surface of the insulation liner within the forward case closure section;		
		in		INSULG
LILHA	$L_{IL_{HA}}$	Length of the hole, for the nozzle, within the insulation liner associated with the aft case closure section;		
		in	Figs. 2, 4	INSULG
LNZB	L_{NZ_B}	Distance nozzle is buried within the case;		
		in	Fig. 4	NOZZLEG

INPUT DATA, INTER-MODEL (Cont.):

Mnemonic	Symbol	Description; Ext. (Int.) Units	Model Type
LSLGN	$L_{SL_{GN}}$	Total slot length; in	IBFLOW
RDILCAI	R_{DILCAI}	Head ratio, inside surface of insulation liner associated with the aft case closure section; N. D.	INSULG
RDILCFI	R_{DILCFI}	Head ratio, inside surface of insulation liner associated with the forward case closure section; N. D.	INSULG
VINPD	$V_{IN_{PD}}$	Volume of propellent displaced by internal insulation. excluding liner; in^3	INSULG
VPPMT	$V_{PP_{MT}}$	Propellent volume; in^3	PROPW

OUTPUT DATA:

The following data is output from this model. It is available for use as inter-model input to other models and to print, plot, and optimization routines.

Mnemonic	Symbol	Description; Ext. (Int.) Units		
APPWEB	$A_{PP_{WEB}}$	Propellent web area. Cross sectional area of propellent volume bounded by the cylindrical grain section and basic cylindrical port section; in^2	Fig. 6	Eq. 6
APT	A_{PT}	Cross sectional area of basic cylindrical section; in^2	Fig. 6	Eq. 3

OUTPUT DATA (Cont.):

Mnemonic	Symbol	Description; Ext. (Int.) Units		
DGN	D_{GN}	Diameter of cylindrical grain section;		
		in	Figs. 2, 6	Eq. 1
DGNCL	$D_{GN_{CL}}$	Equatorial diameter of hemi-ellipsoids associated with the forward and aft grain closure sections;		
		in	Figs. 2, 3, 4	Eq. 7
DGNHA	$D_{GN_{HA}}$	Diameter of aft base of the hemi-ellipsoid frustum associated with the aft grain closure section;		
		in	Figs. 2, 4	Eq. 32
DGNHF	$D_{GN_{HF}}$	Diameter of forward base of the hemi-ellipsoid frustum associated with the forward grain closure section;		
		in	Figs. 2, 3	Eq. 19
DPT	D_{PT}	Diameter of basic cylindrical port section;		
		in	Figs, 2, 3, 4, 6	Eq. 2
LGN	L_{GN}	Length of grain envelope. Distance between the forward base of the hemi-ellipsoid frustum associated with the forward grain closure section and the aft base of the hemi-ellipsoid frustum associated with the aft grain closure section. Includes length penalties for nozzle submergence, slots, joints and internal insulation;		
		in	Fig. 2	Eq. 75
LGNCHA	$L_{GN_{CHA}}$	Length of the axis of revolution of the hemi-ellipsoid frustum associated with the aft grain closure section;		
		in	Figs. 2, 4	Eq. 31

OUTPUT DATA (Cont.):

Mnemonic	Symbol	Description; Ext. (Int.) Units		
LGNCHF	$L_{GN_{CHF}}$	Length of the axis of revolution of the hemi-ellipsoid frustum associated with the forward grain closure section;		
		in	Figs. 2, 3	Eq. 18
LGNCLA	$L_{GN_{CLA}}$	Length of the axis of revolution of the hemi-ellipsoid associated with the aft grain closure section;		
		in	Figs. 2, 4	Eq. 23
LGNCLF	$L_{GN_{CLF}}$	Length of the axis of revolution of the hemi-ellipsoid associated with the forward grain closure section;		
		in	Figs. 2, 3	Eq. 10
LGNCY	$L_{GN_{CY}}$	Length of cylindrical grain section. Includes length penalties for nozzle submergence, slots, joints, and internal insulation;		
		in	Fig. 2	Eq. 71
LGNCY1	$L_{GN_{CY1}}$	Length of basic cylindrical grain section. Does not include length penalties for nozzle submergence, slots, joints and internal insulation;		
		in	Fig. 2	Eq. 36
LGNCY2	$L_{GN_{CY2}}$	Length of cylindrical grain section. Includes length penalty for nozzle submergence;		
		in	Fig. 2	Eq. 55
LGNCY3	$L_{GN_{CY3}}$	Length of cylindrical grain section. Includes length penalties for nozzle submergence and slots;		
		in	Fig. 2	Eq. 64
LGNCY4	$L_{GN_{CY4}}$	Length of cylindrical grain section. Includes length penalties for nozzle submergence, slots and joints;		
		in	Fig. 2	Eq. 66

OUTPUT DATA (Cont.):

Mnemonic	Symbol	Description; Ext. (Int.) Units		
LGNCY5	$L_{GN_{CY5}}$	Length of cylindrical grain section. Includes length penalties for nozzle submergence, slots, joints and internal insulation;		
		in	Fig. 2	Eq. 69
LGNNSCY	$L_{GN_{NSCY}}$	Distance nozzle is submerged in cylindrical grain section;		
		in	Fig. 4	Eq. 40
LGNPDIN	$L_{GN_{PDIN}}$	Cylindrical grain section length penalty for propellent displaced by internal insulation;		
		in	Fig. 2	Eq. 68
LGNPDNS	$L_{GN_{PDNS}}$	Cylindrical grain section length penalty for propellent displaced by submerged nozzle;		
		in	Fig. 2	Eq. 54
LGNSL	$L_{GN_{SL}}$	Cylindrical grain section length penalty for slot cutouts;		
		in	Fig. 2	Eq. 63
LPTCF	$L_{PT_{CF}}$	Total length of port cone frustum section;		
		in	Figs. 2, 4, 6	Eq. 45
LPTCFCA	$L_{PT_{CFCA}}$	Length of the portion of the port cone frustum section within the aft grain closure section;		
		in	Figs. 2, 4	Eq. 42
LPTCFCY	$L_{PT_{CFCY}}$	Length of the portion of the port cone frustum section within the cylindrical grain section;		
		in	Figs. 2, 4	Eq. 44
LPTCFS	$L_{PT_{CFS}}$	Slant height of port cone frustum section;		
		in	Fig. 4	Eq. 47

OUTPUT DATA (Cont.):

Mnemonic	Symbol	Description; Ext. (Int.) Units		
LPTCY1	$L_{PT_{CY1}}$	Total length of cylindrical portion of basic port. Does not include adjustments for nozzle submergence, slots, joints nor internal insulation;		
		in	Fig. 2	Eq. 38
LPTCY2	$L_{PT_{CY2}}$	Length of cylindrical port section. Includes nozzle submergence penalty;		
		in	Figs. 2, 6	Eq. 47
LPTNS	$L_{PT_{NS}}$	Distance nozzle is submerged into port;		
		in	Fig. 4	Eq. 39
LPTNZI	$L_{PT_{NZI}}$	Submerged nozzle inlet allowance;		
		in	Fig. 4	Eq. 43
LPTYCLA	$L_{PT_{YCLA}}$	Length of cylindrical portion of the basic port within the hemi-ellipsoid associated with the aft grain closure section;		
		in	Fig. 4	Eq. 25
LPTYCLF	$L_{PT_{YCLF}}$	Length of cylindrical portion of the basic port within the hemi-ellipsoid associated with the forward grain closure section;		
		in		Eq. 12
QDCFA1	Q_{DCFA1}	Associative quantity, port cone frustum section aft base diameter. See DPTCFA;		
		in		Eq. 76
QDCFA2	Q_{DCFA2}	Associative quantity, port cone frustum section aft base diameter. See DPTCFA;		
		in		Eq. 77
QDCFA3	Q_{DCFA3}	Associative quantity, port cone frustum section aft base diameter. See DPTCFA;		
		in		Eq. 78

OUTPUT DATA (Cont.):

Mnemonic	Symbol	Description; Ext. (Int.) Units	
QDCFF1	Q_{DCFF1}	Associative quantity, port cone frustum section forward base diameter. See DPTCFF; in	Eq. 79
QDCFF2	Q_{DCFF2}	Associative quantity, port cone frustum section forward base diameter. See DPTCFF; in	Eq. 80
QDCFF3	Q_{DCFF3}	Associative quantity, port cone frustum section forward base diameter. See DPTCFF; in	Eq. 81
QDGN1	Q_{DGN1}	Associative quantity, cylindrical grain section diameter. See DGN; in	Eq. 82
QDGN2	Q_{DGN2}	Associative quantity, cylindrical grain section diameter. See DGN; in	Eq. 83
QDGN3	Q_{DGN3}	Associative quantity, cylindrical grain section diameter. See DGN; in	Eq. 84
QDPT1	Q_{DPT1}	Associative quantity, basic cylindrical port section diameter. See DPT; in	Eq. 85
QDPT2	Q_{DPT2}	Associative quantity, basic cylindrical port section diameter. See DPT; in	Eq. 86
QDPT3	Q_{DPT3}	Associative quantity, basic cylindrical port section diameter. See DPT; in	Eq. 87

OUTPUT DATA (Cont.):

Mnemonic	Symbol	Description; Ext. (Int.) Units	
QRAPTH1	Q_{RAPTH1}	Associative quantity, port to nozzle throat area ratio. See RAPTTH;	
		N. D.	Eq. 88
QRAPTH2	Q_{RAPTH2}	Associative quantity, port to nozzle throat area ratio. See RAPTTH;	
		N. D.	Eq. 89
QRAPTH3	Q_{RAPTH3}	Associative quantity, port to nozzle throat area ratio. See RAPTTH;	
		N. D.	Eq. 90
RAPTTH	R_{APTTH}	Area ratio. Ratio of basic cylindrical port section cross sectional area to nozzle throat cross sectional area;	
		N. D.	Eq. 4
RDCFACL	R_{DCFACL}	Diameter ratio. Ratio of port cone frustum section aft base diameter to grain closure equatorial diameter;	
		N. D.	Eq. 41
RDGNCLA	R_{DGNCLA}	Head ratio of ellipsoid associated with the aft grain closure section. Ratio of twice the closure length to the closure equatorial diameter;	
		N. D.	Eq. 22
RDGNCLF	R_{DGNCLF}	Head ratio of ellipsoid associated with the forward grain closure section. Ratio of twice the closure length to the closure equatorial diameter;	
		N. D.	Eq. 9
RDPTCL	R_{DPTCL}	Diameter ratio. Ratio of basic cylindrical port section diameter to grain closure equatorial diameter;	
		N. D.	Eq. 8

OUTPUT DATA (Cont.):

Mnemonic	Symbol	Description; Ext. (Int.) Units	
RLCFCA	R_{LCFCA}	Length ratio. Ratio of length of portion of port cone frustum section within aft grain closure section to length of aft grain closure section;	
		N. D.	Eq. 49
RLDGNCY	R_{LDGNCY}	Length to diameter ratio, cylindrical grain section. Includes nozzle submergence, slot, joint and internal insulation penalties;	
		N. D.	Eq. 72
RLDGNY1	R_{LDGNY1}	Length to diameter ratio, basic cylindrical grain section. Does not include nozzle submergence, slot, joint and internal insulation penalties;	
		N. D.	Eq. 37
RLDGNY2	R_{LDGNY2}	Length to diameter ratio, cylindrical grain section. Includes nozzle submergence penalty;	
		N. D.	Eq. 56
RLDGNY3	R_{LDGNY3}	Length to diameter ratio, cylindrical grain section. Includes nozzle submergence and slot penalties;	
		N. D.	Eq. 65
RL GNY4	R_{LDGNY4}	Length to diameter ratio, cylindrical grain section. Includes nozzle submergence, slot and joint penalties;	
		N. D.	Eq. 67
RLDGNY5	R_{LDGNY5}	Length to diameter ratio, cylindrical grain section. Includes nozzle submergence, slot, joint and internal insulation penalties;	
		N. D.	Eq. 70

OUTPUT DATA (Cont.):

Mnemonic	Symbol	Description; Ext. (Int.) Units		
RLGNCHA	R_{LGNCHA}	Length ratio, aft grain closure section. Ratio of hemi-ellipsoid frustum length to hemi-ellipsoid length;		
		N. D.		Eq. 33
RLGNCHF	R_{LGNCHF}	Length ratio, forward grain closure section. Ratio of hemi-ellipsoid frustum length to hemi-ellipsoid length;		
		N. D.		Eq. 20
RLPTCYA	R_{LPTCYA}	Length ratio. Ratio of the length of the cylindrical portion of the basic port within the hemi-ellipsoid to the length of the hemi-ellipsoid for the aft grain closure section;		
		N. D.		Eq. 27
RLPTCYF	R_{LPTCYF}	Length ratio. Ratio of the length of the cylindrical portion of the basic port within the hemi-ellipsoid to the length of the hemi-ellipsoid for the forward grain closure section;		
		N. D.		Eq. 14
SBSPT	$S_{BS_{PT}}$	Initial propellent burning surface area, excluding slots;		
		in^2	Fig. 6	Eq. 62
SPT2	S_{PT_2}	Propellent surface area associated with the port. Includes submerged nozzle corrections;		
		in^2		Eq. 61
SPTCFB	$S_{PT_{CFB}}$	Port surface area component. Propellent surface at forward base of port cone frustum section;		
		in^2	Fig. 6	Eq. 60
SPTCFS	$S_{PT_{CFS}}$	Port surface area component. Propellent surface associated with lateral area of port cone frustum section;		
		in^2	Fig. 6	Eq. 59

OUTPUT DATA (Cont.):

Mnemonic	Symbol	Description; Ext. (Int.) Units		
SPTCY2	$S_{PT_{CY2}}$	Port surface area component. Propellent surface associated with the lateral area of the cylindrical port section;		
		in^2	Fig. 6	Eq. 58
THETACF	θ_{CF}	Half-angle of port cone frustum section;		
		deg (rad)	Figs. 2, 4	Eq. 46
TPPWEB	$T_{PP_{WEB}}$	Propellent web thickness. Thickness of grain in section where both the grain and port are cylindrical. Radial distance between surface of cylindrical port section and surface of cylindrical grain section;		
		in	Figs. 2, 3, 6	Eq. 5
VGN	V_{GN}	Volume of grain envelope. Includes port, submerged nozzle penalty, slots, joints and all internal insulation except liner. Note that the grain closures of the grain envelope are hemi-ellipsoid frustums, not hemi-ellipsoids;		
		in^3		Eq. 74
VGNCHA	$V_{GN_{CHA}}$	Volume of hemi-ellipsoid frustum associated with the aft grain closure section;		
		in^3	Fig. 5	Eq. 34
VGNCHF	$V_{GN_{CHF}}$	Volume of hemi-ellipsoid frustum associated with the forward grain closure section;		
		in^3	Fig. 3	Eq. 21
VGNCLA	$V_{GN_{CLA}}$	Volume of hemi-ellipsoid associated with the aft grain closure section;		
		in^3	Fig. 5	Eq. 24
VGNCLF	$V_{GN_{CLF}}$	Volume of hemi- ellipsoid associated with the forward grain closure section;		
		in^3	Fig. 3	Eq. 11

OUTPUT DATA (Cont.):

Mnemonic	Symbol	Description; Ext. (Int.) Units
VGNCY	$V_{GN_{CY}}$	Volume of cylindrical grain section. Includes port, submerged nozzle penalty, slots, joints and internal insulation except liner; in^3 Eq. 73
VPPCLA	$V_{PP_{CLA}}$	Volume of propellent associated with the hemi-ellipsoid of the aft grain closure section. Note that this volume is an intermediate quantity and does not include corrections for nozzle submergence, insulation wedges, etc.; in^3 Fig. 5 Eq. 30
VPPCLF	$V_{PP_{CLF}}$	Volume of propellent associated with the hemi-ellipsoid of the forward grain closure section. Note that this volume is an intermediate quantity and does not include corrections for insulation wedges, igniter, etc.; in^3 Fig. 3 Eq. 17
VPPCY1	$V_{PP_{CY1}}$	Volume of propellent within basic cylindrical grain section. Does not include displaced propellent corrections for nozzle submergence, slots, joints nor internal insulation; in^3 Eq. 35
VPPPDNS	$V_{PP_{PDNS}}$	Volume of propellent displaced due to nozzle submergence; in^3 Fig. 5 Eq. 53
VPTCF	$V_{PT_{CF}}$	Total volume of port cone frustum section; in^3 Fig. 5 Eq. 48
VPTCFCY	$V_{PT_{CFCY}}$	Volume of basic port portion of the port cone frustum section within the cylindrical grain section; in^3 Fig. 5 Eq. 51

OUTPUT DATA (Cont.):

Mnemonic	Symbol	Description; Ext. (Int.) Units		
VPTCLA	$V_{PT_{CLA}}$	Volume of basic port within the hemi-ellipsoid associated with the aft grain closure section;		
		in^3	Fig. 5	Eq. 29
VPTCLF	$V_{PT_{CLF}}$	Volume of basic port within the hemi-ellipsoid associated with the forward grain closure section;		
		in^3	Fig. 3	Eq. 16
VPTCYCF	$V_{PT_{CYCF}}$	Volume of basic port section associated with nozzle submergence;		
		in^3	Fig. 5	Eq. 52
VPTECFA	$V_{PT_{ECFA}}$	Volume of ellipsoidal cap at aft base of port cone frustum section within aft grain closure section;		
		in^3	Fig. 5	Eq. 50
VPTECLA	$V_{PT_{ECLA}}$	Volume of ellipsoidal cap at base of cylindrical portion of basic port section within the hemi-ellipsoid associated with the aft grain closure section;		
		in^3	Fig. 5	Eq. 28
VPTECLF	$V_{PT_{ECLF}}$	Volume of ellipsoidal cap at base of cylindrical portion of the basic port section within the hemi-ellipsoid associated with the forward grain closure section;		
		in^3	Fig. 3	Eq. 15
VPTYCLA	$V_{PT_{YCLA}}$	Volume of cylindrical portion of the basic port within the hemi-ellipsoid associated with the aft grain closure section;		
		in^3	Fig. 5	Eq. 26
VPTYCLF	$V_{PT_{YCLF}}$	Volume of cylindrical portion of the basic port within the hemi-ellipsoid associated with the forward grain closure section;		
		in^3	Fig. 3	Eq. 13

PRINT BLOCK KEY:

Nominally, only those lines with an asterisk to the left of the line number will be printed. By input, any of the lines given below may be printed or suppressed (see the section on output models for the details).

			GRAING	GNGM1	GRAIN GEOMETRY	
APPWEB	APT	DGN	*1	DGNCL	DGNHA	DGNHF
DPT	DPTCFA	DPTCFF	*2	KDPT1	KDPT2	KGN1
KGN2	KGN3	KGN4	*3	KGN5	KGN6	KGN7
KGN8	KQDCFA1	KQDCFA2	*4	KQDCFA3	KQDCFF1	KQDCFF2
KQDCFF3	KQDGN1	KQDGN2	*5	KQDGN3	KQDPT1	KQDPT2
KQDPT3	KQRAPH1	KQRAPH2	*6	KQRAPH3	LGN	LGNCHA
LGNCHF	LGNCLA	LGNCLF	*7	LGNCY	LGNCY1	LGNCY2
LGNCY3	LGNCY4	LGNCY5	*8	LGNNSCY	LGNPDIN	LGNPDNS
LGNSL	LJTCUT	LPTCF	*9	LPTCFCA	LPTCFCY	LPTCFHA
LPTCFS	LPTCY1	LPTCY2	*10	LPTNS	LPTNZI	LPTYCLA
LPTYCLF	QDCFA1	QDCFA2	*11	QDCFA3	QDCFF1	QDCFF2
QDCFF3	QDGN1	QDGN2	*12	QDGN3	QDPT1	QDPT2
QDPT3	QRAPTH1	QRAPTH2	*13	QRAPTH3	RAPTTH	RDCFACL
RDGNCLA	RDGNCLF	RDPTCL	*14	RLCFCA	RLDGNCY	RLDGNY1
RLDGNY2	RLDGNY3	RLDGNY4	*15	RLDGNY5	RLGNCHA	RLGNCHF
RLPTCYA	RLPTCYF	SBSPT	*16	SPT2	SPTCFB	SPTCFS
SPTCY2	THETACF	TPPWEB	*17	VGN	VGNCHA	VGNCHF
VGNCLA	VGNCLF	VGNCY	*18	VPPCLA	VPPCLF	VPPCY1
VPPPDNS	VPTCF	VPTCFCY	*19	VPTCLA	VPTCLF	VPTCYCF
VPTECFA	VPTECLA	VPTECLF	*20	VPTYCLA	VPTYCLF	

50.1

MODEL TYPE: IBFLOW (Internal Ballistics, FLOW)

MODEL NAME: IBFM1 (Cylindrical port, slot penalty)

DESCRIPTION:

IBFM1 (Internal Ballistics, Flow Model number 1) evaluates the burn rate and flow characteristics within a cylindrical ported grain to determine the effective slot volume required for a neutral pressure-time history. This required volume (grain length penalty) is sometimes sizable, thereby resulting in a significant degradation of the motor volumetric loading efficiency.

The slot volume requirement is independent of the number of slots and is basically determined by the gas flow requirements from the slots into the center perforate. The calculation of the length of the slots is based upon the following assumptions:

1. The grain is cylindrical;
2. The port burning surface is cylindrical;
3. The gas leaves the slots and enters the center perforate at a Mach number specified by the program user;
4. The pressure and temperature within the slot are equal to the pressure and temperature respectively within the center perforate;
5. The gas flow upstream of the nozzle throat is isentropic flow of a perfect gas.

In addition to the slot penalty, this model also evaluates the maximum and minimum burn rates. These are available as constraint quantities to insure that the web is not thicker than that allowed by the maximum burn rate and burn time or thinner than that allowed by the minimum burn rate and burn time. The model evaluates a set of associative quantities to facilitate setting up these constraints, if required.

An appreciation for the slot geometry may be gained by referring to Figure 1.

PROCEDURE:

Prior to entering IBFM1, the models specified by the PROPELW, IBGAS and IBPERF model types have evaluated the propellent density, gas, and performance properties. The model specified by the GRAING model type then determined the geometry required to design a cylindrical ported grain, including accommodation for nozzle submergence.

The IBFM1 model is then executed and the burn rates and grain length penalty for slots is determined.

After executing IBFM1, the model specified by the GRAING model type will be reentered and the preliminary grain design will be corrected to account for the slot volume. The model specified by the INSULG model type may then utilize data from IBFM1 and the grain geometry to assess internal insulation requirements.

EQUATIONS:

Burn rate at ignition.

$$B_{PP_{IGN}} = \frac{T_{PP_{WEB}}}{T_B} \tag{1}$$

Average burn rate.

$$B_{PP_{AVG}} = K_{BPPAVG} \, B_{PP_{IGN}} \tag{2}$$

Maximum burn rate.

$$B_{PP_{MAX}} = K_{BPPMAX} \, P_{AVG}^{a} \tag{3}$$

Minimum burn rate.

$$B_{PP_{MIN}} = K_{BPPMIN} \, P_{AVG}^{b} \tag{4}$$

Weight flow rate from port surface, excluding slots.

$$\dot{W}_{PT} = \rho_{PP_{MT}} \, S_{BS_{PT}} \, B_{PP_{AVG}} \tag{5}$$

EQUATIONS (Cont.):

Weight flow rate required from all slots.

$$\dot{W}_{SL_{REQ}} = \dot{W}_{PP_{MT}} - \dot{W}_{PT} \tag{6}$$

Area of one burning surface of a slot.

$$A_{BS_{SL}} = A_{PP_{WEB}} \tag{7}$$

Weight flow rate from a slot (two surfaces).

$$\dot{W}_{SL} = 2\, \rho_{PP_{MT}}\, A_{BS_{SL}}\, B_{PP_{AVG}} \tag{8}$$

Length of a slot.

$$L_{SL} = \frac{\dot{W}_{SL}\, C_{GAS}}{\pi\, D_{PT}\, H\, P_{AVG}\, M_{SL}\, g_o} \tag{9}$$

Number of slots required.

$$N_{SL_{REQ}} = \frac{\dot{W}_{SL_{REQ}}}{\dot{W}_{SL}} \tag{10}$$

Grain length penalty for slots cutouts.

$$L_{SL_{GN}} = N_{SL_{REQ}}\, L_{SL} \tag{11}$$

Associative quantities. The following quantities are intended solely for optional utilization by the program user. Their primary usage within this model is for forming constraint quantities.

$$Q_{BI} = K_{QBI}\, B_{PP_{IGN}} \tag{12}$$

$$Q_{BA} = K_{QBA}\, B_{PP_{AVG}} \tag{13}$$

EQUATIONS (Cont.):

$$Q_{BMX} = K_{QBMX}\, B_{PP_{MAX}} \tag{14}$$

$$Q_{BMN} = K_{QBMN}\, B_{PP_{MIN}} \tag{15}$$

OPTIMIZATION CONSIDERATIONS:

Generally, the nature of the problem which would require usage of this model would also require that the following constraints be set up by the program user.

A maximum propellent burn rate constraint will insure that the propellent web is not too thick. (Note that this constraint corresponds to a lower limit on the port fraction.)

$$B_{PP_{AVG}} \leq B_{PP_{MAX}} \tag{16}$$

A minimum propellent burn rate constraint will insure that the propellent web is not too thin. (Note that this constraint corresponds to an upper limit on the port fraction.)

$$B_{PP_{AVG}} \geq B_{PP_{MIN}} \tag{17}$$

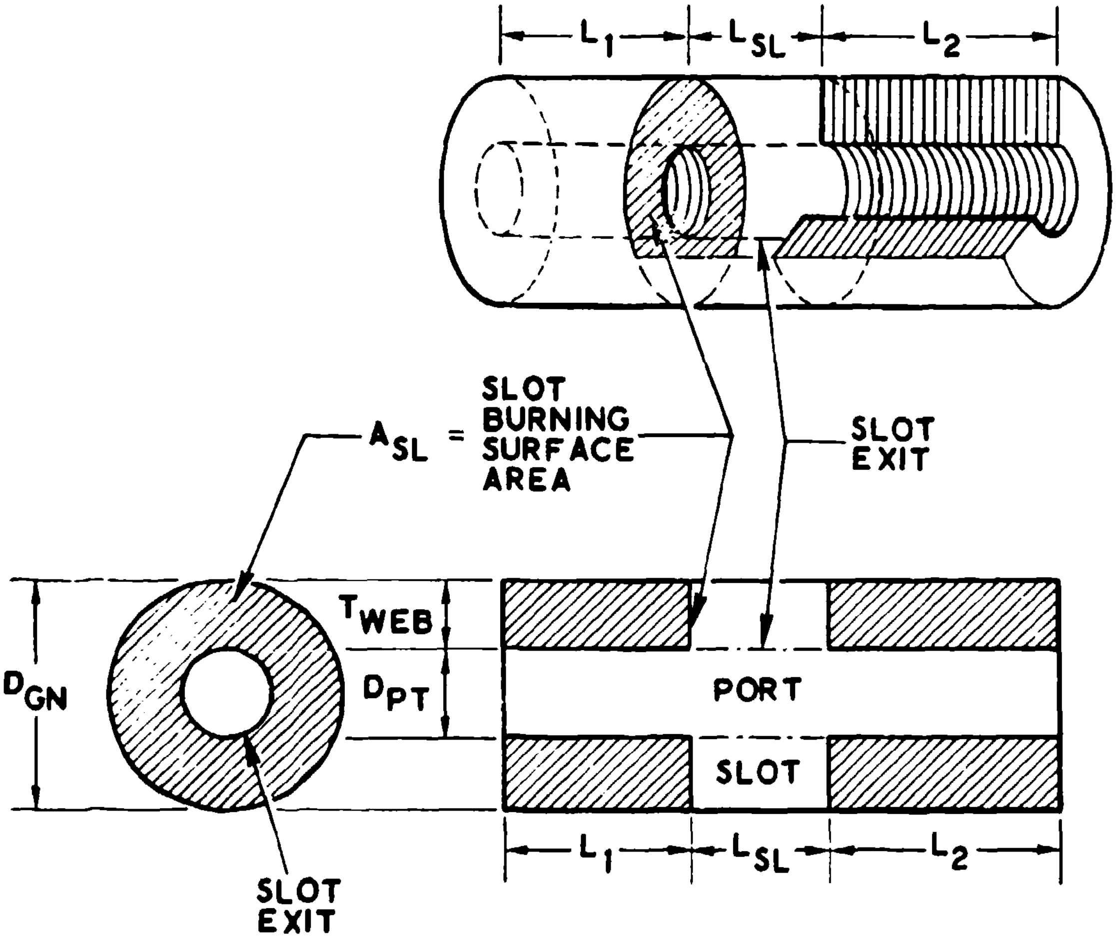

Note that $L_1 + L_2 = L$
Where L is the length such that $S_{PT} = \pi L D_{PT}$

Fig. 50.1-1 Slot Geometry

INPUT DATA, INTRA-MODEL:

The following data is input directly to this model by the program user. If a value is not input, the preset value is used.

Mnemonic	Symbol	Description; Ext. (Int.) Units	Preset
EBPPMAX	a	Exponent for maximum radial propellent burn rate computation; N. D.	0.39
EBPPMIN	b	Exponent for minimum radial propellent burn rate computation; N. D.	0.27
KBPPAVG	K_{BPPAVG}	Coe..icient for average radial propellent burn rate computation; N. D.	1.0
KBPPMAX	K_{BPPMAX}	Coefficient for maximum radial propellent burn rate computation; N. D.	0.054
KBPPMIN	K_{BPPMIN}	Coefficient for minimum radial propellent burn rate computation; N. D.	0.039
KQBAVG	K_{QBA}	Associative quantity coefficient for QBPPAVG computation; N. D.	0
KQBIGN	K_{QBI}	Associative quantity coefficient for QBPPIGN computation; N. D.	0
KQBMAX	K_{QBMX}	Associative quantity coefficient for QBPPMAX computation; N. D.	0
KQBMIN	K_{QBMN}	Associative quantity coefficient for QBPPMIN computation; N. D.	0

INPUT DATA, INTRA-MODEL (Cont.):

Mnemonic	Symbol	Description; Ext. (Int.) Units	Preset
MSLEXT	M_{SL}	Mach number of combustion products at slot exit; N. D.	0.2

INPUT DATA, INTER-MODEL:

This model requires as input certain data which is usually output from a model of the specified model type. If the user has not specified such a source for this data, then it must be input directly with the intra-model input.

Mnemonic	Symbol	Description; Ext. (Int.) Units	Model Type
APPWEB	$A_{PP_{WEB}}$	Cross sectional web area; in^2	GRAING
CGAS	C_{GAS}	Speed of sound in gas; ft/sec	IBGAS
DPT	D_{PT}	Port diameter; in	GRAING
DWPPMT	$\dot{W}_{PP_{MT}}$	Propellent weight flow; lb/sec	IBPERF
PCHAVG	P_{AVG}	Average chamber pressure; PSIA	IBGAS
RHOPPMT	$\rho_{PP_{MT}}$	Propellent density; lb/in^3	PROPELW
RSPHT	H	Specific heat ratio; N. D.	IBGAS
SBSPT	$S_{BS_{PT}}$	Port burning surface area; in^2	GRAING

INPUT DATA, INTER-MODEL (Cont.):

Mnemonic	Symbol	Description; Ext. (Int.) Units	Model Type
TBPPMT	T_B	Propellent burn time; sec	IBPERF
TPPWEB	$T_{PP_{WEB}}$	Web thickness; in	GRAING

OUTPUT DATA:

The following data is output from this model. It is available for use as inter-model input to other models and to print, plot, and optimization routines.

Mnemonic	Symbol	Description; Ext. (Int.) Units	
ABSSL	$A_{BS_{SL}}$	Area of one burning surface of a slot; in^2	Eq. 7
BPPAVG	$B_{PP_{AVG}}$	Average radial propellent burn rate; in/sec	Eq. 2
BPPIGN	$B_{PP_{IGN}}$	Radial burn rate of propellent at ignition; in/sec	Eq. 1
BPPMAX	$B_{PP_{MAX}}$	Maximum radial propellent burn rate; in/sec	Eq. 3
BPPMIN	$B_{PP_{MIN}}$	Minimum radial propellent burn rate; in/sec	Eq. 4
DWBSNSL	$\dot{W}_{PT}$	Propellent weight flow rate from port surface area, excluding slots; lb/sec	Eq. 5
DWSLREQ	$\dot{W}_{SL_{REQ}}$	Propellent weight flow rate required from slots for balanced motor flow; lb/sec	Eq. 6

OUTPUT DATA (Cont.):

Mnemonic	Symbol	Description; Ext. (Int.) Units	
DWSL	$\dot{W}_{SL}$	Propellent weight flow rate from a slot (two surfaces);	
		lb/sec	Eq. 8
LSL	L_{SL}	Length of a slot required for balanced slot flow;	
		in	Eq. 9
LSLGN	$L_{SL_{GN}}$	Grain length penalty for slot cutouts;	
		in	Eq. 11
NSLREQ	$N_{SL_{REQ}}$	Number of slots required for balanced motor flow. NSLREQ will normally be a fractional number. Note the distinction between NSLREQ and NISIH0, NISIH1, which is input to the internal insulation model;	
		N. D.	Eq. 10
QBPPAVG	Q_{BA}	Associative quantity, average burn rate (see BPPAVG);	
		in/sec	Eq. 13
QBPPIGN	Q_{BI}	Associative quantity, burn rate at ignition (see BPPIGN);	
		in/sec	Eq. 12
QBPPMAX	Q_{BMX}	Associative quantity, max. burn rate (see BPPMAX);	
		in/sec	Eq. 14
QBPPMIN	Q_{BMN}	Associative quantity, min. burn rate (see BPPMIN);	
		in/sec	Eq. 15

PRINT BLOCK KEY:

Nominally, only those lines with an asterisk to the left of the line number will be printed. By input, any of the lines given below may be printed or suppressed (see the section on output models for the details).

ABSSL	BPPAVG	BPFIGN	IBFLOW	IBFM1	INTERNAL BALLISTICS, FLOW	
DWSL	DWSLREQ	EBPPMAX	*1	BPPMAX	BPPMIN	DWBSNSL
KBPPMIN	KQBIGN	KQBAVG	*2	EBPPMIN	KBPPAVG	KBPPMAX
LSLGN	MSLEXT	NSLREQ	*3	KQBMAX	KQBMIN	LSL
QBPPMIN			*4	QBPPAVG	QBPPIGN	QBPPMAX
			*5			

60.1

MODEL TYPE: IBGAS (Internal Ballistics, GAS)

MODEL NAME: IBGM1 (Constant vacuum thrust)

DESCRIPTION:

IBGM1 (Internal Ballistics Gas Model number 1) evaluates the gas characteristics and chamber pressures associated with a constant vacuum thrust solid rocket motor.

EQUATIONS:

Average chamber pressure.

$$P_{AVG} = K_{AVG} P \tag{1}$$

Maximum expected operating pressure.

$$P_{MEO} = K_{MEO} P \tag{2}$$

Maximum chamber pressure.

$$P_{MAX} = P_{MEO} \tag{3}$$

Delivered characteristic velocity.

$$C* = \xi C*_{TH} \tag{4}$$

Specific heat ratio constants.

$$H_1 = H + 1 \tag{5}$$

EQUATIONS (Cont.):

$$H_2 = H - 1 \tag{6}$$

$$H_3 = \frac{H_1}{H_2} \tag{7}$$

$$H_4 = \frac{H_1}{H} \tag{8}$$

$$H_5 = \frac{H_2}{H} \tag{9}$$

$$H_6 = \left(\frac{2}{H_1}\right)^{H_3} \tag{10}$$

$$H_7 = \sqrt{\frac{H_2\ H_6}{2}} \tag{11}$$

$$H_8 = \sqrt{\frac{2\ H\ H_6}{H_5}} \tag{12}$$

Gas constant.

$$R_{GAS} = \frac{H\ H_6\ C^{*2}}{T_C} \tag{13}$$

Speed of sound in gas.

$$C_{GAS} = \sqrt{H\ T_C\ R_{GAS}} \tag{14}$$

INPUT DATA, INTRA-MODEL:

The following data is input directly to this model by the program user. If a value is not input, the preset value is used.

Mnemonic	Symbol	Description; Ext. (Int.) Units	Preset
CVTH	C^*_{TH}	Theoretical characteristic velocity; ft/sec	0
KPCHAVG	K_{AVG}	Coefficient, average chamber pressure; N. D.	1
KPCHMEO	K_{MEO}	Coefficient, maximum expected operating chamber pressure; N. D.	1
KCEF	ξ	Combustion efficiency factor; N. D.	1
PCH	P	Chamber pressure; PSIA	0
RSPHT	H	Specific heat ratio; N. D.	0
TCPP	T_C	Propellent combustion temperature; $^\circ R$	0

INPUT DATA, INTER-MODEL:

None

OUTPUT DATA:

The following data is output from this model. It is available for use as inter-model input to other models and to print, plot, and optimization routines.

OUTPUT DATA (Cont.):

Mnemonic	Symbol	Description; Ext. (Int.) Units	
CGAS	C_{GAS}	Speed of sound in gas; ft/sec	Eq. 14
CVDELV	C*	Delivered characteristic velocity; ft/sec	Eq. 4
KRGAS	R_{GAS}	Gas constant; $ft^2/(sec^2 - {}^oR)$	Eq. 13
PCHAVG	P_{AVG}	Average chamber pressure; PSIA	Eq. 1
PCHMAX	P_{MAX}	Maximum chamber pressure; PSIA	Eq. 3
PCHMEO	P_{MEO}	Maximum expected operating chamber pressure; PSIA	Eq. 2
RSPHT1	H_1	Specific heat ratio quantity; N. D.	Eq. 5
RSPHT2	H_2	Specific heat ratio quantity; N. D.	Eq. 6
RSPHT3	H_3	Specific heat ratio quantity; N. D.	Eq. 7
RSPHT4	H_4	Specific heat ratio quantity; N. D.	Eq. 8
RSPHT5	H_5	Specific heat ratio quantity; N. D.	Eq. 9
RSPHT6	H_6	Specific heat ratio quantity; N. D.	Eq. 10

OUTPUT DATA (Cont.):

Mnemonic	Symbol	Description; Ext. (Int.) Units	
RSPHT7	H_7	Specific heat ratio quantity; N. D.	Eq. 11
RSPHT8	H_8	Sp cific heat ratio quantity; N. D.	Eq. 12

PRINT BLOCK KEY:

Nominally, only those lines with an asterisk to the left of the line number will be printed. By input, any of the lines given below may be printed or suppressed (see the section on output models for the details).

CGAS	CVDELV	CVTH	IBGAS	IBGM1	INTERNAL BALLISTICS, GAS	
KHGAS	PCH	PCHAVG	*1	KCEF	KPCHAVG	KPCHMEO
RSPHT1	RSPHT2	RSPHT3	*2	PCHMAX	PCHMEO	RSPHT
RSPHT7	RSPHT8	TCPP	*3	RSPHT4	RSPHT5	RSPHT6
			*4			

70.1

MODEL TYPE: IBPERF (Internal Ballistics, PERFormance)

MODEL NAME: IBPM1 (Conical nozzle divergence losses)

DESCRIPTION:

IBPM1 (Internal Ballistics Performance Model number 1) evaluates the propellent and nozzle dependent vacuum delivered performance quantities. The specific impulse is degraded to account for the nozzle half angle divergence loss (axial direction), due to the directional change of flow as the gas expands in a conical nozzle.

PROCEDURE:

Prior to entering IBPM1, the models specified for the PROPELW and IBGAS model types have evaluated the propellent weight and gas properties.

Upon the first entrance to IBPM1, the propellent weight flow is computed and the model specified by the NOZZLEG model type is executed to determine the nozzle geometry.

IBPM1 is then entered for the second time, the pressure ratio is solved iteratively using Newton's method, and the remainder of the internal ballistics performance dependent quantities are evaluated.

After the IBPM1 computations are completed, the motor geometry and weights are determined, the model specified for the PROPUL model type is executed, and the primary motor propulsion quantities are evaluated.

EQUATIONS (FIRST ENTRANCE):

Propellent weight flow.

$$\dot{W}_{PP_{MT}} = \frac{W_{PP_{MT}}}{T_B} \tag{1}$$

EQUATIONS (SECOND ENTRANCE):

Pressure ratio, nozzle exit pressure to chamber pressure. (transcendental equation solved iteratively for R_P)

$$\epsilon_{NZ} = \frac{H_7}{R_P^{(1/H)} \sqrt{1 - R_P^{H_5}}} \qquad (2)$$

Critical pressure ratio.

$$R_{PC} = \left(\frac{2}{H_1}\right)^{\left(\frac{H}{H_2}\right)} \qquad (3)$$

Nozzle half angle divergence momentum loss.

$$\lambda = \frac{1 + \cos\left(\theta_{NZ}\right)}{2} \qquad (4)$$

Reference nozzle half angle loss.

$$\lambda_R = \frac{1 + \cos\left(\theta_R\right)}{2} \qquad (5)$$

Vacuum thrust coefficient.

$$C_V = \lambda H_8 \sqrt{1 - R_P^{H_5}} + \epsilon_{NZ} R_P \qquad (6)$$

Reference thrust coefficient (exit pressure = atmospheric pressure).

$$C_R = \lambda_R H_8 \sqrt{1 - C_1^{H_5}} \qquad (7)$$

Vacuum specific impulse.

$$I_{SP_V} = \left(\frac{C_V}{C_R}\right) I_{SP_R} \qquad (8)$$

EQUATIONS (SECOND ENTRANCE) (Cont.):

Delivered vacuum specific impulse.

$$I_{SP_{VD}} = K_{VD} I_{SP_V} \quad (9)$$

INPUT DATA, INTRA-MODEL:

The following data is input directly to this model by the program user. If a value is not input, the preset value is used.

Mnemonic	Symbol	Description; Ext. (Int.) Units	Preset
CIBP1	C_1	Ratio of a reference nozzle exit pressure to a reference chamber pressure. The reference nozzle exit pressure must be equal to sea level pressure; N. D.	0.014696
ISPR	I_{SP_R}	Specific impulse for the reference pressure ratio CIBP1 and the reference nozzle half angle NZHAR; sec	0
KISPVD	K_{VD}	Nozzle efficiency factor; N. D.	1
NZHAR	θ_R	Reference nozzle half angle; deg	0
TBPPMT	T_B	Propellent burn time; sec	0

INPUT DATA, INTER-MODEL:

This model requires as input certain data which is usually output from a model of the specified model type. If the user has not specified such a source for this data, then it must be input directly with the intra-model input.

INPUT DATA, INTER-MODEL (Cont.):

Mnemonic	Symbol	Description; Ext. (Int.) Units	Model Type
COSNZHA	$\cos \theta_{NZ}$	Cosine of nozzle half angle; N. D.	NOZZLEG
RAEXTTH	ϵ_{NZ}	Nozzle expansion ratio at exit plane; N. D.	NOZZLEG
RSPHT	H	Specific heat ratio; N. D.	IBGAS
RSPHT1	H_1	Specific heat ratio quantity; N. D.	IBGAS
RSPHT2	H_2	Specific heat ratio quantity; N. D.	IBGAS
RSPHT5	H_5	Specific heat ratio quantity; N. D.	IBGAS
RSPHT7	H_7	Specific heat ratio quantity; N. D.	IBGAS
RSPHT8	H_8	Specific heat ratio quantity; N. D.	IBGAS
WPPMT	$W_{PP_{MT}}$	Propellent weight; lb	PROPELW

OUTPUT DATA:

The following data is output from this model. It is available for use as inter-model input to other models and to print, plot, and optimization routines.

Mnemonic	Symbol	Description; Ext. (Int.) Units	
CFVAC	C_V	Vacuum thrust coefficient; N. D.	Eq. 6

OUTPUT DATA (Cont.):

Mnemonic	Symbol	Description; Ext. (Int.) Units	
CFR	C_R	Reference thrust coefficient corresponding to the reference nozzle half angle NZHAR and the reference pressure ratio CIBP1. The reference nozzle exit pressure is sea level pressure;	
		N. D.	Eq. 7
DWPPMT	$\dot{W}_{PP_{MT}}$	Propellent weight flow;	
		lb/sec	Eq. 1
ISPVC	I_{SP_V}	Vacuum specific impulse;	
		sec	Eq. 8
ISPVD	$I_{SP_{VD}}$	Delivered vacuum specific impulse;	
		sec	Eq. 9
NZHAL	λ	Nozzle half angle loss;	
		N. D.	Eq. 4
NZHALR	λ_R	Reference nozzle half angle loss;	
		N. D.	Eq. 5
RPEPC	R_P	Pressure ratio. Ratio of nozzle exit pressure to chamber pressure;	
		N. D.	Eq. 2
RPEPCC	R_{PC}	Critical pressure ratio. Pressure ratio at nozzle throat;	
		N. D.	Eq. 3

PRINT BLOCK KEY:

Nominally, only those lines with an asterisk to the left of the line number will be printed. By input, any of the lines given below may be printed or suppressed (see the section on output models for the details).

			IBPERF	IBPM1	INTERNAL BALLISTICS, PERFORMANCE	
CFR	CFVAC	CIBP1	*1	DWPPMT	ISPR	ISPVC
ISPVD	KISPVD	NZHAL	*2	NZHALR	NZHAR	RPEPC
RPEPCC	TBPPMT		*3			

80.1

MODEL TYPE: INSULG (internal INSULation Geometry)

MODEL NAME: INGM1 (geometric parameter)

DESCRIPTION:

INGM1 (internal INsulation Geometry Model number 1) evaluates the internal insulation geometry for a solid rocket motor case and propellent grain having a cylindrical section and oblate closures. The basic components may include:

insulation liner

ellipsoidal insulation wedges for the forward and aft closures

insulation required for unjointed grain designs

insulation required for jointed grain designs

The model includes provision for circular cutouts, "holes" in the forward and aft closures, required for the igniter and nozzle. See figures 1 and 2 for an illustration of the basic insulation components and the interface with the case, grain, nozzle, and igniter geometry. Whenever possible, the equations have been formulated such that the geometry for the basic components degenerate to basic geometric forms. In addition, user specified coefficient and bias terms (preset to nominal values) are provided for the principal independent quantities associated with each basic geometric form. Consequently, the actual insulation geometry capable of being simulated is to a large degree a function of the ingenuity of the program user.

The insulation liner, as illustrated in figures 3 - 6, interfaces between the inside case surface and the outside wedge surfaces or grain envelope. Within the cylindrical case section, the liner has constant thickness. Within the closures, the outside and inside liner surfaces are hemi-ellipsoids whose equatorial planes are coincident with the plane separating the closure and cylindrical sections. The liner holes in the forward and aft closures are cylindrical, centered on the axis of revolution of the liner surface hemi-ellipsoids. The principle purposes of the liner geometry are to determine a total volume for insulation weight computations and to specify the head ratios and cylindrical diameter of the basic grain envelope.

DESCRIPTION (Cont.):

The insulation wedges (see figures 7 - 14) are associated with the forward and aft closures and interface between the insulation liner and the grain. The wedges may be completely within a closure, or may extend beyond a closure into the cylindrical section. Since the principle purpose of the wedge geometry is to determine an effective volume for weight evaluations, no corrective action, except for a warning diagnostic, is taken by the program if a wedge extends from within a closure beyond the cylindrical section.

If a wedge is completely within the closure (see figures 7, 13), the inside and outside wedge surfaces are hemi-ellipsoid frustums which are tangent at their bases (the "inside/outside wedge surface osculation plane"). The axis of revolution of these frustums are coincident and the equatorial plane of the hemi-ellipsoid associated with the outside frustum surface is coincident with the plane separating the case closure and case cylindrical sections. However, the "equatorial plane of the hemi-ellipsoid associated with the inside frustum surface" and the "inside/outside wedge surface osculating plane" are normally not coincident with each other or the "plane separating the case closure and case cylindrical sections".

If a wedge extends beyond a closure into the cylindrical section (see figures 9, 14), the outside wedge surface is comprised of a hemi-ellipsoid and a cylinder. The inside wedge surface is a hemi-ellipsoid tangent to the cylindrical portion of the outside wedge surface (the "inside/outside wedge surface osculation plane"). The axis of revolution of the inside and outside wedge surfaces are coincident and the "equatorial plane of the inside surface ellipsoid" is coincident with the "inside/outside wedge surface osculation plane". Further, the "equatorial plane of the hemi-ellipsoid associated with the outside wedge surface" is coincident with the "plane separating the case closure and case cylindrical section". However, normally the equatorial planes of the hemi-ellipsoids associated with the outside wedge surface and the inside wedge surface are not coincident.

The length of the forward closure wedge (figures 7, 9) is normally a function of the propellent web thickness. The igniter cutout is cylindrical, centered on the axis of revolution of the wedge surface hemi-ellipsoids.

The length of the aft closure wedge (figures 11, 13) is normally a function the cone frustum grain cutout half angle. The nozzle cutout is a cone frus- having a half angle equal to the cone frustum grain cutout half angle.

For the purpose of this model, a slot has none or one burning surface inhibited, whereas a joint has both burning surfaces inhibited. The slot and joint insulation, as illustrated in figures 15 - 20, is comprised of the following components:

DESCRIPTION (Cont.):

Port/Liner (PL) component. This component interfaces between the port and the liner. It has a rectangular cross section and its dimensions are normally a function of the maximum insulation thickness and the slot or joint length.

Port/Grain (PG) component. This component, which inhibits a burning surface, interfaces between the port and the grain. It normally has a trapezoid cross section (although it may be a pentagon, rectangle or triangle--see figures 16, 17) and its dimensions are primarily a function of the maximum insulation thickness, propellent web thickness, and a user specified base length. It should be noted that for joints, provision is made for "overlapping" PG components. However, for slots, except for a warning diagnostic, no corrective action is taken by the program if the PG component exceeds the slot cutout length.

Grain/Liner (GL) component. This component interfaces between the grain and the liner. It has a triangular cross section and its dimensions are normally a function of the maximum insulation thickness and the propellent web thickness. The GL component is associated with each non-inhibited slot burning surface.

The number of slots and joints, for insulation purposes, is specified by the program user and should not be a fractional number. The purpose of the slot and joint geometry is to determine an effective volume for insulation weight computations.

PROCEDURE:

INGM1 is a three-entrance model. Inter-model coupling is illustrated by figure 22.

Prior to the first entrance to INGM1, the models specified for the IBGAS, IBPERF, INSULW, and CASEG model types have evaulated the gas characteristics, insulation density and case geometry.

Upon the first entrance to INGM1, the basic insulation material properties are evaluated and, except for the length of the cylindrical section, the insulation liner geometry is determined.

The grain geometry model, GNGM1, then uses the inside liner surface to define the basic grain envelope. After adjusting the basic grain to account for submerged nozzle, slot, and joint penalties, program control is returned to INGM1.

PROCEDURE (Cont.):

Upon the second entrance to INGM1, the insulation wedge geometry, associated with the forward and aft closures, is evaluated, the slot and joint geometry is determined, and the propellent displaced by the closure wedges and the slot/joint insulation components is computed.

The grain geometry model, GNGM1, is then reentered, the cylindrical grain length is adjusted to include the propellent displaced by the insulation, and the total grain geometry is evaluated.

Upon the third entrance to INGM1, the grain geometry has been completely determined and the cylindrical section of the liner is sized. After evaluating the residual insulation volume, the total internal insulation volume is computed.

After executing INGM1, the program evaluates the remaining substage geometry. The model specified by the INSULW model type then uses the volumes obtained in INGM1 as effective volumes to determine the internal insulation weight breakdown.

REFERENCES:

Reference 52, "Some Useful Theorems Associated With Hemi-Ellipsoids" is the basis for the derivations of the following equations:

11, 17, 19, 20, 23, 25, 26, 28, 36, 42, 44, 45, 47, 50, 51, 53, 68, 81, 85, 87, 88, 89, 92, 94, 96, 98, 100, 101, 104, 115, 131, 135, 137, 138, 140, 142, 144, 146, 147, 150.

Reference 54, "Some Useful Theorems Associated With Osculating Ellipses" contains the derivations for the following equations:

74, 75, 76, 126, 127, 128.

Reference 55, "Derivation of LIWCFI and DIWCAI for the GTS INGM1 Internal Insulation Model" contains the derivations and assumptions for the following equations:

107a, 107b, 107c, 107d, 107e, 117, 120, 121, 122, 123, 124.

Reference 56, "PG Internal Insulation Subcomponent for GTS INGM1 Internal Insulation Model" contains the derivations and rationale for equations 156 through 210.

Reference 57, "Derivation of VIWCAPD and VIWCFPD for the GTS INGM1 Internal Insulation Model" contains the derivations and assumptions for equations 211 through 222.

NOTATION:

The following notation convention is used within this model whenever possible.

First Character

A	Plane area. (in^2)
C	Constant or intermediate quantity.
D	Diameter (measured normal to centerline). (in)
K	Coefficient or bias.
L	Length (measured parallel to centerline). (in)
R	Ratio. Next characters will be D or L to indicate diameter or length ratios. (N. D.)
T	Thickness. (in)
V	Volume. (in^3)
Y	Centroid. (in)

Next two characters denote principal insulation component.

IL	Liner.
IJ	Joint.
IN	General.
IS	Slot.
IW	Wedge.

Next characters.

A	Aft.
C or CL	Closure.
CH	Closure Hole.
E	Ellipsoid.
F	Forward.
H	Hole.
PD	Propellent Displaced.

Final character.

I	Inside surface.
O	Outside surface.

EQUATIONS, FIRST ENTRANCE:

Equations 1 through 56 are evaluated at the first entrance to the INGM1 model.

INSULATION PROPERTIES:

Approximate radiative heating rate.

$$Q_{IN_H} = C_{IN_1} \left(\frac{T_{C_{PP}}}{C_{IN_2}} \right)^4 K_{IN_1} + K_{IN_2} \tag{1}$$

Maximum insulation thickness for closure wedges. (See equations 61, 108)

$$T_{IW_{MAX}} = \left(\frac{C_{IN_3} \; T_B \; Q_{IN_H}}{Q^*_{IN} \; \rho_{IW}} \right) K_{IW_{23}} + K_{IW_{24}} \tag{2-a}$$

Maximum insulation thickness for a slot cutout. (Figure 16)

$$T_{IS_{MAX}} = \left(\frac{C_{IN_3} \; T_B \; Q_{IN_H}}{Q^*_{IN} \; \rho_{IS}} \right) K_{IS_1} + K_{IS_2} \tag{2-b}$$

Maximum insulation thickness for a joint cutout. (Figure 17)

$$T_{IJ_{MAX}} = \left(\frac{C_{IN_3} \; T_B \; Q_{IN_H}}{Q^*_{IN} \; \rho_{IJ}} \right) K_{IJ_1} + K_{IJ_2} \tag{2-c}$$

INSULATION LINER, CYLINDRICAL SECTION:

Outside diameter of the cylinder which is the outside surface of the insulation liner in the cylindrical case section. (Figure 2)

$$D_{IL_O} = D_{CS_I} \tag{3}$$

Inside diameter of the cylinder which is the inside surface of the insulation liner in the cylindrical case section. (Figure 2)

$$D_{IL_I} = D_{IL_O} - 2\, T_{IL_{CY}} \tag{4}$$

EQUATIONS, FIRST ENTRANCE (Cont.):

INSULATION LINER, CLOSURE SECTIONS (FORWARD AND AFT):

Equatorial diameter of the ellipsoids formed by the outside surface of the insulation liner associated with the forward and aft case closure sections. (Figures 2, 3, 5)

$$D_{IL_{CLO}} = D_{IL_O} \tag{5}$$

Equatorial diameter of the ellipsoids formed by the inside surface of the insulation liner associated with the forward and aft case closure sections. (Figures 2, 3, 5)

$$D_{IL_{CLI}} = D_{IL_I} \tag{6}$$

INSULATION LINER, FORWARD CLOSURE SECTION:

Head ratio of the ellipsoid formed by the outside surface of the insulation liner within the forward case closure section.

$$R_{DILCFO} = R_{DCSCFI} \tag{7}$$

Length of the axis of revolution of the hemi-ellipsoid formed by the outside surface of the insulation liner within the forward case closure section. (Figures 3, 4)

$$L_{IL_{CLFO}} = \frac{R_{DILCFO} \, D_{IL_{CLO}}}{2} \tag{8}$$

Diameter of circular hole, for the igniter, centered on the axis of revolution of the hemi-ellipsoid formed by the outside surface of the insulation liner within the forward case closure section. (Figures 2, 3)

$$D_{IL_{HFO}} = D_{CS_{HFI}} \, K_{IL_{17}} + K_{IL_{18}} \tag{9}$$

Diameter ratio, hole diameter to equatorial diameter, outside surface of the insulation liner within the forward case closure section. (Figure 3)

$$R_{DILHFO} = \frac{D_{IL_{HFO}}}{D_{IL_{CLO}}} \tag{10}$$

EQUATIONS, FIRST ENTRANCE (Cont.):

INSULATION LINER, FORWARD CLOSURE SECTION (Cont.):

Length of hemi-ellipsoid frustum associated with the outside surface of the insulation liner within the forward closure section. (Figure 3)

$$L_{IL_{CHFO}} = L_{IL_{CLFO}} \sqrt{1 - R^2_{DILHFO}} \tag{11}$$

Thickness of insulation liner at center of forward case closure section. Distance between inside and outside hemi-ellipsoid surfaces of the insulation liner, measured on the axis of revolution. (Figure 3)

$$T_{IL_{CLF}} = T_{IL_{CY}} K_{IL_1} \div K_{IL_2} \tag{12}$$

Length of the axis of revolution of the hemi-ellipsoid formed by the inside surface of the insulation liner within the forward case closure section. (Figure 3)

$$L_{IL_{CLFI}} = L_{IL_{CLFO}} - T_{IL_{CLF}} \tag{13}$$

Head ratio of the ellipsoid formed by the inside surface of the insulation liner within the forward case closure section.

$$R_{DILCFI} = \frac{2\, L_{IL_{CLFI}}}{D_{IL_{CLI}}} \tag{14}$$

Diameter of circular hole, for the igniter, centered on the axis of revolution of the hemi-ellipsoid formed by the inside surface of the insulation liner within the forward case closure section. (Figure 3)

$$D_{IL_{HFI}} = D_{IL_{HFO}} \tag{15}$$

Diameter ratio, hole diameter to equatorial diameter, inside surface of the insulation liner within the forward case closure section. (Figure 3)

$$R_{DILHFI} = \frac{D_{IL_{HFI}}}{D_{IL_{CLI}}} \tag{16}$$

EQUATIONS, FIRST ENTRANCE (Cont.):

INSULATION LINER, FORWARD CLOSURE SECTION (Cont.):

Length of hemi-ellipsoidal frustum associated with the inside surface of the insulation liner within the forward case closure. (Figure 3)

$$L_{IL_{CHFI}} = L_{IL_{CLFI}} \sqrt{1 - R^2_{DILHFI}} \tag{17}$$

Length of the cylindrical hole, for the igniter, in the insulation liner within the forward case closure section. (Figure 3)

$$L_{IL_{HF}} = L_{IL_{CHFO}} - L_{IL_{CHFI}} \tag{18}$$

Volume of the hemi-ellipsoid formed by the outside surface of the insulation liner within the forward case closure section. (Figure 4)

$$V_{IL_{CLFO}} = \left(\frac{\pi}{6}\right) L_{IL_{CLFO}} D^2_{IL_{CLO}} \tag{19}$$

Volume of the cylindrical section, associated with the igniter hole, within the hemi-ellipsoid formed by the outside surface of the insulation liner within the forward case closure section. (Figure 4)

$$V_{IL_{HFOC}} = \left(\frac{\pi}{4}\right) L_{IL_{CHFO}} D^2_{IL_{HFO}} \tag{20}$$

Length ratio, hemi-ellipsoid frustum to hemi-ellipsoid, outside surface, insulation liner, forward case closure. (Figure 3)

$$R_{LILCFO} = \frac{L_{IL_{CHFO}}}{L_{IL_{CLFO}}} \tag{21}$$

Volume of ellipsoidal cap at forward base of the cylindrical section, associated with the ignitor cutout, within the hemi-ellipsoid formed by the outside surface of the insulation liner within the forward case closure section. (Figure 4)

$$V_{IL_{HFOE}} = \left(\frac{V_{IL_{CLFO}}}{2}\right) \left(2 - 3\,R_{LILCFO} + R^3_{LILCFO}\right) \tag{22}$$

EQUATIONS, FIRST ENTRANCE (Cont.):

INSULATION LINER, FORWARD CLOSURE SECTION (Cont.):

Volume of cylinder with ellipsoidal cap, associated with the igniter cutout, within the hemi-ellipsoid formed by the outside surface of the insulation liner within the forward case closure section. (Figure 4)

$$V_{IL_{HFO}} = V_{IL_{HFOE}} + V_{IL_{HFOC}} \tag{23}$$

Volume of hemi-ellipsoid frustum with hole cutout associated with the outside surface of the insulation liner within the forward case closure section. (Figure 4)

$$V_{IL_{CHFO}} = V_{IL_{CLFO}} - V_{IL_{HFO}} \tag{24}$$

Volume of the hemi-ellipsoid formed by the inside surface of the insulation liner within the forward case closure section. (Figure 4)

$$V_{IL_{CLFI}} = \left(\frac{\pi}{6}\right) L_{IL_{CLFI}} D^2_{IL_{CLI}} \tag{25}$$

Volume of the cylindrical section, associated with the igniter hole, within the hemi-ellipsoid formed by the inside surface of the insulation liner within the forward case closure section. (Figure 4)

$$V_{IL_{HFIC}} = \left(\frac{\pi}{4}\right) L_{IL_{CHFI}} D^2_{IL_{HFI}} \tag{26}$$

Length ratio, hemi-ellipsoid frustum to hemi-ellipsoid, inside surface, insulation liner, forward case closure. (Figure 3)

$$R_{LILCFI} = \frac{L_{IL_{CHFI}}}{L_{IL_{CLFI}}} \tag{27}$$

Volume of ellipsoidal cap at forward base of the cylindrical section, associated with the igniter cutout, within the hemi-ellipsoid formed by the inside surface of the insulation liner within the forward case closure section. (Figure 4)

$$V_{IL_{HFIE}} = \left(\frac{V_{IL_{CLFI}}}{2}\right) \left(2 - 3\,R_{LILCFI} + R^3_{LILCFI}\right) \tag{28}$$

EQUATIONS, FIRST ENTRANCE (Cont.):

INSULATION LINER, FORWARD CLOSURE SECTION (Cont.):

Volume of cylinder with ellipsoidal cap, associated with the igniter cutout, within the hemi-ellipsoid formed by the inside surface of the insulation liner within the forward case closure section. (Figure 4)

$$V_{IL_{HFI}} = V_{IL_{HFIE}} + V_{IL_{HFIC}} \tag{29}$$

Volume of hemi-ellipsoid frustum with hole cutout associated with the inside surface of the insulation liner within the forward case closure section. (Figure 4)

$$V_{IL_{CHFI}} = V_{IL_{CLFI}} - V_{IL_{HFI}} \tag{30}$$

Volume of insulation liner within the forward case closure section. (Figure 4)

$$V_{IL_{CLF}} = \left(V_{IL_{CHFO}} - V_{IL_{CHFI}}\right) K_{IL_3} + K_{IL_4} \tag{31}$$

INSULATION LINER, AFT CLOSURE SECTION:

Head ratio of the ellipsoid formed by the outside surface of the insulation liner within the aft case closure section.

$$R_{DILCAO} = R_{DCSCAI} \tag{32}$$

Length of the axis of revolution of the hemi-ellipsoid formed by the outside surface of the insulation liner within the aft case closure section. (Figures 5, 6)

$$L_{IL_{CLAO}} = \frac{R_{DILCAO} \; D_{IL_{CLO}}}{2} \tag{33}$$

Diameter of circular hole, for the nozzle, centered on the axis of revolution of the hemi-ellipsoid formed by the outside surface of the insulation liner within the aft case closure section. (Figure 5)

$$D_{IL_{HAO}} = D_{CS_{HAI}} K_{IL_5} + K_{IL_6} \tag{34}$$

EQUATIONS, FIRST ENTRANCE (Cont.):

INSULATION LINER, AFT CLOSURE SECTION (Cont.):

Diameter ratio, hole diameter to equatorial diameter, outside surface of the insulation liner within the aft case closure section. (Figure 5)

$$R_{DILHAO} = \frac{D_{IL_{HAO}}}{D_{IL_{CLO}}} \tag{35}$$

Length of hemi-ellipsoidal frustum associated with the outside surface of the insulation liner within the aft case closure section. (Figure 5)

$$L_{IL_{CHAO}} = L_{IL_{CLAO}} \sqrt{1 - R^2_{DILHAO}} \tag{36}$$

Thickness of insulation liner at center of aft case closure section. Distance between the inside and outside hemi-ellipsoid surfaces of the insulation liner, measured on the axis of revolution. (Figure 5)

$$T_{IL_{CLA}} = T_{IL_{CY}} K_{IL_7} + K_{IL_8} \tag{37}$$

Length of the axis of revolution of the hemi-ellipsoid formed by the inside surface of the insulation liner within the aft case closure section. (Figure 5)

$$L_{IL_{CLAI}} = L_{IL_{CLAO}} - T_{IL_{CLA}} \tag{38}$$

Head ratio of the ellipsoid formed by the inside surface of the insulation liner within the aft case closure section. (Figure 5)

$$R_{DILCAI} = \frac{2\, L_{IL_{CLAI}}}{D_{IL_{CLI}}} \tag{39}$$

Diameter of circular hole, for the nozzle, centered on the axis of revolution of the hemi-ellipsoid formed by the inside surface of the insulation liner within the aft case closure section. (Figures 2, 5)

$$D_{IL_{HAI}} = D_{IL_{HAO}} \tag{40}$$

EQUATIONS, FIRST ENTRANCE (Cont.):

INSULATION LINER, AFT CLOSURE SECTION (Cont.):

Diameter ratio, hole diameter to equatorial diameter inside surface of the insulation liner within the aft case closure section. (Figure 5)

$$R_{DILHAI} = \frac{D_{IL_{HAI}}}{D_{IL_{CLI}}} \tag{41}$$

Length of hemi-ellipsoidal frustum associated with the inside surface of the insulation liner within the aft case closure. (Figure 5)

$$L_{IL_{CHAI}} = L_{IL_{CLAI}} \sqrt{1 - R^2_{DILHAI}} \tag{42}$$

Length of cylindrical hole, for the nozzle, in the insulation liner within the aft case closure section. (Figure 5)

$$L_{IL_{HA}} = L_{IL_{CHAO}} - L_{IL_{CHAI}} \tag{43}$$

Volume of the hemi-ellipsoid formed by the outside surface of the insulation liner within the aft case closure section. (Figure 6)

$$V_{IL_{CLAO}} = \left(\frac{\pi}{6}\right) L_{IL_{CLAO}} D^2_{IL_{CLO}} \tag{44}$$

Volume of the cylindrical section associated with the nozzle cutout, within the hemi-ellipsoid formed by the outside surface of the insulation liner within the aft case closure section. (Figure 6)

$$V_{IL_{HAOC}} = \left(\frac{\pi}{4}\right) L_{IL_{CHAO}} D^2_{IL_{HAO}} \tag{45}$$

Length ratio, hemi-ellipsoid frustum to hemi-ellipsoid, outside surface, insulation liner, aft case closure. (Figure 5)

$$R_{LILCAO} = \frac{L_{IL_{CHAO}}}{L_{IL_{CLAO}}} \tag{46}$$

EQUATIONS, FIRST ENTRANCE (Cont.):

INSULATION LINER, AFT CLOSURE SECTION (Cont.):

Volume of ellipsoidal cap at aft base of the cylindrical section, associated with the nozzle cutout, within the hemi-ellipsoid formed by the outside surface of the insulation liner within the aft case closure section. (Figure 6)

$$V_{IL_{HAOE}} = \left(\frac{V_{IL_{CLAO}}}{2}\right) \left(2 - 3\,R_{LILCAO} + R^3_{LILCAO}\right) \tag{47}$$

Volume of cylinder with ellipsoidal cap, associated with the nozzle cutout, within the hemi-ellipsoid formed by the outside surface of the insulation liner within the aft closure section. (Figure 6)

$$V_{IL_{HAO}} = V_{IL_{HAOE}} + V_{IL_{HAOC}} \tag{48}$$

Volume of the hemi-ellipsoid frustum with hole cutout associated with the outside surface of the insulation liner within the aft case closure section. (Figure 6)

$$V_{IL_{CHAO}} = V_{IL_{CLAO}} - V_{IL_{HAO}} \tag{49}$$

Volume of the hemi-ellipsoid formed by the inside surface of the insulation liner within the aft case closure section. (Figure 6)

$$V_{IL_{CLAI}} = \left(\frac{\pi}{6}\right) L_{IL_{CLAI}}\, D^2_{IL_{CLI}} \tag{50}$$

Volume of the cylindrical section, associated with the nozzle cutout, within the hemi-ellipsoid formed by the inside surface of the insulation liner within the aft case closure section. (Figure 6)

$$V_{IL_{HAIC}} = \left(\frac{\pi}{4}\right) L_{IL_{CHAI}}\, D^2_{IL_{HAI}} \tag{51}$$

Length ratio, hemi-ellipsoid frustum to hemi-ellipsoid, inside surface, insulation liner, aft case closure. (Figure 5)

$$R_{LILCAI} = \frac{L_{IL_{CHAI}}}{L_{IL_{CLAI}}} \tag{52}$$

EQUATIONS, FIRST ENTRANCE (Cont.):

INSULATION LINER, AFT CLOSURE SECTION (Cont.):

Volume of ellipsoidal cap at aft base of the cylindrical section, associated with the nozzle cutout, within the hemi-ellipsoid formed by the inside surface of the insulation liner within the aft case closure section. (Figure 6)

$$V_{IL_{HAIE}} = \left(\frac{V_{IL_{CLAI}}}{2}\right)\left(2 - 3\,R_{LILCAI} + R^3_{LILCAI}\right) \qquad (53)$$

Volume of cylinder with ellipsoidal cap, associated with the nozzle cutout, within the hemi-ellipsoid formed by the inside surface of the insulation liner within the aft case section. (Figure 6)

$$V_{IL_{HAI}} = V_{IL_{HAIE}} + V_{IL_{HAIC}} \qquad (54)$$

Volume of hemi-ellipsoid frustum with hole cutout associated with the inside surface of the insulation liner within the forward closure section. (Figure 6)

$$V_{IL_{CHAI}} = V_{IL_{CLAI}} - V_{IL_{HAI}} \qquad (55)$$

Volume of insulation liner within the aft case closure section. (Figure 6)

$$V_{IL_{CLA}} = \left(V_{IL_{CHAO}} - V_{IL_{CHAI}}\right) K_{IL_9} + K_{IL_{10}} \qquad (56)$$

EQUATIONS, SECOND ENTRANCE:

Equations 60 through 225 are evaluated at the second entrance to the INGM1 model.

INSULATION WEDGE, FORWARD AND AFT CLOSURE:

Equatorial diameter of the hemi-ellipsoids formed by the outside surface of the insulation wedges associated with the forward and aft closure sections. (Figures 7, 9, 11, 13)

$$D_{IW_{CLO}} = D_{IL_{CLI}} \tag{60}$$

INSULATION WEDGE, FORWARD CLOSURE:

Maximum thickness of the insulation wedge associated with the forward closure. Measured parallel to the motor centerline.

$$T_{IW_{FMAX}} = T_{IW_{MAX}} K_{IW_{21}} + K_{IW_{22}} \tag{61}$$

Diameter of the circular hole, for the igniter, centered on the axis of revolution of the hemi-ellipsoid formed by the outside surface of the insulation wedge associated with the forward case closure section. (Figures 7, 9)

$$D_{IW_{HFO}} = D_{IL_{HFI}} K_{IW_1} + K_{IW_2} \tag{62}$$

Diameter of the circular hole, for the igniter, centered on the axis of revolution of the hemi-ellipsoid formed by the inside surface of the insulation wedge associated with the forward case closure section. (Figures 7, 9)

$$D_{IW_{HFI}} = D_{IW_{HFO}} \tag{63}$$

Length of the cylindrical hole, for the igniter, within the insulation wedge of the forward case closure section. (Figures 7, 9)

$$L_{IW_{HF}} = T_{IW_{FMAX}} K_{IW_3} + K_{IW_4} \tag{64}$$

EQUATIONS, SECOND ENTRANCE (Cont.):

INSULATION WEDGE, FORWARD CLOSURE (Cont.):

Head ratio of the ellipsoid associated with the outside surface of the insulation wedge within the forward closure section.

$$R_{DIWCFO} = R_{DILCFI} \tag{65}$$

Length of the axis of revolution of the hemi-ellipsoid associated with the outside surface of the insulation wedge in the forward closure section. (Figures 7, 9)

$$L_{IW_{CLFO}} = \frac{R_{DIWCFO} \, D_{IW_{CLO}}}{2} \tag{66}$$

Diameter ratio, hole diameter to equatorial diameter, outside surface of the insulation wedge in the forward case closure section. (Figures 7, 9)

$$R_{DIWHFO} = \frac{D_{IW_{HFO}}}{D_{IW_{CLO}}} \tag{67}$$

Length of the hemi-ellipsoid frustum associated with the outside surface of the insulation wedge in the forward case closure section. (Figures 7, 9)

$$L_{IW_{CHFO}} = L_{IW_{CLFO}} \sqrt{1 - R^2_{DIWHFO}} \tag{68}$$

Distance from the equatorial plane of the hemi-ellipsoid associated with the outside surface of the insulation wedge in the forward closure to the inside base of the cylindrical hole cutout for the igniter within the insulation wedge in the forward closure. (Figures 7, 9)

$$L_{IW_{CHFI}} = L_{IW_{CHFO}} - L_{IW_{HF}} \tag{69}$$

Distance from the inside/outside wedge surface osculation plane to the inside base of the cylindrical hole cutout for the igniter. Note that the "inside/outside wedge surface osculation plane" may be within the forward case closure section or within the cylindrical case closure section. For the former case (see Figure 7), it is defined by the circle of osculation formed by the tangency points of the inside wedge surface hemi-ellipsoid and the outside wedge surface hemi-ellipsoid section. For the latter case (see Figure 9), it is defined by the circle of osculation formed by the tangency points of the inside wedge surface hemi-ellipsoid and the outside wedge surface cylindrical section. Note that the proportionality constant, K_{LIWFI1} must be determined by the user.

EQUATIONS, SECOND ENTRANCE (Cont.):

INSULATION WEDGE, FORWARD CLOSURE (Cont.):

$$L_{IW_{HFI}} = T_{PP_{WEB}} K_{LIWFI1} + K_{LIWFI2} \tag{70}$$

Distance from the equatorial plane of the hemi-ellipsoid associated with the outside surface of the insulation wedge in the forward case closure to the "inside/outside wedge surface osculation plane." Note that the insulation wedge is not completely within the forward closure section if $L_{IW_{CFI}}$ is negative. (Figures 7, 9)

$$L_{IW_{CFI}} = L_{IW_{CHFI}} - L_{IW_{HFI}} \tag{71}$$

IWINFCL (Insulation Wedge IN Forward CLosure) is a logical variable which specifies if the insulation wedge associated with the forward closure is completely within the forward closure.

IWINFCL = .TRUE., wedge is completely within the forward closure. See Figure 7.

IWINFCL = .FALSE., wedge extends beyond the forward closure into the cylindrical section or extends to the intersection of the aft closure and cylindrical section. See Figure 9.

IWINFCL = $L_{IW_{CFI}}$.GT.0

INSULATION WEDGE, COMPLETELY WITHIN FORWARD CLOSURE (IWINFCL = .TRUE.):

Equations 73 - 76 are evaluated if IWINFCL = .TRUE. (i.e., $L_{IW_{CFI}} > 0$) as illustrated in Figure 7.

Diameter of the circle of osculation formed by the tangency points of the inside wedge surface hemi-ellipsoid and the outside wedge surface hemi-ellipsoid (Figure 7). See equation 77 for an alternate expression.

$$D_{IW_{CFI}} = \frac{2\sqrt{L^2_{IW_{CLFO}} - L^2_{IW_{CFI}}}}{R_{DIWCFO}} \tag{73}$$

EQUATIONS, SECOND ENTRANCE (Cont.):

INSULATION WEDGE, COMPLETELY WITHIN FORWARD CLOSURE (IWINFCL = .TRUE.)(Cont.):

Distance from the equatorial plane of the hemi-ellipsoid associated with the outside surface of the insulation wedge in the forward closure to the equatorial plane of the hemi-ellipsoid associated with the inside surface of the insulation wedge in the forward case closure. (Figure 7) See equation 78 for an alternate expression. (74)

$$L_{IW_{CEFI}} = \frac{-L_{IW_{CFI}}\left[4\left(L^2_{IW_{CFI}} - L^2_{IW_{CHFI}}\right) + R^2_{DIWCFO}\left(D^2_{IW_{CFI}} - D^2_{IW_{HFI}}\right)\right]}{8\, L_{IW_{CFI}}\, L_{IW_{HFI}} - R^2_{DIWCFO}\left(D^2_{IW_{CFI}} - D^2_{IW_{HFI}}\right)}$$

Length of the axis of revolution of the hemi ellipsoid associated with the inside surface of the insulation wedge in the forward case closure. (Figure 7) See equation 81 for an alternate expression. (75)

$$L_{IW_{EFI}} = \sqrt{\frac{D^2_{IW_{CFI}}\left(L_{IW_{CHFI}} - L_{IW_{CEFI}}\right)^2 - D^2_{IW_{HFI}}\left(L_{IW_{CFI}} - L_{IW_{CEFI}}\right)^2}{D^2_{IW_{CFI}} - D^2_{IW_{HFI}}}}$$

Equatorial diameter of hemi-ellipsoid associated with the inside surface of the insulation wedge in the forward case closure. (Figure 7) See equation 79 for an alternate expression.

$$D_{IW_{EFI}} = \frac{2\, L_{IW_{EFI}}}{R_{DIWCFO}} \sqrt{\frac{L_{IW_{CFI}}}{\left(L_{IW_{CFI}} - L_{IW_{CEFI}}\right)}} \qquad (76)$$

Equations 77 - 81 are evaluated if IWINFCL = .FALSE. (i.e., $L_{IW_{CFI}} \leq 0$) as illustrated in Figure 9.

Diameter of the circle of osculation formed by the tangency points of the inside wedge surface hemi-ellipsoid and the outside wedge surface cylinder. (Figure 9) See equation 73 for an alternate expression.

$$D_{IW_{CFI}} = D_{IW_{CLO}} \qquad (77)$$

Distance from the equatorial plane of the hemi-ellipsoid associated with the outside surface of the insulation wedge in the forward case closure to the equatorial plane of the hemi-ellipsoid associated with the inside surface of the insulation wedge in the forward case closure. (Figure 9) See equation 74 for an alternate expression.

EQUATIONS, SECOND ENTRANCE (Cont.):

INSULATION WEDGE, EXTENDS BEYOND FORWARD CLOSURE (IWINFCL = .FALSE.) (Cont.):

$$L_{IW_{CEFI}} = L_{IW_{CFI}} \tag{78}$$

Equatorial diameter of the hemi-ellipsoid associated with the inside surface of the insulation wedge in the forward case closure. (Figure 9) See equation 76 for an alternate expression.

$$D_{IW_{EFI}} = D_{IW_{CLO}} \tag{79}$$

Diameter ratio, hole diameter to equatorial diameter, inside surface of insulation wedge in the forward case closure. (Figure 9)

$$R_{DIWHFI} = \frac{D_{IW_{HFI}}}{D_{IW_{EFI}}} \tag{80}$$

Length of the axis of revolution of the hemi-ellipsoid associated with the inside surface of the insulation wedge in the forward case closure. (Figure 9) See equation 75 for an alternate expression.

$$L_{IW_{EFI}} = \frac{L_{IW_{HFI}}}{\sqrt{1 - R^2_{DIWHFI}}} \tag{81}$$

INSULATION WEDGE, FORWARD CLOSURE:

Head ratio of the ellipsoid associated with the inside surface of the insulation wedge in the forward case closure section.

$$R_{DIWCFI} = \left(\frac{2\, L_{IW_{EFI}}}{D_{IW_{EFI}}}\right) \tag{81-a}$$

Distance from the pole of the hemi-ellipsoid associated with the inside surface of the insulation wedge in the forward closure to the equatorial plane of the hemi-ellipsoid associated with the outside surface of the insulation wedge in the forward closure. Note that if the wedge extends beyond the closure into the cylindrical section, $L_{IW_{CEFI}}$ has a negative value (Figures 7, 9)

EQUATIONS, SECOND ENTRANCE (Cont.):

INSULATION WEDGE, FORWARD CLOSURE (Cont.):

$$L_{IW_{CLFI}} = L_{IW_{EFI}} + \left(L_{IW_{CEFI}}\right) \tag{82}$$

Distance from the pole of the hemi-ellipsoid associated with the inside surface of the insulation wedge in the forward closure to the forward closure inside/outside surface osculation plane. Note that if the wedge extends beyond the closure into the cylindrical section, $L_{IW_{CFI}}$ has a negative value. (Figures 7, 9)

$$L_{IW_{FI}} = L_{IW_{CLFI}} - \left(L_{IW_{CFI}}\right) \tag{83}$$

Distance from the equatorial plane of the hemi-ellipsoid associated with the inside surface of the insulation wedge in the forward case closure to the inside base of the cylindrical hole cutout for the igniter within the insulation wedge in the forward closure. (Figures 7, 9)

$$L_{IW_{EHFI}} = L_{IW_{EFI}} - L_{IW_{FI}} + L_{IW_{HFI}} \tag{84}$$

Volume of the hemi-ellipsoid associated with the outside surface of the insulation wedge within the forward case closure. (Figures 7, 8, 9, 10)

$$V_{IW_{CLFO}} = \left(\frac{\pi}{6}\right) L_{IW_{CLFO}} D^2_{IW_{CLO}} \tag{85}$$

Length ratio, hemi-ellipsoid frustum to hemi-ellipsoid, outside surface, insulation wedge, forward case closure section. (Figures 7, 9)

$$R_{LIWCF1} = \frac{L_{IW_{CHFO}}}{L_{IW_{CLFO}}} \tag{86}$$

Volume of ellipsoidal cap, at forward base of the cylindrical section associated with the igniter cutout, within the hemi-ellipsoid associated with the outside surface of the insulation wedge in the forward case closure section. (Figures 8, 10)

$$V_{IW_{HFOE}} = \left(\frac{V_{IW_{CLFO}}}{2}\right)\left(2 - 3\,R_{LIWCF1} + R^3_{LIWCF1}\right) \tag{87}$$

EQUATIONS, SECOND ENTRANCE (Cont.):

INSULATION WEDGE, FORWARD CLOSURE (Cont.):

Volume of the cylindrical section, associated with the ignitor hole, within the hemi-ellipsoid associated with the outside surface of the insulation wedge in the forward case closure section. (Figures 8, 10)

$$V_{IW_{HFOC}} = \left(\frac{\pi}{4}\right) L_{IW_{CHFO}} D^2_{IW_{HFI}} \tag{88}$$

INSULATION WEDGE, COMPLETELY WITHIN FORWARD CLOSURE (IWINFCL = .TRUE.):

Equations 89 - 93 are evaluated if the insulation wedge is completely within the forward closure, i.e., $L_{IW_{CFI}} > 0$. (See Figures 7, 8)

Volume of the cylindrical section, associated with the igniter hole, within the hemi-ellipsoid associated with the outside surface of the insulation wedge in the forward case closure section. The bases of the cylindrical section are the equatorial plane of the hemi-ellipsoid and the "inside/outside wedge surface osculation plane". (Figures 7, 8)

$$V_{IW_{HFOL}} = \left(\frac{\pi}{4}\right) L_{IW_{CFI}} D^2_{IW_{HFI}} \tag{89}$$

Volume of the cylinder with ellipsoidal cap, associated with the igniter hole, within the hemi-ellipsoid associated with the outside surface of the insulation wedge in the forward case closure section. The cylindrical base is the "inside/outside wedge surface osculation plane". (Figures 7, 8) See equation 95 for an alternate expression.

$$V_{IW_{HFO}} = V_{IW_{HFOE}} + V_{IW_{HFOC}} - V_{IW_{HFOL}} \tag{90}$$

Length ratio, hemi-ellipsoid frustum (with equatorial and "inside/outside wedge surface osculation plane" bases) to hemi-ellipsoid, outside surface, insulation wedge, forward base closure section. (Figures 7, 8)

$$R_{LIWCF2} = \frac{L_{IW_{CFI}}}{L_{IW_{CLFO}}} \tag{91}$$

EQUATIONS, SECOND ENTRANCE (Cont.):

INSULATION WEDGE, COMPLETELY WITHIN FORWARD CLOSURE (IWINFCL = .TRUE.) (Cont.):

Volume of the ellipsoidal cap formed by the intersection of the "inside/outside wedge surface osculation plane" and the hemi-ellipsoid associated with the outside surface of the insulation wedge in the forward case closure section. (Figures 8, 9)

$$V_{IW_{CFOE}} = \left(\frac{V_{IW_{CLFO}}}{2}\right)\left(2 - 3\,R_{LIWCF2} + R^3_{LIWCF2}\right) \tag{92}$$

Volume of the ellipsoidal cap with hole cutout for the igniter, formed by the intersection of the "inside/outside wedge surface osculation plane" and the hemi-ellipsoid associated with the outside surface of the insulation wedge in the forward case closure section. (Figure 8) See equation 97 for an alternate expression.

$$V_{IW_{CHFO}} = V_{IW_{CFOE}} - V_{IW_{HFO}} \tag{93}$$

INSULATION WEDGE, EXTENDS BEYOND FORWARD CLOSURE (IWINFCL = .FALSE.):

Equations 94 - 97 are evaluated if the insulation wedge is not completely within the forward closure, i.e., $L_{IW_{CFI}} \leq 0.$ (See Figures 9, 10)

Volume of the cylindrical section, associated with the igniter hole, within the cylindrical case section associated with the outside surface of the insulation wedge in the forward case closure section. The bases of the cylindrical section are the equatorial plane of the hemi-ellipsoid and the "inside/outside wedge surface osculation plane". (Figures 9, 10) Note that this is a positive volume. See equation 90 for an alternate expression.

$$V_{IW_{HFOY}} = \left(\frac{\pi}{4}\right)\left(-L_{IW_{CFI}}\right) D^2_{IW_{HFO}} \tag{94}$$

EQUATIONS, SECOND ENTRANCE (Cont.):

INSULATION WEDGE, EXTENDS BEYOND FORWARD CLOSURE (IWINFCL = .FALSE.) (Cont.):

Volume of the cylinder, with ellipsoidal cap, associated with the igniter hole, in the hemi-ellipsoid and cylinder associated with the outside surface of the insulation wedge in the forward case closure section. (Figure 10) See equation 90 for an alternate expression.

$$V_{IW_{HFO}} = V_{IW_{HFOE}} + V_{IW_{HFOC}} + V_{IW_{HFOY}} \tag{95}$$

Volume of the cylindrical section associated with the outside surface of the insulation wedge in the forward case closure section. (Figures 9, 10) Note that this is a positive volume.

$$V_{IW_{FOY}} = \left(\frac{\pi}{4}\right) \left(- L_{IW_{CFI}}\right) D^2_{IW_{CLO}} \tag{96}$$

Volume of hemi-ellipsoid and cylinder, with hole cutout for the igniter, which forms the outside surface of the insulation wedge in the forward case closure section. (Figures 8, 10) See equation 93 for an alternate expression.

$$V_{IW_{CHFO}} = V_{IW_{CLFO}} + V_{IW_{FOY}} - V_{IW_{HFO}} \tag{97}$$

INSULATION WEDGE, FORWARD CLOSURE:

Volume of the hemi-ellipsoid associated with the inside surface of the insulation wedge within the forward case closure section. (Figures 7, 9)

$$V_{IW_{EFI}} = \left(\frac{\pi}{6}\right) L_{IW_{EFI}} \; D^2_{IW_{EFI}} \tag{98}$$

Length ratio, hemi-ellipsoid frustum (with equatorial and inside cylindrical hole cutout for the igniter bases) to hemi-ellipsoid, inside surface, insulation wedge, forward case closure section. (Figures 7, 9)

$$R_{LIWCF3} = \frac{L_{IW_{EHFI}}}{L_{IW_{EFI}}} \tag{99}$$

EQUATIONS, SECOND ENTRANCE (Cont.):

INSULATION WEDGE, FORWARD CLOSURE (Cont.):

Volume of ellipsoidal cap, at forward base of the cylindrical section associated with the igniter cutout, within the hemi-ellipsoid associated with the inside surface of the insulation wedge in the forward case closure section. (Figures 8, 10)

$$V_{IW_{HFIE}} = \left(\frac{V_{IW_{EFI}}}{2}\right)\left(2 - 3\,R_{LIWCF3} + R^3_{LIWCF3}\right) \qquad (100)$$

Volume of the cylindrical section, associated with the igniter hole, within the hemi-ellipsoid associated with the inside surface of the insulation wedge in the forward case closure section. (Figures 8, 10)

$$V_{IW_{HFIC}} = \left(\frac{\pi}{4}\right)\; L_{IW_{EHFI}}\; D^2_{IW_{HFI}} \qquad (101)$$

Volume of the cylinder with ellipsoidal cap, associated with the igniter hole, in the hemi-ellipsoid associated with the inside surface of the insulation wedge in the forward case closure section. (Figures 8, 10)

$$V_{IW_{HFI}} = V_{IW_{HFIE}} + V_{IW_{HFIC}} \qquad (102)$$

Length ratio, hemi-ellipsoid frustum (with equatorial and "inside/outside wedge surface osculation plane" bases) to hemi-ellipsoid, inside surface, insulation wedge, forward case closure section. (Figures 7, 9)

$$R_{LIWCF4} = \frac{\left(L_{IW_{EFI}} - L_{IW_{FI}}\right)}{L_{IW_{EFI}}} \qquad (103)$$

Volume of the ellipsoidal cap associated with the inside surface of the insulation wedge in the forward case closure section. If the insulation wedge extends beyond the closure, $V_{IW_{EFIE}}$ is the hemi-ellipsoid volume. (Figures 8, 10)

$$V_{IW_{EFIE}} = \left(\frac{V_{IW_{EFI}}}{2}\right)\left(2 - 3\,R_{LIWCF4} + R^3_{LIWCF4}\right) \qquad (104)$$

EQUATIONS, SECOND ENTRANCE (Cont.):

INSULATION WEDGE, FORWARD CLOSURE (Cont.):

Volume of the ellipsoidal cap, with hole cutout for the igniter, which forms the inside surface of the insulation wedge in the forward case closure section. (Figures 8, 10)

$$V_{IW_{CHFI}} = \left(V_{IW_{EFIE}} - V_{IW_{HFI}}\right) \tag{105}$$

Volume of insulation material required for the insulation wedge associated with the forward case closure section. (Figures 8, 10)

$$V_{IW_{CLF}} = \left(V_{IW_{CHFO}} - V_{IW_{CHFI}}\right) K_{IW_7} + K_{IW_8} \tag{106}$$

INSULATION WEDGE, AFT CLOSURE, BOUNDS FOR AN ACCEPTABLE SOLUTION:

The following conditions must be satisfied for acceptable solutions in determining the insulation wedge volume requirements associated with the aft closure. If the conditions are not satisfied, a diagnostic is usually printed and computations of sizing quantities may be terminated. See Figures 11, 13 and the figures associated with the GRAING model type.

The forward base of the submerged nozzle cone frustum grain cutout must not be aft of the aft closure.

$$\left(-L_{CF_{CY}}\right) \leq L_{IW_{CLAO}} \tag{107-a}$$

If the forward base of the submerged nozzle cone frustum grain cutout is in the cylindrical section, its diameter may not exceed the diameter of the inside surface of the insulation liner within the cylindrical section.

$$\text{For} \quad \left(-L_{CF_{CY}}\right) \leq 0; \quad 0 < D_{CFF} \leq D_{IL_I} \tag{107-b}$$

If the forward base of the submerged nozzle cone frustum grain cutout is in the closure section, its diameter may not exceed the diameter of the inside surface of the insulation liner within the closure section.

$$\text{For} \quad \left(-L_{CF_{CY}}\right) \geq 0; \quad 0 < \left(\frac{D_{CFF}}{2}\right) \leq \left[\sqrt{\frac{L^2_{IL_{CLAI}} - L^2_{CF_{CY}}}{R_{DILCAI}}}\right] \tag{107-c}$$

EQUATIONS, SECOND ENTRANCE (Cont.):

INSULATION WEDGE, AFT CLOSURE. BOUNDS FOR AN ACCEPTABLE SOLUTION (Cont.):

The "inside/outside wedge surface osculation plane" must be forward of the forward base of the submerged nozzle cone frustum insulation wedge cutout. See Figures 11, 13.

$$L_{IW_{HAI}} > \left[L_{IW_{CHAI}} + L_{CF_{CY}}\right] \tag{107-d}$$

The forward base of the submerged nozzle cone frustum grain cutout must be forward of the aft base of the submerged nozzle cone frustum grain cutout.

$$-\left(\frac{\pi}{2}\right) < \theta_{CF} < \left(\frac{\pi}{2}\right) \tag{107-e}$$

INSULATION WEDGE, AFT CLOSURE:

Maximum thickness of the insulation wedge associated with the aft closure. Measured parallel to the slant height of the cone frustum grain cutout. See Figures 11, 13.

$$T_{IW_{AMAX}} = T_{IW_{MAX}} K_{IW_9} + K_{IW_{10}} \tag{108}$$

Diameter of the aft base of the cone frustum hole, for the nozzle cutout, centered on the axis of revolution of the hemi-ellipsoid formed by the outside surface of the insulation wedge associated with the aft case closure section. (Figures 11, 13)

$$D_{IW_{HAO}} = D_{IL_{HAI}} K_{IW_{11}} + K_{IW_{12}} \tag{109}$$

Diameter of the forward base of the cone frustum hole, for the nozzle cutout, centered on the axis of revolution of the hemi-ellipsoid formed by the inside surface of the insulation wedge associated with the aft case closure section. (Figures 11, 13)

$$D_{IW_{HAI}} = \left|D_{IW_{HAO}} K_{IW_{13}} - \left[2\, T_{IW_{AMAX}} \sin\left(\theta_{CF}\right)\right] K_{IW_{14}}\right| K_{IW_{15}} + K_{IW_{16}} \tag{110}$$

EQUATIONS, SECOND ENTRANCE (Cont.):

INSULATION WEDGE, AFT CLOSURE (Cont.):

Altitude of the cone frustum, for the nozzle cutout, within the insulation wedge of the aft case closure section. (Figures 11, 13)

$$L_{IW_{HA}} = \left[T_{IW_{AMAX}} \cos\left(\theta_{CF}\right)\right] K_{IW_{17}} + K_{IW_{18}} \tag{111}$$

Head ratio of the ellipsoid associated with the outside surface of the insulation wedge in the aft case closure section. See equation 39.

$$R_{DIWCAO} = R_{DILCAI} \tag{112}$$

Length of the axis of revolution of the hemi-ellipsoid associated with the outside surface of the insulation wedge in ther aft closure section. (Figures 11, 13)

$$L_{IW_{CLAO}} = \frac{R_{DIWCAO} D_{IW_{CLO}}}{2} \tag{113}$$

Diameter ratio, aft base of cone frustum hole to equatorial diameter, outside surface of the insulation wedge in the aft case closure section. (Figures 11, 13)

$$R_{DIWHAO} = \frac{D_{IW_{HAO}}}{D_{IW_{CLO}}} \tag{114}$$

Length of the hemi-ellipsoid frustum associated with the outside surface of the insulation wedge in the aft case closure section. (Figures 11, 13)

$$L_{IW_{CHAO}} = L_{IW_{CLAO}} \sqrt{1 - R^2_{DIWHAO}} \tag{115}$$

Distance from the equatorial plane of the hemi-ellipsoid associated with the outside surface of the insulation wedge in the aft case closure section to forward base of the cone frustum hole, for the nozzle cutout, within the insulation wedge in the aft case closure section. (Figures 11, 13)

$$L_{IW_{CHAI}} = L_{IW_{CHAO}} - L_{IW_{HA}} \tag{116}$$

EQUATIONS, SECOND ENTRANCE (Cont.):

DETERMINATION IF AFT CLOSURE WEDGE EXTENDS BEYOND THE CLOSURE:

To determine if the insulation wedge lies completely within the aft case closure section (see Figure 11), or extends beyond the aft closure section into the cylindrical section (see Figure 13), the following procedure is utilized.

$L_{IW_{CAI}}$ is first evaluated using the cylindrical geometry of equation 117.

If $L_{IW_{CAI}} \leq 0$, (i.e., IWINACL = .FALSE.), the "inside/outside wedge surface osculation plane" lies within the cylindrical section and equation 119 is used to evaluate $D_{IW_{CAI}}$. See Figure 13.

If $L_{IW_{CAI}} > 0$, (i.e., IWINACL = .TRUE.), the "inside/outside wedge surface osculation plane" lies within the aft closure section and the ellipsoidal geometry of equations 120 - 124 must be used to reevaluate $L_{IW_{CAI}}$ and $D_{IW_{CAI}}$.

For a derivation of equations 117 - 124, and root selection rationale, see reference 55.

Distance from the "equatorial plane of the aft closure outside wedge surface hemi-ellipsoid" to the "inside/outside wedge surface osculation plane". Measured along the axis of revolution, positive sense aft. A positive value indicates that the wedge is completely within the aft closure. A negative value indicates that the wedge extends beyond the aft closure into the cylindrical section. See IWINACL, equation 118. See equation 124 for an alternate expression.

$$L_{IW_{CAI}} = \left(-L_{CF_{CY}}\right) - \left(\frac{1}{2}\right) \left(D_{IW_{CLO}} - D_{CFF}\right) \tan \left(\theta_{CF}\right) \qquad (117)$$

EQUATIONS, SECOND ENTRANCE (Cont.):

DETERMINATION IF AFT CLOSURE WEDGE EXTENDS BEYOND THE CLOSURE (Cont.):

IWINACL (Insulation Wedge IN Aft CLosure) is a logical variable which specifies if the insulation wedge associated with the aft closure is completely within the aft closure.

If IWINACL = .TRUE.; the insulation wedge is completely within the aft closure. Equations 124, 123 are used to evaluate $L_{IW_{CAI}}$ and $D_{IW_{CAI}}$. See Figures 11, 12.

If IWINACL = .FALSE.; the insulation wedge extends beyond the aft closure into the cylindrical section, or extends to the intersection of the aft closure and cylindrical section. Equations 117, 119 are used to evaluate $L_{IW_{CAI}}$ and $D_{IW_{CAI}}$. See Figures 13, 14.

For the following logical expression, $L_{IW_{CAI}}$ is evaluated using equation 117.

$$IWINACL = L_{IW_{CAI}} .GT. 0 \tag{118}$$

INSULATION WEDGE, EXTENDS BEYOND AFT CLOSURE (IWINACL = .FALSE.):

Equation 119 is evaluated if the insulation wedge extends beyond the aft closure into the cylindrical section, i.e., $L_{IW_{CAI}} \leq 0$.

Note that $L_{IW_{CAI}}$ is evaluated using equation 117 above.

Diameter of the "inside/outside osculation circle" associated with the aft closure insulation wedge. (Figure 15) See equation 123 for an alternate expression.

$$D_{IW_{CAI}} = D_{IW_{CIO}} \tag{119}$$

EQUATIONS, SECOND ENTRANCE (Cont.):

INSULATION WEDGE, COMPLETELY WITHIN AFT CLOSURE (IWINACL = .TRUE.):

Equations 120 - 124 are evaluated if the insulation wedge lies completely within the aft closure, i.e., $L_{IW_{CAI}} > 0$ as evaluated by equation 117.

Note that $L_{IW_{CAI}}$ is reevaluated using equation 124.

Equations 120 - 122 are intermediate computations for $D_{IW_{CAI}}$ as shown in reference 55.

$$C_{IW_A} = \tan^2(\theta_{CF}) + R^2_{DIWCAO} \tag{120}$$

$$C_{IW_B} = -\tan(\theta_{CF})\left[2\left(-L_{CF_{CY}}\right) + D_{CFF}\tan(\theta_{CF})\right] \tag{121}$$

$$C_{IW_C} = L^2_{CF_{CY}} - L^2_{IW_{CLAO}} + \left(\frac{D_{CFF}}{2}\right)\tan(\theta_{CF})\left[\left(\frac{D_{CFF}}{2}\right)\tan(\theta_{CF}) + 2\left(-L_{CF_{CY}}\right)\right] \tag{122}$$

Diameter of the "inside/outside osculation circle" associated with the aft closure insulation wedge. Se IWINACL, equation 118 and Figure 11. See equation 119 for an alternate expression.

$$D_{IW_{CAI}} = \frac{-C_{IW_B} + \sqrt{C^2_{IW_B} - 4\,C_{IW_A}\,C_{IW_C}}}{C_{IW_A}} \tag{123}$$

Distance from the "equatorial plane of the aft closure outside wedge surface hemi-ellipsoid" to the "inside/outside wedge surface osculation plane". Measured along the axis of revolution, positive sense aft. Since the wedge is completely within the aft closure, the value will be positive. Se IWINACL, equation 118, and Figure 11. See equation 117 for an alternate expression.

$$L_{IW_{CAI}} = \left(-L_{CF_{CY}}\right) - \left(\frac{1}{2}\right)\left(D_{IW_{CAI}} - D_{CFF}\right)\tan(\theta_{CF}) \tag{124}$$

EQUATIONS, SECOND ENTRANCE (Cont.):

INSULATION WEDGE, AFT CLOSURE:

Distance from the "inside/outside wedge surface osculation plane" to the inside base of the cone frustum hole cutout of the insulation wedge for the nozzle. Note that the "inside/outside wedge surface osculation plane" may be within the aft case closure section or within the cylindrical case closure section. For the former case (see Figure 11), it is defined by the circle of osculation formed by the tangency points of the inside wedge surface hemi-ellipsoid and the outside wedge surface hemi-ellipsoid section. For the latter case (see Figure 13), it is defined by the circle of osculation formed by the tangency points of the inside wedge surface hemi-ellipsoid and the outside wedge surface cylindrical section.

$$L_{IW_{HAI}} = L_{IW_{CHAI}} - L_{IW_{CAI}} \tag{125}$$

INSULATION WEDGE, COMPLETELY WITHIN THE AFT CLOSURE (IWINACL = TRUE.):

Equations 126 - 128 are evaluated if the insulation wedge lies completely within the aft closure. See equations 129 - 131 if the wedge extends beyond the aft closure into the cylindrical section.

Distance from the equatorial plane of the hemi-ellipsoid associated with the outside surface of the insulation wedge in the aft case closure section to the equatorial plane of the hemi-ellipsoid associated with the inside surface of the insulation wedge in the aft case closure section. (Figure 11) See equation 129 for an alternate expression.

$$L_{IW_{CEAI}} = \frac{-L_{IW_{CAI}}\left[4\left(L^2_{IW_{CAI}} - L^2_{IW_{CHAI}}\right) + R^2_{DIWCAO}\left(D^2_{IW_{CAI}} - D^2_{IW_{HAI}}\right)\right]}{8\,L_{IW_{CAI}}\,L_{IW_{HAI}} - R^2_{DIWCAO}\left(D^2_{IW_{CAI}} - D^2_{IW_{HAI}}\right)} \tag{126}$$

Length of the axis of revolution of the hemi-ellipsoid associated with the inside surface of the insulation wedge in the aft case closure. (Figure 11) See equation 131 for an alternate expression.

$$L_{IW_{EAI}} = \sqrt{\frac{-D^2_{IW_{HAI}}\left(L_{IW_{CAI}} - L_{IW_{CEAI}}\right)^2 + D^2_{IW_{CAI}}\left(L_{IW_{CHAI}} - L_{IW_{CEAI}}\right)^2}{D^2_{IW_{CAI}} - D^2_{IW_{HAI}}}} \tag{127}$$

EQUATIONS, SECOND ENTRANCE (Cont.):

INSULATION WEDGE, COMPLETELY WITHIN THE AFT CLOSURE (IWINACL = .TRUE.)(Cont.):

Equatorial diameter of the hemi-ellipsoid associated with the inside surface of the insulation wedge in the aft case closure section. (Figure 11) See equation 130 for an alternate expression.

$$D_{IW_{EAI}} = \left(\frac{2\,L_{IW_{EAI}}}{R_{DIWCAO}}\right)\sqrt{\frac{L_{IW_{CAI}}}{\left(L_{IW_{CAI}} - L_{IW_{CEAI}}\right)}} \qquad (128)$$

INSULATION WEDGE, EXTENDS BEYOND AFT CLOSURE (IWINACL = .FALSE.):

Equations 129 - 131 below are evaluated if the insulation wedge extends beyond the aft closure into the cylindrical section, as illustrated by Figure 13.

Distance from the equatorial plane of the hemi-ellipsoid associated with the outside surface of the insulation wedge in the aft case closure section to the equatorial plane of the hemi-ellipsoid associated with the inside surface of the insulation wedge in the aft case closure section. (Figure 13) See equation 126 for an alternate expression.

$$L_{IW_{CEAI}} = L_{IW_{CAI}} \qquad (129)$$

Equatorial diameter of the hemi-ellipsoid associated with the inside surface of the insulation wedge in the aft case closure section. (Figure 13) See equation 128 for an alternate expression.

$$D_{IW_{EAI}} = D_{IW_{CLO}} \qquad (130)$$

Length of the axis of revolution of the hemi-ellipsoid associated with the inside surface of the insulation wedge in the aft case closure section. (Figure 13) See equation 127 for an alternate expression.

$$L_{IW_{EAI}} = \frac{L_{IW_{HAI}}}{\sqrt{1 - \left(\frac{D_{IW_{HAI}}}{D_{IW_{EAI}}}\right)^2}} \qquad (131)$$

EQUATIONS, SECOND ENTRANCE (Cont.):

INSULATION WEDGE, AFT CLOSURE:

Head ratio of the ellipsoid associated with the inside surface of the insulation wedge in the aft case closure section.

$$R_{DIWCAI} = \left(\frac{2\, L_{IW_{EAI}}}{D_{IW_{EAI}}} \right) \tag{131-a}$$

Distance from the pole of the hemi-ellipsoid associated with the inside surface of the insulation wedge in the aft closure to the equatorial plane of the hemi-ellipsoid associated with the outside surface of the insulation wedge in the aft closure. Note that if the wedge extends beyond the closure into the cylindrical section, $L_{IW_{CEAI}}$ has a negative value. (Figures 11, 13)

$$L_{IW_{CLAI}} = L_{IW_{EAI}} + \left(L_{IW_{CEAI}} \right) \tag{132}$$

Distance from the pole of the hemi-ellipsoid associated with the inside surface of the insulation wedge in the aft closure to the aft closure "inside/outside wedge surface osculation plane". Note that if the wedge extends beyond the closure into the cylindrical section, $L_{IW_{CAI}}$ has a negative value. (Figures 11, 13)

$$L_{IW_{AI}} = L_{IW_{CLAI}} - \left(L_{IW_{CAI}} \right) \tag{133}$$

Distance from the equatorial plane of the hemi-ellipsoid associated with the inside surface of the insulation wedge in the aft case closure to the inside base of the cone frustum cutout within the insulation wedge in the aft case closure section. (Figures 11, 13)

$$L_{IW_{EHAI}} = L_{IW_{EAI}} - L_{IW_{AI}} + L_{IW_{HAI}} \tag{134}$$

Volume of the hemi-ellipsoid associated with the outside surface of the insulation wedge in the aft case closure section. (Figures 11, 13, 14)

$$V_{IW_{CLAO}} = \left(\frac{\pi}{6} \right) L_{IW_{CLAO}}\, D^2_{IW_{CLO}} \tag{135}$$

EQUATIONS, SECOND ENTRANCE (Cont.):

INSULATION WEDGE, AFT CLOSURE (Cont.):

Length ratio, hemi-ellipsoid frustum to hemi-ellipsoid, outside surface, insulation wedge, aft case closure section. (Figures 11, 13)

$$R_{LIWCA1} = \frac{L_{IW_{CHAO}}}{L_{IW_{CLAO}}} \tag{136}$$

Volume of the ellipsoidal cap, at aft base of the cone frustum section associated with the nozzle cutout, within the hemi-ellipsoid associated with the outside surface of the insulation wedge in the aft case closure section. (Figures 12,14)

$$V_{IW_{HAOE}} = \left(\frac{V_{IW_{CLAO}}}{2}\right)\left(2 - 3\,R_{LIWCA1} + R^{3}_{LIWCA1}\right) \tag{137}$$

Volume of the cylindrical section, associated with the nozzle cutout, within the hemi-ellipsoid frustum associated with the outside surface of the insulation wedge in the aft case closure section. (Figures 12, 14)

$$V_{IW_{HAOC}} = \left(\frac{\pi}{4}\right)\left(L_{IW_{CHAO}} - L_{IW_{CAI}}\right) D^{2}_{IW_{HAI}} \tag{138}$$

INSULATION WEDGE, COMPLETELY WITHIN CLOSURE (IWINACL = .TRUE.):

Equations 139 - 141 are evaluated if the insulation wedge lies completely within the aft closure. See Figures 11, 12.

Length ratio, hemi-ellipsoid frustum (with equatorial and "inside/outside wedge surface osculation plane" bases) to hemi-ellipsoid, outside surface, insulation wedge, aft case closure section. (Figures 11, 12)

$$R_{LIWCA2} = \frac{L_{IW_{CAI}}}{L_{IW_{CLAO}}} \tag{139}$$

EQUATIONS, SECOND ENTRANCE (Cont.):

INSULATION WEDGE, COMPLETELY WITHIN CLOSURE (IWINACL = .TRUE.)(Cont.):

Volume of the ellipsoidal cap formed by the intersection of the "inside/outside wedge surface osculation plane" and the hemi-ellipsoid associated with the outside surface of the insulation wedge in the aft case closure section. (Figure 12)

$$V_{IW_{CAOE}} = \left(\frac{V_{IW_{CLAO}}}{2}\right)\left(2 - 3\ R_{LIWCA2} + R^3_{LIWCA2}\right) \tag{140}$$

Volume of the hemi-ellipsoid frustum, with cylindrical hole cutout, associated with the outside surface of the insulation wedge in the aft case closure section. (Figure 12) See equation 143 for an alternate expression.

$$V_{IW_{CHAO}} = V_{IW_{CAOE}} - V_{IW_{HAOE}} - V_{IW_{HAOC}} \tag{141}$$

INSULATION WEDGE, EXTENDS BEYOND AFT CLOSURE (IWINACL = .FALSE.):

Equations 142, 143, are evaluated if the insulation wedge extends beyond the aft closure into the cylindrical section. See Figures 13, 14.

Volume of the cylindrical section associated with the outside surface of the insulation wedge in the aft case closure section. (Figures 13, 14) Note that this is a positive volume.

$$V_{IW_{AOY}} = \left(\frac{\pi}{4}\right)\left(-L_{IW_{CAI}}\right) D^2_{IW_{CLO}} \tag{142}$$

Volume of the hemi-ellipsoid frustum, with cylindrical hole cutout, associated with the outside surface of the insulation wedge in the aft closure section. (Figure 14) See equation 141 for an alternate expression.

$$V_{IW_{CHAO}} = V_{IW_{AOY}} + V_{IW_{CLAO}} - V_{IW_{HAOE}} - V_{IW_{HAOC}} \tag{143}$$

EQUATIONS, SECOND ENTRANCE (Cont.):

INSULATION WEDGE, AFT CLOSURE:

Volume of the hemi-ellipsoid associated with the inside surface of the insulation wedge within the aft case closure. (Figures 11, 13)

$$V_{IW_{EAI}} = \left(\frac{\pi}{6}\right) L_{IW_{EAI}} D^2_{IW_{EAI}} \tag{144}$$

Length ratio, hemi-ellipsoid frustum (with equatorial base and inside nozzle cutout base) to hemi-ellipsoid, inside surface, insulation wedge, aft case closure section. (Figures 11, 13)

$$R_{LIWCA3} = \frac{L_{IW_{EHAI}}}{L_{IW_{EAI}}} \tag{145}$$

Volume of the ellipsoidal cap, at the aft base of the cone frustum section associated with the nozzle cutout, within the hemi-ellipsoid associated with the inside surface of the insulation wedge in the aft case closure section. (Figures 12, 14)

$$V_{IW_{HAIE}} = \left(\frac{V_{IW_{EAI}}}{2}\right)\left(2 - 3\,R_{LIWCA3} + R^3_{LIWCA3}\right) \tag{146}$$

Volume of the cylindrical section, associated with the nozzle cutout, within the hemi-ellipsoid associated with the inside surface of the insulation wedge in the aft case closure section. (Figures 12, 14)

$$V_{IW_{HAIC}} = \left(\frac{\pi}{4}\right) L_{IW_{HAI}} D^2_{IW_{HAI}} \tag{147}$$

Volume of the cylinder, with ellipsoidal cap, associated with the nozzle cutout cone frustum, in the hemi-ellipsoid associated with the inside surface of the insulation wedge in the aft case closure section. (Figures 12, 14)

$$V_{IW_{HAI}} = V_{IW_{HAIE}} + V_{IW_{HAIC}} \tag{148}$$

EQUATIONS, SECOND ENTRANCE (Cont.):

INSULATION WEDGE, AFT CLOSURE (Cont.):

Length ratio, hemi-ellipsoid frustum (with equatorial and "inside/outside wedge surface osculation plane" bases) to hemi-ellipsoid, inside surface, insulation wedge, aft case closure section. (Figures 11, 13)

$$R_{LIWCA4} = \frac{\left(L_{IW_{CAI}} - L_{IW_{CEAI}}\right)}{L_{IW_{EAI}}} \tag{149}$$

Volume of the ellipsoidal cap associated with the inside surface of the insulation wedge in the aft case closure. If the insulation wedge extends beyond the closure, $V_{IW_{EAIE}}$ is the hemi-ellipsoid volume. (Figures 12, 14)

$$V_{IW_{EAIE}} = \left(\frac{V_{IW_{EAI}}}{2}\right) \left(2 - 3\,R_{LIWCA4} + R^3_{LIWCA4}\right) \tag{150}$$

Volume of the ellipsoidal cap, with cylindrical hole cutout associated with the core frustum hole cutout for the nozzle, which forms the inside surface of the insulation wedge in the aft case closure section. (Figures 12, 14)

$$V_{IW_{CHAI}} = V_{IW_{EAIE}} - V_{IW_{HAI}} \tag{151}$$

Area of triangular section, associated with the cone frustum cutout for the nozzle, within the aft case closure section. (Figures 12, 14)

$$A_{IW_{HAT}} = \left(\frac{1}{4}\right)\left(D_{IW_{HAO}} - D_{IW_{HAI}}\right) L_{IW_{HA}} \tag{152}$$

Distance from axis of revolution to centroid of triangular section in insulation wedge, associated with the cone frustum cutout for the nozzle, within the aft case closure section. (Figures 11, 13)

$$Y_{IW_{HAT}} = \frac{D_{IW_{HAI}}}{3} + \left(\frac{1}{6}\right) D_{IW_{HAO}} \tag{153}$$

Volume of triangular section in the insulation wedge, associated with the cone frustum cutout for the nozzle, within the aft case closure section. (Figures 12, 14)

EQUATIONS, SECOND ENTRANCE (Cont.):

INSULATION WEDGE, AFT CLOSURE (Cont.):

$$V_{IW_{HAT}} = 2\pi\, Y_{IW_{HAT}}\, A_{IW_{HAT}} \tag{154}$$

Volume of insulation material required for the insulation wedge associated with the aft case closure section. (Figures 12, 14)

$$V_{IW_{CLA}} = \left(V_{IW_{CHAO}} - V_{IW_{CHAI}} - V_{IW_{HAT}}\right) K_{IW_{19}} + K_{IW_{20}} \tag{155}$$

SLOT AND JOINT INSULATION, BOUNDS FOR ACCEPTABLE SOLUTIONS:

The following conditions must be satisfied for acceptable solutions in determining the insulation slot and joint volume requirements. If the conditions are not satisfied, a diagnostic is usually printed and computations of sizing quantities may be terminated. (Figures 16, 17)

$$D_{IL_I} \geq T_{PP_{WEB}} \tag{156-a}$$

$$T_{PP_{WEB}} > 0 \tag{156-b}$$

$$T_{PP_{WEB}} \geq T_{IS_{MAX}} \tag{156-c}$$

$$T_{PP_{WEB}} \geq T_{IJ_{MAX}} \tag{156-d}$$

$$T_{IS_{MAX}} \geq 0 \tag{156-e}$$

$$T_{IJ_{MAX}} \geq 0 \tag{156-f}$$

$$L_{IS_{CUT}} \geq 0 \tag{156-g}$$

$$L_{IJ_{CUT}} \geq 0 \tag{156-h}$$

$$L_{IS_{PG1}} \geq 0 \tag{156-i}$$

$$L_{IJ_{PG1}} \geq 0 \tag{156-j}$$

EQUATIONS, SECOND ENTRANCE (Cont.):

SLOT AND JOINT INSULATION, CUTOUT REQUIREMENTS:

Number of slot cutouts in grain to be insulated. Integer valued real number (floating point integer).

$$N_{IS_{CUT}} = N_{IS_{IH0}} + N_{IS_{IH1}} \tag{157}$$

CUTOUTS (CUT OUT in grain for Slot) is a logical variable which specifies if there are slot cutouts within the grain which require insulation.

If CUTOUTS = .TRUE.; there is at least one slot cutout requiring insulation. Either one or no slot burning surface may be inhibited.

If CUTOUTS = .FALSE.; there are no slot cutouts requiring insulation.

$$CUTOUTS = N_{IS_{CUT}} \ .GT.\ O \tag{157-a}$$

CUTOUTJ (CUT OUT in grain for Joint) is a logical variable which specifies if there are joint cutouts within the grain which require insulation.

If CUTOUTJ = .TRUE.; there is at least one joint cutout requiring insulation. Both burning surfaces of a joint are inhibited.

If CUTOUTJ = .FALSE.; there are no joint cutouts requiring insulation.

$$CUTOUTJ = N_{IJ_{CUT}} \ .GT.\ O \tag{157-b}$$

SLOT INSULATION, COMPONENT VOLUMES (CUTOUTS = .FALSE.):

If CUTOUTS = .FALSE.; there is no slot insulation and equations 158-160 are evaluated. See Figures 15, 16, 20. See equations 162, 164, 165, 170 for alternate expression

EQUATIONS, SECOND ENTRANCE (Cont.):

SLOT INSULATION, COMPONENT VOLUMES (CUTOUTS = .FALSE.)(Cont.):

$$V_{IS_{PL}} = 0 \quad (158)$$

$$V_{IS_{GL}} = 0 \quad (159)$$

$$V_{IS_{PG}} = 0 \quad (160)$$

SLOT INSULATION, COMPONENT VOLUMES (CUTOUTS = .TRUE.):

If CUTOUTS = .TRUE.; equations 162 - 170 are evaluated to determine the slot insulation component volumes, as illustrated by Figures 15, 16, 20.

Length of a single slot cutout for insulation computations. (Figure 16)

$$L_{IS_{CUT}} = \left(\frac{L_{SL_{GN}}}{N_{IS_{CUT}}}\right) K_{IS_3} + K_{IS_4} \quad (162)$$

Volume of port/liner insulation component for a slot cutout. (Figures 15, 16, 20) See equation 158 for an alternate expression.

$$V_{IS_{PL}} = \left[\pi\left(D_{IL_I} - T_{IS_{MAX}}\right) L_{IS_{CUT}} T_{IS_{MAX}}\right] K_{IS_5} + K_{IS_6} \quad (163)$$

Volume of grain/liner insulation component for a slot cutout. (Figures 15, 16, 20) See equation 159 for an alternate expression.

$$V_{IS_{GL}} = \left|\pi\left[\left(\frac{D_{IL_I}}{2}\right) - \left(\frac{T_{IS_{MAX}}}{3}\right)\right] T_{PP_{WEB}} T_{IS_{MAX}}\right| K_{IS_7} + K_{IS_8} \quad (164)$$

Volume of the port/grain insulation component for slot cutouts. See Figures 15, 16, 20. See equations 160, 170 for alternate expressions.

If $N_{IS_{IH1}} = 0$, there are no slots having one grain burning surface inhibited, and equation 165 is used to evaluate $V_{IS_{PG}}$.

$$V_{IS_{PG}} = 0 \quad (165)$$

EQUATIONS, SECOND ENTRANCE (Cont.):

SLOT INSULATION, COMPONENT VOLUMES (CUTOUTS = .TRUE.)(Cont.):

If $N_{IS_{IH1}} > 0$, equations 166 - 170 are evaluated to determine $V_{IS_{PG}}$.

Altitude of the polygon cross section associated with the port/grain insulation component for slot cutouts. (Figure 16)

$$T_{IS_{PG1}} = T_{PP_{WEB}} - T_{IS_{MAX}} \tag{166}$$

Length of outside base of the polygon cross section associated with the port/grain insulation component for slot cutouts. (Figure 16)

$$L_{IS_{PGO}} = \left(\frac{T_{IS_{MAX}}}{T_{PP_{WEB}}}\right)\left(T_{PP_{WEB}} - T_{IS_{MAX}} + L_{IS_{PGI}}\right) \tag{167}$$

Area of the polygon cross section associated with the port/grain insulation component for slot cutouts. (Figure 16)

$$A_{IS_{PG}} = \left(\frac{T_{IS_{PG1}}}{2}\right)\left(L_{IS_{PGI}} + L_{IS_{PGO}}\right) \tag{168}$$

Centroid, measured with respect to the motor centerline, of the polygon cross section associated with the port/grain insulation component for slot cutouts. (Figure 16)

$$Y_{IS_{PG}} = \left(\frac{D_{IL_1}}{2}\right) - T_{IS_{MAX}} - \left(\frac{T_{IS_{PG1}}}{3}\right)\left(\frac{2\,L_{IS_{PGI}} + L_{IS_{PGO}}}{L_{IS_{PGI}} + L_{IS_{PGO}}}\right)$$

Volume of the port/grain insulation component for slot cutouts. (Figures 15, 16, 20) See equations 160, 165 for alternate expressions.

$$V_{IS_{PG}} = \left[2\,\pi\,Y_{IS_{PG}}\,A_{IS_{PG}}\right] K_{IS_9} + K_{IS_{10}} \tag{170}$$

EQUATIONS, SECOND ENTRANCE(Cont.):

SLOT INSULATION, PORT/GRAIN COMPONENT POLYGON CLASSIFICATION:

The following logical expressions are used to classify the polygon cross section associated with the port/grain insulation component for slot cutouts.

If $N_{IS_{IH1}} = 0$; there is no port/grain insulation component and all elements of the PGIS logical valued array are .FALSE.

If $N_{IS_{IH1}} > 0$; one, and only one, of the elements of the PGIS logical array must have a .TRUE. value for an acceptable port/grain insulation component solution.

If $N_{IS_{IH1}} > 0$; and either all of the elements of PGIS evaluated using equations 171, 177 are .FALSE., or more than one element is .TRUE., the logical variable PGISBAD is set .TRUE.

See Figure 18 for a geometrical interpretation and "Optimization Considerations" of the REMARKS section for discontinuity considerations.

Vertical line solution.

$$PGIS(1) = \left(T_{IS_{MAX}} .EQ. 0\right) .AND. \left(L_{IS_{PGI}} .EQ. 0\right) \tag{171}$$

Horizontal line solution.

$$PGIS(2) = \left(T_{PP_{WEB}} .EQ. T_{IS_{MAX}}\right) \tag{172}$$

Intermediate quantity, solution is not a line.

$$ISNOTLN = .NOT. \left|PGIS(1) .OR. PGIS(2)\right| \tag{173}$$

Triangle solution.

$$PGIS(3) = ISNOTLN .AND. \left(L_{IS_{PGI}} .EQ. 0\right) .AND. \left(T_{IS_{MAX}} .GT. 0\right) \tag{174}$$

EQUATIONS, SECOND ENTRANCE (Cont.):

SLOT INSULATION, PORT/GRAIN COMPONENT POLYGON CLASSIFICATION (Cont.):

Trapezoid solutions.

$$PGIS(4) = ISNOTLN \;.AND.\; \left(L_{IS_{PGI}} \;.LT.\; L_{IS_{PGO}}\right) \;.AND.\; \left(L_{IS_{PGI}} \;.GT.\; 0\right) \tag{175}$$

$$PGIS(5) = ISNOTLN \;.AND.\; \left(T_{IS_{MAX}} \;.GT.\; 0\right) \;.AND.\; \left(T_{IS_{MAX}} \;.EQ.\; L_{IS_{PGI}}\right) \tag{176}$$

$$PGIS(6) = ISNOTLN \;.AND.\; \left(L_{IS_{PGI}} \;.GT.\; L_{IS_{PGO}}\right) \tag{177}$$

JOINT INSULATION, COMPONENT VOLUMES (CUTOUTJ = .FALSE.):

If CUTOUTJ = .FALSE., there is no joint insulation and equations 178, 179 are evaluated. See Figures 15, 17, 20, and equations 182, 195 for alternate definition if CUTOUTJ = .TRUE. .

$$V_{IJ_{PL}} = 0 \tag{178}$$

$$V_{IJ_{PG}} = 0 \tag{179}$$

JOINT INSULATION, COMPONENT VOLUMES (CUTOUTJ = .TRUE.):

If CUTOUTJ = .TRUE., equations 181 - 195 are evaluated to determine the joint insulation component volumes as illustrated by Figures 15, 17, 20.

Length of a unit joint cutout for insulation computations. (Figure 17)

$$L_{IJ_{CUT}} = \left(\frac{L_{JT_{CUT}}}{N_{IJ_{CUT}}}\right) K_{IJ_3} + K_{IJ_4} \tag{181}$$

EQUATIONS, SECOND ENTRANCE (Cont.):

JOINT INSULATION, COMPONENT VOLUMES (CUTOUTJ = .TRUE.)(Cont.):

Volume of port/liner insulation component for joint cutouts. (Figures 17, 20)

$$V_{IJ_{PL}} = \left| \pi \left(D_{IL_I} - T_{IJ_{MAX}} \right) L_{IJ_{CUT}} T_{IJ_{MAX}} \right| K_{IJ_5} + K_{IJ_6} \tag{182}$$

Intermediate quantity required for the determination of the outside base of the polygon cross section associated with the port/grain insulation component for joint cutouts. (Figure 17)

$$L_{IJ_{PG3}} = \left(\frac{T_{IJ_{MAX}}}{T_{PP_{WEB}}} \right) \left(T_{PP_{WEB}} - T_{IJ_{MAX}} + L_{IJ_{PGI}} \right) \tag{183}$$

PGIJLAP is a logical valued variable which indicates overlapping of the polygon cross sections associated with the port/grain insulation component for joint cutouts. (Figure 19)

PGIJLAP = .TRUE., PG components overlap.

PGIJLAP = .FALSE., PG components do not overlap.

$$PGIJLAP = L_{IJ_{PG3}} \text{ .GT. } \left(\frac{L_{IJ_{CUT}}}{2} \right) \tag{183-a}$$

Outside base of the polygon cross section associated with the port/grain insulation components for grain cutouts. (Figure 17)

$$\text{If PGIJLAP = .FALSE.,} \quad L_{IJ_{PGO}} = L_{IJ_{PG3}} \tag{184}$$

$$\text{If PGIJLAP = .TRUE.,} \quad L_{IJ_{PGO}} = \left(\frac{L_{IJ_{CUT}}}{2} \right) \tag{185}$$

Component altitude of the polygon cross section associated with the port/grain insulation component for joint cutouts. (Figure 17)

$$T_{IJ_{PG3}} = T_{PP_{WEB}} - T_{IJ_{MAX}} + L_{IJ_{PGI}} - \left(\frac{T_{PP_{WEB}}}{T_{IJ_{MAX}}} \right) L_{IJ_{PGO}} \tag{186}$$

EQUATIONS, SECOND ENTRANCE (Cont.):

JOINT INSULATION, COMPONENT VOLUMES (CUTOUTJ = .TRUE.)(Cont.):

Component altitude of the polygon cross section associated with the port/grain insulation component for joint cutouts. (Figure 17)

$$T_{IJ_{PG1}} = \left(\frac{T_{PP_{WEB}}}{T_{IJ_{MAX}}}\right) L_{IJ_{PGO}} - L_{IJ_{PGI}} \tag{187}$$

Area of the polygon cross section associated with the port/grain insulation component for joint cutouts. (Figure 17)

$$A_{IJ_{PG}} = \left(\frac{T_{IJ_{PG1}}}{2}\right) \left(L_{IJ_{PGI}} + L_{IJ_{PGO}}\right) + T_{IJ_{PG3}} L_{IJ_{PGO}} \tag{188}$$

Centroid, measured with respect to the motor centerline, of the polygon cross section for joint cutouts. (Figure 17)

$$Y_2 = \left(\frac{T^2_{IJ_{PG1}}}{3}\right) \left(2 L_{IJ_{PGI}} + L_{IJ_{PGO}}\right) \tag{189}$$

$$Y_3 = T_{IJ_{PG1}} T_{IJ_{PG3}} \left(L_{IJ_{PGI}} + L_{IJ_{PGO}}\right) \tag{190}$$

$$Y_4 = T^2_{IJ_{PG3}} L_{IJ_{PGO}} \tag{191}$$

$$Y_5 = T_{IJ_{PG1}} \left(L_{IJ_{PGI}} + L_{IJ_{PGO}}\right) + 2 T_{IJ_{PG3}} L_{IJ_{PGO}} \tag{192}$$

$$Y_1 = \frac{Y_2 + Y_3 + Y_4}{Y_5} \tag{193}$$

$$Y_{IJ_{PG}} = \left(\frac{D_{IL_1}}{2}\right) - T_{IJ_{MAX}} - Y_1 \tag{194}$$

EQUATIONS, SECOND ENTRANCE (Cont.):

JOINT INSULATION, COMPONENT VOLUMES (CUTOUTJ = .TRUE.) (Cont.):

Volume of a port/grain insulation component for slot cutouts. (Figure 20) See equation 179 for an alternate expression.

$$V_{IJ_{PG}} = \left|2\,\pi\, Y_{IJ_{PG}}\, A_{IJ_{PG}}\right| K_{IJ_7} + K_{IJ_8} \qquad (195)$$

JOINT INSULATION, PORT/GRAIN COMPONENT POLYGON CLASSIFICATION:

The following logical expressions are used to classify the polygon cross section associated with the port/grain insulation component for joint cutouts.

If CUTOUTJ = .FALSE., there is no joint insulation and all elements of the PGIJ logical valued array are .FALSE. .

If CUTOUTJ = .TRUE., one, and only one, of the elements of the PGIJ logical valued array must have a .TRUE. value for an acceptable port/grain insulation component solution.

If CUTOUTJ = .TRUE., and either all of the elements of the PGIJ array are false, or more than one element is true, the logical variable PGIJBAD is set .TRUE. .

See Figure 19 for a geometrical interpretation and "Optimization Considerations" of the REMARKS section for discontinuity considerations.

Vertical line solution.

$$PGIJ(1) = \left(T_{IJ_{MAX}}\ .EQ.\ 0\right)\ .AND.\ \left(L_{IJ_{PGI}}\ .EQ.\ 0\right) \qquad (196)$$

Horizontal line solution.

$$PGIJ(2) = \left(T_{PP_{WEB}}\ .EQ.\ T_{IJ_{MAX}}\right) \qquad (197)$$

Intermediate quantity, solution is not a line.

$$IJNOTLN = .NOT.\ \left[PGIJ(1)\ .OR.\ PGIJ(2)\right] \qquad (198)$$

EQUATIONS, SECOND ENTRANCE (Cont.):

JOINT INSULATION, PORT/GRAIN COMPONENT POLYGON CLASSIFICATION (Cont.):

Triangle solution.

$$PGIJ(3) = \left(T_{IJ_{PG3}}\ .EQ.\ O\right)\ .AND.\ IJNOTLN\ .AND.\ \left(L_{IJ_{PGI}}\ .EQ.\ O\right)\ .AND.\ \left(T_{IJ_{MAX}}\ .GT.\ O\right) \tag{199}$$

Trapezoid solutions.

$$PGIJ(4) = \left(T_{IJ_{PG3}}\ .EQ.\ O\right)\ .AND.\ IJNOTLN\ .AND.\ \left(L_{IJ_{PGI}}\ .LT.\ L_{IJ_{PGO}}\right)\ .AND.\ \left(L_{IJ_{PGI}}\ .GT.\ O\right) \tag{200}$$

$$PGIJ(5) = \left(T_{IJ_{PG3}}\ .EQ.\ O\right)\ .AND.\ IJNOTLN\ .AND.\ \left(T_{IJ_{MAX}}\ .GT.\ O\right)\ .AND.\ \left(L_{IJ_{PGI}}\ .EQ.\ T_{IJ_{MAX}}\right) \tag{201}$$

$$PGIJ(6) = \left(T_{IJ_{PG3}}\ .EQ.\ O\right)\ .AND.\ IJNOTLN\ .AND.\ \left(L_{IJ_{PGI}}\ .GT.\ L_{IJ_{PGO}}\right) \tag{202}$$

$$PGIJ(7) = \left(T_{IJ_{PG3}}\ .GT.\ O\right)\ .AND.\ \left(L_{IJ_{PGI}}\ .EQ.\ T_{IJ_{MAX}}\right) \tag{203}$$

$$PGIJ(8) = \left(T_{IJ_{PG3}}\ .GT.\ O\right)\ .AND.\ \left(L_{IJ_{PGI}}\ .EQ.\ O\right)\ .AND.\ \left(T_{IJ_{MAX}}\ .GT.\ O\right) \tag{204}$$

Pentagon solution.

$$PGIJ(9) = \left(T_{IJ_{PG3}}\ .GT.\ O\right)\ .AND.\ \left(L_{IJ_{PGI}}\ .GT.\ O\right)\ .AND.\ \left(L_{IJ_{PGI}}\ .LT.\ L_{IJ_{PGO}}\right) \tag{205}$$

EQUATIONS, SECOND ENTRANCE (Cont.):

SLOT AND JOINT VOLUMES:

Volume of insulation for a slot with no sides inhibited. (Figure 20)

$$V_{IS_{IHO}} = \left[V_{IS_{PL}} + 2\, V_{IS_{GL}}\right] K_{IS_{11}} + K_{IS_{12}} \tag{206}$$

Volume of insulation for a slot with one side inhibited. (Figure 20)

$$V_{IS_{IH1}} = \left[V_{IS_{PL}} + V_{IS_{GL}} + V_{IS_{PG}}\right] K_{IS_{13}} + K_{IS_{14}} \tag{207}$$

Total volume of insulation required for slots.

$$V_{IS} = \left[N_{IS_{IH0}}\, V_{IS_{IH0}} + N_{IS_{IH1}}\, V_{IS_{IH1}}\right] K_{IS_{15}} + K_{IS_{16}} \tag{208}$$

Volume of insulation required for a joint. (Figure 20)

$$V_{IJ_{IH2}} = \left[V_{IJ_{PL}} + 2\, V_{IJ_{PG}}\right] K_{IJ_{9}} + K_{IJ_{10}} \tag{209}$$

Total volume of insulation required for joints.

$$V_{IJ} = N_{IJ_{CUT}}\, V_{IJ_{IH2}}\, K_{IJ_{11}} + K_{IJ_{12}} \tag{210}$$

PROPELLENT DISPLACEMENT:

Volume of propellent displaced by the insulation wedge associated with the forward closure. (Figure 21)

$$\begin{aligned} V_{IW_{CFPD}} = \Bigg\{ V_{IW_{CLF}} - \left(\frac{\pi}{12}\right) \Big\{ & R_{DIWCFO}\left[\left(D^2_{IW_{CLO}} - D^2_{IW_{HFO}}\right)^{3/2} - \left(D^2_{IW_{CLO}} - D^2_{PT}\right)^{3/2}\right] \\ & + 3\, L_{IW_{CEFI}} \left(D^2_{IW_{HFO}} - D^2_{PT}\right) \\ & + R_{DIWCFI}\left[\left(D^2_{IW_{EFI}} - D^2_{PT}\right)^{3/2} - \left(D^2_{IW_{EFI}} - D^2_{IW_{HFO}}\right)^{3/2}\right]\Big\}\Bigg\} K_{PD_1} + K_{PD_2} \end{aligned} \tag{211}$$

EQUATIONS, SECOND ENTRANCE (Cont.):

PROPELLENT DISPLACEMENT (Cont.):

Determination of propellent displaced by the insulation wedge associated with the aft closure.

If $\theta_{CF} = 0$, the grain cone frustum is a cylinder and equation 212 is used to evaluate $V_{IW_{CAPD}}$.

If $L_{CF_{CA}} > 0$. and $\theta_{CF} \neq 0$, the grain cone frustum intersects the ellipsoid portion of the aft outside insulation wedge and equations 213 - 221 are used to evaluate $V_{IW_{CAPD}}$.

If $L_{CF_{CA}} \leq 0$, and $\theta_{CF} \neq 0$, the grain cone frustum intersects the cylindrical portion of the aft outside insulation wedge and equations 213 - 220, 222 are used to evaluate $V_{IW_{CAPD}}$.

Volume of propellent displaced by the insulation wedge associated with the aft closure (cylindrical grain cone frustum). See equations 221, 222 for alternate expressions. (Figure 21)

$$V_{IW_{CAPD}} = \Bigg\{ V_{IW_{CLA}} - \left(\frac{\pi}{12}\right)\Big\{ R_{DIWCAO}\left[\left(D^2_{IW_{CLO}} - D^2_{IW_{HAO}}\right)^{3/2} - \left(D^2_{IW_{CLO}} - D^2_{CFA}\right)^{3/2}\right]$$

$$+ 3\, L_{IW_{CEAI}}\left(D^2_{IW_{HAO}} - D^2_{CFA}\right) \tag{212}$$

$$+ R_{DIWCAI}\left[\left(D^2_{IW_{EAI}} - D^2_{CFA}\right)^{3/2} - \left(D^2_{IW_{EAI}} - D^2_{IW_{HAO}}\right)^{3/2}\right]\Big\}\Bigg\} K_{PD_3} + K_{PD_4}$$

Equations 213 - 220 are intermediate computations required for the evaluation of equations 221 and 222. They are evaluated if $\theta_{CF} \neq 0$.

$$L_{IW_{A1}} = L_{IW_{CHAO}} - \left(\frac{D_{IW_{HAO}}}{2}\right)\cot\left(\theta_{CF}\right) \tag{213}$$

EQUATIONS, SECOND ENTRANCE (Cont.):

PROPELLENT DISPLACEMENT (Cont.):

$$L_{IW_{A2}} = L_{CF_{CA}} - \left(\frac{D_{CFA}}{2}\right) \cot\left(\theta_{CF}\right) \qquad (214)$$

$$D_{IW_{A1}} = \left(\frac{D_{CFA}}{2}\right) - L_{CF_{CA}} \tan\left(\theta_{CF}\right) \qquad (215)$$

$$C_{IW_{AP}} = R^2_{DIWCAI} \tan^2\left(\theta_{CF}\right) + 1 \qquad (216)$$

$$C_{IW_{BP}} = 2\ R^2_{DIWCAI}\ D_{IW_{A1}} \tan\left(\theta_{CF}\right) - 2\ L_{IW_{CEAI}} \qquad (217)$$

$$C_{IW_{CP}} = D^2_{IW_{A1}}\ R^2_{DIWCAI} - L^2_{IW_{EAI}} + L^2_{IW_{CEAI}} \qquad (218)$$

Distance from the equatorial plane of the hemi-ellipsoid associated with the outside surface of the insulation wedge in the aft closure to the intersection of the grain cone frustum cutout with the inside surface of the insulation wedge in the aft closure. Measured parallelto centerline. (Figure 21)

$$L_{IW_{CFAI}} = \frac{-C_{IW_{BP}} + \sqrt{C^2_{IW_{BP}} - 4\ C_{IW_{AP}}\ C_{IW_{CP}}}}{2\ C_{IW_{AP}}} \qquad (219)$$

Diameter of the circle formed by the intersection of the grain cone frustum cutout with the inside surface of the insulation wedge associated with the aft closure section. (Figure 21)

$$D_{IW_{CFAI}} = 2\left[D_{IW_{A1}} + L_{IW_{CFAI}} \tan\left(\theta_{CF}\right)\right] \qquad (220)$$

Volume of propellent displaced by the insulation wedge associated with the aft closure $\left(L_{CF_{CA}} > 0\right)$. See Figure 21. See equations 212, 222 for alternate expressions.

EQUATIONS, SECOND ENTRANCE (Cont.):

PROPELLENT DISPLACEMENT (Cont.):

$$V_{IW_{CAPD}} = \Bigg\{ V_{IW_{CLA}} - \left(\frac{\pi}{12}\right) \Bigg\{ R_{DIWCAO} \left[\left(D^2_{IW_{CLO}} - D^2_{IW_{HAO}}\right)^{3/2} - \left(D^2_{IW_{CLO}} - D^2_{IW_{CFA}}\right)^{3/2} \right]$$

$$+ R_{DIWCAI} \left[\left(D^2_{IW_{EAI}} - D^2_{IW_{CFAI}}\right)^{3/2} - \left(D^2_{IW_{EAI}} - D^2_{IW_{HAI}}\right)^{3/2} \right]$$

$$+ 3 \left[L_{IW_{A1}} D^2_{IW_{HAO}} + \left(L_{IW_{A2}} - L_{IW_{CEAI}}\right) D^2_{IW_{CFAI}} \right.$$

$$\left. + \left(L_{IW_{CEAI}} - L_{IW_{A1}}\right) D^2_{IW_{HAI}} - L_{IW_{A2}} D^2_{CFA} \right] \qquad (221)$$

$$+ \left[D^3_{IW_{HAO}} + D^3_{IW_{CFAI}} - D^3_{IW_{HAI}} - D^3_{CFA} \right] \cot\left(\theta_{CF}\right) \Bigg\} \Bigg\} K_{PD_3} + K_{PD_4}$$

Volume of propellent displaced by the insulation wedge associated with the aft closure $L_{CF_{CA}} \leq 0$. See Figure 21. See equations 212, 221 for alternate expressions.

$$V_{IW_{CAPD}} = \left(\frac{\pi}{12}\right) \Bigg\{ 3 \left(L_{IW_{A2}} - L_{IW_{CEAI}}\right)\left(D^2_{CFA} - D^2_{IW_{CFAI}}\right)$$

$$+ \left(D^3_{CFA} - D^3_{IW_{CFAI}}\right) \cot\left(\theta_{CF}\right) \qquad (222)$$

$$+ R_{DIWCAI} \left[\left(D^2_{IW_{EAI}} - D^2_{CFA}\right)^{3/2} - \left(D^2_{IW_{EAI}} - D^2_{IW_{CFAI}}\right)^{3/2} \right] \Bigg\} K_{PD_3} + K_{PD_4}$$

Volume of propellent displaced by the insulation wedges associated with the forward and aft closures. (Figure 21)

$$V_{IW_{PD}} = \left(V_{IW_{CAPD}} + V_{IW_{CFPD}}\right) K_{PD_5} + K_{PD_6} \qquad (223)$$

EQUATIONS, SECOND ENTRANCE (Cont.):

PROPELLENT DISPLACEMENT (Cont.):

Volume of propellent displaced by the grain/liner components of the slot insulation. (Figure 21)

$$V_{IS_{PD}} = \left(2\, N_{IS_{IH0}} + N_{IS_{IH1}}\right) V_{IS_{GL}}\, K_{PD_7} + K_{PD_8} \tag{224}$$

Total volume of propellent displaced by the insulation wedges and slots. (Figure 21)

$$V_{IN_{PD}} = \left(V_{IW_{PD}} + V_{IS_{PD}}\right) K_{PD_9} + K_{PD_{10}} \tag{225}$$

EQUATIONS, THIRD ENTRANCE:

Equations 226 - 230 are evaluated at the third entrance to the INGM1 model.

INSULATION LINER, CYLINDRICAL SECTION:

Length of insulation liner within the cylindrical case section. Includes length adjustment for submerged nozzle, slots and joints. (Figure 2)

$$L_{IL_{CY}} = L_{GN_{CY4}} K_{IL_{11}} + K_{IL_{12}} \tag{226}$$

Volume of cylindrical insulation liner section within the cylindrical case section.

$$V_{IL_{CY}} = \left(\frac{\pi}{4}\right) \left(D^2_{IL_O} - D^2_{IL_I}\right) L_{IL_{CY}} K_{IL_{13}} + K_{IL_{14}} \tag{227}$$

INSULATION LINER, TOTAL VOLUME:

Total volume of insulation material required for the insulation liner. Includes adjustment for igniter hole in forward closure, nozzle hole in aft closure, length penalty for submerged nozzle, slots, and joints in the grain.

$$V_{IL} = \left(V_{IL_{CY}} + V_{IL_{CLF}} + V_{IL_{CLA}}\right) K_{IL_{15}} + K_{IL_{16}} \tag{228}$$

RESIDUAL INSULATION:

Volume of residual insulation.

$$V_{IN_R} = T_{IN_R} \left(\frac{V_{IL}}{T_{IL_{CY}}}\right) K_{IN_5} + K_{IN_6} \tag{229}$$

TOTAL INSULATION VOLUME:

Total internal insulation volume. Includes liner, wedges in forward and aft closure, inhibited slots and joints. (Figures 1, 2)

$$V_{IN} = \left(V_{IL} + V_{IW_{CLA}} + V_{IW_{CLF}} + V_{IS} + V_{IJ}\right) K_{IN_7} + K_{IN_8} \tag{230}$$

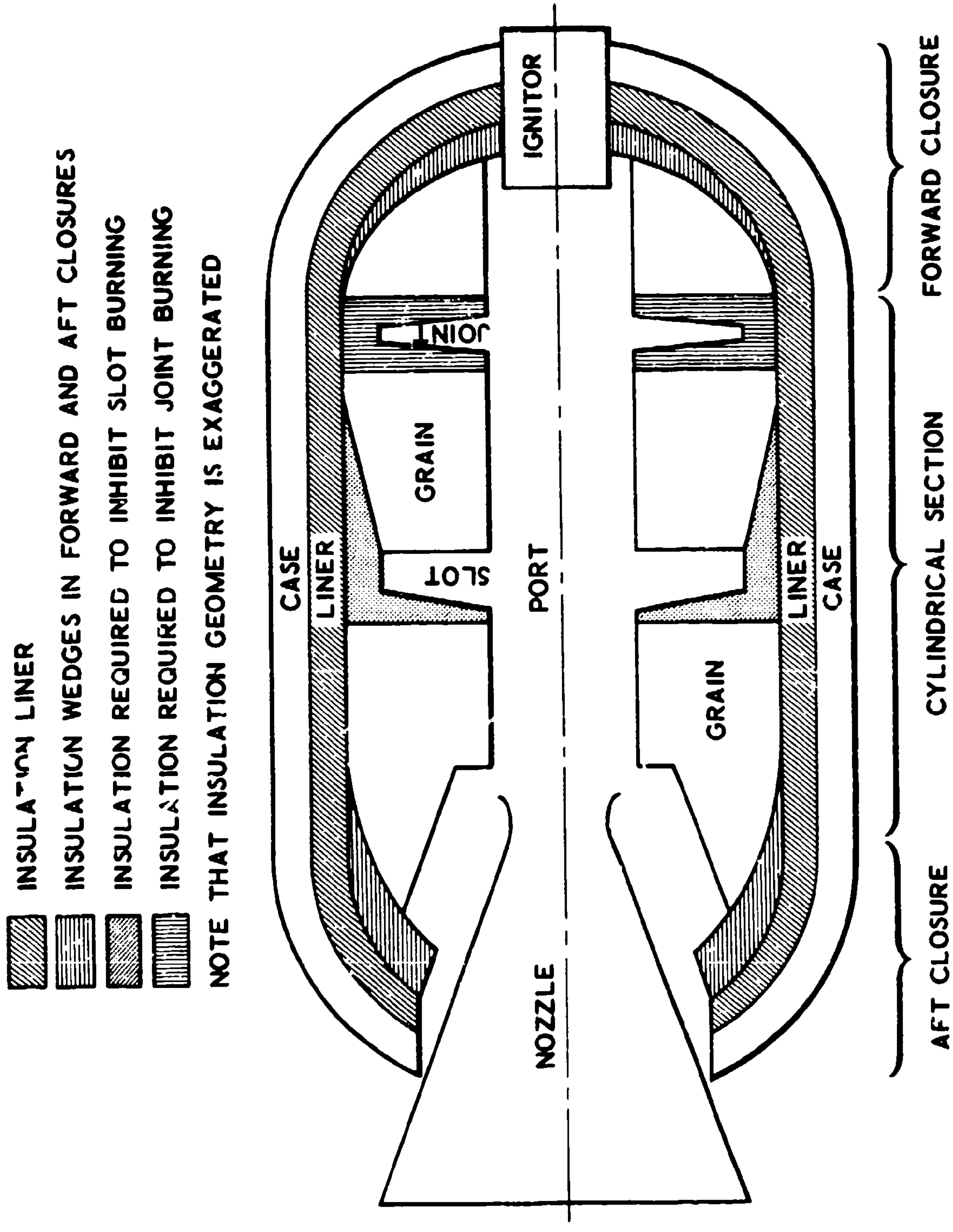

Fig. 80.1-1 Basic Insulation Components

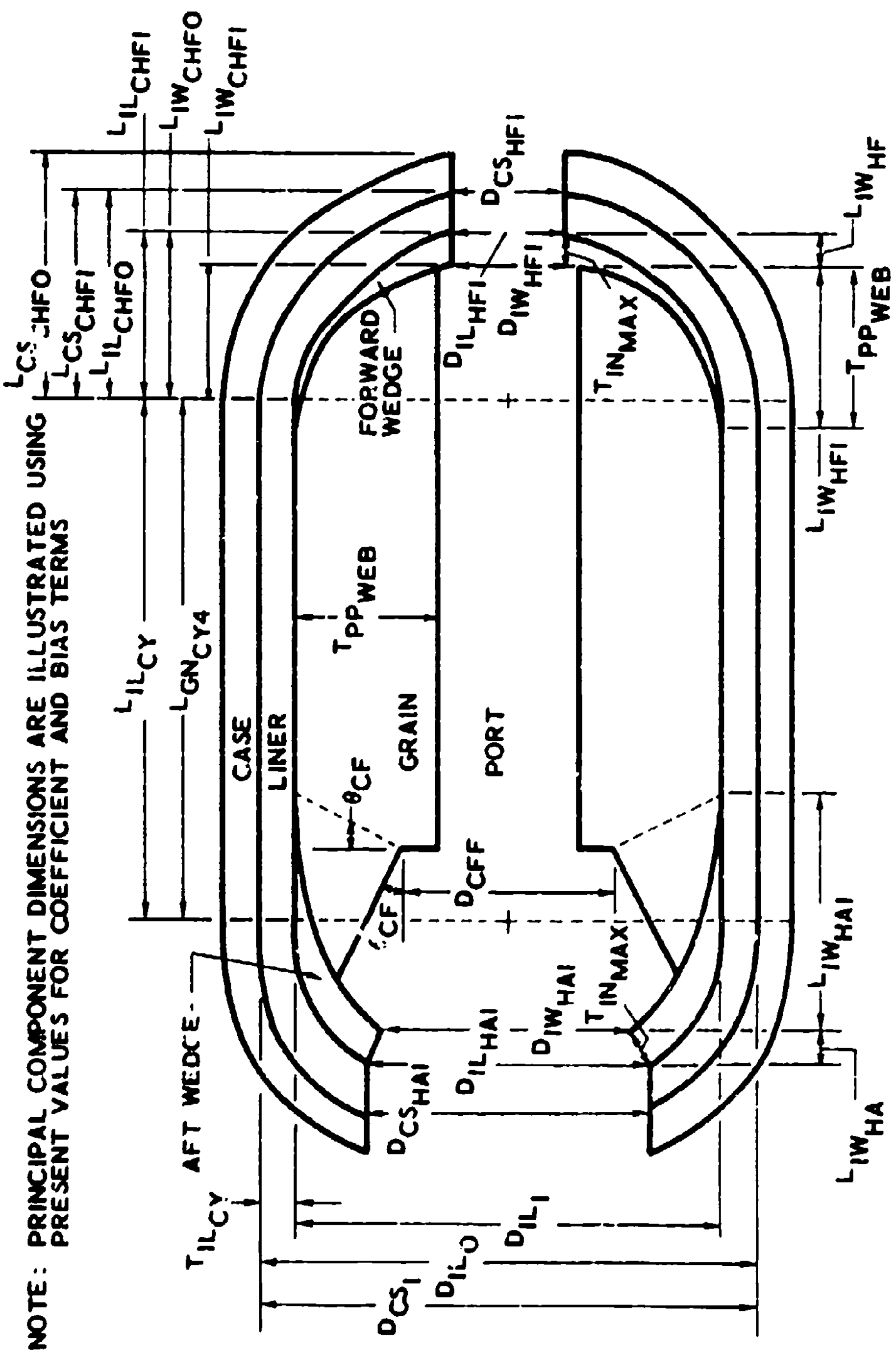

Fig. 80.1-2 Typical Insulation Liner and Wedge Geometry

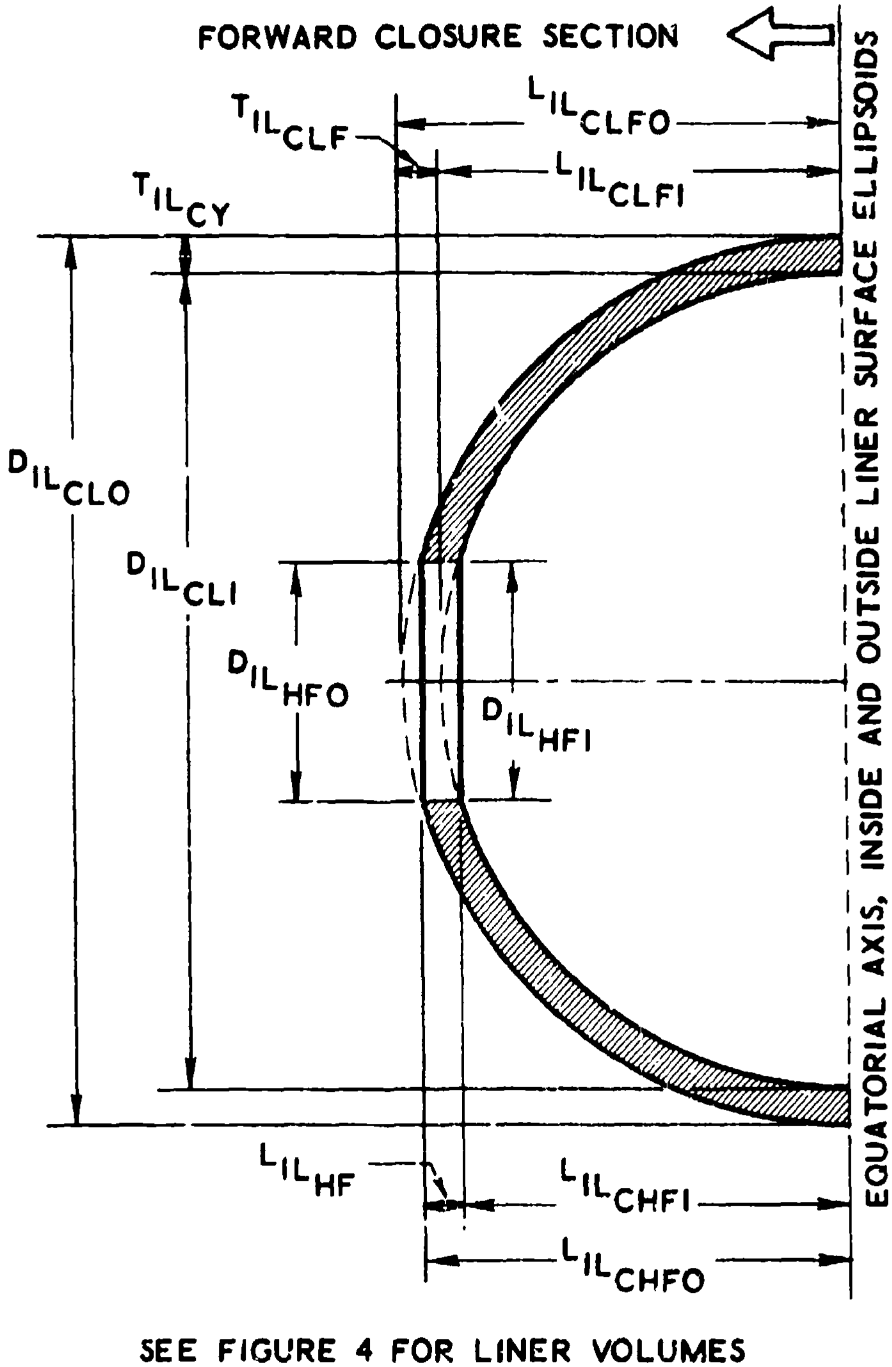

Fig. 80.1-3 Liner Within Forward Closure, Detailed Geometry

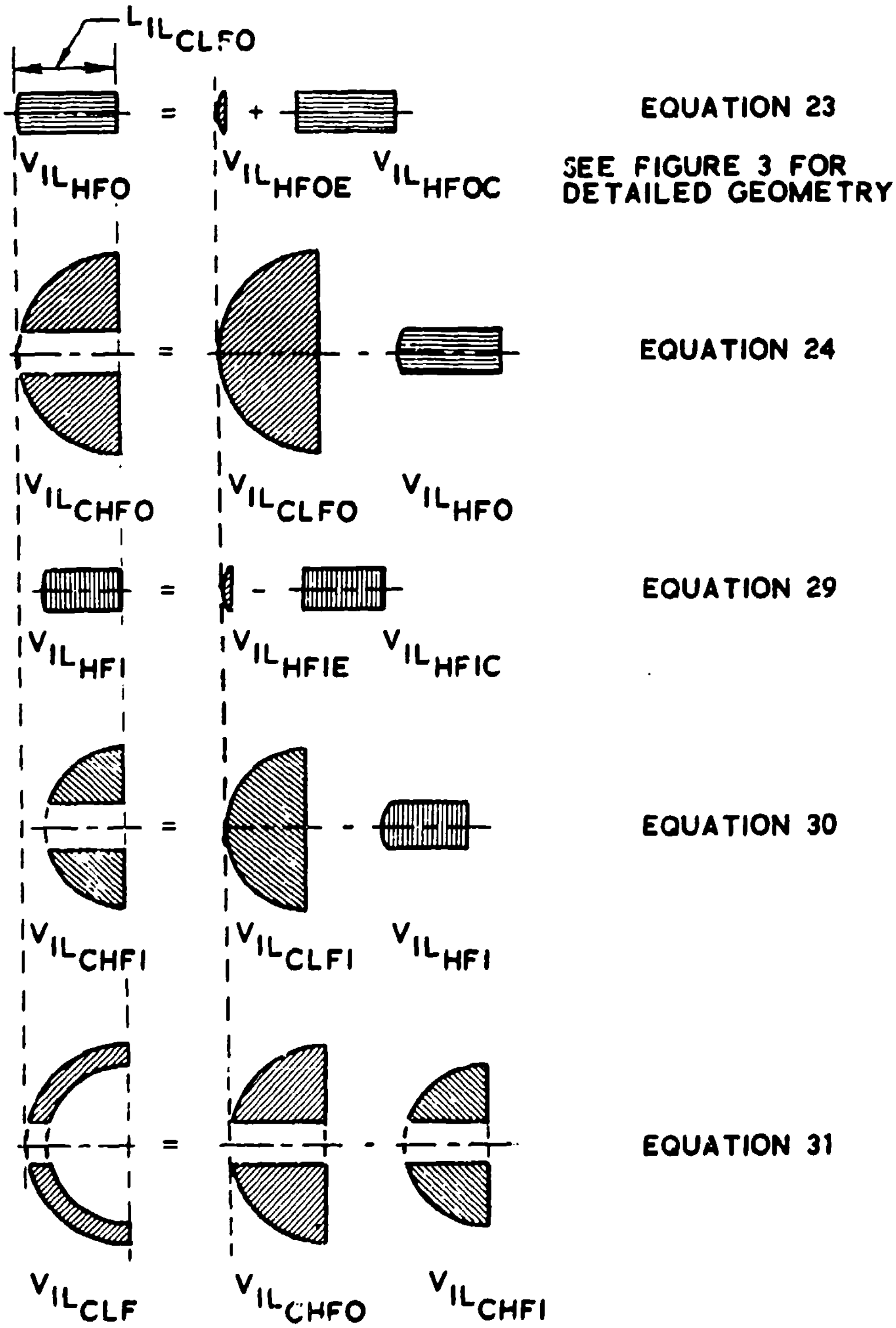

Fig. 80.1-4 Liner Within Forward Closure, Volumes

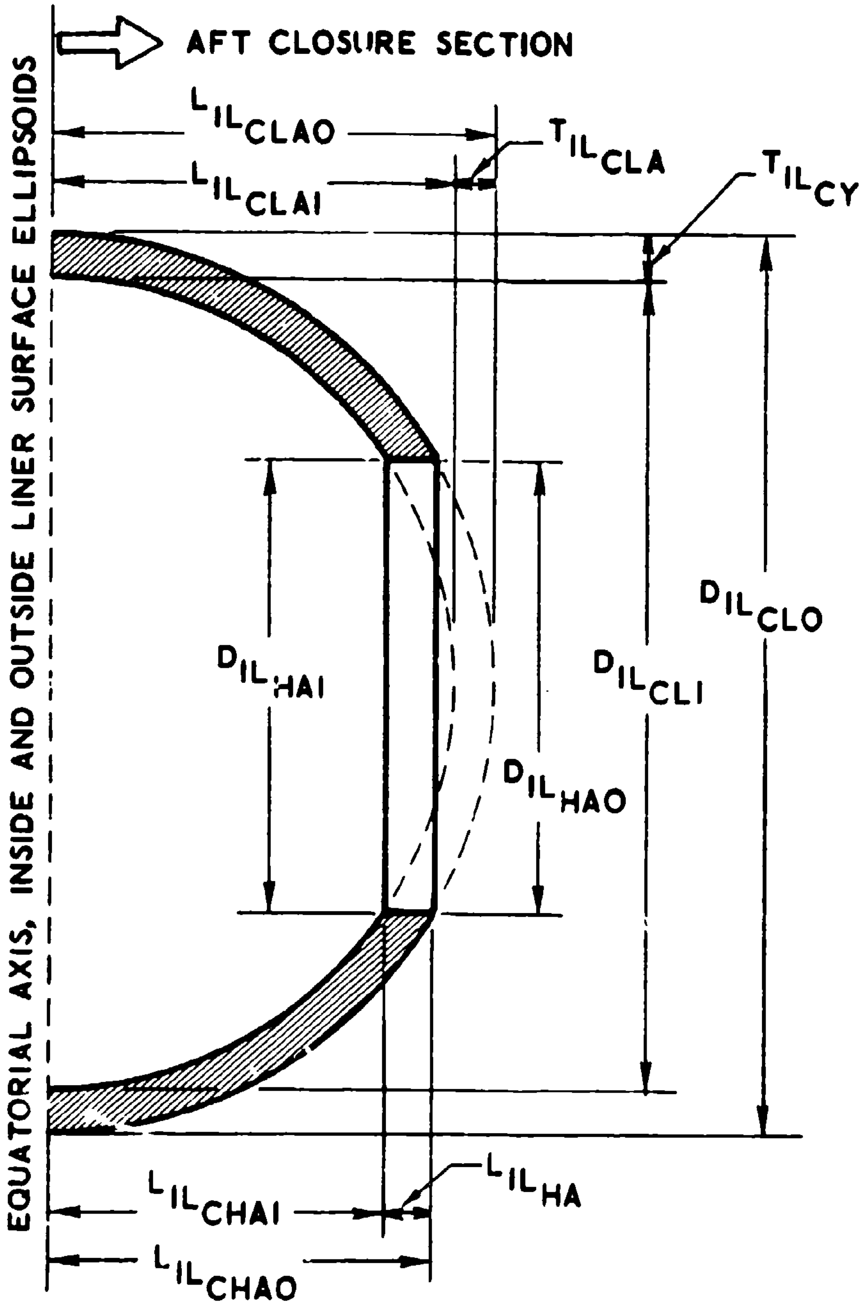

SEE FIGURE 6 FOR LINER VOLUMES

Fig. 80.1-5 Liner Within Aft Closure, Detailed Geometry

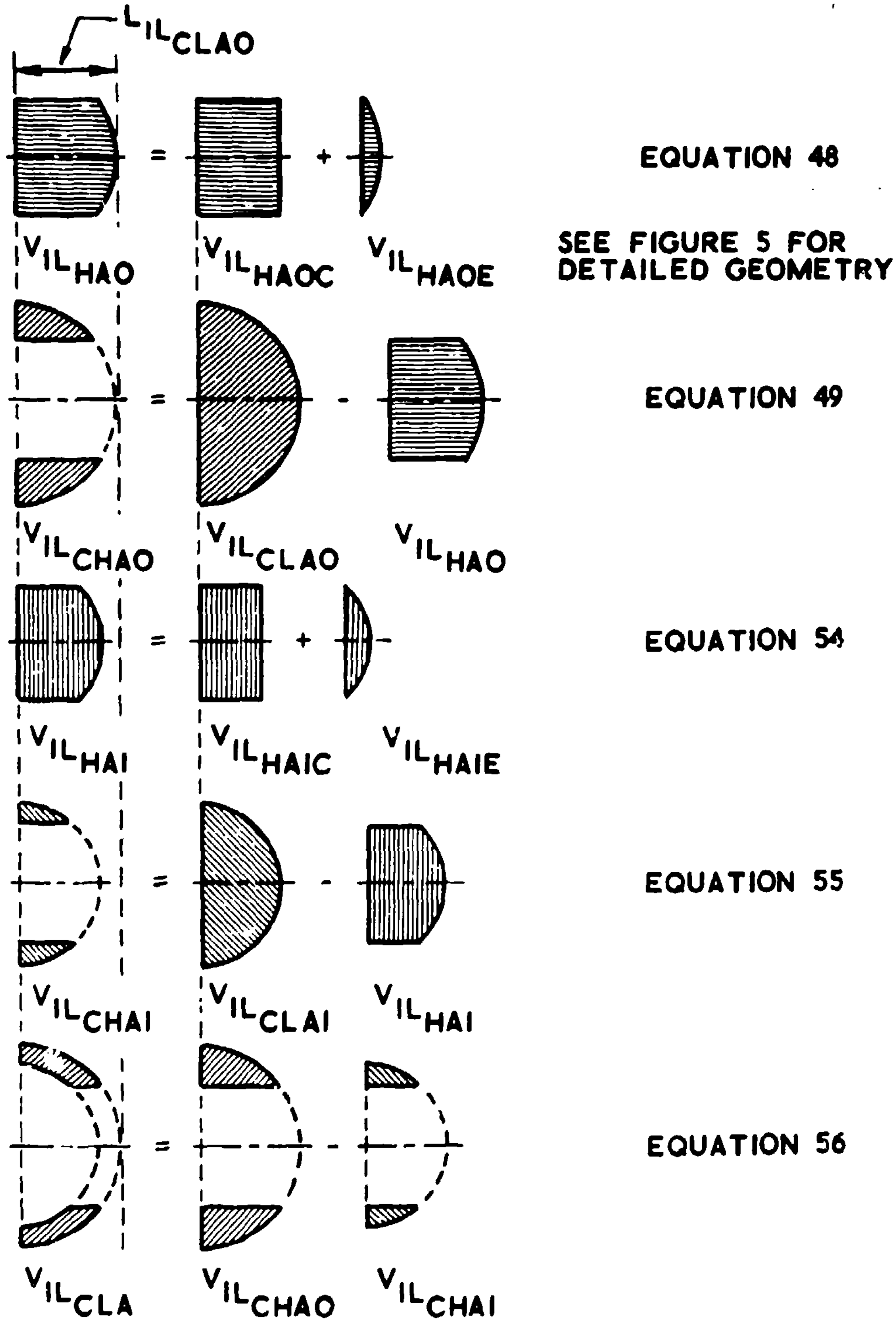

Fig. 80.1-6 Liner Within Aft Closure, Volumes

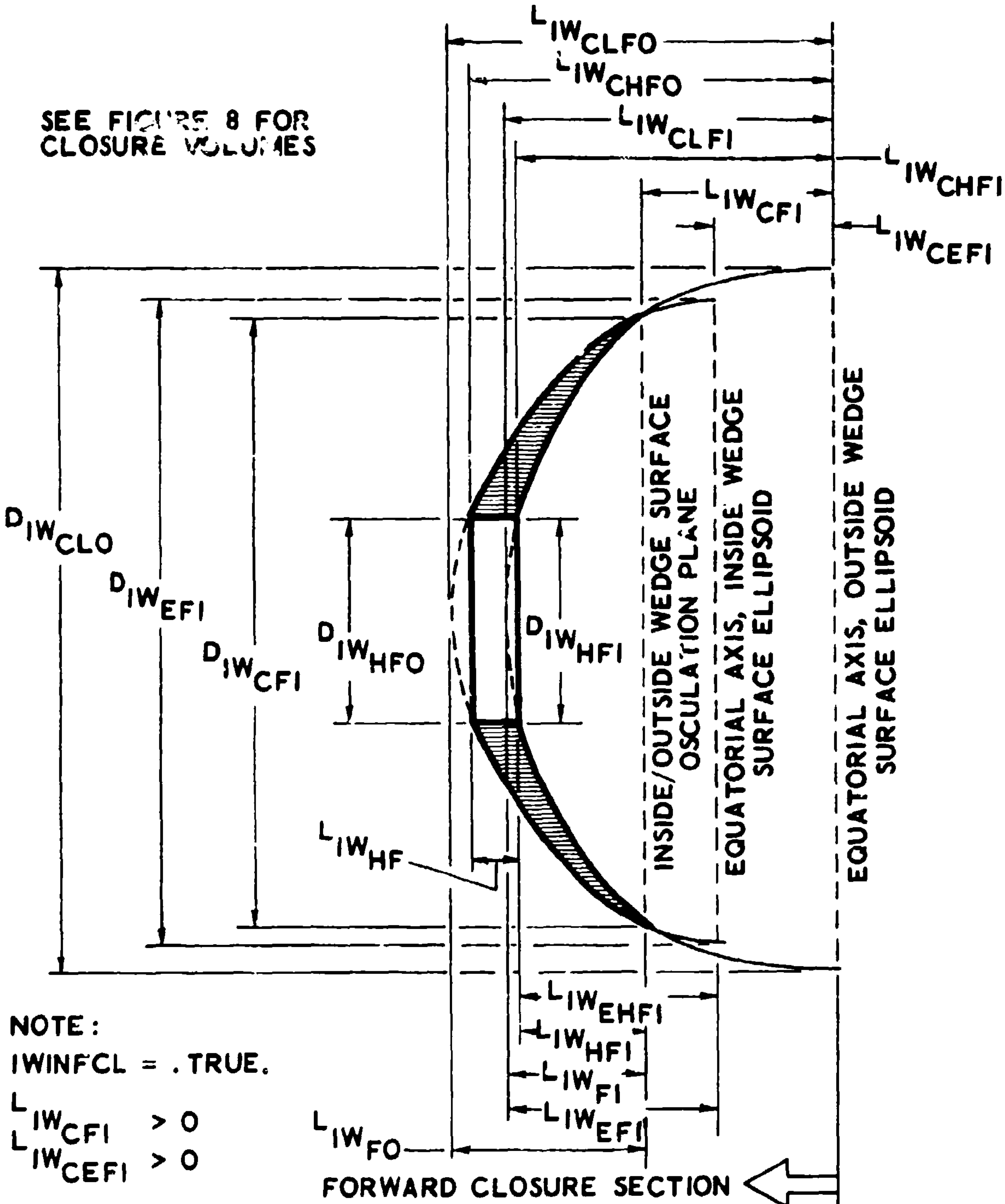

Fig. 80.1-7 Wedge Within Forward Closure, Detailed Geometry

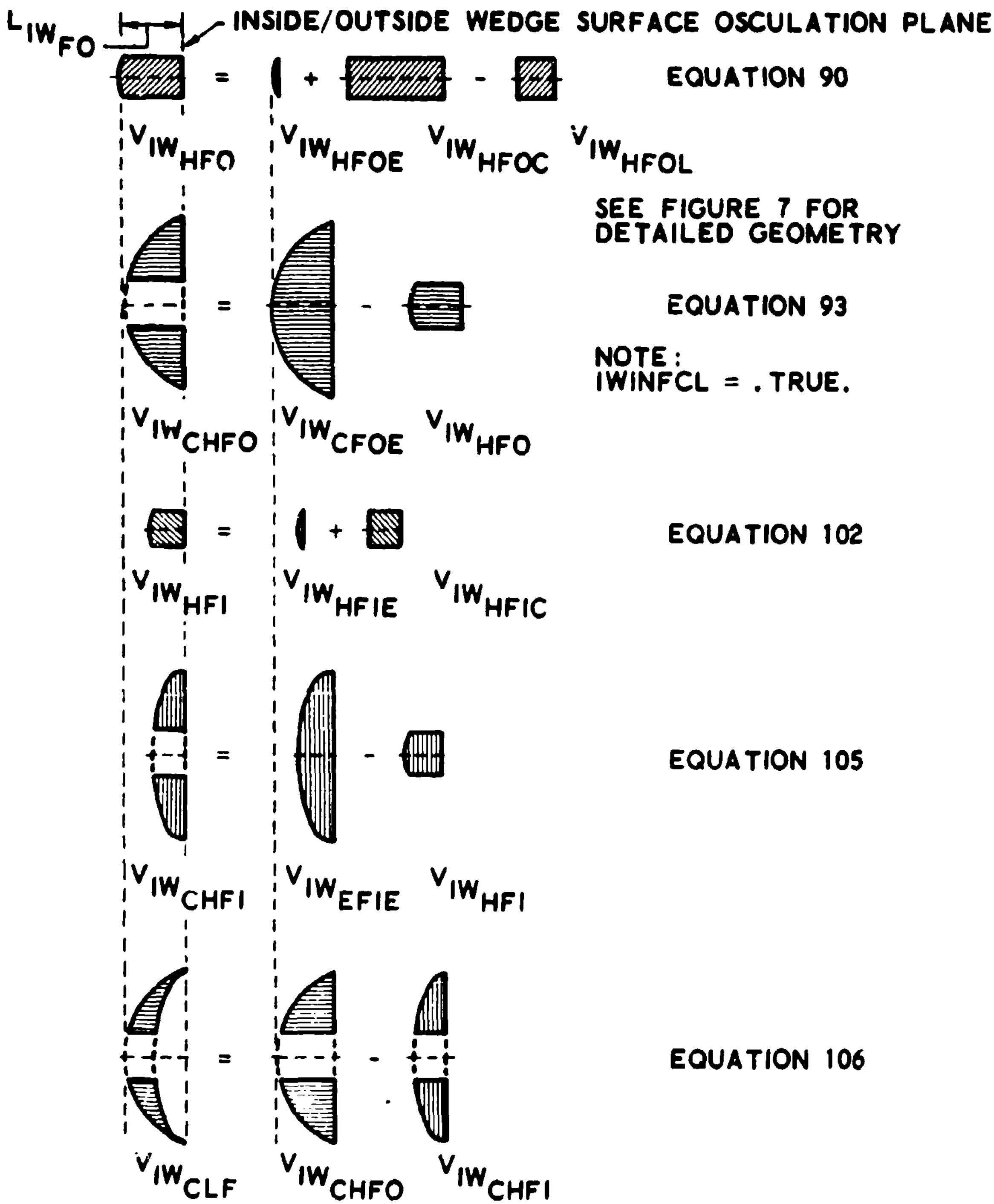

Fig. 80.1-8 Wedge Within Forward Closure, Volumes

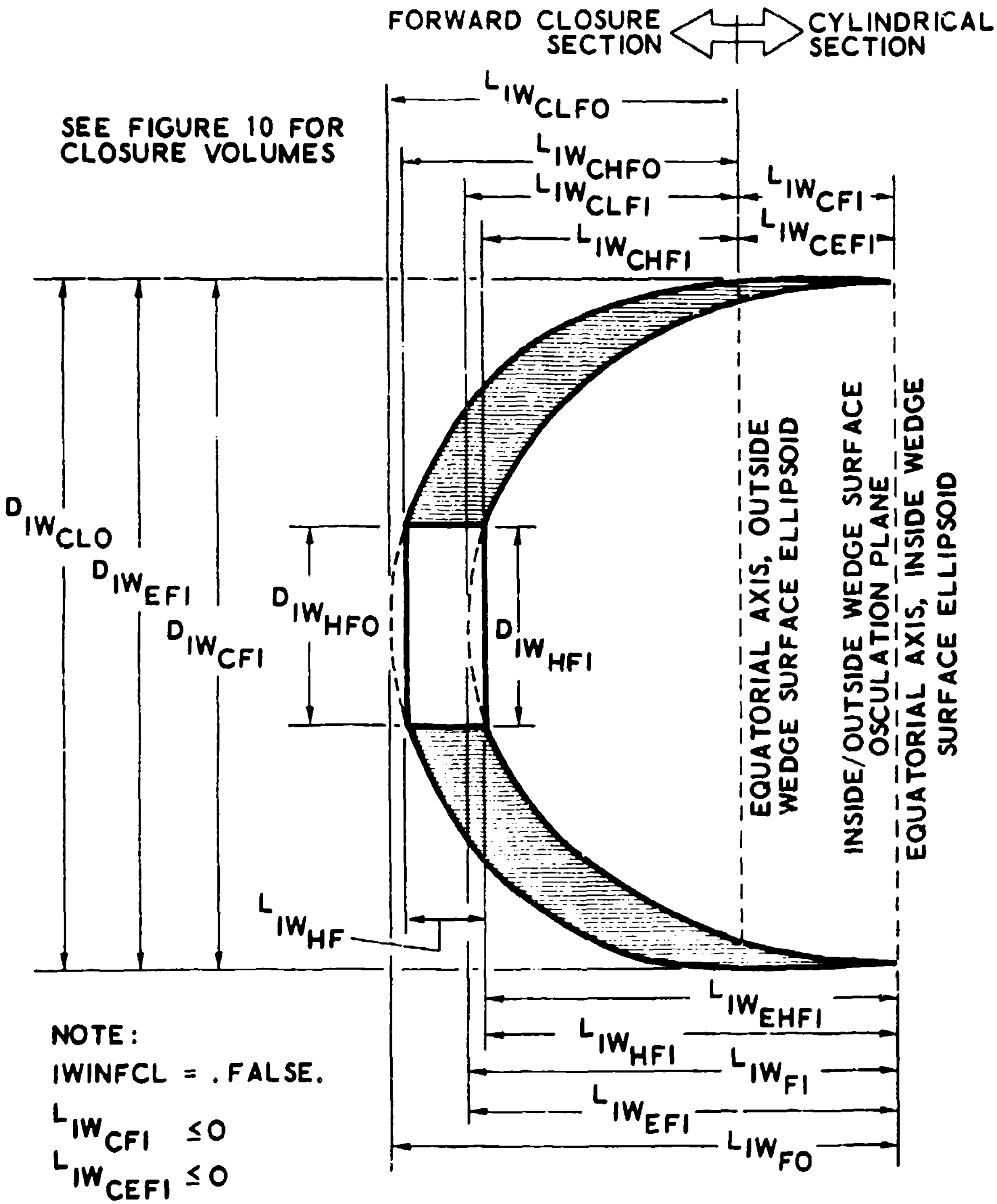

Fig. 80.1-9 Wedge Beyond Forward Closure, Detailed Geometry

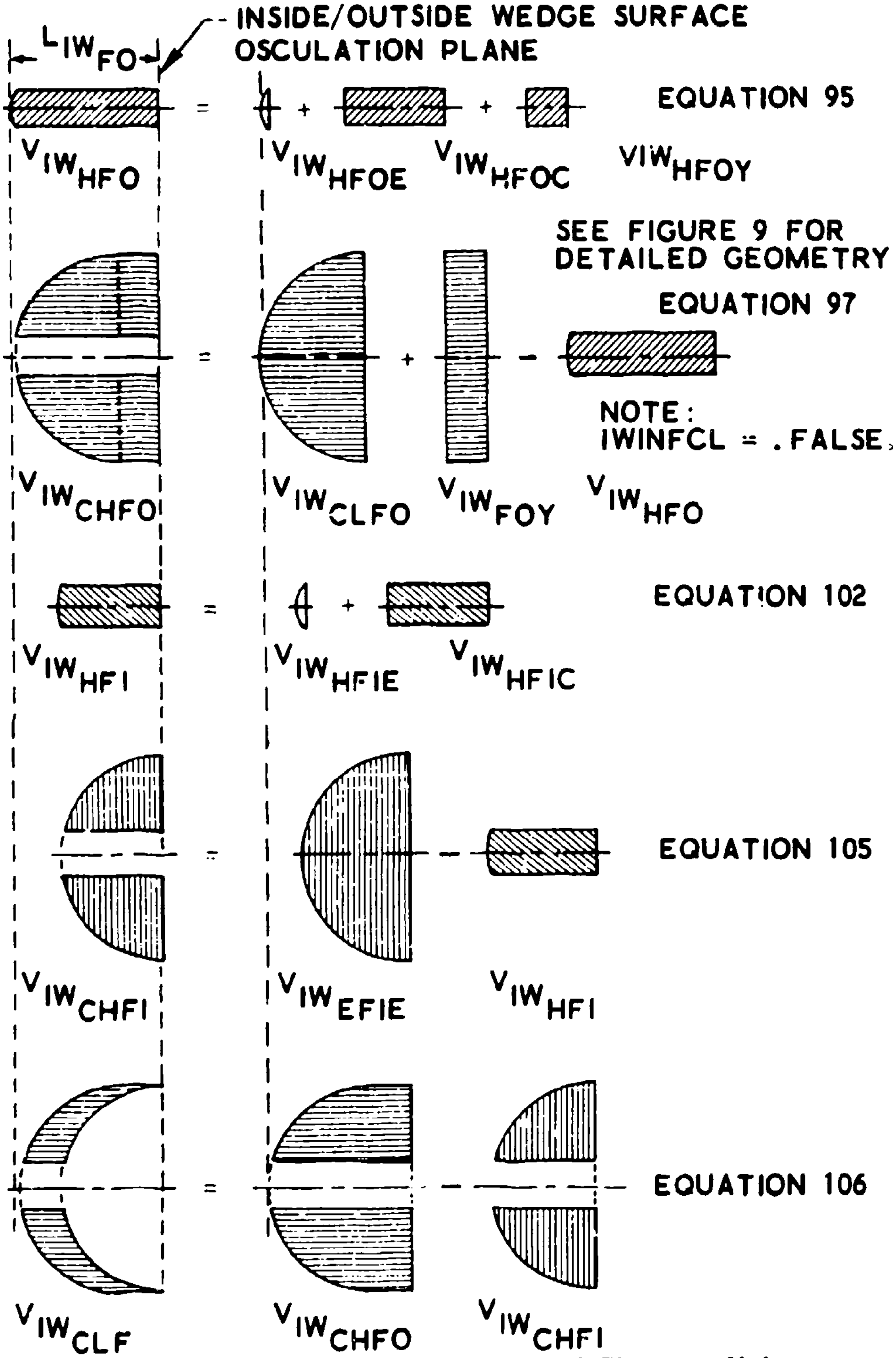

Fig. 80.1-10 Wedge Beyond Forward Closure, Volumes

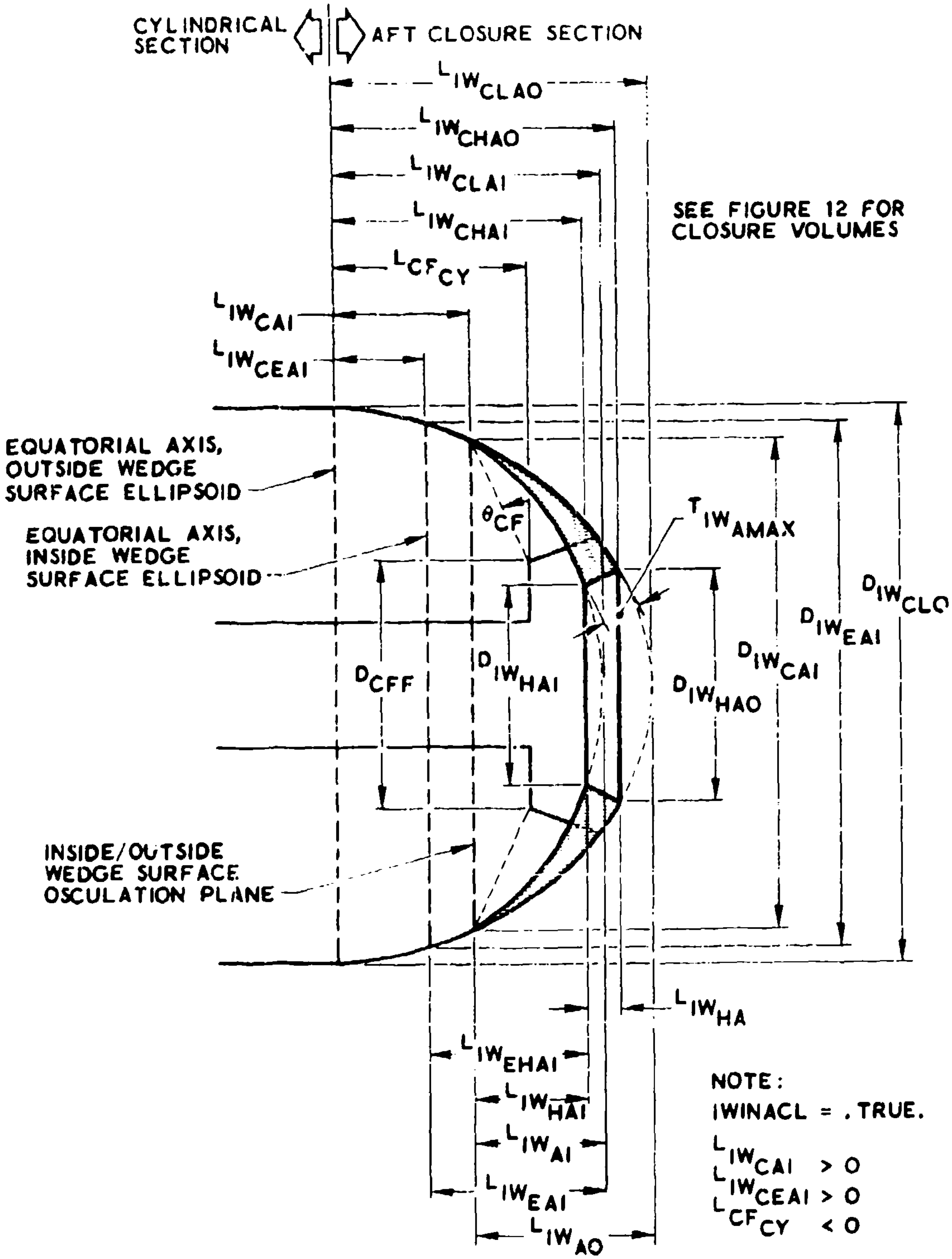

Fig. 80.1-11 Wedge Within Aft Closure, Detailed Geometry

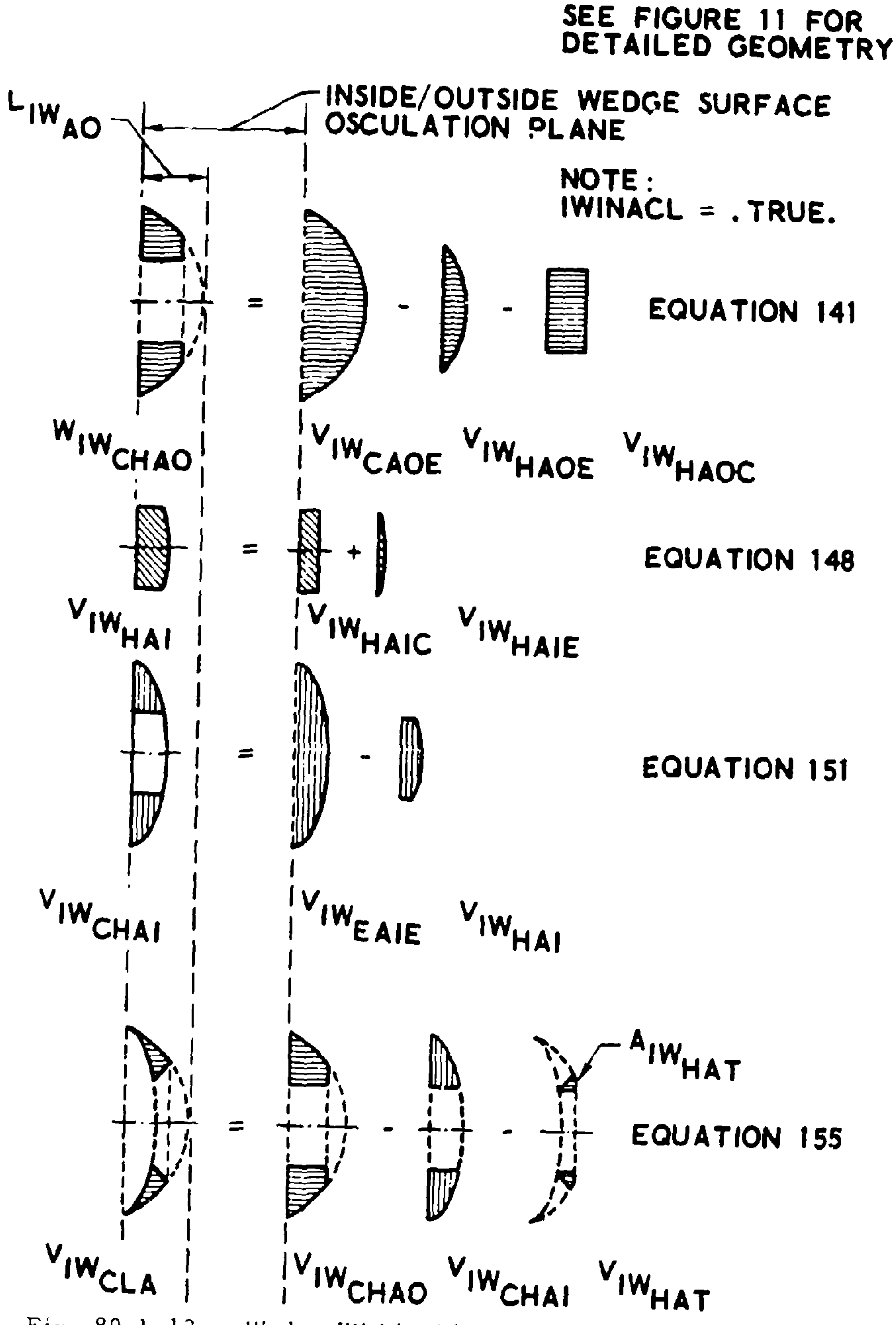

Fig. 80.1-12 Wedge Within Aft Closure, Volumes

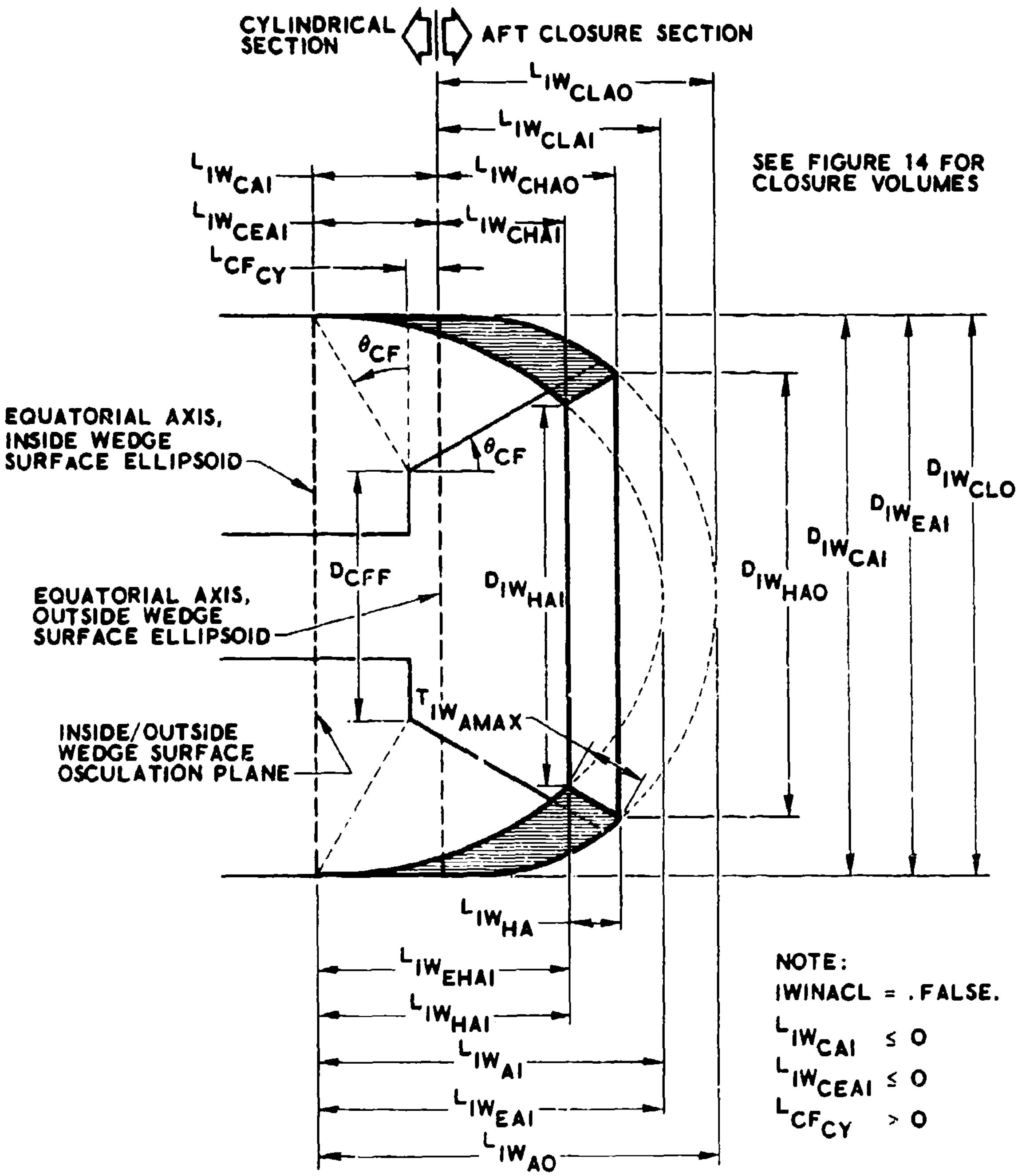

Fig. 80.1-13 Wedge Beyond Aft Closure, Detailed Geometry

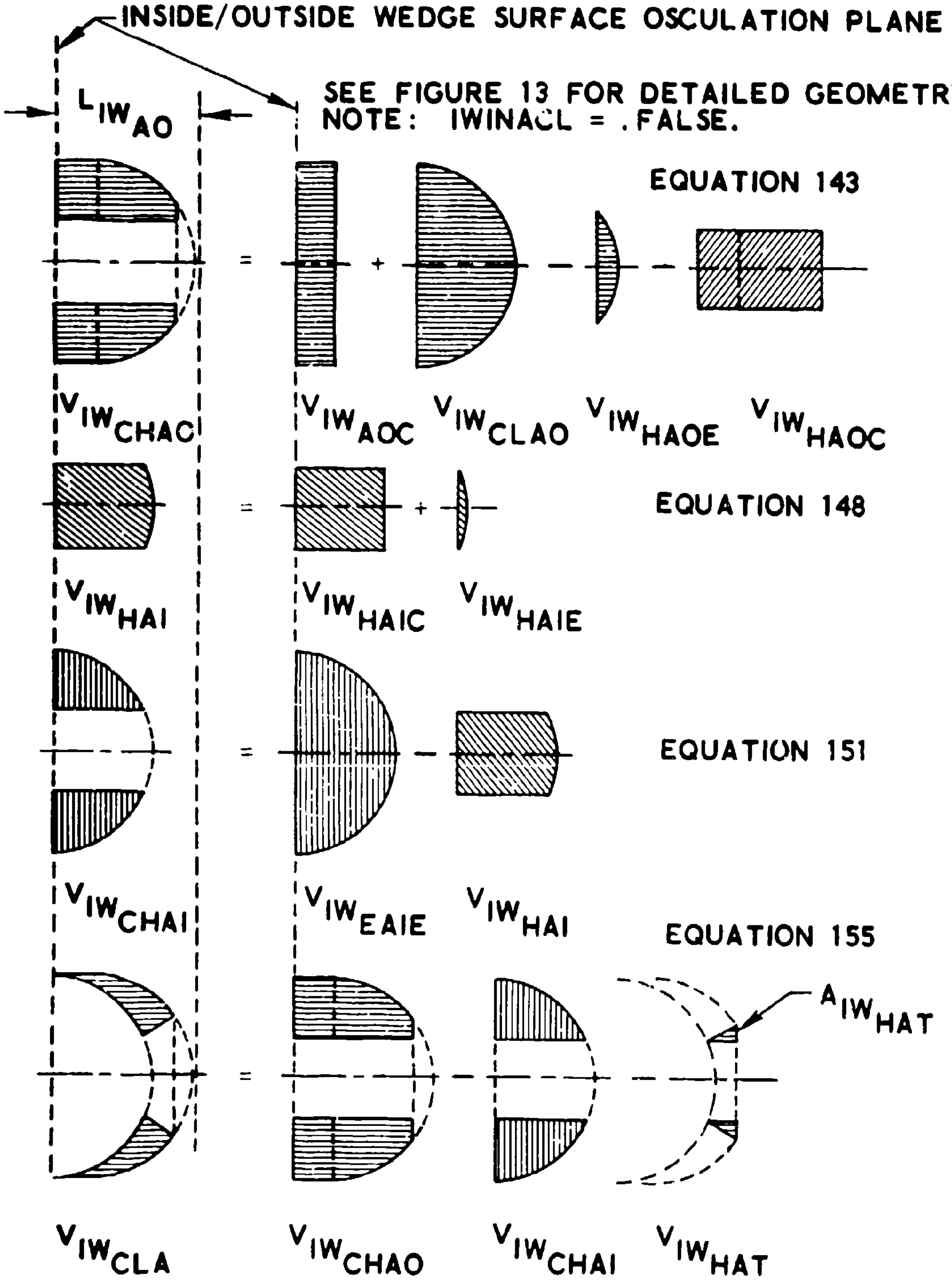

Fig. 80.1-14 Wedge Beyond Aft Closure, Volumes

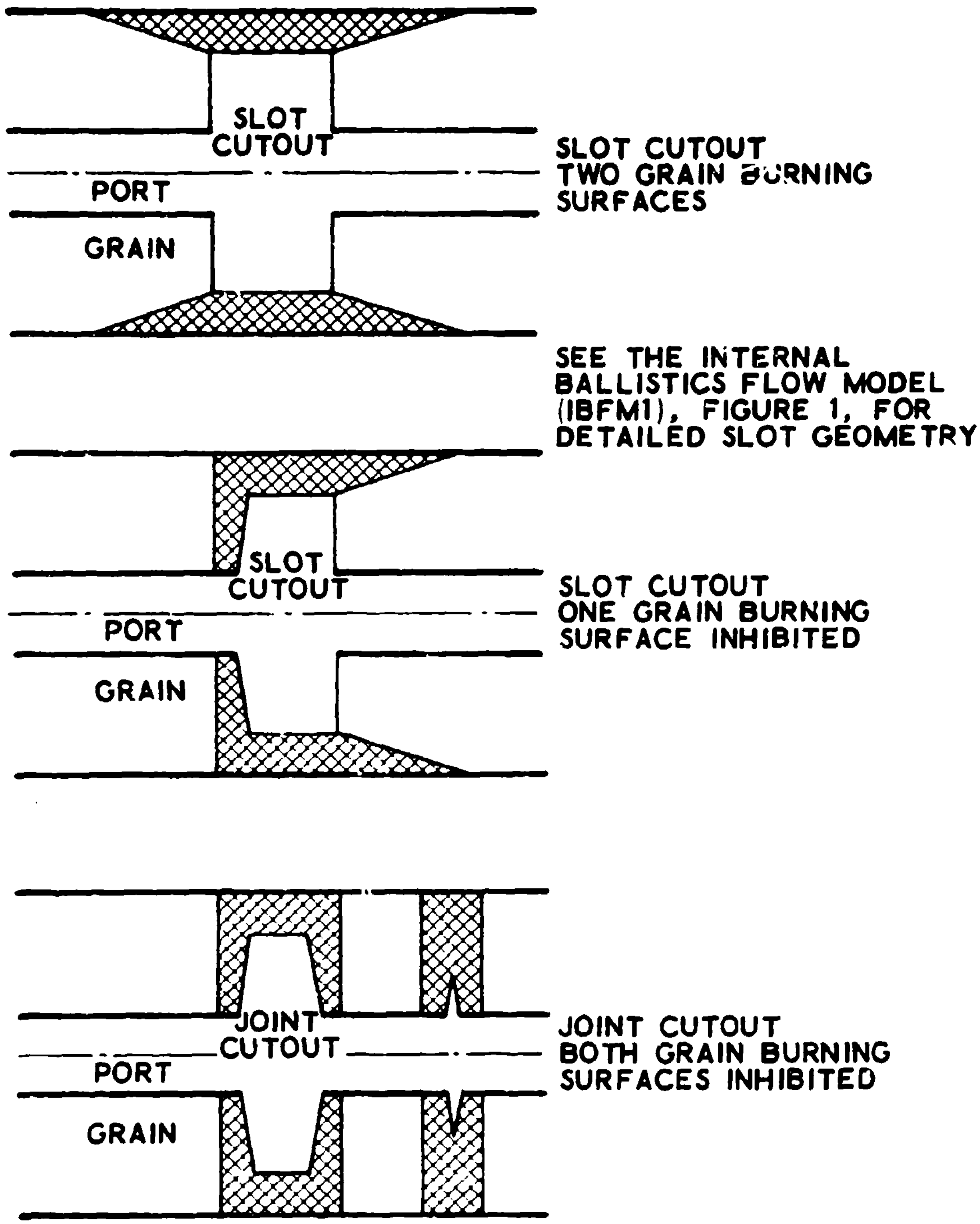

Fig. 80.1-15 Slot and Joint Insulation Configurations

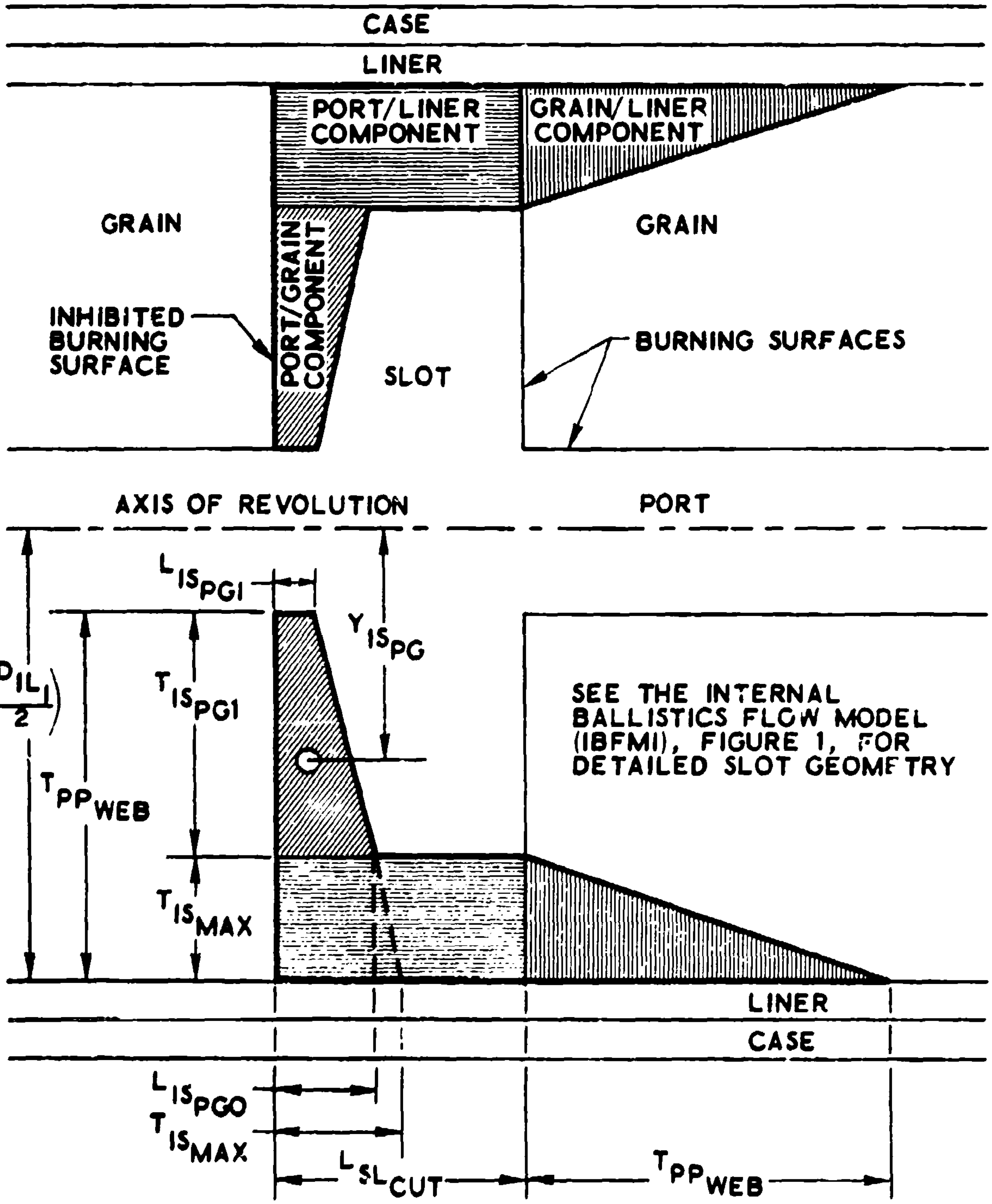

Fig. 80.1-16 Slot Insulation Subcomponents and Geometry

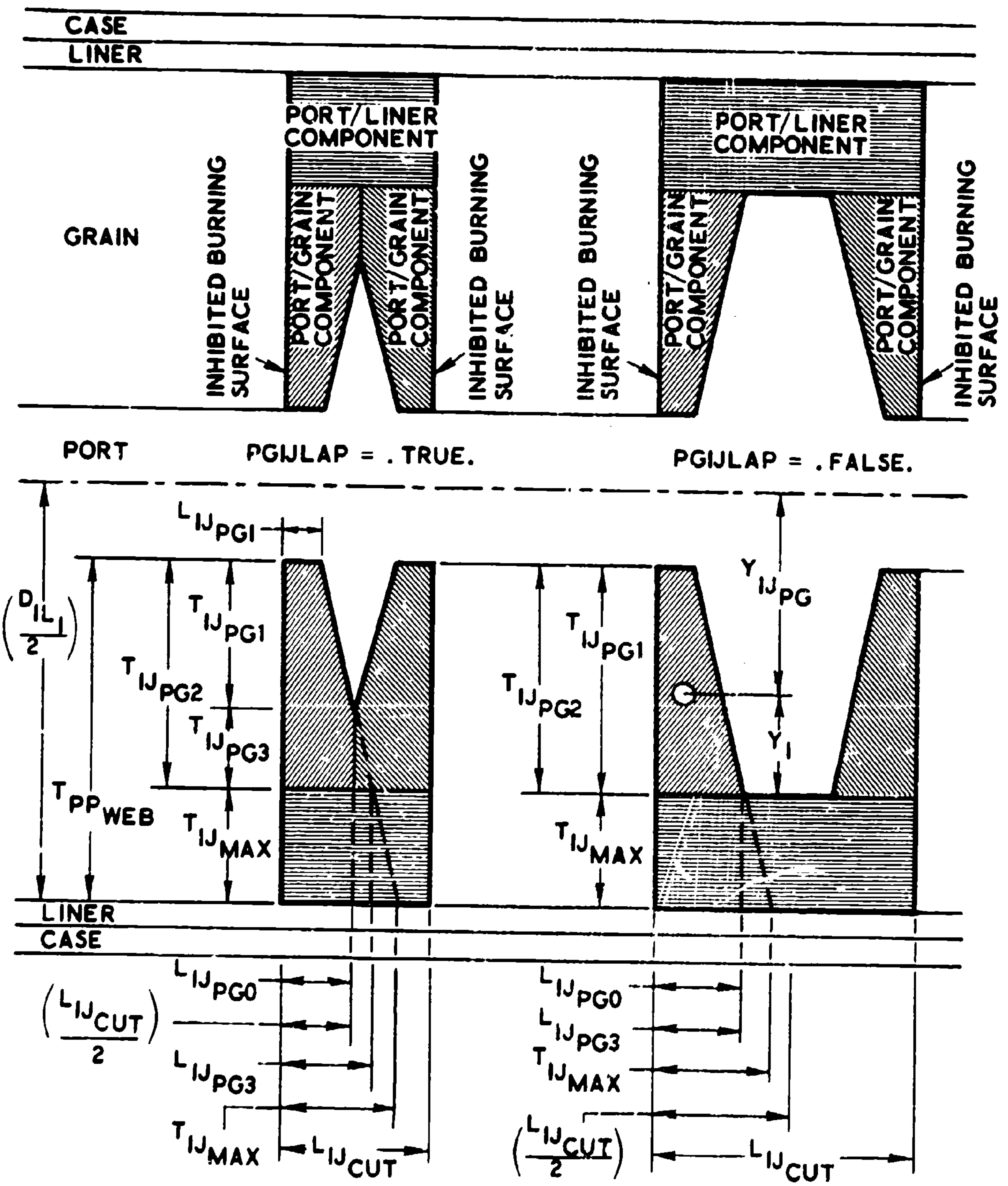

Fig. 80.1-17 Joint Insulation Subcomponents and Geometry

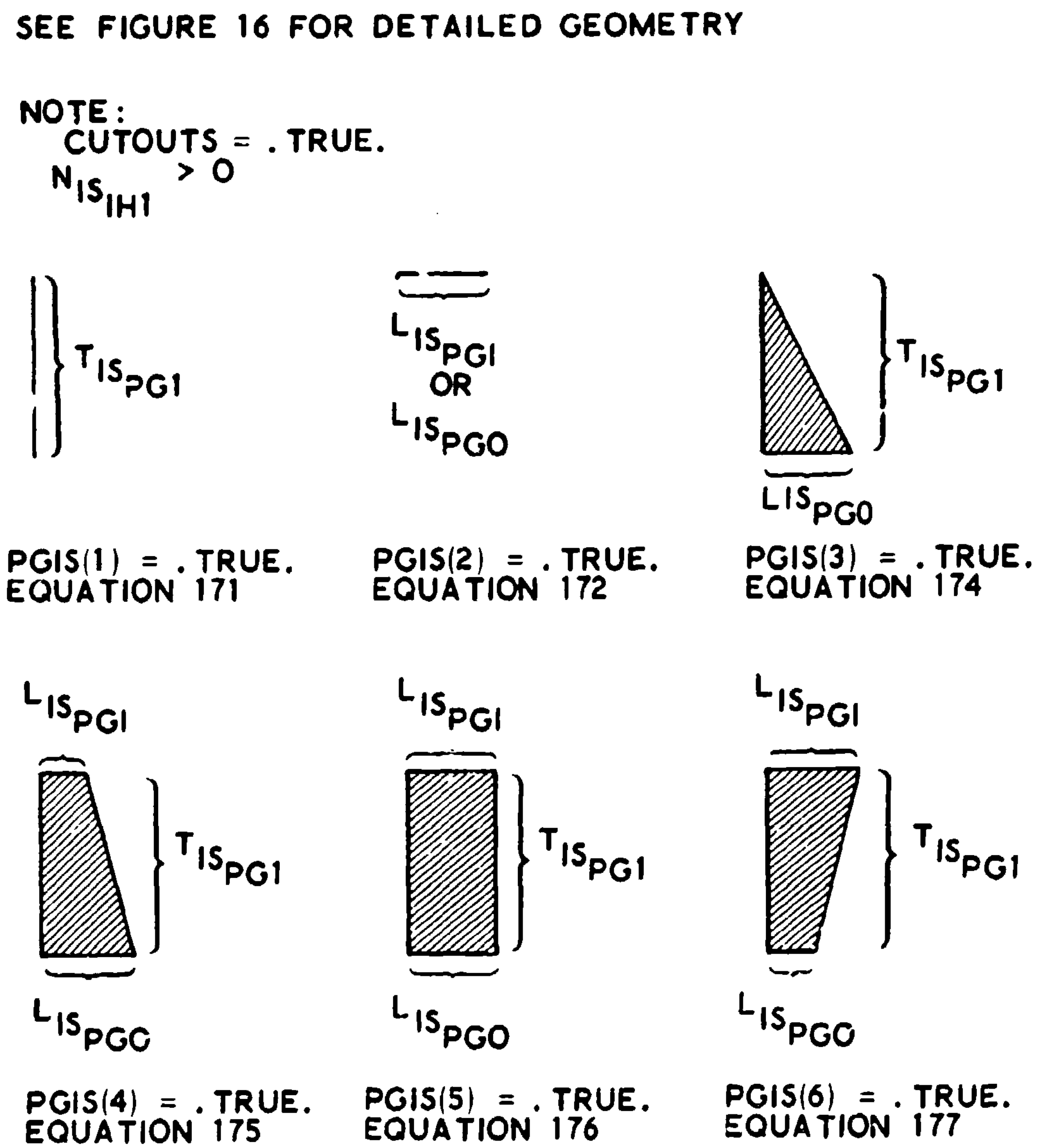

Fig. 80.1-18 Acceptable Polygons for Slot Port/Grain Component

SEE FIGURE 17 FOR DETAILED GEOMETRY.
NOTE: CUTOUT J = .TRUE.

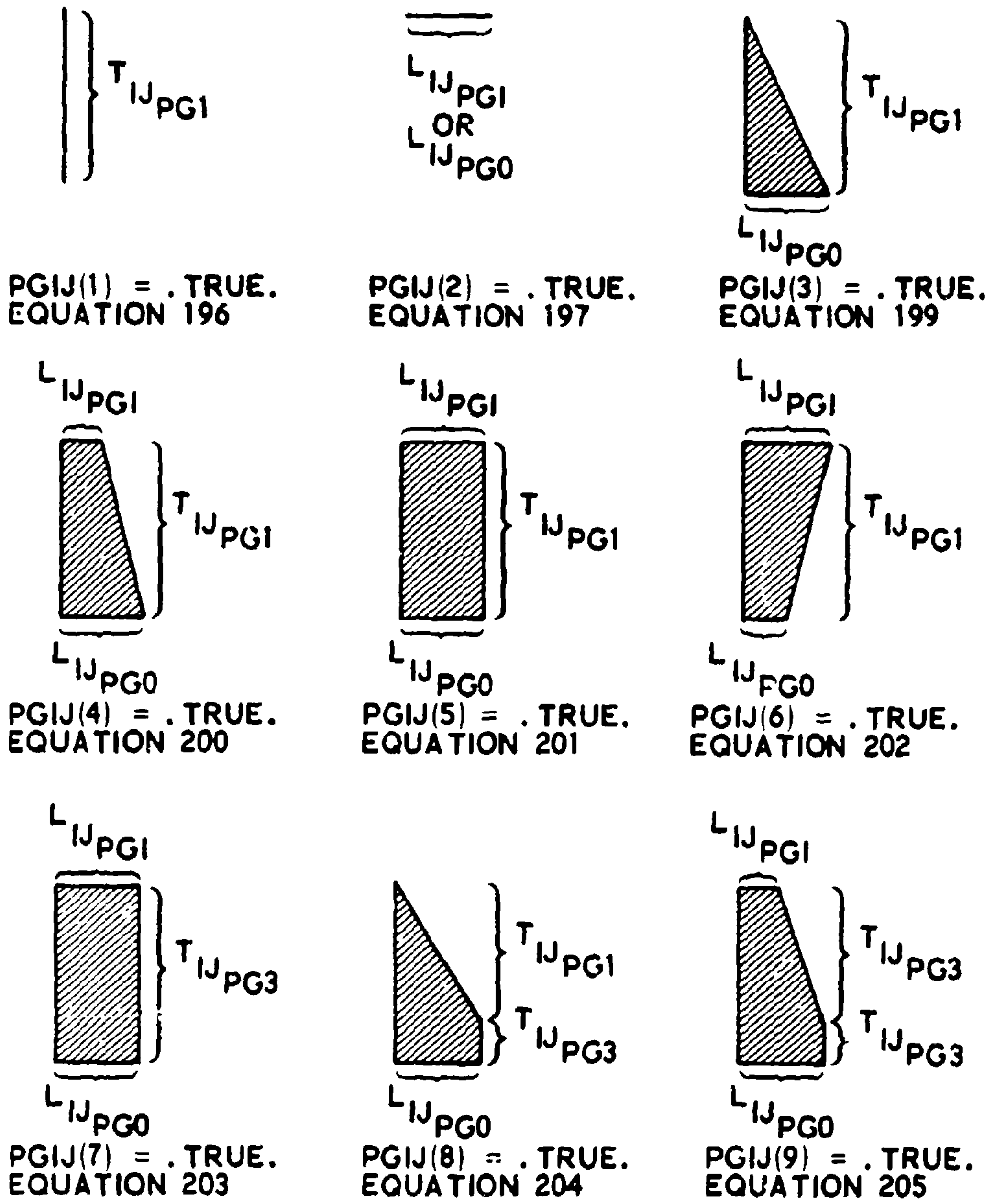

Fig. 80.1-19 Acceptable Polygons for Joint Port/Grain Component

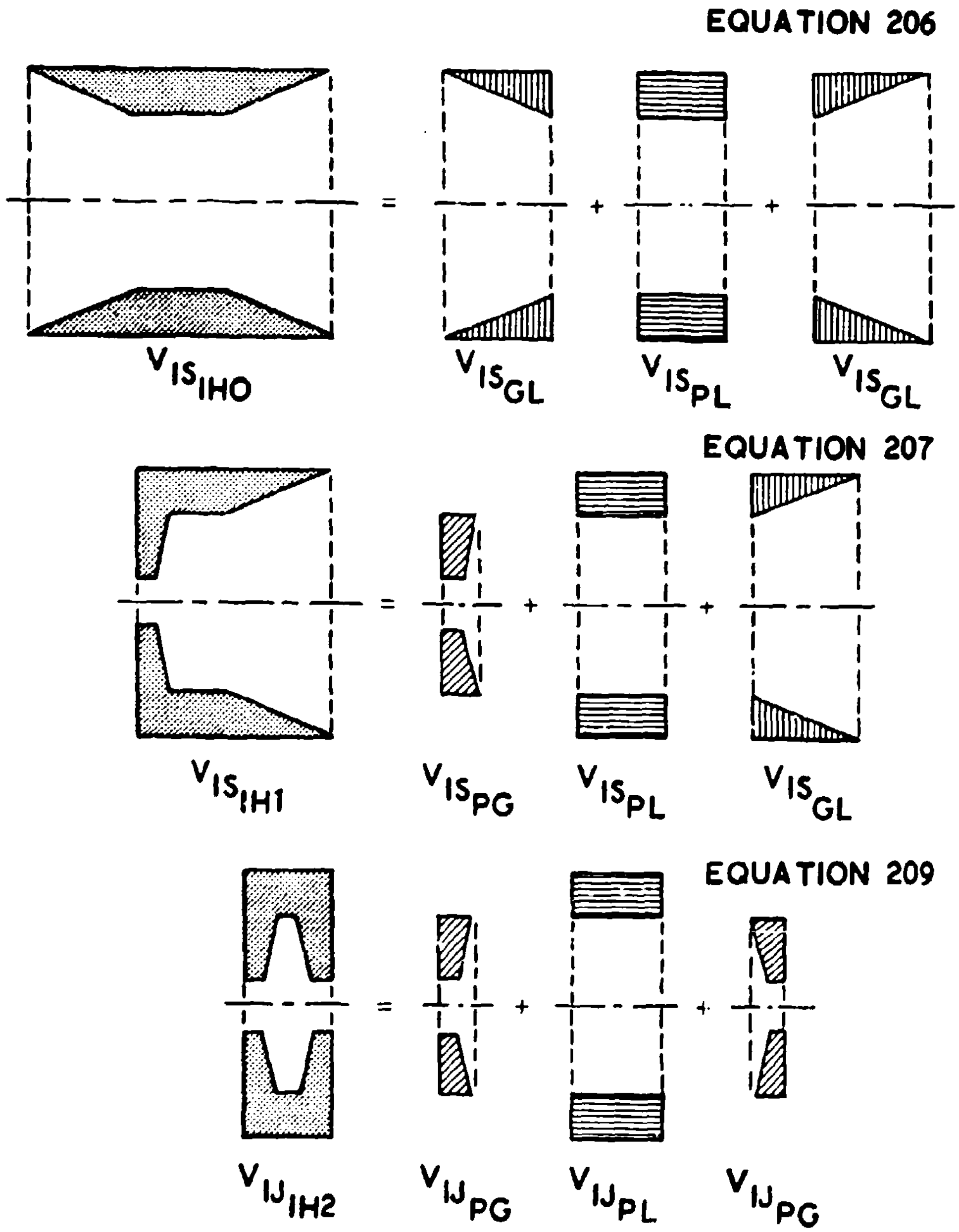

Fig. 80.1-20 Slot and Joint Insulation Volumes

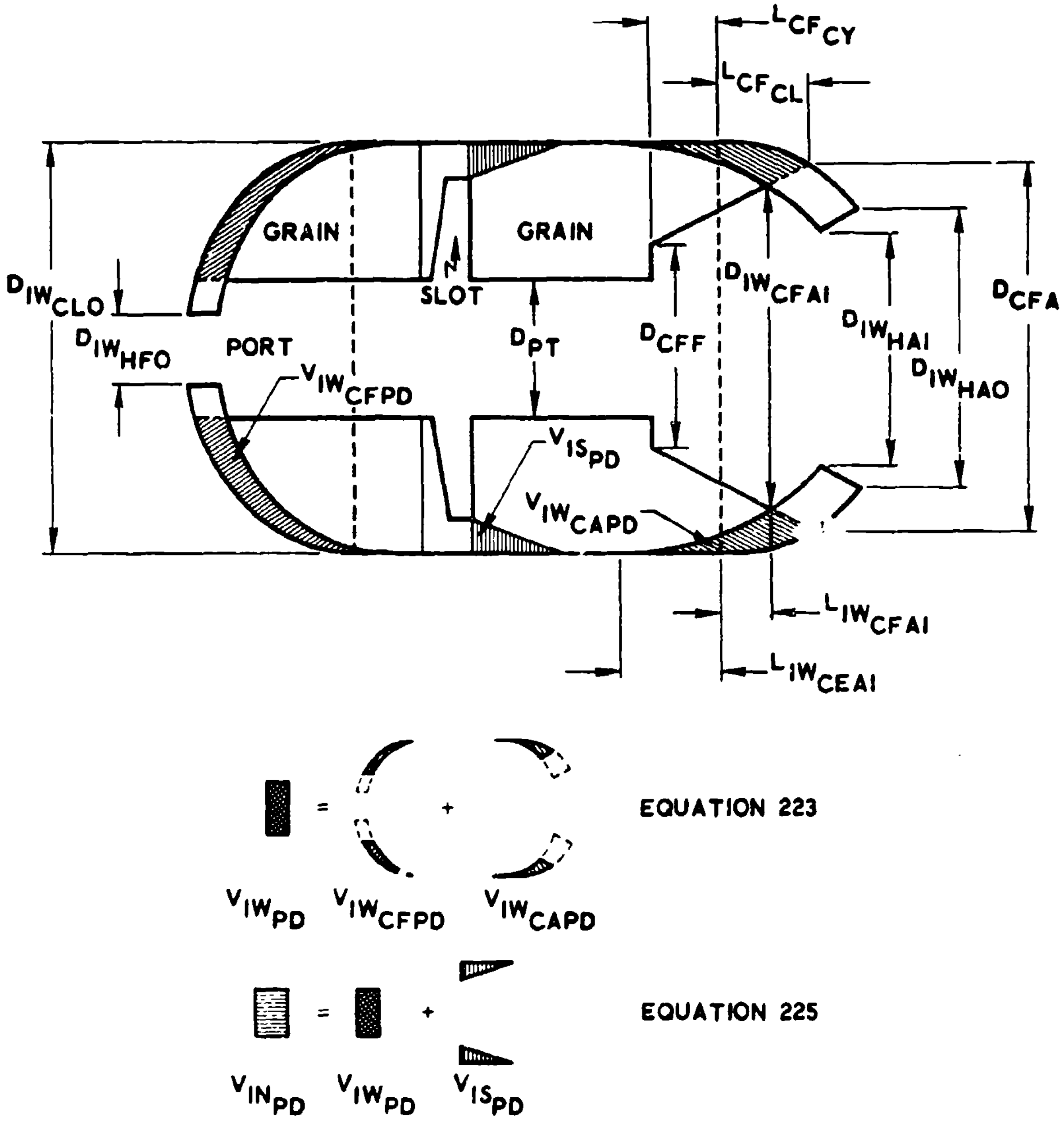

Fig. 80.1-21 Displaced Propellent

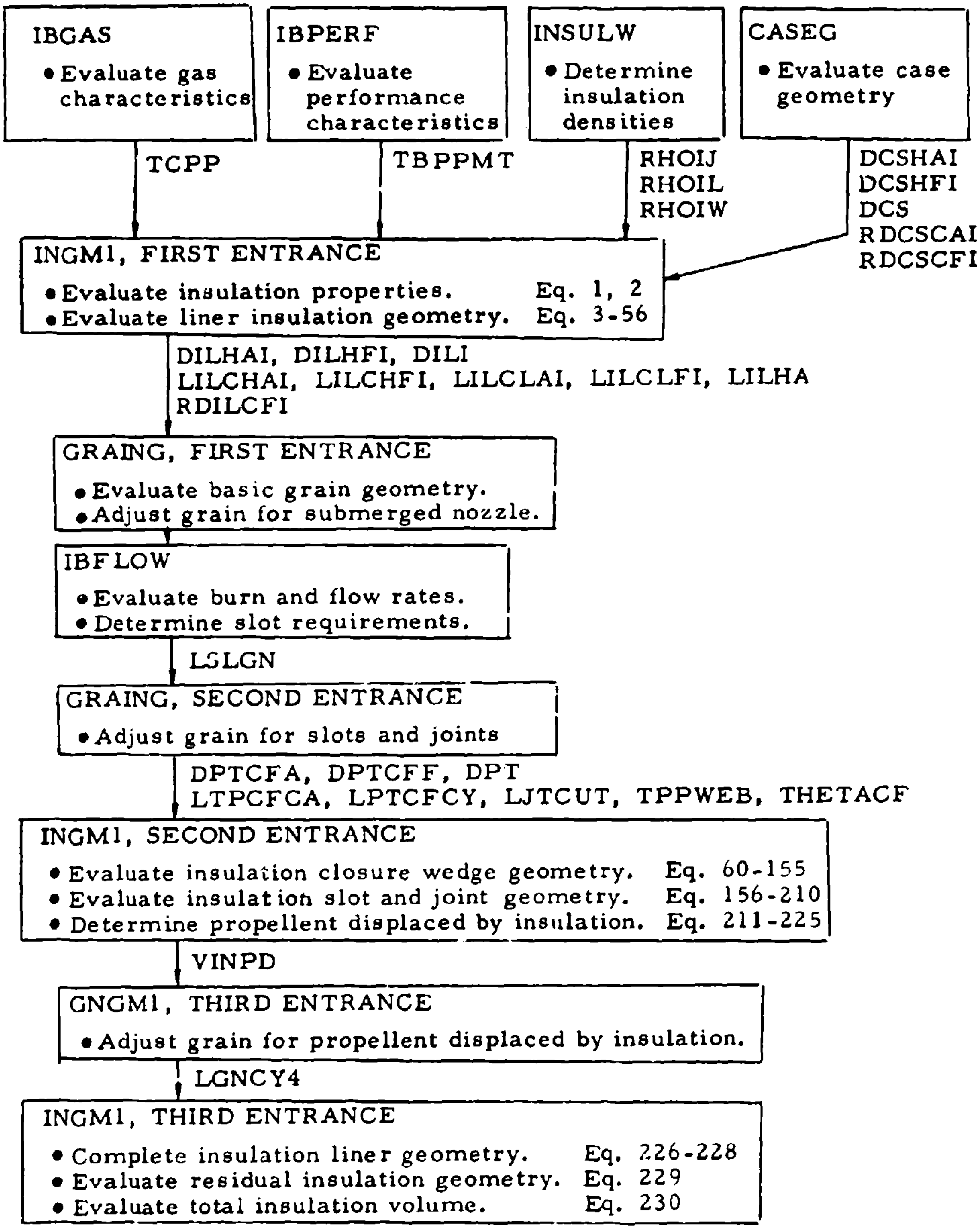

Fig. 80.1-22 Inter-Model Coupling

INPUT DATA, INTRA-MODEL:

The following data is input directly to this model by the program user. If a value is not input, the preset value is used.

Mnemonic	Symbol	Description; Ext. (Int.) Units		Preset
CING1	C_{IN_1}	Constant for QINH computation.		0.43
CING2	C_{IN_2}	Constant for QINH computation.		1000.
CING3	C_{IN_3}	Constant for TIWMAX, TISMAX and TIJMAX computations.		0.00868
KLIWFI1	K_{LIWFI1}	Proportionality coefficient for LIWHFI computation; N. D.		1
KLIWFI2	K_{LIWFI2}	Bias for LIWHFI computation; in		0
LIJPGI	$L_{IJ_{PGI}}$	Inside base of the polygon cross section associated with the port/grain insulation component for joint cutouts; in	Fig. 17	.1
LISPGI	$L_{IS_{PGI}}$	Inside base of the polygon cross section associated with the port/grain insulation component for slot cutouts; in	Fig. 16	.1
NIJCUT	$N_{IJ_{CUT}}$	Number of joint cutouts having both grain burning surfaces inhibited. Integer valued real number (floating point integer); N. D.		0
NISIH0	$N_{IS_{IH0}}$	Number of slot cutouts having no grain burning surfaces inhibited. Integer valued real number (floating point integer); N. D.		0

INPUT DATA, INTRA-MODEL (Cont.):

Mnemonic	Symbol	Description; Int. (Int.) Units		Preset
NISIH1	$N_{IS_{IH1}}$	Number of slot cutouts having one grain burning surface inhibited. Integer valued real number (floating point integer);		
		N. D.		0
QINSTAR	Q^{*}_{IN}	Effective heat of ablation of internal insulation;		
		btu/lb		0
TILCY	$T_{IL_{CY}}$	Thickness of insulation liner in the cylindrical section;		
		in	Fig. 2	0
TINR	T_{IN_R}	Thickness of residual insulation;		
		in		.1

Due to the nature of this model, a very large number of coefficient and bias quantities (mnemonic with first character K) are made available for input. However, in normal applications the preset values are used for most, if not all, of these quantities. Note that these coefficient quantities are preset (1) and the bias quantities are preset (0).

LINER INSULATION COEFFICIENTS AND BIAS

KIL1	K_{IL_1}	Coefficient for TILCLF computation;	
		N. D.	1
KIL2	K_{IL_2}	Bias for TILCLF computation;	
		in	0
KIL3	K_{IL_3}	Coefficient for VILCLF computation;	
		N. D.	1

INPUT DATA, INTRA-MODEL (Cont.):

Mnemonic	Symbol	Description; Ext. (Int.) Units	Preset
KIL4	K_{IL_4}	Bias for VILCLF computation; in^3	0
KIL5	K_{IL_5}	Coefficient for DILHAO computation; N. D.	1
KIL6	K_{IL_6}	Bias for DILHAO computation; in	0
KIL7	K_{IL_7}	Coefficient for TILCLA computation; N. D.	1
KIL8	K_{IL_8}	Bias for TILCLA computation; in	0
KIL9	K_{IL_9}	Coefficient for VILCLA computation; N. D.	1
KIL10	$K_{IL_{10}}$	Bias for VILCLA computation; in^3	0
KIL11	$K_{IL_{11}}$	Coefficient for LILCY computation; N. D.	1
KIL12	$K_{IL_{12}}$	Bias for LILCY computation; in	0
KIL13	$K_{IL_{13}}$	Coefficient for VILCY computation; N. D.	1
KIL14	$K_{IL_{14}}$	Bias for VILCY computation; in	0

INPUT DATA, INTRA-MODEL (Cont.):

Mnemonic	Symbol	Description; Ext. (Int.) Units	Preset
KIL15	$K_{IL_{15}}$	Coefficient for VIL computation; N. D.	1
KIL16	$K_{IL_{16}}$	Bias for VIL computation; in^3	0
KIL17	$K_{IL_{17}}$	Coefficient for DILHFO computation; N. D.	1
KIL18	$K_{IL_{18}}$	Bias for DILHFO computation; in	0

JOINT INSULATION COEFFICIENTS AND BIAS

Mnemonic	Symbol	Description; Ext. (Int.) Units	Preset
KIJ1	K_{IJ_1}	Coefficient for TIJMAX computation; N. D.	1
KIJ2	K_{IJ_2}	Bias for TIJMAX computation; in	0
KIJ3	K_{IJ_3}	Coefficient for LIJCUT computation; N. D.	1
KIJ4	K_{IJ_4}	Bias for LIJCUT computation; in	0
KIJ5	K_{IJ_5}	Coefficient for VIJPL computation; N. D.	1
KIJ6	K_{IJ_6}	Bias for VIJPL computation; in^3	0

INPUT DATA, INTRA-MODEL (Cont.):

Mnemonic	Symbol	Description; Ext. (Int.) Units	Preset
KIJ7	K_{IJ_7}	Coefficient for VIJPG computation; N. D.	1
KIJ8	K_{IJ_8}	Bias for VIJPG computation; in^3	0
KIJ9	K_{IJ_9}	Coefficient for VIJIH2 computation; N. D.	1
KIJ10	$K_{IJ_{10}}$	Bias for VIJIH2 computation; in^3	0
KIJ11	$K_{IJ_{11}}$	Coefficient for VIJ computation; N. D.	1
KIJ12	$K_{IJ_{12}}$	Bias for VIJ computation; in^3	0

GENERAL INSULATION COEFFICIENTS AND BIAS

Mnemonic	Symbol	Description; Ext. (Int.) Units	Preset
KIN1	K_{IN_1}	Coefficient for QINH computation; N. D.	1
KIN2	K_{IN_2}	Bias for QINH computation;	0
KIN3	K_{IN_3}	Coefficient for TINMAX computation; N. D.	1
KIN4	K_{IN_4}	Bias for TINMAX computation; in	0

INPUT DATA, INTRA-MODEL (Cont.):

Mnemonic	Symbol	Description; Ext. (Int.) Units	Preset
KIN5	K_{IN_5}	Coefficient for VINR computation; N. D.	1
KIN6	K_{IN_6}	Bias for VINR computation; in^3	0
KIN7	K_{IN_7}	Coefficient for VIN computation; N. D.	1
KIN8	K_{IN_8}	Bias for VIN computation; in^3	0

SLOT INSULATION COEFFICIENTS AND BIAS

Mnemonic	Symbol	Description; Ext. (Int.) Units	Preset
KIS1	K_{IS_1}	Coefficient for TISMAX computation; N. D.	1
KIS2	K_{IS_2}	Bias for TISMAX computation; in	0
KIS3	K_{IS_3}	Coefficient for LISCUT computation; N. D.	1
KIS4	K_{IS_4}	Bias for LISCUT computation; in	0
KIS5	K_{IS_5}	Coefficient for VISPL computation; N. D.	1
KIS6	K_{IS_6}	Bias for VISPL computation; in^3	0

INPUT DATA, INTRA-MODEL (Cont.):

Mnemonic	Symbol	Description; Ext. (Int.) Units	Preset
KIS7	K_{IS_7}	Coefficient for VISGL computation; N. D.	1
KIS8	K_{IS_8}	Bias for VISGL computation; in^3	0
KIS9	K_{IS_9}	Coefficient for VISPG computation; N. D.	1
KIS10	$K_{IS_{10}}$	Bias for VISPG computation; in^3	0
KIS11	$K_{IS_{11}}$	Coefficient for VISIH0 computation; N. D.	1
KIS12	$K_{IS_{12}}$	Bias for VISIH0 computation; in^3	0
KIS13	$K_{IS_{13}}$	Coefficient for VISIH1 computation; N. D.	1
KIS14	$K_{IS_{14}}$	Bias for VISIH1 computation; in^3	0
KIS15	$K_{IS_{15}}$	Coefficient for VIS computation; N. D.	1
KIS16	$K_{IS_{16}}$	Bias for VIS computation; in^3	0

INPUT DATA, INTRA-MODEL (Cont.):

Mnemonic	Symbol	Description; Ext. (Int.) Units	Preset
WEDGE INSULATION COEFFICIENTS AND BIAS			
KIW1	K_{IW_1}	Coefficient for DIWHFO computation; N. D.	1
KIW2	K_{IW_2}	Bias for DIWHFO computation; in	0
KIW3	K_{IW_3}	Coefficient for LIWHF computation; N. D.	1
KIW4	K_{IW_4}	Bias for LIWHF computation; in	0
KIW7	K_{IW_7}	Coefficient for VIWCLF computation; N. D.	1
KIW8	K_{IW_8}	Bias for VIWCLF computation; in^3	0
KIW9	K_{IW_9}	Coefficient for TIWAMAX computation; N. D.	1
KIW10	$K_{IW_{10}}$	Bias for TIWAMAX computation; in	0
KIW11	$K_{IW_{11}}$	Coefficient for DIWHAO computation; N. D.	1
KIW12	$K_{IW_{12}}$	Bias for DIWHAO computation; in	0
KIW13	$K_{IW_{13}}$	Coefficient for DIWHAI computation; N. D.	1

INPUT DATA, INTRA-MODEL (Cont.):

Mnemonic	Symbol	Description; Ext. (Int.) Units	Preset
KIW14	$K_{IW_{14}}$	Coefficient for DIWHAI computation; N. D.	1
KIW15	$K_{IW_{15}}$	Coefficient for DIWHAI computation; N. D.	1
KIW16	$K_{IW_{16}}$	Bias for DIWHAI computation; in	0
KIW17	$K_{IW_{17}}$	Coefficient for LIWHA computation; N. D.	1
KIW18	$K_{IW_{18}}$	Bias for LIWHA computation; in	0
KIW19	$K_{IW_{19}}$	Coefficient for VIWCLA computation; N. D.	1
KIW20	$K_{IW_{20}}$	Bias for VIWCLA computation; in^3	0
KIW21	$K_{IW_{21}}$	Coefficient for TIWFMAX computation; N. D.	1
KIW22	$K_{IW_{22}}$	Bias for TIWFMAX computation; in	0
KIW23	$K_{IW_{23}}$	Coefficient for TIWMAX computation; N. D.	1
KIW24	$K_{IW_{24}}$	Bias for TIWMAX computation; in	0

INPUT DATA, INTRA-MODEL (Cont.):

Mnemonic	Symbol	Description; Ext. (Int.) Units	Preset
KPD1	K_{PD_1}	Coefficient for VIWCFPD computation; N. D.	1
KPD2	K_{PD_2}	Bias for VIWCFPD computation; in^3	0
KPD3	K_{PD_3}	Coefficient for VIWCAPD computation; N. D.	1
KPD4	K_{PD_4}	Bias for VIWCAPD computation; in^3	0
KPD5	K_{PD_5}	Coefficient for VIWPD computation; N. D.	1
KPD6	K_{PD_6}	Bias for VIWPD computation; in^3	0
KPD7	K_{PD_7}	Coefficient for VISPD computation; N. D.	1
KPD8	K_{PD_8}	Bias for VISPD computation; in^3	0
KPD9	K_{PD_9}	Coefficient for VINPD computation; N. D.	1
KPD10	$K_{PD_{10}}$	Bias for VINPD computation; in^3	0

INPUT DATA, INTER-MODEL:

This model requires as input certain data which is usually output from a model of the specified model type. If the user has not specified such a source for this data, then it must be input directly with the intra-model input.

Mnemonic	Symbol	Description; Ext. (Int.) Units		Model Type
DCSHAI	$D_{CS_{HAI}}$	Diameter of hole in aft inside case closure surface;		
		in	Figs. 2, 22	CASEG
DCSHFI	$D_{CS_{HFI}}$	Diameter of hole in forward inside case closure surface;		
		in	Figs. 2, 22	CASEG
DCSI	$D_{CS_{I}}$	Inside case diameter, cylindrical section;		
		in	Figs. 2, 22	CASEG
DPT	D_{PT}	Diameter of cylindrical section of port;		
		in	Figs. 2, 21, 22	GRAING
DPTCFA	D_{CFA}	Aft base diameter of the port cone frustum section required for nozzle submergence;		
		in	Figs. 21, 22	GRAING
DPTCFF	D_{CFF}	Forward base diameter of the port cone frustum section required for nozzle submergence;		
		in	Figs. 11, 13, 21, 22	GRAING
LGNCY4	$L_{GN_{CY4}}$	Length of cylindrical grain section. Includes length penalty for nozzle submergence, joint cutouts and slot cutouts;		
		in	Figs. 2, 21, 22	GRAING
LJTCUT	$L_{JT_{CUT}}$	Total length of cut in grain for joints;		
		in	Fig. 22	GRAING

INPUT DATA, INTER-MODEL (Cont.):

Mnemonic	Symbol	Description; Ext. (Int.) Units		Model Type
LPTCFCA	$L_{CF_{CA}}$	Length of the portion of the port cone frustum section, required for nozzle submergence, within the aft closure. Positive sense from closure equatorial plane towards aft;		
		in	Figs. 21, 22	GRAING
LPTCFCY	$L_{CF_{CY}}$	Length of the portion of the port cone frustum which is within the cylindrical section;		
		in	Figs. 11, 13, 21, 22	GRAING
LSLGN	$L_{SL_{GN}}$	Total slot length;		
		in	Fig. 22	IBFLOW
RDCSCAI	R_{DCSCAI}	Head ratio, aft inside case closure surface;		
		N. D.	Fig. 22	CASEG
RDCSCFI	R_{DCSCFI}	Head ratio, forward inside case closure surface;		
		N. D.	Figs. 21, 22	CASEG
RHOIJ	ρ_{IJ}	Density of insulation for joint cutouts;		
		lb/in^3	Fig. 22	INSULW
RHOIS	ρ_{IS}	Density of insulation for slot cutouts;		
		lb/in^3	Fig. 22	INSULW
RHOIW	ρ_{IW}	Density of insulation for closure wedges;		
		lb/in^3	Fig. 22	INSULW
TBPPMT	T_B	Propellent burn time;		
		sec	Fig. 22	IBPERF

INPUT DATA, INTER-MODEL (Cont.):

Mnemonic	Symbol	Description; Ext. (Int.) Units		Model Type
TCPP	$T_{C_{PP}}$	Propellent combustion temperature; °R	Fig. 22	IBGAS
THETACF	θ_{CF}	Half-angle of port cone frustum section; deg (rad)	Figs. 2, 11, 13, 21, 22	GRAING
TPPWEB	$T_{PP_{WEB}}$	Thickness of propellent web; in	Figs. 2, 16, 17, 22	GRAING

OUTPUT DATA:

The following data is output from this model. It is available for use as inter-model input to other models and to print, plot, and optimization routines.

Mnemonic	Symbol	Description; Ext. (Int.) Units
AIJPG	$A_{IJ_{PG}}$	Area of the polygon cross section associated with the port/grain insulation component for joint cutouts; in^2 Fig. 17 Eq. 188
AISPG	$A_{IS_{PG}}$	Area of the polygon cross section associated with the port/grain insulation component for slot cutouts; in^2 Fig. 16 Eq. 168
AIWHAT	$A_{IW_{HAT}}$	Area of triangular wedge section, associated with the cone frustum cutout for the nozzle, within the aft case closure section; in^2 Figs. 12, 14 Eq. 152
COSTCF	$\cos\left(\theta_{CF}\right)$	Cosine of THETACF; N. D.
CUTOUTJ	CUTOUTJ	CUTOUTJ (CUT OUT in grain for Joint) is a logical variable which specifies if there are joint cutouts within the grain which require insulation. .TRUE.; there is at least one joint cutout requiring insulation. Both surfaces of a joint are inhibited. .FALSE.; there are no joint cutouts requiring insulation; N. D. Eq. 157-b
CUTOUTS	CUTOUTS	CUTOUTS (CUT OUT in grain for Slot) is a logical variable which specifies if there are slot cutouts within the grain which require insulation.

OUTPUT DATA (Cont.):

Mnemonic	Symbol	Description; Ext. (Int.) Units		
		.TRUE.;	there is at least one slot cutout requiring insulation. Either one or no slot burning surface may be inhibited.	
		.FALSE.;	there are no slot cutouts requiring insulation.	
		N. D.		Eq. 157-a
CIWA	C_{IW_A}	Intermediate computation for DIWCAI evaluation;		
		N. D.		Eq. 120
CIWAP	$C_{IW_{AP}}$	Intermediate computation for LIWCFAI evaluation;		
		N. D.		Eq. 216
CIWB	C_{IW_B}	Intermediate computation for DIWCAI evaluation;		
		in		Eq. 121
CIWBP	$C_{IW_{BP}}$	Intermediate computation for LIWCFAI evaluation;		
		in		Eq. 217
CIWC	C_{IW_C}	Intermediate computation for DIWCAI evaluation;		
		in^2		Eq. 122
CIWCP	$C_{IW_{CP}}$	Intermediate computation for LIWCFAI evaluation;		
		in^2		Eq. 218
DILCLI	$D_{IL_{CLI}}$	Equatorial diameter of the ellipsoids formed by the inside surface of the insulation liner associated with the forward and aft case closure sections;		
		in	Figs. 3, 5	Eq. 6

OUTPUT DATA (Cont.):

Mnemonic	Symbol	Description; Ext. (Int.) Units		
DILCLO	$D_{IL_{CLO}}$	Equatorial diameter of the ellipsoids formed by the outside surface of the insulation liner associated with the forward and aft case closure sections;		
		in	Figs. 3, 5	Eq. 5
DILHAI	$D_{IL_{HAI}}$	Diameter of circular hole, for the nozzle, centered on the axis of revolution of the hemi-ellipsoid formed by the inside surface of the insulation liner within the aft case closure section;		
		in	Figs. 2, 5	Eq. 40
DILHAO	$D_{IL_{HAO}}$	Diameter of circular hole, for the nozzle, centered on the axis of revolution of the hemi-ellipsoid formed by the outside surface of the insulation liner within the aft case closure section;		
		in	Fig. 5	Eq. 34
DILHFI	$D_{IL_{HFI}}$	Diameter of circular hole, for the ignitor, centered on the axis of revolution of the hemi-ellipsoid formed by the inside surface of the insulation liner within the forward case closure section;		
		in	Fig. 3	Eq. 15
DILHFO	$D_{IL_{HFO}}$	Diameter of circular hole, for the ignitor, centered on the axis of revolution of the hemi-ellipsoid formed by the outside surface of the insulation liner within the forward case closure section;		
		in	Fig. 3	Eq. 9
DILI	D_{IL_I}	Inside diameter of the cylinder which is the inside surface of the insulation liner in the cylindrical case section;		
		in	Fig. 2	Eq. 4
DILO	D_{IL_O}	Outside diameter of the cylinder which is the outside surface of the insulation liner in the cylindrical case section;		
		in	Fig. 2	Eq. 3

OUTPUT DATA (Cont.):

Mnemonic	Symbol	Description; Ext. (Int.) Units		
DIWAI	$D_{IW_{AI}}$	Intermediate computation for LIWCFAI, DIWCFAI evaluation;		
		in		Eq. 215
DIWCAI	$D_{IW_{CAI}}$	Diameter of the circle of osculation formed by the tangency points of the inside aft wedge surface hemi-ellipsoid and the outside aft wedge surface hemi-ellipsoid. See IWINACL;		
		in	Figs. 11, 15	Eqs. 119, 123
DIWCFAI	$D_{IW_{CFAI}}$	Diameter of the circle formed by the intersection of the grain cone frustum cutout with the inside surface of the insulation wedge associated with the aft closure section;		
		in		Eq. 220
DIWCFI	$D_{IW_{CFI}}$	Diameter of the circle of osculation formed by the tangency points of the inside forward wedge surface hemi-ellipsoid and the outside forward wedge surface hemi-ellipsoid. See IWINFCL;		
		in	Figs. 7, 9	Eqs. 73, 77
DIWCLO	$D_{IW_{CLO}}$	Equatorial diameter of the hemi-ellipsoids formed by the outside surface of the insulation wedges associated with the forward and aft closure sections;		
		in	Figs. 7, 9, 11, 13	Eq. 60
DIWEAI	$D_{IW_{EAI}}$	Equatorial diameter of the hemi-ellipsoid associated with the inside surface of the insulation wedge in the aft case closure section. See IWINACL;		
		in	Figs. 11, 13	Eqs. 128, 130
DIWEFI	$D_{IW_{EFI}}$	Equatorial diameter of the hemi-ellipsoid associated with the inside surface of the insulation wedge in the forward case closure. See IWINFCL;		
		in	Figs. 7, 9	Eqs. 76, 79

OUTPUT DATA (Cont.):

Mnemonic	Symbol	Description; Ext. (Int.) Units
DIWHAI	$D_{IW_{HAI}}$	Diameter of the forward base of the cone frustum hole, for the nozzle cutout, centered on the axis of revolution of the hemi-ellipsoid formed by the inside surface of the insulation wedge associated with the aft case closure section; in Figs. 11, 13 Eq. 110
DIWHAO	$D_{IW_{HAO}}$	Diameter of the aft base of the cone frustum hole, for the nozzle cutout, centered on the axis of revolution of the hemi-ellipsoid formed by the outside surface of the insulation wedge associated with the aft case closure section; in Figs. 11, 13 Eq. 109
DIWHFI	$D_{IW_{HFI}}$	Diameter of the circular hole, for the ignitor, centered on the axis of revolution of the hemi-ellipsoid formed by the inside surface of the insulation wedge associated with the forward case closure section; in Figs. 7, 9 Eq. 63
DIWHFO	$D_{IW_{HFO}}$	Diameter of the circular hole, for the ignitor, centered on the axis of revolution of the hemi-ellipsoid formed by the outside surface of the insulation wedge associated with the forward case closure section; in Figs. 7, 9 Eq. 62
GOODPGJ	GOODPGJ	GOODPGJ is a logical valued variable which indicates an acceptable polygon cross section for the port/grain insulation component associated with the joint cutouts. =.TRUE.; PG component for joint insulation is an acceptable polygon. The particular polygon may be determined by referring to PGIJ.

OUTPUT DATA (Cont.):

Mnemonic	Symbol	Description; Ext. (Int.) Units
		=.FALSE.; PG component for joint insulation is not an acceptable polygon. Joint insulation geometry may be bad. N.D.
GOODPGS	GOODPGS	GOODPGS is a logical valued variable which indicates an acceptable polygon cross section for the port/grain insulation component associated with the slot cutouts; =.TRUE., PG component for slot insulation is an acceptable polygon. the particular polygon may be determined by referring to PGIS. =.FALSE., PG component for slot insulation is not an acceptable polygon. Slot insulation geometry may be bad; N.D.
IJNOTLN	IJNOTLN	Intermediate logical quantity for PGIJ computation; N.D. Eq. 198
ISNOTLN	ISNOTLN	Intermediate logical quantity for PGIS computation; N.D. Eq. 173
IWINACL	$I_{WIN_{ACL}}$	IWINACL (Insulation Wedge IN Aft Closure) is a logical variable which specifies if the insulation wedge associated with the aft closure is completely within the aft closure; =.TRUE.; the insulation wedge is completely within the aft closure. See Figs. 11, 12.

OUTPUT DATA (Cont.):

Mnemonic	Symbol	Description; Ext. (Int.) Units
		=.FALSE.; the insulation wedge extends beyond the aft closure into the cylindrical section, or extends to the intersection of the aft closure and cylindrical section. See Figs. 13, 14;
		N.D. Eq. 118
IWINFCL	IWINFCL	IWINFCL (Insulation Wedge IN Forward CLosure) is a logical variable which specifies if the insulation wedge associated with the forward closure is completely within the forward closure;
		=.TRUE.; wedge is completely within the forward closure. See Fig. 7.
		=.FALSE.; wedge extends beyond the forward closure into the cylindrical section or extends to the intersection of the forward closure and cylindrical section. See Fig. 9;
		N.D. Eq. 72
LIJCUT	$L_{IJ_{CUT}}$	Length of a single joint cutout for insulation computation;
		in Fig. 17 Eq. 181
LIJPG3	$L_{IJ_{PG3}}$	Intermediate quantity required for the determination of the outside base of the polygon cross section associated with the port/grain insulation component for joint cutouts;
		in Fig. 17 Eq. 183
LIJPGO	$L_{IJ_{PGO}}$	Outside base of the polygon cross section associated with the port/grain insulation components for grain cutouts;
		in Fig. 17 Eqs. 184,185

OUTPUT DATA (Cont.):

Mnemonic	Symbol	Description; Ext. (Int.) Units		
LILCHAI	$L_{IL_{CHAI}}$	Length of hemi-ellipsoidal frustum associated with the inside surface of the insulation liner within the aft case closure;		
		in	Fig. 5	Eq. 42
LILCHAO	$L_{IL_{CHAO}}$	Length of hemi-ellipsoidal frustum associated with the outside surface of the insulation liner within the aft case closure section;		
		in	Fig. 5	Eq. 36
LILCHFI	$L_{IL_{CHFI}}$	Length of the hemi-ellipsoidal frustum associated with the inside surface of the insulation liner within the forward case closure;		
		in	Figs. 2, 3	Eq. 17
LILCHFO	$L_{IL_{CHFO}}$	Length of hemi-ellipsoidal frustum associated with the outside surface of the insulation liner within the forward closure section;		
		in	Figs. 2, 3	Eq. 11
LILCLAI	$L_{IL_{CLAI}}$	Length of the axis of revolution of the hemi-ellipsoid formed by the inside surface of the insulation liner within the aft case closure section;		
		in	Fig. 5	Eq. 38
LILCLAO	$L_{IL_{CLAO}}$	Length of the axis of revolution of the hemi-ellipsoid formed by the outside surface of the insulation liner within the aft case closure section;		
		in	Figs. 5, 6	Eq. 33
LILCLFI	$L_{IL_{CLFI}}$	Length of the axis of revolution of the hemi-ellipsoid formed by the inside surface of the insulation liner within the forward case closure section;		
		in	Fig. 3	Eq. 13

OUTPUT DATA (Cont.):

Mnemonic	Symbol	Description; Ext. (Int.) Units		
LILCLFO	$L_{IL_{CLFO}}$	Length of the axis of revolution of the hemi-ellipsoid formed by the outside surface of the insulation liner within the forward case closure section;		
		in	Figs. 3, 4	Eq. 8
LILCY	$L_{IL_{CY}}$	Length of insulation liner within the cylindrical case section. Includes length adjustment for submerged nozzle, slots and joints;		
		in	Fig. 2	Eq. 226
LILHA	$L_{IL_{HA}}$	Length of cylindrical hole, for the nozzle, in the insulation liner within the aft case closure section;		
		in	Fig. 5	Eq. 43
LILHF	$L_{IL_{HF}}$	Length of cylindrical hole, for the ignitor, in the insulation liner within the forward case closure section;		
		in	Fig. 3	Eq. 18
LISCUT	$L_{IS_{CUT}}$	Length of a single slot cutout for insulation computations;		
		in	Fig. 16	Eq. 162
LISPGO	$L_{IS_{PGO}}$	Length of outside base of the polygon cross section associated with the port/grain insulation component for slot cutouts;		
		in	Fig. 16	Eq.
LIWAI	$L_{IW_{AI}}$	Distance from the pole of the hemi-elli[illegible] associated with the inside surface of the insulation wedge in the aft closure to the a[illegible] closure "inside/outside surface wedge osculation plane";		
		in	Figs. 11, 13	Eq. 133

OUTPUT DATA (Cont.):

Mnemonic	Symbol	Description; Ext. (Int.) Units
LIWA1	$L_{IW_{A1}}$	Intermediate computation for VIWCAPD evaluation; in Eq. 213
LIWA2	$L_{IW_{A2}}$	Intermediate computation for VIWCAPD evaluation; in Eq. 214
LIWCAI	$L_{IW_{CAI}}$	Distance from the "equatorial plane of the aft closure outside wedge surface hemi-ellipsoid" to the "inside/outside wedge surface osculation plane". Measured along the axis of revolution, positive sense aft. A positive value indicates that the wedge is completely within the aft closure. A negative value indicates that the wedge extends beyond the aft closure into the cylindrical section. See IWINACL; in Figs. 11, 13 Eqs. 117, 124
LIWCEAI	$L_{IW_{CEAI}}$	Distance from the equatorial plane of the hemi-ellipsoid associated with the outside surface of the insulation wedge in the aft case closure section to the equatorial plane of the hemi-ellipsoid associated with the inside surface of the insulation wedge in the aft case closure section. See IWINACL; in Figs. 11, 13 Eqs. 126, 129
LIWCEFI	$L_{IW_{CEFI}}$	Distance from the equatorial plane of the hemi-ellipsoid associated with the outside surface of the insulation wedge in the forward case closure to the equatorial plane of the hemi-ellipsoid associated with the inside surface of the insulation wedge in the forward case closure; in Figs. 7, 9 Eqs. 74, 78

OUTPUT DATA (Cont.):

Mnemonic	Symbol	Description; Ext. (Int.) Units		
LIWCFAI	$L_{IW_{CFAI}}$	Distance from the equatorial plane of the hemi-ellipsoid associated with the outside surface of the insulation wedge in the aft closure to the intersection of the grain cone frustum cutout with the inside surface of the insulation wedge in the aft closure. Measured parallel to centerline;		
		in		Eq. 219
LIWCFI	$L_{IW_{CFI}}$	Distance from the equatorial plane of the hemi-ellipsoid associated with the outside surface of the insulation wedge in the forward case closure to the "inside/outside wedge surface osculation plane." Note that the insulation wedge is not completely within the forward closure section if LIWCFI is negative. See IWINFCL;		
		in	Figs. 7, 9	Eq. 71
LIWCHAI	$L_{IW_{CHAI}}$	Distance from the equatorial plane of the hemi-ellipsoid associated with the outside surface of the insulation wedge in the aft case closure section to forward base of the cone frustum hole, for the nozzle cutout, within the insulation wedge in the aft case closure section;		
		in	Figs. 11, 13	Eq. 116
LIWCHAO	$L_{IW_{CHAO}}$	Length of the hemi-ellipsoid frustum associated with the outside surface of the insulation wedge in the aft case closure section;		
		in	Figs. 11, 13	Eq. 115
LIWCHFI	$L_{IW_{CHFI}}$	Distance from the equatorial plane of the hemi-ellipsoid associated with the outside surface of the insulation wedge in the forward closure to the inside base of the cylindrical hole cutout for the ignitor within the insulation wedge in the forward closure;		
		in	Figs. 7, 9	Eq. 69

OUTPUT DATA (Cont.):

Mnemonic	Symbol	Description; Ext. (Int.) Units
LIWCHFO	$L_{IW_{CHFO}}$	Length of the hemi-ellipsoid frustum associated with the outside surface of the insulation wedge in the forward case closure section; in Figs. 7, 9 Eq. 68
LIWCLAI	$L_{IW_{CLAI}}$	Distance from the pole of the hemi-ellipsoid associated with the inside surface of the insulation wedge in the aft closure to the equatorial plane of the hemi-ellipsoid associated with the outside surface of the insulation wedge in the aft closure; in Figs. 11, 13 Eq. 132
LIWCLAO	$L_{IW_{CLAO}}$	Length of the axis of revolution of the hemi-ellipsoid associated with the outside surface of the insulation wedge in the aft closure section; in Figs. 11, 13 Eq. 113
LIWCLFI	$L_{IW_{CLFI}}$	Distance from the pole of the hemi-ellipsoid associated with the inside surface of the insulation wedge in the forward closure to the equatorial plane of the hemi-ellipsoid associated with the outside surface of the insulation wedge in the forward closure; in Figs. 7, 9 Eq. 82
LIWCLFO	$L_{IW_{CLFO}}$	Length of the axis of revolution of the hemi-ellipsoid associated with the outside surface of the insulation wedge in the forward closure section; in Figs. 7, 9 Eq. 66
LIWEAI	$L_{IW_{EAI}}$	Length of the axis of revolution of the hemi-ellipsoid associated with the inside surface of the insulation wedge in the aft case closure section; in Figs. 11, 13 Eqs. 127, 131

OUTPUT DATA (Cont.):

Mnemonic	Symbol	Description; Ext. (Int.) Units
LIWEFI	$L_{IW_{EFI}}$	Length of the axis of revolution of the hemi-ellipsoid associated with the inside surface of the insulation wedge in the forward case closure. See IWINFCL; in Figs. 7, 9 Eqs. 75, 81
LIWEHAI	$L_{IW_{EHAI}}$	Distance from the equatorial plane of the hemi-ellipsoid associated with the inside surface of the insulation wedge in the aft case closure to the inside base of the cone frustum cutout within the insulation wedge in the aft case closure section; in Figs. 11, 13 Eq. 134
LIWEHFI	$L_{IW_{EHFI}}$	Distance from the equatorial plane of the hemi-ellipsoid associated within the inside surface of the insulation wedge in the forward case closure to the inside base of the cylindrical hole cutout for the ignitor within the insulation wedge in the forward closure; in Figs. 7, 9 Eq. 84
LIWFI	$L_{IW_{FI}}$	Distance from the pole of the hemi-ellipsoid associated with the inside surface of the insulation wedge in the forward closure to the forward closure inside/outside wedge surface osculation plane; in Figs. 7, 9 Eq. 83
LIWHA	$L_{IW_{HA}}$	Altitude of the cone frustum, for the nozzle cutout, within the insulation wedge of the aft case closure section; in Figs. 11, 13 Eq. 111
LIWHAI	$L_{IW_{HAI}}$	Distance from the "inside/outside wedge surface osculation plane" to the inside base of the cone frustum hole cutout of the insulation wedge for the nozzle; in Figs. 11, 13 Eq. 125

OUTPUT DATA (Cont.):

Mnemonic	Symbol	Description; Ext. (Int.) Units
LIWHF	$L_{IW_{HF}}$	Length of the cylindrical hole, for the ignitor, within the insulation wedge of the forward case closure section; in Figs. 7, 9 Eq. 64
LIWHFI	$L_{IW_{HFI}}$	Distance from the inside/outside wedge surface osculation plane to the inside base of the cylindrical hole cutout for the ignitor; in Figs. 7, 9 Eq. 70
NISCUT	$N_{IS_{CUT}}$	Number of slot cutouts in grain to be insulated. Integer valued real number (floating point integer); N. D. Eq. 157
PGIJ(i)	PGIJ(i)	Logical value array which identifies the particular polygon cross section of the port/grain insulation component associated with joint cutouts. The i-th element of PGIJ will have the value .TRUE. (all other elements will be .FALSE.), thereby indicating the particular polygon shape (e.g., line, triangle, trapezoid, pentagon) for the PG component. See Fig. 19 for the key identifying the i-th element; N. D. Fig. 19 Eqs. 196-205
PGIJLAP	PGIJLAP	Logical valued variable which indicates overlapping of the polygon cross sections associated with the port/grain insulation component for joint cutouts; =.TRUE.; PG components overlap. =.FALSE.; PG components do not overlap; N. D. Fig. 19 Eq. 183-a

OUTPUT DATA (Cont.):

Mnemonic	Symbol	Description; Ext. (Int.) Units
PGIS(i)	PGIS(i)	Logical valued array which identifies the particular polygon cross section of the port/grain insulation component associated with slot cutouts. If a slot burning surface is inhibited, the i-th element of PGIS will have the value .TRUE. (all other elements will be .FALSE.), thereby indicating the particular polygon shape (e.g., line, triangle, trapezoid) for the PG component. See Fig. 18 for the key identifying the i-th element; N. D. Fig. 18 Eqs. 171-177
QINH	Q_{IN_H}	Approximate radiative heating rate; N. D. Eq. 1
RDILCAI	R_{DILCAI}	Head ratio of the ellipsoid formed by the inside surface of the insulation liner within the aft case closure section; N. D. Eq. 39
RDILCAO	R_{DILCAO}	Head ratio of the ellipsoid formed by the outside surface of the insulation liner within the aft case closure section; N. D. Eq. 32
RDILCFI	R_{DILCFI}	Head ratio of the ellipsoid formed by the inside surface of the insulation liner within the forward case closure section; N. D. Eq. 14
RDILCFO	R_{DILCFO}	Head ratio of the ellipsoid formed by the outside surface of the insulation liner within the forward case closure section; N. D. Eq. 7

OUTPUT DATA (Cont.):

Mnemonic	Symbol	Description; Ext. (Int.) Units
RDILHAI	R_{DILHAI}	Diameter ratio, hole diameter to equatorial diameter, inside surface of the insulation liner within the aft case closure section; N. D. Eq. 41
RDILHAO	R_{DILHAO}	Diameter ratio, hole diameter to equatorial diameter, outside surface of the insulation liner within the aft case closure section; N. D. Eq. 35
RDILHFI	R_{DILHFI}	Diameter ratio, hole diameter to equatorial diameter, inside surface of the insulation liner within the forward case closure section; N. D. Eq. 16
RDILHFO	R_{DILHFO}	Diameter ratio, hole diameter to equatorial diameter, outside surface of the insulation liner within the forward case closure section; N. D. Eq. 10
RDIWCAI	R_{DIWCAI}	Head ratio of the ellipsoid associated with the inside surface of the insulation wedge in the aft closure section; N. D. Eq. 131-a
RDIWCAO	R_{DIWCAO}	Head ratio of the ellipsoid associated with the outside surface of the insulation wedge within the aft case closure section; N. D. Eq. 112
RDIWCFI	R_{DIWCFI}	Head ratio of the ellipsoid associated with the inside surface of the insulation wedge in the forward closure section; N. D. Eq. 81-a

OUTPUT DATA (Cont.):

Mnemonic	Symbol	Description; Ext. (Int.) Units
RDIWCFO	R_{DIWCFO}	Head ratio of the ellipsoid associated with the outside surface of the insulation wedge within the forward case closure section; N. D. Eq. 65
RDIWHAO	R_{DIWHAO}	Diameter ratio, aft base of cone frustum hole to equatorial diameter, outside surface of the insulation wedge in the aft case closure section; N. D. Eq. 114
RDIWHFI	R_{DIWHFI}	Diameter ratio, hole diameter to equatorial diameter, inside surface of insulation wedge in the forward case closure; N. D. Eq. 80
RDIWHFO	R_{DIWHFO}	Diameter ratio, hole diameter to equatorial diameter, outside surface of the insulation wedge in the forward case closure section; N. D. Eq. 67
RLILCAI	R_{LILCAI}	Length ratio, hemi-ellipsoid frustum to hemi-ellipsoid, inside surface, insulation liner, forward case closure; N. D. Eq. 52
RLILCAO	R_{LILCAO}	Length ratio, hemi-ellipsoid frustum to hemi-ellipsoid, outside surface, insulation liner, aft case closure; N. D. Eq. 46
RLILCFI	R_{LILCFI}	Length ratio, hemi-ellipsoid frustum to hemi-ellipsoid, inside surface, insulation liner, forward case closure; N. D. Eq. 27

OUTPUT DATA (Cont.):

Mnemonic	Symbol	Description; Ext. (Int.) Units	
RLILCFO	R_{LILCFO}	Length ratio, hemi-ellipsoid frustum to hemi-ellipsoid, outside surface, insulation liner, forward case closure;	
		N. D.	Eq. 21
RLIWCA1	R_{LIWCA1}	Length ratio, hemi-ellipsoid frustum to hemi-ellipsoid, outside surface, insulation wedge, aft case closure section;	
		N. D.	Eq. 136
RLIWCA2	R_{LIWCA2}	Length ratio, hemi-ellipsoid frustum (with equatorial and "inside/outside wedge surface osculation plane" bases) to hemi-ellipsoid, outside surface, insulation wedge, aft case closure section;	
		N. D.	Eq. 139
RLIWCA3	R_{LIWCA3}	Length ratio, hemi-ellipsoid frustum (with equatorial base and inside nozzie cutout base) to hemi-ellipsoid, inside surface, insulation wedge, aft case closure section;	
		N. D.	Eq. 145
RLIWCA4	R_{LIWCA4}	Length ratio, hemi-ellipsoid frustum (with equatorial and "inside/outside wedge surface osculation plane" bases) to hemi-ellipsoid inside surface, insulation wedge, aft case closure section;	
		N. D.	Eq. 149
RLIWCF1	R_{LIWCF1}	Length ratio, hemi-ellipsoid frustum to hemi-ellipsoid, outside surface, insulation wedge, forward case closure section;	
		N. D.	Eq. 86

OUTPUT DATA (Cont.):

Mnemonic	Symbol	Description; Ext. (Int.) Units
RLIWCF2	R_{LIWCF2}	Length ratio, hemi-ellipsoid frustum (with equatorial and "inside/outside wedge surface osculation plane" bases) to hemi-ellipsoid outside surface, insulation wedge, forward base closure section; N. D. Eq. 91
RLIWCF3	R_{LIWCF3}	Length ratio, hemi-ellipsoid frustum (with equatorial and inside cylindrical hole cutout for the ignitor bases) to hemi-ellipsoid, inside surface, insulation wedge, forward case closure section; N. D. Eq. 99
RLIWCF4	R_{LIWCF4}	Length ratio, hemi-ellipsoid frustum (with equatorial and "inside/outside wedge surface osculation plane" bases) to hemi-ellipsoid, inside surface, insulation wedge, forward case closure section; N. D. Eq. 103
SINTCF	$\sin\left(\theta_{CF}\right)$	Sin of THETACF; N. D.
TANTCF	$\tan\left(\theta_{CF}\right)$	Tangent of THETACF; N. D.
TIJMAX	$T_{IJ_{MAX}}$	Maximum insulation thickness for a joint cutout; in Fig. 17 Eq. 2-c
TIJPG1	$T_{IJ_{PG1}}$	Component altitude of the polygon cross section associated with the port/grain insulation component for joint cutouts; in Fig. 17 Eq. 187

OUTPUT DATA (Cont.)

Mnemonic	Symbol	Description; Ext. (Int.) Units		
TIJPG3	$T_{IJ_{PG3}}$	Component altitude of the polygon cross section associated with the port/grain insulation component for joint cutouts;		
		in	Fig. 17	Eq. 186
TILCLA	$T_{IL_{CLA}}$	Thickness of insulation liner at center of aft case closure section. Diatance between the inside and outside hemi-ellipsoid surfaces of the insulation liner, measured on the axis of revolution;		
		in	Fig. 5	Eq. 37
TILCLF	$T_{IL_{CLF}}$	Thickness of insulation liner at center of forward case closure section. Distance between inside and outside hemi-ellipsoid surfaces of the insulation liner, measured on the axis of revolution;		
		in	Fig. 3	Eq. 12
TISMAX	$T_{IS_{MAX}}$	Maximum insulation thickness for a slot cutout;		
		in	Fig. 16	Eq. 2-b
TISPG1	$T_{IS_{PG1}}$	Altitude of the polygon cross section associated with the port/grain insulation component for slot cutouts;		
		in	Fig. 16	Eq. 166
TIWMAX	$T_{IW_{MAX}}$	Maximum insulation thickness for closure wedges (excluding liner);		
		in		Eq. 2-a
TIWAMAX	$T_{IW_{AMAX}}$	Maximum thickness of the insulation wedge associated with the aft closure. Measured parallel to the slant height of the cone frustum grain cutout;		
		in		Eq. 108

OUTPUT DATA (Cont.):

Mnemonic	Symbol	Description; Ext. (Int.) Units		
TIWFMAX	$T_{IW_{FMAX}}$	Maximum thickness of the insulation wedge associated with the forward closure. Measured parallel to the motor centerline See LIWHF;		
		in		Eq. 61
VIJ	V_{IJ}	Total volume of insulation required for joints;		
		in^3		Eq. 210
VIJIH2	$V_{IJ_{IH2}}$	Volume of insulation required for a joint;		
		in^3	Fig. 20	Eq. 209
VIJPG	$V_{IJ_{PG}}$	Volume of a port/grain insulation component for slot cutouts;		
		in^3	Fig. 20	Eqs. 179, 195
VIJPL	$V_{IJ_{PL}}$	Volume of port/liner insulation component for joint cutouts;		
		in^3	Figs. 17, 20	Eqs. 178, 182
VIL	V_{IL}	Total volume of insulation material required for the insulation liner. Includes adjustment for ignitor hole in forward closure, nozzle hole in aft closure, length penalty for submerged nozzle, slots and joints in grain;		
		in^3		Eq. 228
VILCHAI	$V_{IL_{CHAI}}$	Volume of hemi-ellipsoid frustum with hole cutout associated with the inside surface of the insulation liner within the aft case closure section;		
		in^3	Fig. 6	Eq. 55
VILCHAO	$V_{IL_{CHAO}}$	Volume of the hemi-ellipsoid frustum with hole cutout associated with the outside surface of the insulation liner within the aft case closure section;		
		in^3	Fig. 6	Eq. 49

OUTPUT DATA (Cont.):

Mnemonic	Symbol	Description; Ext. (Int.) Units		
VILCHFI	$V_{IL_{CHFI}}$	Volume of hemi-ellipsoid frustum with hole cutout associated with the inside surface of the insulation liner within the forward case closure section;		
		in^3	Fig. 4	Eq. 30
VILCHFO	$V_{IL_{CHFO}}$	Volume of hemi-ellipsoid frustum with hole cutout associated with the outside surface of the insulation liner within the forward case closure section;		
		in^3	Fig. 4	Eq. 24
VILCLA	$V_{IL_{CLA}}$	Volume of insulation liner within the forward case closure section;		
		in^3	Fig. 6	Eq. 56
VILCLAI	$V_{IL_{CLAI}}$	Volume of the hemi-ellipsoid formed by the inside surface of the insulation liner within the aft case closure section;		
		in^3	Fig. 6	Eq. 50
VILCLAO	$V_{IL_{CLAO}}$	Volume of the hemi-ellipsoid formed by the outside surface of the insulation liner within the aft case closure section;		
		in^3	Fig. 6	Eq. 44
VILCLF	$V_{IL_{CLF}}$	Volume of insulation liner within the forward case closure section;		
		in^3	Fig. 4	Eq. 31
VILCLFI	$V_{IL_{CLFI}}$	Volume of the hemi-ellipsoid formed by the inside surface of the insulation liner within the forward case closure section;		
		in^3	Fig. 4	Eq. 25
VILCLFO	$V_{IL_{CLFO}}$	Volume of the hemi-ellipsoid formed by the outside surface of the insulation liner within the forward case closure section;		
		in^3	Fig. 4	Eq. 19

OUTPUT DATA (Cont.):

Mnemonic	Symbol	Description; Ext. (Int.) Units		
VILCY	$V_{IL_{CY}}$	Volume of cylindrical insulation liner section within the cylindrical case section;		
		in^3		Eq. 227
VILHAI	$V_{IL_{HAI}}$	Volume of cylinder with ellipsoidal cap, associated with the nozzle cutout, within the hemi-ellipsoid formed by the inside surface of the insulation liner within the aft case section;		
		in^3	Fig. 6	Eq. 54
VILHAIC	$V_{IL_{HAIC}}$	Volume of the cylindrical section, associated with the nozzle cutout, within the hemi-ellipsoid formed by the inside surface of the insulation liner within the aft case closure section;		
		in^3	Fig. 6	Eq. 51
VILHAIE	$V_{IL_{HAIE}}$	Volume of ellipsoidal cap at aft base of the cylindrical section, associated with the nozzle cutout, within the hemi-ellipsoid formed by the inside surface of the insulation liner within the aft case closure section;		
		in^3	Fig. 6	Eq. 53
VILHAO	$V_{IL_{HAO}}$	Volume of cylinder with ellipsoidal cap, associated with the nozzle cutout, within the hemi-ellipsoid formed by the outside surface of the insulation liner within the aft closure section;		
		in^3	Fig. 6	Eq. 48
VILHAOC	$V_{IL_{HAOC}}$	Volume of the cylindrical section associated with the nozzle cutout, within the hemi-ellipsoid formed by the outside surface of the insulation liner within the aft case closure section;		
		in^3	Fig. 6	Eq. 45

OUTPUT DATA (Cont.):

Mnemonic	Symbol	Description; Ext. (Int.) Units
VILHAOE	$V_{IL_{HAOE}}$	Volume of ellipsoidal cap at aft base of the cylindrical section, associated with the nozzle cutout, within the hemi-ellipsoid formed by the outside surface of the insulation liner within the aft case closure section; in^3 Fig. 6 Eq. 47
VILHFI	$V_{IL_{HFI}}$	Volume of cylinder with ellipsoidal cap, associated with the ignitor cutout, within the hemi-ellipsoid formed by the inside surface of the insulation liner within the forward case closure section; in^3 Fig. 4 Eq. 29
VILHFIC	$V_{IL_{HFIC}}$	Volume of the cylindrical section, associated with the ignitor hole, within the hemi-ellipsoid formed by the inside surface of the insulation liner within the forward case closure section; in^3 Fig. 4 Eq. 26
VILHFIE	$V_{IL_{HFIE}}$	Volume of ellipsoidal cap at forward base of the cylindrical section, associated with the ignitor cutout, within the hemi-ellipsoid formed by the inside surface of the insulation liner within the forward case closure section; in^3 Fig. 4 Eq. 28
VILHFO	$V_{IL_{HFO}}$	Volume of cylinder with ellipsoidal cap, associated with the ignitor cutout, within the hemi-ellipsoid formed by the outside surface of the insulation liner within the forward case closure section; in^3 Fig. 4 Eq. 23

OUTPUT DATA (Cont.):

Mnemonic	Symbol	Description; Ext. (Int.) Units
VILHFOC	$V_{IL_{HFOC}}$	Volume of the cylindrical section, associated with the ignitor hole, within the hemi-ellipsoid formed by the outside surface of the insulation liner within the forward case closure section; in^3 Fig. 4 Eq. 20
VILHFOE	$V_{IL_{HFOE}}$	Volume of ellipsoidal cap at forward base of the cylindrical section, associated with the ignitor cutout, within the hemi-ellipsoid formed by the outside surface of the insulation liner within the forward case closure section; in^3 Fig. 4 Eq. 22
VIN	V_{IN}	Total internal insulation volume. Includes liner, wedges in forward and aft closures, inhibited slots and joints; in^3 Eq. 230
VINPD	$V_{IN_{PD}}$	Total volume of propellent displaced by the closure insulation wedges and the slot grain/liner insulation components; in^3 Eq. 225
VINR	V_{IN_R}	Volume of residual insulation; in^3 Eq. 229
VIS	V_{IS}	Total volume of insulation required for slots; in^3 Eq. 208
VISGL	$V_{IS_{GL}}$	Volume of grain/liner insulation component for slot cutout; in^3 Figs. 15, 16, 20 Eqs. 159, 164
VISIH0	$V_{IS_{IH0}}$	Volume of insulation for a slot with no sides inhibited; in^3 Fig. 20 Eq. 206

OUTPUT DATA (Cont.):

Mnemonic	Symbol	Description; Ext. (Int.) Units		
VISIH1	$V_{IS_{IH1}}$	Volume of insulation for a slot with one side inhibited;		
		in^3	Fig. 20	Eq. 207
VISPD	$V_{IS_{PD}}$	Volume of propellent displaced by the slot grain/liner insulation components;		
		in^3		Eq. 224
VISPG	$V_{IS_{PG}}$	Volume of the port/grain insulation component for slot cutouts;		
		in^3	Figs. 15, 16, 20	Eqs. 160, 165, 170
VISPL	$V_{IS_{PL}}$	Volume of port/liner insulation component for a slot cutout;		
		in^3	Figs. 15, 16, 20	Eqs. 158, 163
VIWAOY	$V_{IW_{AOY}}$	Volume of the cylindrical section associated with the outside surface of the insulation wedge in the aft case closure section;		
		in^3	Fig. 13	Eq. 142
VIWCAOE	$V_{IW_{CAOE}}$	Volume of the ellipsoidal cap formed by the intersection of the "inside/outside wedge surface osculation plane" and the hemi-ellipsoid associated with the outside surface of the insulation wedge in the aft closure section;		
		in^3	Fig. 12	Eq. 140
VIWCAPD	$V_{IW_{CAPD}}$	Volume of propellent displaced by the insulation wedge associated with the aft closure;		
		in^3		Eqs. 212, 221, 222

OUTPUT DATA (Cont.):

Mnemonic	Symbol	Description; Ext. (Int.) Units
VIWCFOE	$V_{IW_{CFOE}}$	Volume of the ellipsoidal cap formed by the intersection of the "inside/outside wedge surface osculation plane" and the hemi-ellipsoid associated with the outside surface of the insulation wedge in the forward case closure section; in^3 Figs. 8, 9 Eq. 92
VIWCFPD	$V_{IW_{CFPD}}$	Volume of propellent displaced by the insulation wedge associated with the forward closure; in^3 Eq. 211
VIWCHAI	$V_{IW_{CHAI}}$	Volume of the ellipsoidal cap, with cylindrical hole cutout associated with the cone frustum hole cutout for the nozzle, which forms the inside surface of the insulation wedge in the aft case closure section; in^3 Figs. 12, 14 Eq. 151
VIWCHAO	$V_{IW_{CHAO}}$	Volume of the hemi-ellipsoid frustum, with cylindrical hole cutout, associated with the outside surface of the insulation wedge in the aft closure section; in^3 Figs. 12, 14 Eqs. 141, 143
VIWCHFI	$V_{IW_{CHFI}}$	Volume of the ellipsoidal cap, with hole cutout for the ignitor, which forms the inside surface of the insulation wedge in the forward case closure section; in^3 Figs. 8, 10 Eq. 105
VIWCHFO	$V_{IW_{CHFO}}$	Volume associated with the outside surface of the insulation wedge in the forward case closure section, adjusted for ignitor hole; in^3 Figs. 8, 10 Eqs. 93, 97
VIWCLA	$V_{IW_{CLA}}$	Volume of insulation material required for the insulation wedge associated with the aft case closure section; in^3 Figs. 12, 14 Eq. 155

OUTPUT DATA (Cont.):

Mnemonic	Symbol	Description; Ext. (Int.) Units		
VIWCLAO	$V_{IW_{CLAO}}$	Volume of the hemi-ellipsoid associated with the outside surface of the insulation wedge in the aft case closure section;		
		in^3	Fig. 14	Eq. 135
VIWCLF	$V_{IW_{CLF}}$	Volume of insulation material required for the insulation wedge associated with the forward case closure section;		
		in^3	Figs. 8, 10	Eq. 106
VIWCLFO	$V_{IW_{CLFO}}$	Volume of the hemi-ellipsoid associated with the outside surface of the insulation wedge within the forward case closure;		
		in^3	Figs. 8, 10	Eq. 85
VIWEAI	$V_{IW_{EAI}}$	Volume of the hemi-ellipsoid associated with the inside surface of the insulation wedge within the aft case closure;		
		in^3		Eq. 144
VIWEAIE	$V_{IW_{EAIE}}$	Volume of the ellipsoidal cap associated with the inside surface of the insulation wedge in the aft case closure. If the insulation wedge extends beyond the closure, VIWEAIE is the hemi-ellipsoid volume;		
		in^3	Figs. 12, 14	Eq. 150
VIWEFI	$V_{IW_{EFI}}$	Volume of the hemi-ellipsoid associated with the inside surface of the insulation wedge within the forward case closure section;		
		in^3	Figs. 7, 9	Eq. 98
VIWEFIE	$V_{IW_{EFIE}}$	Volume of the ellipsoidal cap associated with the inside surface of the insulation wedge in the forward case closure section. If the insulation wedge extends beyond the closure, VIWEFIE is the hemi-ellipsoid volume;		
		in^3	Figs. 8, 10	Eq. 104

OUTPUT DATA (Cont.):

Mnemonic	Symbol	Description; Ext. (Int.) Units		
VIWFOY	$V_{IW_{FOY}}$	Volume of the cylindrical section associated with the outside surface of the insulation wedge in the forward case closure section;		
		in^3	Fig. 10	Eq. 96
VIWHAI	$V_{IW_{HAI}}$	Volume of the cylinder, with ellipsoidal cap, associated with the nozzle cutout cone frustum, in the hemi-ellipsoid associated with the inside surface of the insulation wedge in the aft case closure section;		
		in^3	Figs. 12, 14	Eq. 148
VIWHAIC	$V_{IW_{HAIC}}$	Volume of the cylindrical section, associated with the nozzle cutout, within the hemi-ellipsoid associated with the inside surface of the insulation wedge in the aft case closure section;		
		in^3	Figs. 12, 14	Eq. 147
VIWHAIE	$V_{IW_{HAIE}}$	Volume of the ellipsoidal cap, at the aft base of the cone frustum associated with the nozzle cutout, within the hemi-ellipsoid associated with the inside surface of the insulation wedge in the aft case closure section;		
		in^3	Figs. 12, 14	Eq. 146
VIWHAOC	$V_{IW_{HAOC}}$	Volume of the cylindrical section, associated with the nozzle cutout, within the hemi-ellipsoid frustum associated with the outside surface of the insulation wedge in the aft case closure section;		
		in^3	Figs. 12, 14	Eq. 138
VIWHAOE	$V_{IW_{HAOE}}$	Volume of the ellipsoidal cap, at aft base of the cone frustum section associated with the nozzle cutout, within the hemi-ellipsoid associated with the outside surface of the insulation wedge in the aft case closure section;		
		in^3	Figs. 12, 14	Eq. 137

OUTPUT DATA (Cont.):

Mnemonic	Symbol	Description; Ext. (Int.) Units
VIWHAT	$V_{IW_{HAT}}$	Volume of triangular section, in insulation wedge, associated with the cone frustum cutout for the nozzle within the aft case closure section; in^3 Figs. 12, 14 Eq. 154
VIWHFI	$V_{IW_{HFI}}$	Volume of the cylinder with ellipsoidal cap, associated with the ignitor hole, in the hemi-ellipsoid associated with the inside surface of the insulation wedge in the forward case closure section; in^3 Figs. 8, 10 Eq. 102
VIWHFIC	$V_{IW_{HFIC}}$	Volume of the cylindrical section, associated with the ignitor hole, within the hemi-ellipsoid associated with the inside surface of the insulation wedge in the forward case closure section; in^3 Figs. 8, 10 Eq. 101
VIWHFIE	$V_{IW_{HFIE}}$	Volume of ellipsoidal cap, at forward base of the cylindrical section associated with the ignitor cutout, within the hemi-ellipsoid associated with the inside surface of the insulation wedge in the forward case closure section; in^3 Figs. 8, 10 Eq. 100
VIWHFO	$V_{IW_{HFO}}$	Volume of the cylinder, with ellipsoidal cap, associated with the ignitor hole, in the hemi-ellipsoid and cylinder associated with the outside surface of the insulation wedge in the forward case closure section; in^3 Figs. 8, 10 Eqs. 90, 95
VIWHFOC	$V_{IW_{HFOC}}$	Volume of the cylindrical section, associated with the ignitor hole, within the hemi-ellipsoid associated with the outside surface of the insulation wedge in the forward case closure section; in^3 Figs. 8, 10 Eq. 88

OUTPUT DATA (Cont.):

Mnemonic	Symbol	Description; Ext. (Int.) Units		
VIWHFOE	$V_{IW_{HFOE}}$	Volume of ellipsoidal cap, at forward base of the cylindrical section associated with the ignitor cutout, within the hemi-ellipsoid associated with the outside surface of the insulation wedge in the forward case closure section;		
		in^3	Figs. 8, 10	Eq. 87
VIWHFOL	$V_{IW_{HFOL}}$	Volume of the cylindrical section, associated with the ignitor hole, within the hemi-ellipsoid associated with the outside surface of the insulation wedge in the forward case closure section. The bases of the cylindrical section are the equatorial plane of the hemi-ellipsoid and the "inside/outside wedge surface osculation plane";		
		in^3	Figs. 7, 8	Eq. 89
VIWHFOY	$V_{IW_{HFOY}}$	Volume of the cylindrical section, associated with the ignitor hole, within the cylindrical case section associated with the outside surface of the insulation wedge in the forward case closure section. The bases of the cylindrical section are the equatorial plane of the hemi-ellipsoid and the "inside/outside wedge surface osculation plane";		
		in^3	Fig. 10	Eq. 94
VIWPD	$V_{IW_{PD}}$	Volume of propellent displaced by the insulation wedges associated with the forward and aft closures;		
		in^3		Eq. 223
YIJ1	Y_1	Intermediate quantity for YIJPG computation;		
		in^3		Eq. 193
YIJ2	Y_2	Intermediate quantity for YIJPG computation;		
		in^3		Eq. 189

OUTPUT DATA (Cont.):

Mnemonic	Symbol	Description; Ext. (Int.) Units
YIJ3	Y_3	Intermediate quantity for YIJPG computation; in — Eq. 190
YIJ4	Y_4	Intermediate quantity for YIJPG computation; in^3 — Eq. 191
YIJ5	Y_5	Intermediate quantity for YIJPG computation; in^2 — Eq. 192
YIJPG	$Y_{IJ_{PG}}$	Centroid, measured with respect to the motor centerline, of the polygon cross section for joint cutouts; in — Fig. 17 — Eq. 194
YISPG	$Y_{IS_{PG}}$	Centroid, measured with respect to the motor centerline, of the polygon cross section associated with the port/grain insulation component for slot cutouts; in — Fig. 16 — Eq. 169
YIWHAT	$Y_{IW_{HAT}}$	Distance from axis of revolution to centroid of triangular section in insulation wedge, associated with the cone frustum cutout for the nozzle, within the aft case closure section; in — Figs. 11, 13 — Eq. 153

PRINT BLOCK KEY:

Nominally, only those lines with an asterisk to the left of the line number will be printed. By input, any of the lines given below may be printed or suppressed (see the section on output models for the details).

			INSULG	INGM1	INTERNAL	INSULATION GEOMETRY
AIJPG	AISPG	AIWHAT	*1	CING1	CING2	CING3
CIWA	CIWAP	CIWB	*2	CIWBP	CIWC	CIWCP
COSTCF	CUTOUTJ	CUTOUTS	*3	DILCLI	DILCLO	DILHAI
DILHAO	DILHFI	DILHFO	*4	DILI	DILO	DIWA1
DIWCAI	DIWCFAI	DIWCFI	*5	DIWCLO	DIWEAI	DIWEFI
DIWHAI	DIWHAO	DIWHFI	*6	DIWHFO	GOODPGJ	GOODPGS
IJNOTLN	ISNOTLN	IWINACL	*7	IWINFCL	KIJ1	KIJ2
KIJ3	KIJ4	KIJ5	*8	KIJ6	KIJ7	KIJ8
KIJ9	KIJ10	KIJ11	*9	KIJ12	KIJTRUE	KIL1
KIL2	KIL3	KIL4	*10	KIL5	KIL6	KIL7
KIL8	KIL9	KIL10	*11	KIL11	KIL12	KIL13
KIL14	KIL15	KIL16	*12	KIL17	KIL18	KIN1
KIN2	KIN3	KIN4	*13	KIN5	KIN6	KIN7
KIN8	KIS1	KIS2	*14	KIS3	KIS4	KIS5
KIS6	KIS7	KIS8	*15	KIS9	KIS10	KIS11
KIS12	KIS13	KIS14	*16	KIS15	KIS16	KISTRUE
KIW1	KIW2	KIW3	*17	KIW4	KIW7	KIW8
KIW9	KIW10	KIW11	*18	KIW12	KIW13	KIW14
KIW15	KIW16	KIW17	*19	KIW18	KIW19	KIW20
KIW21	KIW22	KIW23	*20	KIW24	KLIWFI1	KLIWFI2
KPD1	KPD2	KPD3	*21	KPD4	KPD5	KPD6
KPD7	KPD8	KPD9	*22	KPD10	LIJCUT	LIJPGI
LIJPGO	LIJPG3	LILCHAI	*23	LILCHAO	LILCHFI	LILCHFO
LILCLAI	LILCLAO	LILCLFI	*24	LILCLFO	LILCY	LILHA
LILHF	LISCUT	LISPGI	*25	LISPGO	LIWA1	LIWA2
LIWAI	LIWCAI	LIWCEAI	*26	LIWCEFI	LIWCFAI	LIWCFI
LIWCHAI	LIWCHAO	LIWCHFI	*27	LIWCHFO	LIWCLAI	LIWCLAO
LIWCLFI	LIWCLFO	LIWEAI	*28	LIWEFI	LIWEHAI	LIWEHFI
LIWFI	LIWHA	LIWHAI	*29	LIWHF	LIWHFI	NIJCUT
NISCUT	NISIHO	NISIH1	*30	PGIJ(1)	PGIJ(2)	PGIJ(3)
PGIJ(4)	PGIJ(5)	PGIJ(6)	*31	PGIJ(7)	PGIJ(8)	PGIJ(9)

PRINT BLOCK KEY (Cont.):

PGIJLAP	PGIS(1)	PGIS(2)	*32	PGIS(3)	PGIS(4)	PGIS(5)
PGIS(6)	QINH	QINSTAR	*33	RDILCAI	RDILCAO	RDILCFI
RDILCFO	RDILHAI	RDILHAO	*34	RDILHFI	RDILHFO	RDIWCAI
RDIWCAO	RDIWCFI	RDIWCFO	*35	RDIWHAO	RDIWHFI	RDIWHFO
RLILCAI	RLILCAO	RLILCFI	*36	RLILCFO	RLIWCA1	RLIWCA2
RLIWCA3	RLIWCA4	RLIWCF1	*37	RLIWCF2	RLIWCF3	RLIWCF4
SINTCF	TANTCF	TIJMAX	*38	TIJPG1	TIJPG3	TILCLA
TILCLF	TILCY	TINR	*39	TISMAX	TISPG1	TIWAMAX
TIWFMAX	TIWMAX	VIJ	*40	VIJIH2	VIJPG	VIJPL
VIL	VILCHAI	VILCHAO	*41	VILCHFI	VILCHFO	VILCLA
VILCLAI	VILCLAO	VILCLF	*42	VILCLFI	VILCLFO	VILCY
VIL AI	VILHAIC	VILHAIE	*43	VILHAO	VILHAOC	VILHAOE
VILHFI	VILHFIC	VILHFIE	*44	VILHFO	VILHFOC	VILHFOE
VIN	VINPD	VINR	*45	VIS	VISGL	VISIHO
VISIH1	VISPD	VISPG	*46	VISPL	VIWAOY	VIWCAOE
VIWCAPD	VIWCFOE	VIWCFPD	*47	VIWCHAI	VIWCHAO	VIWCHFI
VIWCHFO	VIWCLA	VIWCLAO	*48	VTWCLF	VIWCLFO	VIWEAI
VIWEAIE	VIWEFI	VIWEFIE	*49	VIWFOY	VIWHAI	VIWHAIC
VIWHAIE	VIWHAOC	VIWHAOE	*50	VIWHAT	VIWHFI	VIWHFIC
VIWHFIE	VIWHFC	VIWHFOC	*51	VIWHFOE	VIWHFOL	VIWHFOY
VIWPD	YIJ1	YIJ2	*52	YIJ3	YIJ4	YIJ5
YIJPG	YISPG	YIWHAT	*53			

90.1

MODEL TYPE: INSULW (internal INSULation Weight)

MODEL NAME: INWM1 (Geometry dependent)

DESCRIPTION:

INWM1 (internal INsulation Weight Model number 1) uses volumes, determined by an insulation geometry model, to evaluate the internal insulation component weights for a solid rocket motor. The computed insulation weight breakdown may include the following components.

Insulation liner.

Insulation wedges associated with the forward and aft closures.

Joint insulation.

Slot insulation.

Residual insulation.

PROCEDURE:

This is a two entrance model. At the first entrance, the insulation densities are picked up and made available to define the insulation properties required for the insulation geometry computations. No equations are evaluated.

The internal insulation geometry is then evaluated by the model specified for the INSULG model type and the component volumes are evaluated.

The second entrance of INWM1 uses these volumes to evaluate the component weights, then uses these component weights to compute the internal insulation weight breakdown.

EQUATIONS:

Weight of insulation liner within forward case closure section.

$$W_{IL_{CLF}} = K_{WILCLF} \, \rho_{IL} \, V_{IL_{CLF}} \qquad (1)$$

EQUATIONS (Cont.):

Weight of insulation liner within aft case closure section.

$$W_{IL_{CLA}} = K_{WILCLA} \rho_{IL} V_{IL_{CLA}} \tag{2}$$

Weight of insulation liner within cylindrical case section.

$$W_{IL_{CY}} = K_{WILCY} \rho_{IL} V_{IL_{CY}} \tag{3}$$

Total weight of insulation liner. Includes forward closure, aft closure and cylindrical section components.

$$W_{IL} = K_{WIL} \rho_{IL} V_{IL} \tag{4}$$

Weight of insulation wedge associated with forward case closure section.

$$W_{IW_{CLF}} = K_{WIWCLF} \rho_{IW} V_{IW_{CLF}} \tag{5}$$

Weight of insulation wedge associated with aft case closure section.

$$W_{IW_{CLA}} = K_{WIWCLA} \rho_{IW} V_{IW_{CLA}} \tag{6}$$

Total weight of closure insulation wedges. Includes forward case closure and aft case closure components.

$$W_{IW} = K_{WIW} \left(W_{IW_{CLF}} + W_{IW_{CLA}} \right) \tag{7}$$

Weight of insulation for a single slot having no sides inhibited.

$$W_{IS_{IH0}} = K_{WISIH0} \rho_{IS} V_{IS_{IH0}} \tag{8}$$

Weight of insulation for a single slot having one side inhibited.

$$W_{IS_{IH1}} = K_{WISIH1} \rho_{IS} V_{IS_{IH1}} \tag{9}$$

EQUATIONS (Cont.):

Total weight for slot insulation.

$$W_{IS} = K_{WIS}\,\rho_{IS}\,V_{IS} \tag{10}$$

Weight of insulation for a single joint having both sides inhibited.

$$W_{IJ_{IH2}} = K_{WIJIH2}\,\rho_{IJ}\,V_{IJ_{IH2}} \tag{11}$$

Total weight for joint insulation.

$$W_{IJ} = K_{WIJ}\,\rho_{IJ}\,V_{IJ} \tag{12}$$

Density of residual internal insulation material.

$$\rho_R = K_{\rho RL}\,\rho_{IL} + K_{\rho RJ}\,\rho_{IJ} + K_{\rho RW}\,\rho_{IW} + K_{\rho RS}\,\rho_{IS} + K_{\rho R} \tag{12-a}$$

Total residual insulation weight.

$$W_{IN_R} = K_{WINR}\,\rho_R\,V_{IN_R} \tag{13}$$

Total internal insulation weight. Includes liner, closure wedge, slot, and joint components.

$$W_{IN} = K_{WIN}\left(W_{IL} + W_{IW} + W_{IS} + W_{IJ}\right) \tag{14}$$

Total non-expended internal insulation weight component.

$$W_{IN_{NX}} = K_{WINNX}\,W_{IN_R} \tag{15}$$

Total expended internal insulation weight component.

$$W_{IN_X} = K_{WINX}\left(W_{IN} - W_{IN_R}\right) \tag{16}$$

Expended (thrust producing) internal insulation weight component.

$$W_{IN_{XT}} = K_{WINXT}\,W_{IN_X} \tag{17}$$

Expended (non-thrust producing) internal insulation weight component.

$$W_{IN_{XI}} = W_{IN_X} - W_{IN_{XT}} \tag{18}$$

INPUT DATA, INTRA-MODEL:

The following data is input directly to this model by the program user. If a value is not input, the preset value is used.

Mnemonic	Symbol	Description; Ext. (Int.) Units	Preset
KRHOINR	$K_{\rho R}$	Bias for RHOINR computation; lb/in^3	0
KRHOIRJ	$K_{\rho RJ}$	Coefficient for RHOINR computation; N. D.	0
KRHOIRL	$K_{\rho RL}$	Coefficient for RHOINR computation; N. D.	1
KRHOIRS	$K_{\rho RS}$	Coefficient for RHOINR computation; N. D.	0
KRHOIRW	$K_{\rho RW}$	Coefficient for RHOINR computation; N. D.	0
KWIJ	K_{WIJ}	Coefficient for WIJ computation; N. D.	1
KWIJIH2	K_{WIJIH2}	Coefficient for WIJIH2 computation; N. D.	1
KWIL	K_{WIL}	Coefficient for WIL computation; N. D.	1
KWILCLA	K_{WILCLA}	Coefficient for WILCLA computation; N. D.	1
KWILCLF	K_{WILCLF}	Coefficient for WILCLF computation; N. D.	1
KWILCY	K_{WILCY}	Coefficient for WILCY computation; N. D.	1
KWIN	K_{WIN}	Coefficient for WIN computation; N. D.	1

INPUT DATA, INTRA-MODEL (Cont.):

Mnemonic	Symbol	Description; Ext. (Int.) Units	Preset
KWINR	K_{WINR}	Coefficient for WINR computation; N. D.	1
KWINNX	K_{WINNX}	Coefficient for WINNX computation; N. D.	1
KWINX	K_{WINX}	Coefficient for WINX computation; N. D.	1
KWINXT	K_{WINXT}	Coefficient for WINXT computation; N. D.	1
KWIS	K_{WIS}	Coefficient for WIS computation; N. D.	1
KWISIH0	K_{WISIH0}	Coefficient for WISIH0 computation; N. D.	1
KWISIH1	K_{WISIH1}	Coefficient for WISIH1 computation; N. D.	1
KWIW	K_{WIW}	Coefficient for WIW computation; N. D.	1
KWIWCLA	K_{WIWCLA}	Coefficient for WIWCLA computation; N. D.	1
KWIWCLF	K_{WIWCLF}	Coefficient for WIWCLF computation; N. D.	1
RHOIJ	ρ_{IJ}	Density of internal insulation material for joints; lb/in^3	0
RHOIL	ρ_{IL}	Density of internal insulation material for liner; lb/in^3	0

INPUT DATA, INTRA-MODEL (Cont.):

Mnemonic	Symbol	Description; Ext. (Int.) Units	Preset
RHOIS	ρ_{IS}	Density of internal insulation material for slots; lb/in^3	0
RHOIW	ρ_{IW}	Density of internal insulation material for closure wedges; lb/in^3	0

INPUT DATA, INTER-MODEL:

This model requires as input certain data which is usually output from a model of the specified model type. If the user has not specified such a source for this data, then it must be input directly with the intra-model input.

Mnemonic	Symbol	Description; Ext. (Int.) Units	Model Type
VIJ	V_{IJ}	Total volume of internal insulation required for joints; in^3	INSULG
VIJIH2	$V_{IJ_{IH2}}$	Volume of internal insulation required for a single joint having both sides inhibited; in^3	INSULG
VIL	V_{IL}	Total volume of internal insulation required for insulation liner. Includes cylindrical section and closure components; in^3	INSULG
VILCLA	$V_{IL_{CLA}}$	Volume of internal insulation liner within the aft closure; in^3	INSULG
VILCLF	$V_{IL_{CLF}}$	Volume of internal insulation liner within the forward closure; in^3	INSULG

INPUT DATA, INTER-MODEL (Cont.):

Mnemonic	Symbol	Description; Ext. (Int.) Units	Model Type
VILCY	$V_{IL_{CY}}$	Volume of internal insulation liner within the cylindrical case section; in^3	INSULG
VINR	V_{IN_R}	Volume of residual internal insulation; in^3	INSULG
VIS	V_{IS}	Total volume of internal insulation required for slots; in^3	INSULG
VISIH0	$V_{IS_{IH0}}$	Volume of internal insulation required for a single slot having no sides inhibited; in^3	INSULG
VISIH1	$V_{IS_{IH1}}$	Volume of internal insulation required for a single slot having one side inhibited; in^3	INSULG
VIWCLA	$V_{IW_{CLA}}$	Volume of internal insulation wedge associated with the aft closure; in^3	INSULG
VIWCLF	$V_{IW_{CLF}}$	Volume of internal insulation wedge associated with the forward closure; in^3	INSULG

OUTPUT DATA:

The following data is output from this model. It is available for use as inter-model input to other models and to print, plot, and optimization routines.

Mnemonic	Symbol	Description; Ext. (Int.) Units	
RHOINR	ρ_R	Density of residual insulation material; lb	Eq. 12-a

OUTPUT DATA (Cont.):

Mnemonic	Symbol	Description; Ext. (Int.) Units	
WIJ	W_{IJ}	Total weight for joint insulation;	
		lb	Eq. 12
WIJIH2	$W_{IJ_{IH2}}$	Weight of insulation for a single joint having both sides inhibited;	
		lb	Eq. 11
WIL	W_{IL}	Total weight of insulation liner. Includes forward closure, aft closure, and cylindrical section components;	
		lb	Eq. 4
WILCLA	$W_{IL_{CLA}}$	Weight of insulation liner within aft case closure section;	
		lb	Eq. 2
WILCLF	$W_{IL_{CLF}}$	Weight of insulation liner within forward case closure section;	
		lb	Eq. 1
WILCY	$W_{IL_{CY}}$	Weight of insulation liner within cylindrical case section;	
		lb	Eq. 3
WIN	W_{IN}	Total internal insulation weight. Includes liner, closure wedge, slot and joint components;	
		lb	Eq. 14
WINNX	$W_{IN_{NX}}$	Total non expended internal insulation weight exponent;	
		lb	Eq. 15
WINR	W_{IN_R}	Weight of residual internal insulation;	
		lb	Eq. 13
WINX	W_{IN_X}	Total expended internal insulation weight component;	
		lb	Eq. 16

OUTPUT DATA (Cont.):

Mnemonic	Symbol	Description; Ext. (Int.) Units	
WINXI	$W_{IN_{XI}}$	Expended (non-thrust producing) internal insulation weight component;	
		lb	Eq. 18
WINXT	$W_{IN_{XT}}$	Expended (thrust producing) internal insulation weight component;	
		lb	Eq. 17
WIS	W_{IS}	Total weight for slot insulation;	
		lb	Eq. 10
WISIH0	$W_{IS_{IH0}}$	Weight of insulation for a single slot having no sides inhibited;	
		lb	Eq. 8
WISIH1	$W_{IS_{IH1}}$	Weight of insulation for a single slot having one side inhibited;	
		lb	Eq. 9
WIW	W_{IW}	Total weight of insulation of insulation wedges. Includes forward case closure and aft case closure components;	
		lb	Eq. 7
WIWCLA	$W_{IW_{CLA}}$	Weight of insulation wedge associated with aft closure section;	
		lb	Eq. 6
WIWCLF	$W_{IW_{CLF}}$	Weight of insulation wedge associated with forward closure section;	
		lb	Eq. 5

PRINT BLOCK KEY:

Nominally, only those lines with an asterisk to the left of the line number will be printed. By input, any of the lines given below may be printed or suppressed (see the section on output models for the details).

			INSULW	INWM1	INTERNAL INSULATION WEIGHT	
WIN	WINNX	WINX	*1	WINXI	WINXT	
KRHOINR	KRHOIRJ	KRHOIRL	*2	KRHOIRS	KRHOIRW	KWIJ
KWIJIH2	KWIL	KWILCLA	*3	KWILCLF	KWILCY	KWIN
KWINNX	KWINR	KWINX	*4	KWINXT	KWIS	KWISIHO
KWISIH1	KWIW	KWIWCLA	*5	KWIWCLF	RHOIJ	RHOIL
RHOINR	RHOIS	RHOIW	*6	WIJIH2	WIJ	WIL
WILCLA	WILCLF	WILCY	*7	WINR	WIS	WISIHO
WISIH1	WIW	WIWCLA	*8	WIWCLF		

100.1

MODEL TYPE: INTSTGG (INTerSTaGe Geometry)

MODEL NAME: ITGM1 (Cone frustum)

DESCRIPTION:

ITGM1 (InTerstage Geometry Model number 1) evaluates the geometry for a simple cone frustum or cylindrical interstage connecting either two substages (see figure 1) or the top substage and the payload (see figure 2).

PROCEDURE:

Prior to entering ITGM1, all substage and payload models have been executed.

ITGM1 is then executed. If this is not the uppermost interstage in the propulsion system, the geometry requirements of the substage below and the substage above this interstage are used to determine the pertinent interstage geometry. If this is the uppermost interstage in the propulsion system, the substage below and the payload above are utilized to determine interstage geometry.

After leaving ITGM1, the weight models for this particular interstage are executed. After all interstages are sized, the stage models will be executed and, utilizing the interstage and substage data, the stage will be sized.

EQUATIONS:

Required interstage length component associated with the substage above this interstage. Figs. 1, 2

$$L_{IT_{SSF}} = \left(L_{SS_{ITA}}\right)_{above} \tag{1}$$

Required interstage length component associated with the substage below this interstage. Figs. 1, 2

$$L_{IT_{SSA}} = \left(L_{SS_{ITF}}\right)_{below} \tag{2}$$

EQUATIONS (Cont.):

Interstage length. Figs. 1, 2

$$L_{IT} = L_{IT_{SSA}} + L_{IT_{SSF}} + L_{IT_S} \tag{3}$$

Forward interstage base diameter. Figs. 1, 2

$$D_{IT_F} = \left(D_{SS_{ITA}}\right)_{above} \tag{4}$$

Aft interstage base diameter. Figs. 1, 2

$$D_{IT_A} = \left(D_{SS_{ITF}}\right)_{below} \tag{5}$$

Interstage half angle. Figs. 1, 2

$$\theta_{IT} = \arctan\left[\frac{D_{IT_A} - D_{IT_F}}{2\, L_{IT}}\right] \tag{6}$$

Interstage slant height. Figs. 1, 2

$$L_{IT_L} = \frac{L_{IT}}{\cos\ \theta_{IT}} \tag{7}$$

Interstage surface area.

$$S_{IT} = \left(\frac{\pi}{2}\right) L_{IT_L} \left(D_{IT_F} + D_{IT_A}\right) \tag{8}$$

Interstage aft base cross-sectional area.

$$A_{IT_A} = \left(\frac{\pi}{4}\right) D^2_{IT_A} \tag{9}$$

Interstage forward base cross-sectional area.

$$A_{IT_F} = \left(\frac{\pi}{4}\right) D^2_{IT_F} \tag{10}$$

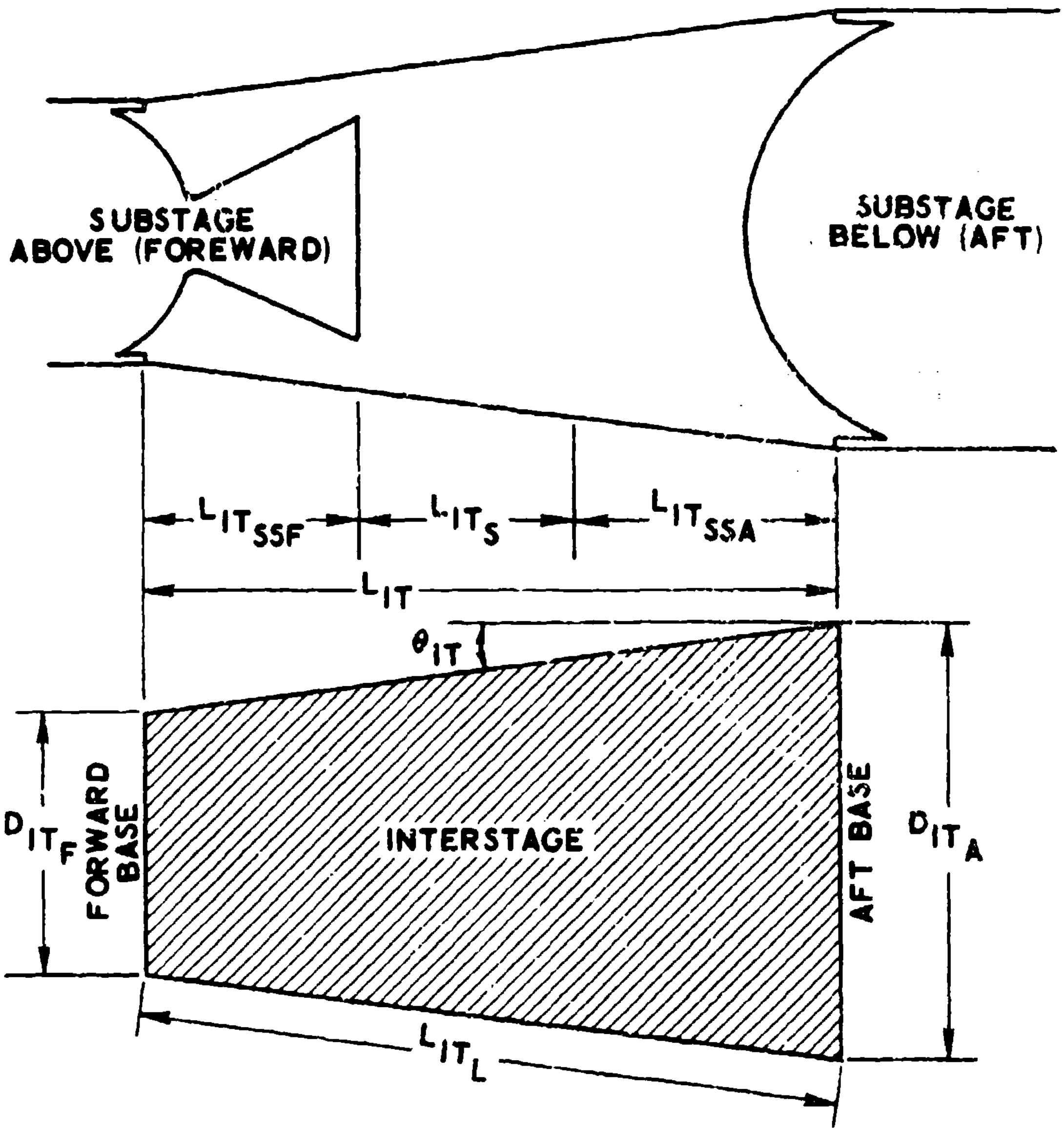

Fig. 100.1-1 Geometry, Interstage Between Substages

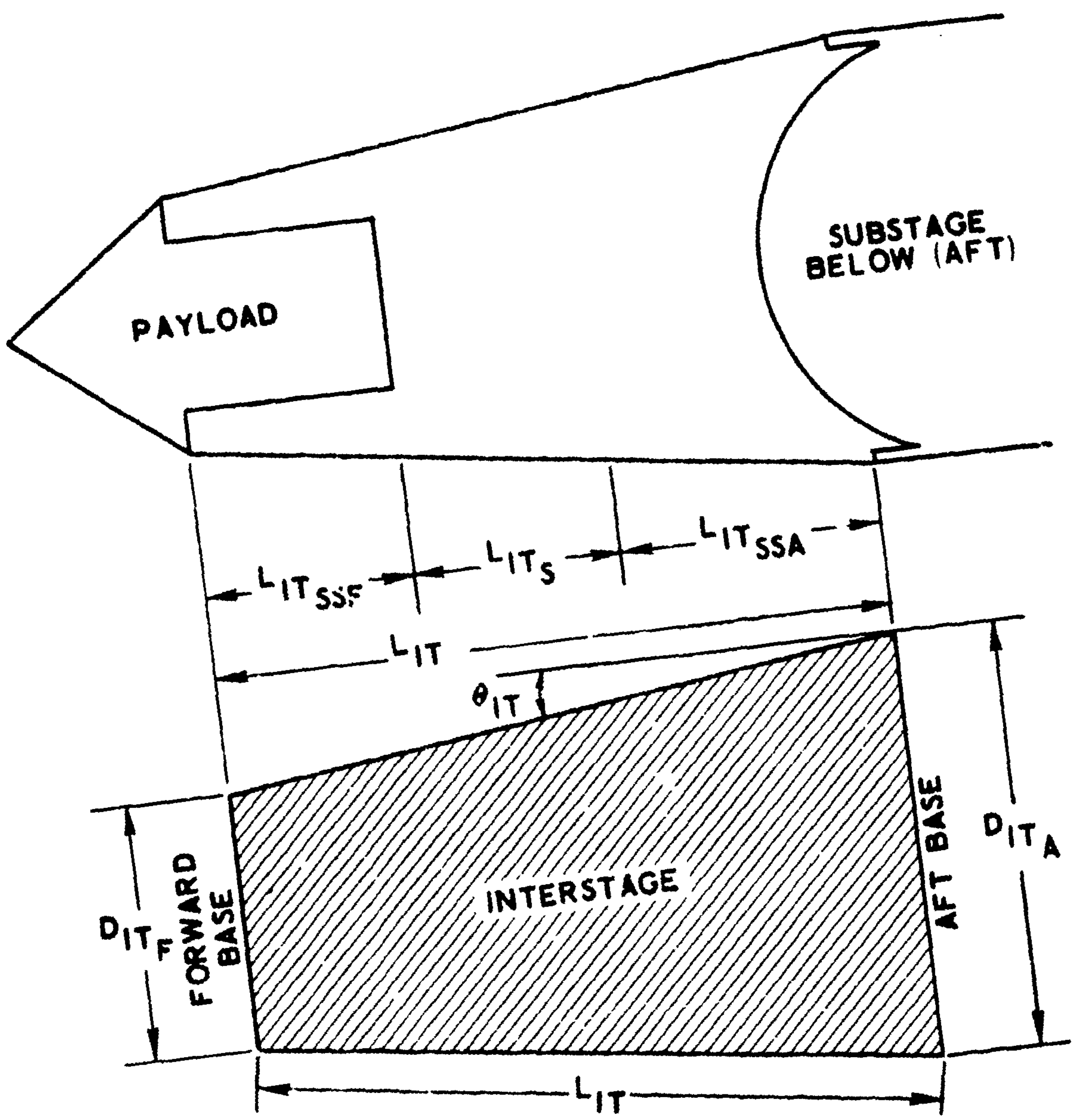

Fig. 100.1-2 Geometry, Interstage Between Substage and Payload

INPUT DATA, INTRA-MODEL:

The following data is input to this model directly by the program user. If a value is not input, the preset value is used.

Mnemonic	Symbol	Description; Ext. (Int.) Units	Preset
LITS	L_{IT_S}	Spacing distance associated with the interstage. (Figs. 1, 2); in	0

INPUT DATA, INTER-MODEL:

This model requires as input certain data which is usually output from a model of the specified model type. If the user has not specified such a source for this data, then it must be input directly with the intra-model input.

Mnemonic	Symbol	Description; Ext. (Int.) Units	Model Type
DSSITA	$D_{SS_{ITA}}$	Substage aft diameter for interstage attachment Associated with the substage above, or forward of, the interstage; in	SUBSTGG
DSSITF	$D_{SS_{ITF}}$	Substage forward diameter for interstage attachment. Associated with the substage below, or aft of, the interstage; in	SUBSTGG
LSSITA	$L_{SS_{ITA}}$	Length of interstage required for substage above, or forward of, the interstage. Includes nozzle protruding beyond aft substage skirt, etc.; in	SUBSTGG
LSSITF	$L_{SS_{ITF}}$	Length of interstage required for substage below, or aft of, the interstage. Includes closure protruding beyond forward skirt, etc.; in	SUBSTGG

OUTPUT DATA:

The following data is output from this model. It is available for use as inter-model input to other models and to print, plot, and optimization routines.

Mnemonic	Symbol	Description; Ext. (Int.) Units		
AITA	A_{IT_A}	Cross-sectional area, interstage aft base; in^2		Eq. 9
AITF	A_{IT_F}	Cross-sectional area, interstage fore base; in^2		Eq. 10
DITA	D_{IT_A}	Interstage aft (below) base diameter; in	Figs. 1, 2	Eq. 5
DITF	D_{IT_F}	Interstage forward (above) base diameter; in	Figs. 1, 2	Eq. 4
ITHA	θ_{IT}	Interstage half angle. (internal units, radians); deg	Figs. 1, 2	Eq. 6
LIT	L_{IT}	Interstage length. Measured along centerline. Altitude of cone frustum or cylinder; in	Figs. 1, 2	Eq. 3
LITL	L_{IT_L}	Interstage slant height; in	Figs. 1, 2	Eq. 7
LITSSA	$L_{IT_{SSA}}$	Required interstage length component associated with the substage above (forward); in	Figs. 1, 2	Eq. 2
LITSSF	$L_{IT_{SSF}}$	Required interstage length component associated with the substage below (aft); in	Figs. 1, 2	Eq. 1
SIT	S_{IT}	Interstage surface area; in	Figs. 1, 2	Eq. 8

PRINT BLOCK KEY:

Nominally, only those lines with an asterisk to the left of the line number will be printed. By input, any of the lines given below may be printed or suppressed (see the section on output models for the details).

```
                                     INTSTGG      ITGM1        INTERSTAGE GEOMETRY
AITA        AITF        DITA              *1      DITF         ITHA            LIT
LITL        LITS        LITSSA            *2      LITSSF       SIT
```

110.1

MODEL TYPE: INTINSW (INTerstage External INSulation Weight)

MODEL NAME: ITIWM1 (Geometry Dependent)

DESCRIPTION:

ITIWM1 (InTerstage external Insulation Weight Model number 1) uses a geometry dependent equation to evaluate the interstage external insulation weight as a function of the interstage surface area and the external insulation weight per unit area.

PROCEDURE:

Prior to entering ITIWM1, the model specified for the INTSTGG model type has determined the interstage surface area.

The ITIWM1 model uses the interstage surface area, together with the external insulation weight per unit area, to determine the external insulation weight breakdown.

After leaving ITIWM1, the model specified for the INTSTGW model type will use the external insulation weights to evaluate the interstage weights.

EQUATIONS:

Total interstage external insulation weight.

$$W_{IT_{IE}} = K_{WITIE} \left(K_{WITIE1} S_{IT} W_{IT_{IUA}} + K_{WITIE2} \right) \quad (1)$$

Total non-expended interstage external insulation weight component.

$$W_{IT_{IENX}} = K_{WITINX} W_{IT_{IE}} \quad (2)$$

Total expended interstage external insulation weight component.

$$W_{IT_{IEX}} = K_{WITIX} W_{IT_{IE}} \quad (3)$$

EQUATIONS (Cont.):

Expended (non-thrust producing) interstage external insulation weight component.

$$W_{IT_{IEXI}} = W_{IT_{IEX}} \tag{4}$$

Expended (thrust producing) interstage external insulation weight component.

$$W_{IT_{IEXT}} = 0 \tag{5}$$

INPUT DATA, INTRA-MODEL:

The following data is input to this model directly by the program user. If a value is not input, the preset value is used.

Mnemonic	Symbol	Description; Ext. (Int.) Units	Preset
KWITIE	K_{WITIE}	Coefficient for WITIE computation; N. D.	1
KWITIE1	K_{WITIE1}	Coefficient for WITIE computation; N. D.	1
KWITIE2	K_{WITIE2}	Bias for WITIE computation; lb	0
KWITINX	K_{WITINX}	Coefficient for WITIENX computation; N. D.	1
KWITIX	K_{WITIX}	Coefficient for WITIEX computation; N. D.	0
WITIUA	$W_{IT_{IUA}}$	Weight of interstage external insulation per unit interstage surface area; lb/in^2	0

INPUT DATA, INTER-MODEL:

This model requires as input certain data which is usually output from a model of the specified model type. If the user has not specified such a source for this data, then it must be input directly with the intra-model input.

Mnemonic	Symbol	Description; Ext. (Int.) Units	Model Type
SIT	S_{IT}	Interstage surface area; in^2	INTSTGG

OUTPUT DATA:

The following data is output from this model. It is available for use as inter-model input to other models and to print, plot, and optimization routines.

Mnemonic	Symbol	Description; Ext. (Int.) Units	
WITIE	$W_{IT_{IE}}$	Total interstage external insulation weight; lb	Eq. 1
WITIENX	$W_{IT_{IENX}}$	Total non-expended interstage external insulation weight component; lb	Eq. 2
WITIEX	$W_{IT_{IEX}}$	Total expended interstage external insulation weight component; lb	Eq. 3
WITIEXI	$W_{IT_{IEXI}}$	Expended (non-thrust producing) interstage external insulation weight component; lb	Eq. 4
WITIEXT	$W_{IT_{IEXT}}$	Expended (thrust producing) interstage external insulation weight component; lb	Eq. 5

PRINT BLOCK KEY:

Nominally, only those lines with an asterisk to the left of the line number will be printed. By input, any of the lines given below may be printed or suppressed (see the section on output models for the details).

```
                                  INTINSW   ITIWM1    INTERSTAGE EXTERNAL INSULATION WEIGHT
WITIE     WITIENX   WITIEX             *1   WITIEXI   WITIEXT
KWITIE    KWITIE1   KWITIE2            *2   KWITINX   KWITIX    WITIUA
```

120.1

MODEL TYPE: INTSTRW (INTerstage STRucture Weight)

MODEL NAME: ITSWM1 (Parametric weight scaling)

DESCRIPTION:

ITSWM1 (InTerstage Structure Weight Model number 1) utilizes a parametric weight scaling equation to determine the interstage structure weight. The actual flight loads are not used explicitly as parameters by this model. However, axial thrust loads are implicitly accounted for since the theoretical equation, upon which the correlation analysis is based, uses motor thrust as a loading parameter. See reference 8 for a description of the equation and scaling rationale.

The interstage structure includes all of the interstage except the external insulation.

The model is applicable for performance parameters within the following limits (see Input Data - Inter Model).

5 < RAEXTTH < 75

300 < PCHAVG < 1000 psia

40 < TBPPMT < 140 sec.

3000 < WPPMT < 2,000,000 lbs.

PROCEDURE:

Prior to entering ITSWM1, the geometry, weights, internal ballistics, and propulsion characteristics for all of the substages have been evaluated. For the substage immediately above this interstage, the models specified for the IBGAS, IBPERF, and NOZZLEG model types have evaluated the internal ballistics and nozzle geometry. For the substage immediately below this interstage, the models specified for the IBPERF and PROPELW model types have evaluated the internal ballistics and propellent characteristics.

The ITSWM1 model is then executed and the interstage structure weight is evaluated using parametric weight scaling equations. In addition, the interstage structure weight is broken down into expended and non-expended components.

PROCEDURE (Cont.):

After leaving ITSWM1, these expended and non-expended components will be used by the model specified for the INSTGW model type to determine the interstage weights.

EQUATIONS:

Total interstage structure weight.

$$W_{IT_{ST}} = K_{WITST}\, C_1 \left\{ \left[\frac{W_{PP_{MT}}\, I_{SP_{VD}}}{T_B} \right]^{C_2}_{\text{below}} \right. \tag{1}$$

$$\left. \left[R_{LNZP} \left(\sqrt{\epsilon_{NZ}} - 1 \right) \sqrt{\frac{W_{PP_{MT}}\, \overline{C^*}}{P_{AVG}\, T_B}} \right]^{C_3}_{\text{above}} \right\}$$

Total non-expended interstage structure weight component.

$$W_{IT_{STNX}} = K_{WITSNX}\, W_{IT_{ST}} \tag{2}$$

Total expended interstage structure weight component.

$$W_{IT_{STX}} = 0 \tag{3}$$

Expended (non-thrust producing) interstage structure weight component.

$$W_{IT_{STXI}} = 0 \tag{4}$$

Expended (thrust producing) interstage structure weight component.

$$W_{IT_{STXT}} = 0 \tag{5}$$

INPUT DATA, INTRA-MODEL:

The following data is input to this model directly by the program user. If a value is not input, the preset value is used.

INPUT DATA, INTRA-MODEL (Cont.):

Mnemonic	Symbol	Description; Ext. (Int.) Units	Preset
CITST1	C_1	Scaling constant for WITST computation; N. D.	0.00114
CITST2	C_2	Scaling constant for WITST computation; N. D.	0.665
CITST3	C_3	Scaling constant for WITST computation; N. D.	0.828
KWITST	K_{WITST}	Proportionality factor for total interstage structure weight; N. D.	1
KWITSNX	K_{WITSNX}	Proportionality factor for non-expended interstage structure weight component; N. D.	1

INPUT DATA, INTER-MODEL:

This model requires as input certain data which is usually output from a model of the specified model type. If the user has not specified such a source for this data, then it must be input directly with the intra-model input.

Mnemonic	Symbol	Description; Ext. (Int.) Units	Model Type
CVDELV	C^*	Delivered characteristic velocity of substage above this interstage; ft/sec	IBGAS
ISPVD	$I_{SP_{VD}}$	Delivered vacuum specific impulse of substage below this interstage; sec	IBPERF
PCHAVG	P_{AVG}	Average chamber pressure of substage above this interstage; psia	IBGAS

INPUT DATA, INTER-MODEL (Cont.):

Mnemonic	Symbol	Description; Ext. (Int.) Units	Model Type
RAEXTTH	ϵ_{NZ}	Expansion ratio of substage above this interstage; N. D.	NOZZLEG
RLNZP	R_{LNZP}	Protruding nozzle ratio of substage above this interstage; N. D.	NOZZLEG
TBPPMT	T_B	Propellent burn time of substage above this interstage; sec	IBPERF
TBPPMT	T_B	Propellent burn time of substage below this interstage; sec	IBPERF
WPPMT	$W_{PP_{MT}}$	Propellent weight of substage above this interstage; sec	PROPELW
WPPMT	$W_{PP_{MT}}$	Propellent weight of substage below this interstage; lb	PROPEL

OUTPUT DATA:

The following data is output from this model. It is available for use as inter-model input to other models and to print, plot, and optimization routines.

Mnemonic	Symbol	Description; Ext. (Int.) Units	
WITST	$W_{IT_{ST}}$	Total interstage structure weight. Includes all interstage weight except external insulation; lb	Eq. 1

OUTPUT DATA (Cont.):

Mnemonic	Symbol	Description; Ext. (Int.) Units	
WITSTNX	$W_{IT_{STNX}}$	Total non-expended interstage structure weight component;	
		lb	Eq. 2
WITSTX	$W_{IT_{STX}}$	Total expended interstage structure weight component;	
		lb	Eq. 3
WITSTXI	$W_{IT_{STXI}}$	Expended (non-thrust producing) interstage structure weight component;	
		lb	Eq. 4
WITSTXT	$W_{IT_{STXT}}$	Expended (thrust producing) interstage structure weight component;	
		lb	Eq. 5

PRINT BLOCK KEY:

Nominally, only those lines with an asterisk to the left of the line number will be printed. By input, any of the lines given below may be printed or suppressed (see the section on output models for the details).

```
                                        INTSTRW   ITSWM1     INTERSTAGE STRUCTURE WEIGHT
WITSST      WITSTNX      WITSTX              *1   WITSTXI    WITSTXT
KWITSST     KWITSNX                          *2
CITST1      CITST2       CITST3              *3
```

120.2

MODEL TYPE: INTSTRW (INTerstage STRucture Weight)

MODEL NAME: ITSWM2 (Geometry Dependent Weight)

DESCRIPTION:

ITSWM2 (InTerstage Structure Weight Model number 2) uses a geometry dependent equation to evaluate the interstage structure weight as a function of the interstage surface area and the weight per unit surface area. Although this model may be utilized for any interstage, its primary usage is for simulating the top interstage within the propulsion system (i.e., payload adapter).

The interstage structure includes all of the interstage except the external insulation.

PROCEDURE:

Prior to entering ITSWM2, the model specified for the INTSTGG model type has determined the interstage surface area.

The ITSWM2 model then uses the interstage surface area, together with the structure weight per unit surface area, to determine the interstage structure weight breakdown.

After leaving ITSWM2, the model specified for the INTSTGW model type will use the interstage structure weight to determine the interstage weight.

EQUATIONS:

Total interstage structure weight.

$$W_{IT_{ST}} = K_{WITST}\left(K_{WITST1}\, S_{IT}\, W_{IT_{SUA}} + K_{WITST2}\right) \qquad (1)$$

Total non-expended interstage structure weight component.

$$W_{IT_{STNX}} = W_{IT_{ST}} \qquad (2)$$

Total expended interstage structure weight component.

$$W_{IT_{STX}} = 0 \qquad (3)$$

EQUATIONS (Cont.):

Expended (thrust producing) interstage structure weight component.

$$W_{IT_{STXT}} = 0 \tag{4}$$

Expended (non-thrust producing) interstage structure weight component.

$$W_{IT_{STXI}} = 0 \tag{5}$$

INPUT DATA, INTRA-MODEL:

The following data is input to this model directly by the program user. If a value is not input, the preset value is used.

Mnemonic	Symbol	Description; Ext. (Int.) Units	Preset
KWITST	K_{WITST}	Coefficient for WITST computation; N. D.	1
KWITST1	K_{WITST1}	Coefficient for WITST computation; N. D.	1
KWITST2	K_{WITST2}	Bias for WITST computation; lb	0
WITSUA	$W_{IT_{SUA}}$	Interstage structure weight per unit surface area; lb/in^2	0

INPUT DATA, INTER-MODEL:

This model requires as input certain data which is usually output from a model of the specified model type. If the user has not specified such a source for this data, then it must be input directly with the intra-model input.

Mnemonic	Symbol	Description; Ext. (Int.) Units	Model Type
SIT	S_{IT}	Interstage structure surface area; in^2	INTSTGG

OUTPUT DATA:

The following data is output from this model. It is available for use as inter-model input to other models and to print, plot, and optimization routines.

Mnemonic	Symbol	Description; Ext. (Int.) Units	
WITST	$W_{IT_{ST}}$	Total interstage structure weight, includes all interstage weight except external insulation; lb	Eq. 1
WITSTNX	$W_{IT_{STNX}}$	Total non-expended interstage structure weight component; lb	Eq. 2
WITSTX	$W_{IT_{STX}}$	Total expended interstage structure weight component; lb	Eq. 3
WITSTXI	$W_{IT_{STXI}}$	Expended (non-thrust producing) interstage structure weight component; lb	Eq. 5
WITSTXT	$W_{IT_{STXT}}$	Expended (thrust producing) interstage structure weight component; lb	Eq. 4

PRINT BLOCK KEY:

Nominally, only those lines with an asterisk to the left of the line number will be printed. By input, any of the lines given below may be printed or suppressed (see the section on output models for the details).

			INTSTRW	ITSWM2	INTERSTAGE STRUCTURE WEIGHT
WITST	WITSTNX	WITSTX	*1	WITSTXI	WITSTXT
KWITST	KWITSNX		*2		
KWITST1	KWITST2	WITSUA	*4		

130.1

MODEL TYPE: INTSTGW (INTerSTaGe Weight)

MODEL NAME: ITWM1 (Weight Synthesis)

DESCRIPTION:

ITWM1 (InTerstage Weight Model number 1) is a weight synthesis model which evaluates the interstage weight breakdown. The interstage weight is comprised of the following subsystems:

Interstage structure

Interstage external insulation

PROCEDURE:

Prior to entering ITWM1, the models specified by the INTSTRW and INTINSW model types have evaluated the interstage structure and external insulation weights. In addition to evaluating subcomponent weights peculiar to their particular requirements, they have defined a set of component weights in terms of expended or non-expended attributes.

These expended and non-expended weight components are input to ITWM1. The ITWM1 model will combine these quantities to determine the interstage weight components.

After all of the interstages are sized, the model specified by the STAGEW model type will use the substage and interstage quantities to determine the stage weights and mass fractions.

EQUATIONS:

Total interstage weight.

$$W_{IT} = K_{WIT} \left(W_{IT_{ST}} + W_{IT_{IE}} \right) \qquad (1)$$

EQUATIONS (Cont.):

Total non-expended interstage weight component.

$$W_{IT_{NX}} = K_{WITNX} \left(W_{IT_{STNX}} + W_{IT_{IENX}} \right) \qquad (2)$$

Total expended interstage weight component.

$$W_{IT_X} = K_{WITX} \left(W_{IT_{STX}} + W_{IT_{IEX}} \right) \qquad (3)$$

Expended (thrust producing) interstage weight component.

$$W_{IT_{XT}} = K_{WITXT} \left(W_{IT_{STXT}} + W_{IT_{IEXT}} \right) \qquad (4)$$

Expended (non-thrust producing) interstage weight component.

$$W_{IT_{XI}} = K_{WITXI} \left(W_{IT_{STXI}} + W_{IT_{IEXI}} \right) \qquad (5)$$

INPUT DATA, INTRA-MODEL:

The following data is input to this model directly by the program user. If a value is not input, the preset value is used.

Mnemonic	Symbol	Description; Ext. (Int.) Units	Preset
KWIT	K_{WIT}	Proportionality factor for total interstage weight;	
		N. D.	1
KWITNX	K_{WITNX}	Proportionality factor for total non-expended interstage weight component;	
		N. D.	1
KWITX	K_{WITX}	Proportionality factor for total expended interstage weight component;	
		N. D.	1
KWITXI	K_{WITXI}	Proportionality factor for expended (non-thrust producing) interstage weight component;	
		N. D.	1

INPUT DATA, INTRA-MODEL (Cont.):

Mnemonic	Symbol	Description; Ext. (Int.) Units	Preset
KWITXT	K_{WITXT}	Proportionality factor for expended (thrust producing) interstage weight component; N. D.	1

INPUT DATA, INTER-MODEL:

This model requires as input certain data which is usually output from a model of the specified model type. If the user has not specified such a source for this data, then it must be input directly with the intra-model input.

Mnemonic	Symbol	Description; Ext. (Int.) Units	Model Type
WITIE	$W_{IT_{IE}}$	Total interstage external insulation weight; lb	INTINSW
WITIENX	$W_{IT_{IENX}}$	Total non-expended interstage external insulation weight component; lb	INTINSW
WITIEX	$W_{IT_{IEX}}$	Total expended interstage external insulation weight component; lb	INTINSW
WITIEXI	$W_{IT_{IEXI}}$	Expended (non-thrust producing) external insulation weight component; lb	INTINSW
WITIEXT	$W_{IT_{IEXT}}$	Expended (thrust producing) external insulation weight component; lb	INTINSW
WITST	$W_{IT_{ST}}$	Total interstage structure weight; lb	INTSTRW
WITSTNX	$W_{IT_{STNX}}$	Total non-expended interstage structure weight component; lb	INTSTRW

INPUT DATA, INTER-MODEL (Cont.):

Mnemonic	Symbol	Description; Ext. (Int.) Units	Model Type
WITSTX	$W_{IT_{STX}}$	Total expended interstage structure weight component; lb	INTSTRW
WITSTXI	$W_{IT_{STXI}}$	Expended (non-thrust producing) interstage structure weight component; lb	INTSTRW
WITSTXT	$W_{IT_{STXT}}$	Expended (thrust producing) interstage structure weight component; lb	INTSTRW

OUTPUT DATA:

The following data is output from this model. It is available for use as inter-model input to other models and to print, plot, and optimization routines.

Mnemonic	Symbol	Description; Ext. (Int.) Units	
WIT	W_{IT}	Total interstage weight. Includes structure and external insulation; lb	Eq. 1
WITNX	$W_{IT_{NX}}$	Total non-expended interstage weight component. Includes structure and external insulation; lb	Eq. 2
WITX	W_{IT_X}	Total expended interstage weight component. Includes structure and external insulation; lb	Eq. 3
WITXI	$W_{IT_{XI}}$	Expended (non-thrust producing) interstage weight component. Includes structure and external insulation; lb	Eq. 5

OUTPUT DATA (Cont.):

Mnemonic	Symbol	Description; Ext. (Int.) Units
WITXT	$W_{IT_{XT}}$	Expended (thrust producing) interstage weight component. Includes structure and external insulation; lb Eq. 4

PRINT BLOCK KEY:

Nominally, only those lines with an asterisk to the left of the line number will be printed. By input, any of the lines given below may be printed or suppressed (see the section on output models for the details).

```
                                     INTSTGW    ITIWM1     INTERSTAGE WEIGHT
WIT        WITNX        WITX              *1    WITXI      WITXT
KWIT       KWITNX       KWITX             *2    KWITXI     KWITXT
```

140.1

MODEL TYPE: MISCMTW (MISCellaneous MoTor Weight)

MODEL NAME: MMWM1 (Collective Miscellaneous Subsystems, Parametric Scaling)

DESCRIPTION:

MMWM1 (Miscellaneous Motor Weight Model number 1) utilizes a parametric scaling equation to determine collectively the weight of a set of miscellaneous solid rocket motor subsystems. The subsystems considered are:

Raceways

Base heat protection

Igniter

Ordnance

See reference 8 for a description of the equation and parametric scaling rationale.

The model is applicable for performance parameters within the following limits (see Input Data, Inter-Model and reference 8, figure 15).

$$1000 \text{ lb} < WPPMT < 5,000,000 \text{ lb}$$

PROCEDURE:

In addition to evaluating the miscellaneous motor weight, the MMWM1 model determines the weight breakdown in terms of expended and non-expended components.

These expended and non-expended component weights will later be used by the model specified for the MOTORW model type to determine the motor weights and mass fractions.

EQUATIONS:

Total miscellaneous motor weight.

$$W_{MM} = K_{WMM} C_1 \left(W_{PP_{MT}}\right)^{C_2} \qquad (1)$$

Total non-expended miscellaneous motor weight component.

$$W_{MM_{NX}} = K_{WMMNX} W_{MM} \qquad (2)$$

Total expended miscellaneous motor weight component.

$$W_{MM_X} = 0 \qquad (3)$$

Expended (thrust producing) miscellaneous motor weight component.

$$W_{MM_{XI}} = 0 \qquad (4)$$

Expended (non-thrust producing) miscellaneous motor weight component.

$$W_{MM_{XT}} = 0 \qquad (5)$$

INPUT DATA, INTRA-MODEL:

The following data is input to this model directly by the program user. If a value is not input, the preset value is used.

Mnemonic	Symbol	Description; Ext. (Int.) Units	Preset
CMMW1	C_1	Scaling constant for WMM computations; N. D.	0.05
CMMW2	C_2	Scaling constant for WMM computation; N. D.	0.8

INPUT DATA, INTRA-MODEL (Cont.):

Mnemonic	Symbol	Description; Ext. (Int.) Units	Preset
KWMM	K_{WMM}	Proportionality factor for total miscellaneous motor weight; N. D.	1
KWMMNX	K_{WMMNX}	Proportionality factor for non-expended miscellaneous motor weight component; N. D.	1

INPUT DATA, INTER-MODEL:

This model requires as input certain data which is usually output from a model of the specified model type. If the user has not specified such a source for this data, then it must be input directly with the intra-model input.

Mnemonic	Symbol	Description; Ext. (Int.) Units	Model Type
WPPMT	$W_{PP_{MT}}$	Propellent weight; lb	PROPELW

OUTPUT DATA:

The following data is output by this model. It is available for use as inter-model input to other models and to print, plot, and optimization routines.

Mnemonic	Symbol	Description; Ext. (Int.) Units	
WMM	W_{MM}	Total miscellaneous motor weight, includes weights of raceways, base heat protection, igniters, and ordnance; lb	Eq. 1
WMMNX	$W_{MM_{NX}}$	Total non-expended miscellaneous motor weight component, includes weights of raceways, base heat protection, igniters, and ordnance; lb	Eq. 2

OUTPUT DATA (Cont.):

Mnemonic	Symbol	Description; Ext. (Int.) Units	
WMMX	W_{MM_X}	Total expended miscellaneous motor weight component, includes weights of raceways, base heat protection, igniters, and ordnance; lb	Eq. 3
WMMXI	$W_{MM_{XI}}$	Expended (non-thrust producing) miscellaneous motor weight component, includes weights of raceways, base heat protection, igniters, and ordnance; lb	Eq. 4
WMMXT	$W_{MM_{XT}}$	Expended (thrust producing) weight component, includes weights of raceways, base heat protection, igniters, and ordnance; lb	Eq. 5

PRINT BLOCK KEY:

Nominally, only those lines with an asterisk to the left of the line number will be printed. By input, any of the lines given below may be printed or suppressed (see the section on output models for the details).

			MISCMTW	MMWM1	MISCELLANEOUS MOTOR WEIGHT
WMM	WMMNX	WMMX	*1	WMMXI	WMMXT
CMMW1	CMMW2	KWMM	*2	KWMMNX	

150.1

MODEL TYPE: MOTORG (MOTOR Geometry)

MODEL NAME: MTGM1 (Solid Rocket Motor)

DESCRIPTION:

MTGM1 (MoTor Geometry Model number 1) evaluates the geometry of a basic solid rocket motor. The motor includes only the cylindrical case section, forward case closure section and aft case closure section. It may include diameter corrections for raceways, etc., but does not include the protruding portion of the nozzle, thrust termination ports, etc. The latter quantities are evaluated by the substage geometry model. The motor geometry is illustrated by figure 1.

PROCEDURE:

Prior to entering MTGM1, the models specified by the PROPELW, CASEG, and GRAING model types have evaluated the geometry of the major motor components.

MTGM1 then determines the basic motor geometry.

After executing MTGM1, the model specified by the SUBSTGG model type will utilize the motor geometry and nozzle geometry to determine the substage geometry.

EQUATIONS:

Length of forward motor closure. (Figure 1)

$$L_{MT_{CHF}} = K_{MT_1} L_{CS_{CHFO}} + K_{MT_2} \tag{1}$$

Length of aft motor closure. (Figure 1)

$$L_{MT_{CHA}} = K_{MT_3} L_{CS_{CHAO}} + K_{MT_4} \tag{2}$$

EQUATIONS (Cont.):

Length of motor cylindrical section. (Figure 1)

$$L_{MT_{CY}} = K_{MT_5} L_{CS_{CY}} + K_{MT_6} \tag{3}$$

Total motor length. (Figure 1)

$$L_{MT} = L_{MT_{CY}} + L_{MT_{CHF}} + L_{MT_{CHA}} \tag{4}$$

Total motor diameter. (Figure 1)

$$D_{MT} = K_{MT_7} D_{CS_O} + K_{MT_8} \tag{5}$$

Motor cross sectional area.

$$A_{MT} = \left(\frac{\pi}{4}\right) D_{MT}^2 \tag{6}$$

Ratio; motor length to case diameter.

$$R_{LDMTCS} = \frac{L_{MT}}{D_{CS_O}} \tag{7}$$

Ratio; motor length to motor diameter.

$$R_{LDMT} = \frac{L_{MT}}{D_{MT}} \tag{8}$$

Motor volume.

$$V_{MT} = V_{GN} \tag{9}$$

Motor volumetric loading efficiency.

$$\eta_{PP_{MT}} = \frac{V_{PP_{MT}}}{V_{MT}} \tag{10}$$

EQUATIONS (Cont.):

Motor forward skirt length. (Figure 1)

$$L_{MT_{SKF}} = K_{MTSKF1} D_{CS_O} + K_{MTSKF2} \tag{11}$$

Motor aft skirt length. (Figure 1)

$$L_{MT_{SKA}} = K_{MTSKA1} D_{CS_O} + K_{MTSKA2} \tag{12}$$

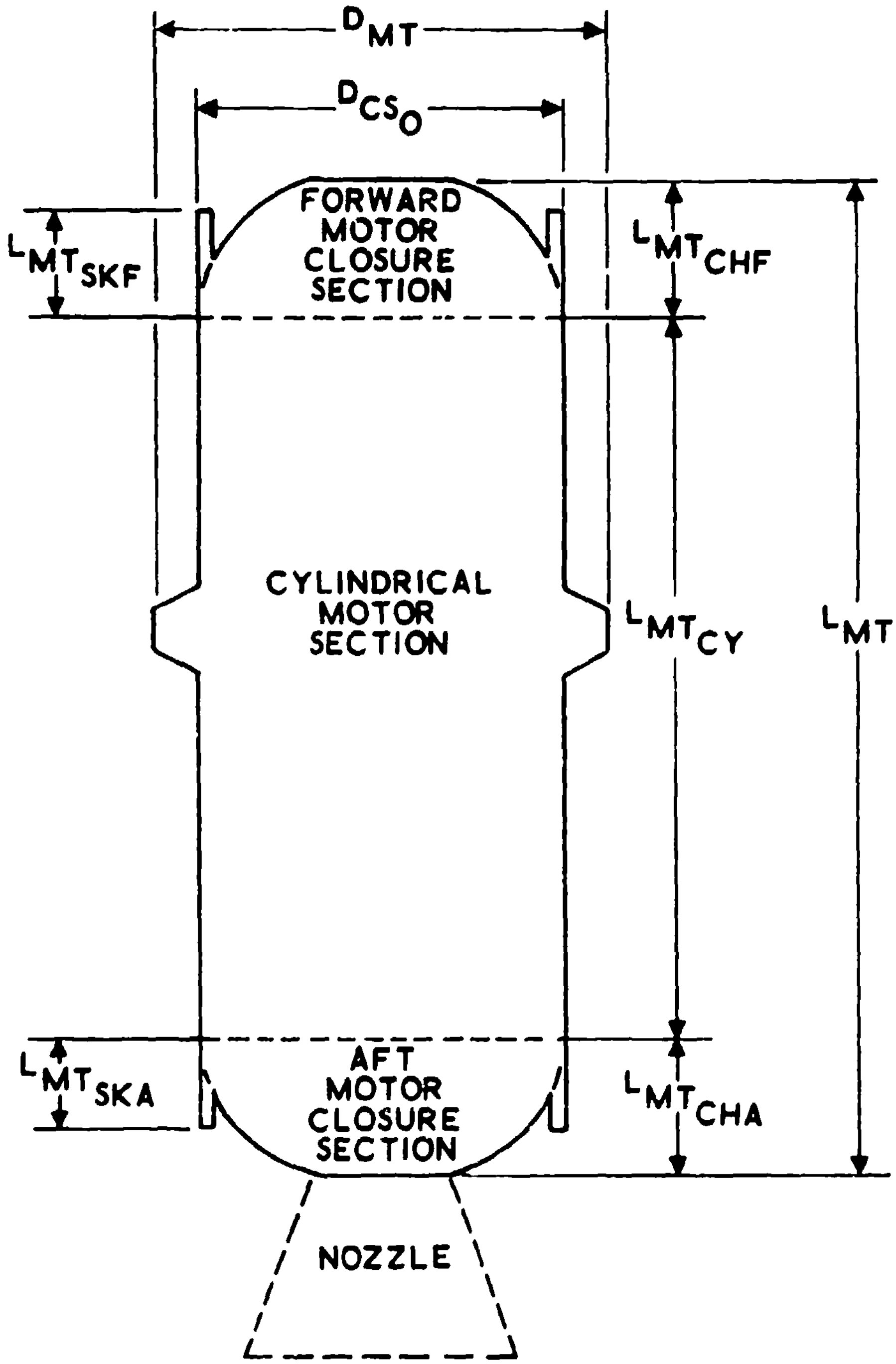

Fig. 150.1-1 Basic Motor Geometry

INPUT DATA, INTRA-MODEL:

The following data is input directly to this model by the program user. If a value is not input, the preset value is used.

Mnemonic	Symbol	Description; Ext. (Int.) Units	Preset
KMTSKA1	K_{MTSKA1}	Proportionality factor relating the motor aft skirt length to the outside case diameter; N. D.	0.1
KMTSKA2	K_{MTSKA2}	Bias for motor aft skirt length computation; in	0
KMTSKF1	K_{MTSKF1}	Proportionality factor relating the motor forward skirt length to the outside case diameter; N. D.	0.1
KMTSKF2	K_{MTSKF2}	Bias for motor forward skirt length computation; in	0

The following coefficient and bias quantities are made available for input. However, in normal applications, the preset values are used for most, if not all, of these quantities. Note that these coefficient quantities are preset (1) and the bias quantities are preset (0).

KMT1	K_{MT1}	Coefficient for LMTCHF computation; N. D.	1
KMT2	K_{MT2}	Bias for LMTCHF computation; in	0
KMT3	K_{MT3}	Coefficient for LMTCHA computation; N. D.	1
KMT4	K_{MT4}	Bias for LMTCHA computation; in	0

INPUT DATA, INTRA-MODEL (Cont.):

Mnemonic	Symbol	Description; Ext. (Int.) Units	Preset
KMT5	K_{MT5}	Coefficient for LMTCY computation; N. D.	1
KMT6	K_{MT6}	Bias for LMTCY computation; in	0
KMT7	K_{MT7}	Coefficient for DMT computation; N. D.	1
KMT8	K_{MT8}	Bias for DMT computation; in	0

INPUT DATA, INTER-MODEL:

This model requires as input certain data which is usually output from a model of the specified model type. If the user has not specified such a source for this data, then it must be input directly with the intra-model input.

Mnemonic	Symbol	Description; Ext. (Int.) Units	Model Type
DCSO	D_{CS_O}	Outside case diameter; in Fig. 1	CASEG
LCS	L_{CS}	Case length; in	CASEG
LCSCY	$L_{CS_{CY}}$	Cylindrical case section length; in	CASEG
LCSCHAO	$L_{CS_{CHAO}}$	Aft case closure length; in	CASEG
LCSCHFO	$L_{CS_{CHFO}}$	Forward case closure length; in	CASEG

INPUT DATA, INTER-MODEL (Cont.):

Mnemonic	Symbol	Description; Ext. (Int.) Units	Model Type
VGN	V_{GN}	Volume of grain envelope; in^3	GRAING
VPPMT	$V_{PP_{MT}}$	Propellent volume; in^3	PROPELW

OUTPUT DATA:

The following data is output from this model. It is available for use as inter-model input to other models and to print, plot, and optimization routines.

Mnemonic	Symbol	Description; Ext. (Int.) Units		
AMT	A_{MT}	Motor cross sectional area. May include raceways and other protrusions; in		Eq. 6
DMT	D_{MT}	Motor diameter. May include allowance for raceways and other protrusions; in	Fig. 1	Eq. 5
LMT	L_{MT}	Motor length. Does not include protruding nozzle, outside igniter attachment, thrust termination parts, etc.; in	Fig. 1	Eq. 4
LMTCHA	$L_{MT_{CHA}}$	Aft motor closure length; in	Fig. 1	Eq. 2
LMTCHF	$L_{MT_{CHF}}$	Forward motor closure length. Does not include outside igniter attachments, thrust termination ports, etc.; in	Fig. 1	Eq. 1
LMTCY	$L_{MT_{CY}}$	Motor cylinder length; in	Fig. 1	Eq. 3

OUTPUT DATA (Cont.):

Mnemonic	Symbol	Description; Ext. (Int.) Units		
LMTSKA	$L_{MT_{SKA}}$	Motor aft skirt length. Measured along outside of skirt from intersection of cylindrical motor section and aft closure section;		
		in	Fig. 1	Eq. 12
LMTSKF	$L_{MT_{SKF}}$	Motor forward skirt length. Measured along outside of skirt from intersection of cylindrical motor section and forward motor section;		
		in	Fig. 1	Eq. 11
RLDMT	R_{LDMT}	Ratio, motor length to motor diameter;		
		N. D.		Eq. 8
RLDMTCS	R_{LDMTCS}	Ratio, motor length to case outside diameter;		
		N. D.		Eq. 7
RVPPMT	$\eta_{PP_{MT}}$	Motor volumetric loading efficiency. Ratio of propellent volume to motor volume;		
		N. D.		Eq. 10
VMT	V_{MT}	Motor volume. Volume of grain envelope. Excludes case liner;		
		in^3		Eq. 9

PRINT BLOCK KEY:

Nominally, only those lines with an asterisk to the left of the line number will be printed. By input, any of the lines given below may be printed or suppressed (see the section on output models for the details).

			MOTORG	MTGM1	MOTOR GEOMETRY	
AMT	DMT	KMT1	*1	KMT2	KMT3	KMT4
KMT5	KMT6	KMT7	*2	KMT8	KMCSKA1	KMTSKA2
KMTSKF1	KMTSKF2	LMT	*3	LMTCHA	LMTCHF	LMTCY
LMTSKA	LMTSKF	RLDMT	*4	RLDMTCS	RVPPMT	VMT

160.1

MODEL TYPE: MOTORW (MOTOR Weight)

MODEL NAME: MTWM1 (Weight Synthesis)

DESCRIPTION:

MTWM1 (MoTor Weight Model number 1) is a weight synthesis model which evaluates the motor weight breakdown. The motor weight is comprised of the following subsystems.

- Propellent
- Case (includes joint weight penalty if applicable)
- Thrust termination mechanism
- Internal insulation
- Thrust vector control system
- Miscellaneous motor weight (includes raceways, base heat protection, igniters, and ordnance)

Note that the above subsystems do NOT include the nozzle. See the SUBSTGW model type for substage (motor plus nozzle) weight quantities.

PROCEDURE:

Prior to entering MTWM1, all of the models which evaluate motor subsystem weights have been executed. In addition to evaluating sub-component weights peculiar to its particular requirement, each model has defined a set of component weights in terms of expended or non-expended attributes.

These expended or non-expended subsystem weights are input to the MTWM1 model which, in turn, combines these quantities to determine the motor weight breakdown. The motor mass fractions are also evaluated.

After MTWM1 is executed, the model specified by the SUBSTGW model type will utilize these motor quantities, with the nozzle quantities, to determine the total substage weights and mass fractions.

EQUATIONS:

Total motor weight.

$$W_{MT} = K_{WMT} \left(W_{PP_{MT}} + W_{CS} + W_{TT} + W_{MM} + W_{IN} + W_{TV}\right) \quad (1)$$

Total non-expended motor weight component.

$$W_{MT_{NX}} = K_{WMTNX} \left(W_{CS_{NX}} + W_{TT_{NX}} + W_{MM_{NX}} + W_{IN_{NX}} + W_{TV_{NX}}\right) \quad (2)$$

Total expended motor weight component (excluding propellent).

$$W_{MT_X} = K_{WMTX} \left(W_{CS_X} + W_{TT_X} + W_{MM_X} + W_{IN_X} + W_{TV_X}\right) \quad (3)$$

Expended (thrust producing) motor weight component.

$$W_{MT_{XT}} = K_{WMTXT} \left(W_{CS_{XT}} + W_{TT_{XT}} + W_{MM_{XT}} + W_{IN_{XT}} + W_{TV_{XT}}\right) \quad (4)$$

Expended (non-thrust producing) motor weight component.

$$W_{MT_{XI}} = K_{WMTXI} \left(W_{CS_{XI}} + W_{TT_{XI}} + W_{MM_{XI}} + W_{IN_{XI}} + W_{TV_{XI}}\right) \quad (5)$$

INPUT DATA, INTRA-MODEL:

The following data is input to this model directly by the program user. If a value is not input, the preset value is used.

Mnemonic	Symbol	Description; Ext. (Int.) Units	Preset
KWMT	K_{WMT}	Proportionality factor for total motor weight; N. D.	1
KWMTNX	K_{WMTNX}	Proportionality factor for non-expended motor weight component; N. D	1

INPUT DATA, INTRA-MODEL (Cont.):

Mnemonic	Symbol	Description; Ext. (Int.) Units	Preset
KWMTX	K_{WMTX}	Proportionality factor for total expended motor weight component; N. D.	1
KWMTXI	K_{WMTXI}	Proportionality factor for expended (non-thrust producing) motor weight component; N. D.	1
KWMTXT	K_{WMTXT}	Proportionality factor for expended (thrust producing) motor weight component; N. D.	1

INPUT DATA, INTER-MODEL:

This model requires as input certain data which is usually output from a model of the specified model type. If the user has not specified such a source for this data, then it must be input directly with the intra-model input.

Mnemonic	Symbol	Description; Ext. (Int.) Units	Model Type
WCS	W_{CS}	Case weight, total; lb	CASEW
WCSNX	$W_{CS_{NX}}$	Case weight component, total non-expended; lb	CASEW
WCSX	W_{CS_X}	Case weight component, total expended; lb	CASEW
WCSXI	$W_{CS_{XI}}$	Case weight component, expended, (non-thrust producing); lb	CASEW

INPUT DATA, INTER-MODEL (Cont.):

Mnemonic	Symbol	Description; Ext. (Int.) Units	Model Type
WCSXT	$W_{CS_{XT}}$	Case weight component, expended, (thrust producing); lb	CASEW
WIN	W_{IN}	Internal insulation weight, total; lb	INSULW
WINNX	$W_{IN_{NX}}$	Internal insulation weight component, total non-expended; lb	INSULW
WINX	W_{IN_X}	Internal insulation weight component, total expended; lb	INSULW
WINXI	$W_{IN_{XI}}$	Internal insulation weight component, expended, (non-thrust producing); lb	INSULW
WINXT	$W_{IN_{XT}}$	Internal insulation weight component, expended, (thrust producing); lb	INSULW
WMM	W_{MM}	Miscellaneous motor weight, total; lb	MISCMTW
WMMNX	$W_{MM_{NX}}$	Miscellaneous motor weight component, total non-expended; lb	MISCMTW
WMMX	W_{MM_X}	Miscellaneous motor weight component, total expended; lb	MISCMTW
WMMXI	$W_{MM_{XI}}$	Miscellaneous motor weight component, expended, (non-thrust producing); lb	MISCMTW

INPUT DATA, INTER-MODEL (Cont.):

Mnemonic	Symbol	Description; Ext. (Int.) Units	Model Type
WMMXT	$W_{MM_{XT}}$	Miscellaneous motor weight component, expended, (thrust producing); lb	MISCMTW
WPPMT	$W_{PP_{MT}}$	Propellent weight; lb	PROPELW
WTT	W_{TT}	Thrust termination weight, total; lb	TTERMW
WTTNX	$W_{TT_{NX}}$	Thrust termination weight component, total non-expended; lb	TTERMW
WTTX	$W_{TT_{X}}$	Thrust termination weight component, total expended; lb	TTERMW
WTTXI	$W_{TT_{XI}}$	Thrust termination weight component, expended, (non-thrust producing); lb	TTERMW
WTTXT	$W_{TT_{XT}}$	Thrust termination weight component, expended, (thrust producing); lb	TTERMW
WTV	W_{TV}	Thrust vector control weight, total; lb	TVCW
WTVNX	$W_{TV_{NX}}$	Thrust vector control weight component, total non-expended; lb	TVCW
WTVX	$W_{TV_{X}}$	Thrust vector control weight component, total expended; lb	TVCW

INPUT DATA, INTER-MODEL (Cont.):

Mnemonic	Symbol	Description; Ext. (Int.) Units	Model Type
WTVXI	$W_{TV_{XI}}$	Thrust vector control weight component, expended, (non-thrust producing); lb	TVCW
WTVXT	$W_{TV_{XT}}$	Thrust vector control weight component, expended, (thrust producing); lb	TVCW

OUTPUT DATA:

The following data is output from this model. It is available for use as inter-model input to other models and to print, plot, and optimization routines.

Mnemonic	Symbol	Description; Ext. (Int.) Units	
WMT	W_{MT}	Total motor weight. Includes propellent, case, thrust termination, miscellaneous, internal insulation, and thrust vector control subsystems. Does not include nozzle; lb	Eq. 1
WMTNX	$W_{MT_{NX}}$	Total non-expended motor weight component. Includes case, thrust termination, miscellaneous, internal insulation, and thrust vector control subsystems. Does not include nozzle; lb	Eq. 2
WMTX	W_{MT_X}	Total expended motor weight component. Includes case, thrust termination, miscellaneous, internal insulation and thrust vector control subsystems. Does not include propellent or nozzle; lb	Eq. 3

OUTPUT DATA (Cont.):

Mnemonic	Symbol	Description; Ext. (Int.) Units	
WMTXI	$W_{MT_{XI}}$	Expended (non-thrust producing) motor weight component. Includes case, thrust termination, miscellaneous motor, internal insulation, and thrust vector control subsystems. Does not include nozzle;	
		lb	Eq. 5
WMTXT	$W_{MT_{XT}}$	Expended (thrust producing) motor weight component. Includes case, thrust termination, miscellaneous, internal insulation, and thrust vector control subsystems. Does not include propellent or nozzle;	
		lb	Eq. 4

PRINT BLOCK KEY:

Nominally, only those lines with an asterisk to the left of the line number will be printed. By input, any of the lines given below may be printed or suppressed (see the section on output models for the details).

```
                                  MOTORW    MTWM1     MOTOR WEIGHT
WMT       WMTNX       WMTX            *1    WMTXI     WMTXT
KWMT      KWMTNX      KWMTX           *2    KWMTXI    KWMTXT
```

170.1

MODEL TYPE: NOZZLEG (NOZZLE Geometry)

MODEL NAME: NZGM1 (Conical nozzle)

DESCRIPTION:

NZGM1 (NoZzle Geometry Model number 1) evaluates the geometrical expressions required for a simple conical nozzle design having circular convergent and transition section contours. Due to the requirement that the nozzle contour be smooth (continuous function and continuous first derivative) where the major sections join at the throat and transition planes, the conical section half angle is equal to the transition section arc angle.

The model assumes:

1. The length of the convergent section is directly proportional to the throat diameter.

2. The radius of curvature of the convergent section contour is directly proportional to the throat diameter.

3. The radius of curvature of the transition section contour is directly proportional to the throat diameter.

4. The conical section half angle is equal to the transition section arc angle.

5. The nozzle has zero thickness.

It should be noted that the placement of the buried nozzle plane with respect to the motor is not determined by this model. Although always associated with the outside surface of the aft case closure, the actual placement of the buried nozzle plane is normally specified by the model associated with the GRAING model type.

For an appreciation of the basic nozzle terminology used within this model, see figure 1. Figures 2 through 5 illustrate the nozzle geometry and are useful when referring to the symbol definitions and equations.

PROCEDURE:

Prior to entering NZGM1, the models specified by the IBGAS and IBPERF model types have evaluated the gas characteristics, chamber pressures and propellent weight flow for the solid rocket motor.

The NZGM1 is then executed and the conical nozzle geometry is evaluated.

After executing NZGM1, the model specified by the IBPERF model type is reentered (if required) to evaluate the performance quantities which are dependent upon the nozzle geometry.

EQUATIONS:

Nozzle throat area.

$$A_{NZ_{TH}} = \frac{\dot{W}_{PP_{MT}} C*}{g_o P_{AVG}} \qquad (1)$$

Nozzle throat diameter. (Figures 2, 3, 4, 5)

$$D_{NZ_{TH}} = \sqrt{\frac{4 A_{NZ_{TH}}}{\pi}} \qquad (2)$$

Proportionality factor relating nozzle entrance diameter to nozzle throat diameter.

$$K_{DENT} = 1 + 2\left(C_2 - \sqrt{C_2^2 - C_1^2}\right) \qquad (3)$$

Porportionality factor relating nozzle transition diameter to nozzle throat diameter.

$$K_{DTR} = 1 + 2\, C_3 \left[1 - \cos\left(\theta_{NZ}\right)\right] \qquad (4)$$

Ratio, nozzle transition diameter to nozzle throat diameter.

$$R_{DTRTH} = K_{DTR} \qquad (5)$$

Expansion ratio at nozzle transition plane.

$$\epsilon_{TR} = \left(R_{DTRTH}\right)^2 \qquad (6)$$

EQUATIONS (Cont.):

Ratio, nozzle exit diameter to nozzle throat diameter.

$$R_{DEXTTH} = \sqrt{\epsilon_{NZ}} \tag{7}$$

Radius of curvature, convergent nozzle section. (Figure 3)

$$R_{C_{CV}} = C_2 \, D_{NZ_{TH}} \tag{8}$$

Radius of curvature, transition nozzle section. (Figure 4)

$$R_{C_{TR}} = C_3 \, D_{NZ_{TH}} \tag{9}$$

Nozzle entrance diameter. (Figure 3)

$$D_{NZ_{ENT}} = K_{DENT} \, D_{NZ_{TH}} \tag{10}$$

Nozzle transition diameter. (Figure 4)

$$D_{NZ_{TR}} = R_{DTRTH} \, D_{NZ_{TH}} \tag{11}$$

Nozzle exit diameter. (Figure 5)

$$D_{NZ_{EXT}} = R_{DEXTTH} \, D_{NZ_{TH}} \tag{12}$$

Nozzle entrance area. (Figure 3)

$$A_{NZ_{ENT}} = \left(\frac{\pi}{4}\right) D^2_{NZ_{ENT}} \tag{13}$$

Nozzle transition area. (Figure 4)

$$A_{NZ_{TR}} = \left(\frac{\pi}{4}\right) D^2_{NZ_{TR}} \tag{14}$$

EQUATIONS (Cont.):

Nozzle exit area. (Figure 5)

$$A_{NZ_{EXT}} = \left(\frac{\pi}{4}\right) D^2_{NZ_{EXT}} \tag{15}$$

Convergent nozzle section length. (Figure 3)

$$L_{NZ_{CV}} = C_1 \; D_{NZ_{TH}} \tag{16}$$

Transition nozzle section length. (Figure 4)

$$L_{NZ_{TR}} = R_{C_{TR}} \sin\left(\theta_{NZ}\right) \tag{17}$$

Conic nozzle section length. (Figure 5)

$$L_{NZ_{CN}} = \frac{\left(D_{NZ_{EXT}} - D_{NZ_{TR}}\right)}{2 \tan\left(\theta_{NZ}\right)} \tag{18}$$

Body nozzle section length. (Figure 2)

$$L_{NZ_{BDY}} = L_{NZ_{CV}} + L_{NZ_{TR}} \tag{19}$$

Divergent nozzle section length. (Figure 2)

$$L_{NZ_{DV}} = L_{NZ_{TR}} + L_{NZ_{CN}} \tag{20}$$

Total nozzle length. (Figure 2)

$$L_{NZ} = L_{NZ_{CV}} + L_{NZ_{DV}} \tag{21}$$

Buried nozzle section length. (Figure 2)

$$L_{NZ_B} = K_{LNZB} \; L_{NZ} \tag{22}$$

EQUATIONS (Cont.):

Protruding nozzle section length. (Figure 2)

$$L_{NZ_P} = L_{NZ} - L_{NZ_B} \tag{23}$$

Buried nozzle length ratio.

$$R_{LNZB} = \frac{L_{NZ_B}}{L_{NZ}} \tag{23-a}$$

Protruding nozzle length ratio.

$$R_{LNZP} = \frac{L_{NZ_P}}{L_{NZ}} \tag{23-b}$$

Length buried in convergent nozzle section. (Positive sense towards entrance.) (Figure 4)

$$L_{NZ_{BCV}} = L_{NZ_{CV}} - L_{NZ_B} \tag{24}$$

Length buried in transition nozzle section. (Positive sense towards exit.) (Figure 4)

$$L_{NZ_{BTR}} = L_{NZ_B} - L_{NZ_{CV}} \tag{25}$$

Length buried in conic nozzle section. (Positive sense towards exit.) (Figure 5)

$$L_{NZ_{BCN}} = L_{NZ_B} - L_{NZ_{BDY}} \tag{26}$$

Buried nozzle diameter evaluation:

If the buried nozzle plane is within the convergent nozzle section, (Figure 3)

$$D_{NZ_B} = D_{NZ_{TH}} + 2\left(R_{C_{CV}} - \sqrt{R^2_{C_{CV}} - L^2_{NZ_{BCV}}}\right) \tag{27}$$

EQUATIONS (Cont.):

If the buried nozzle plane is within the transition nozzle section, (Figure 4)

$$D_{NZ_B} = D_{NZ_{TH}} + 2\left(R_{C_{TR}} - \sqrt{R^2_{C_{TR}} - L^2_{NZ_{BTR}}}\right) \quad (28)$$

If the buried nozzle plane is within the conic nozzle section, (Figure 5)

$$D_{NZ_B} = D_{NZ_{TR}} + 2\,L_{NZ_{BCN}} \tan\left(\theta_{NZ}\right) \quad (29)$$

Associative Quantities. The following quantities are intended solely for optional utilization by the program user. (Their primary usage within this model is for forming constraint quantities.)

$$Q_{DB} = K_{QDB}\, D_{NZ_B} \quad (30)$$

$$Q_{DENT} = K_{QDEN}\, D_{NZ_{ENT}} \quad (31)$$

$$Q_{DEXT} = K_{QDEX}\, D_{NZ_{EXT}} \quad (32)$$

$$Q_{LNZ} = K_{QL}\, L_{NZ} \quad (33)$$

$$Q_{LB} = K_{QLB}\, L_{NZ_B} \quad (34)$$

$$Q_{DTH} = K_{QDTH}\, D_{NZ_{TH}} \quad (35)$$

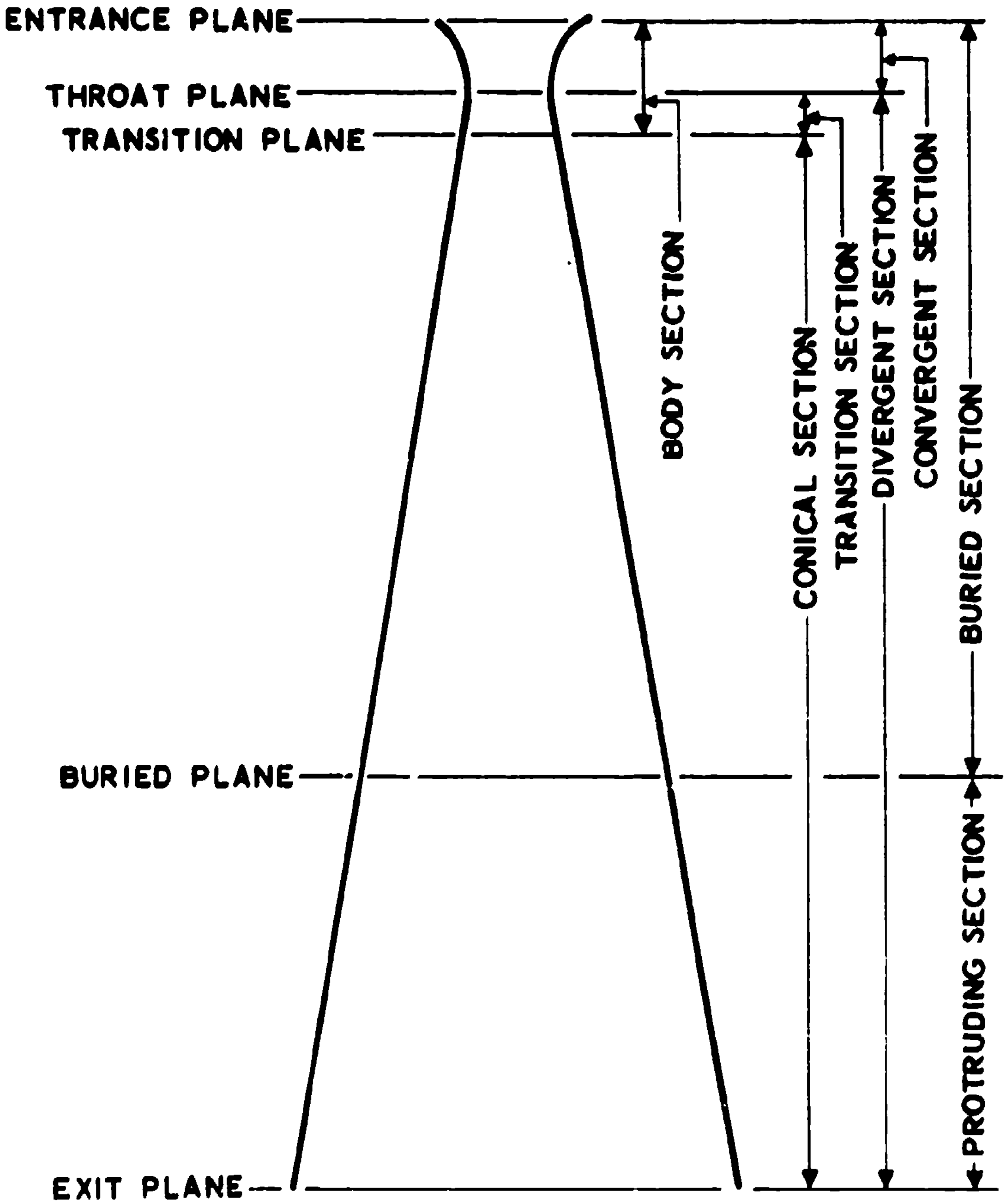

Fig. 170.1-1 Conical Nozzle Sections and Planes

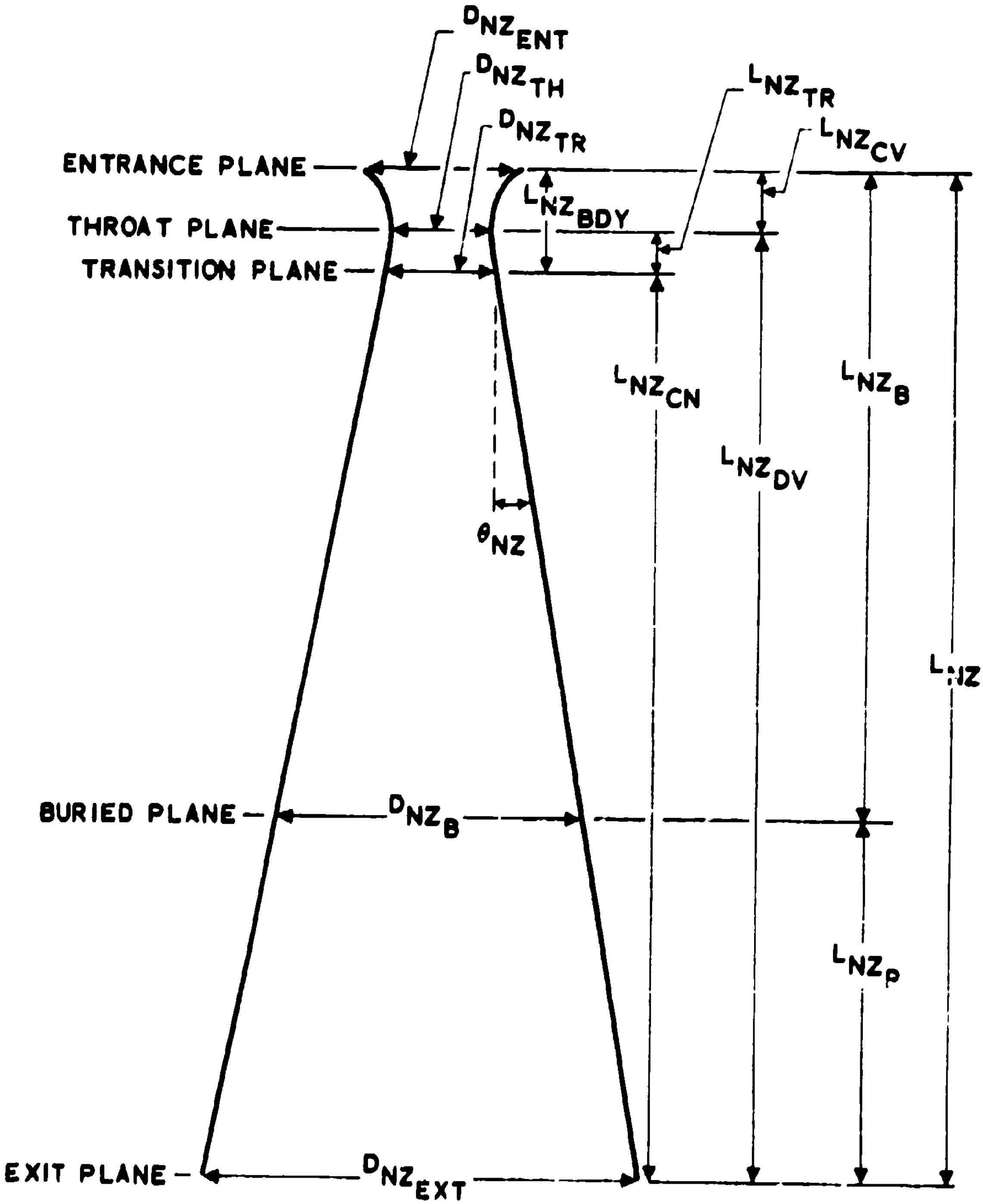

Fig. 170.1-2 Conical Nozzle, Total Geometry

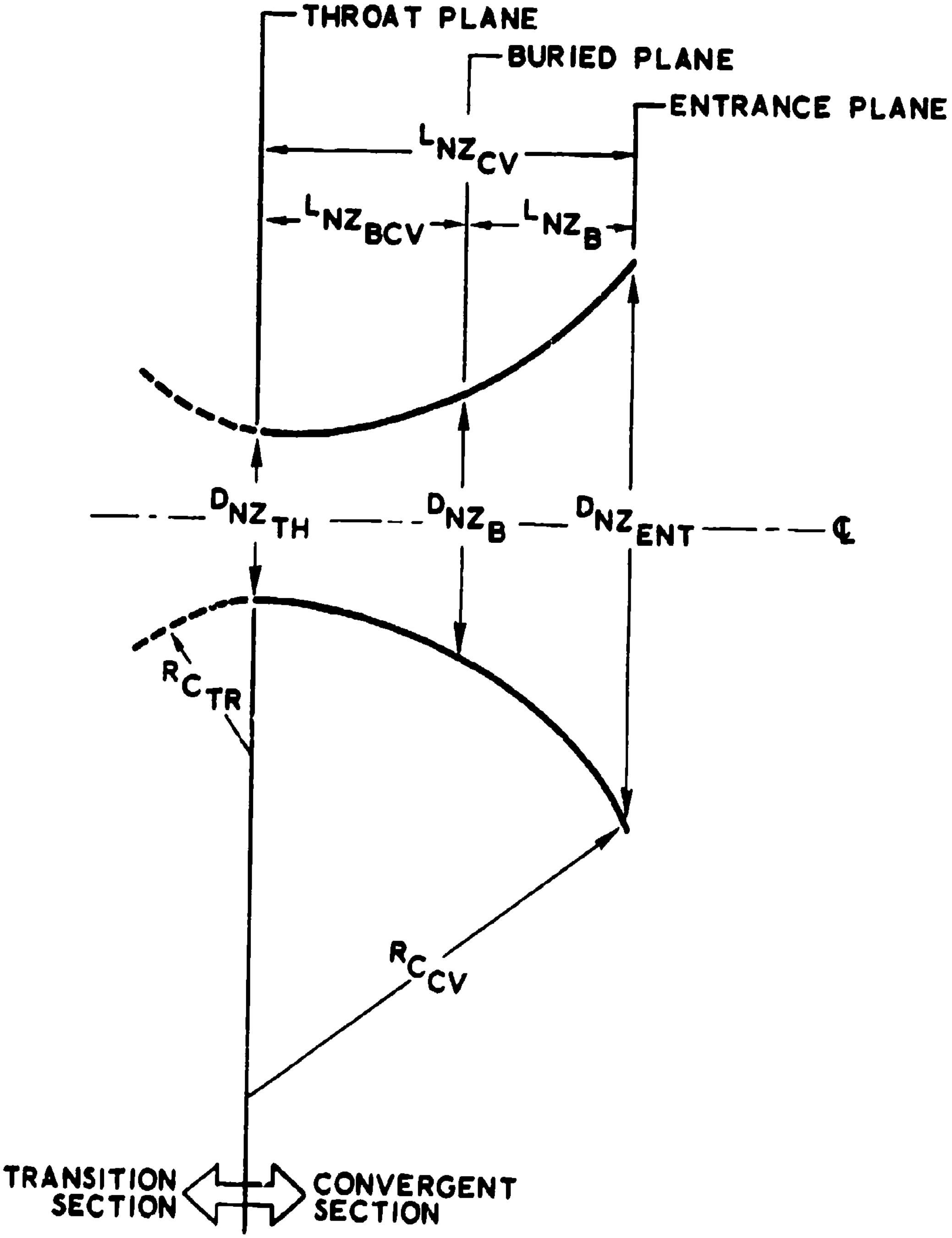

Fig. 170.1-3 Conical Nozzle, Convergent Section

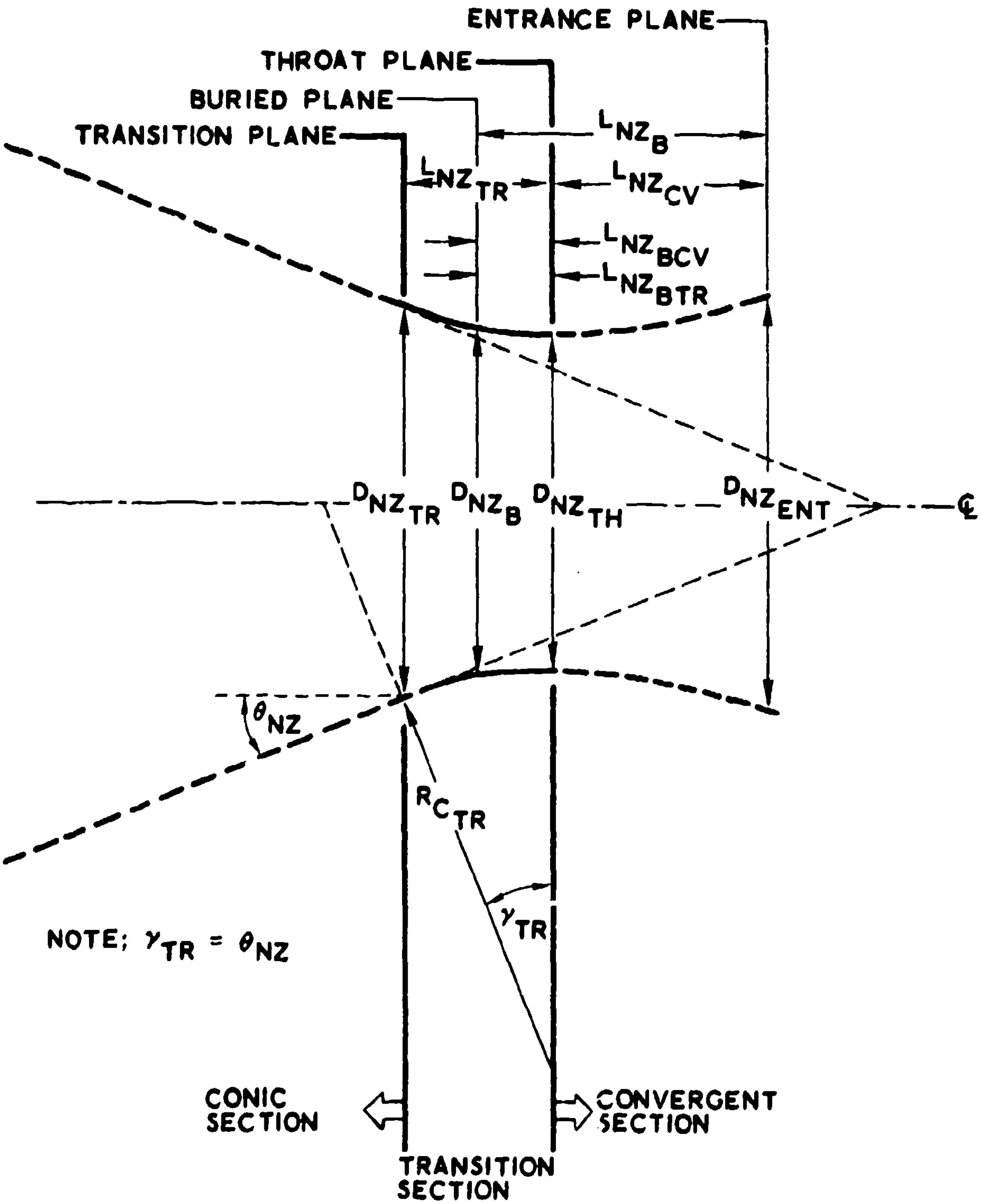

Fig. 170.1-4 Conical Nozzle, Transition Section

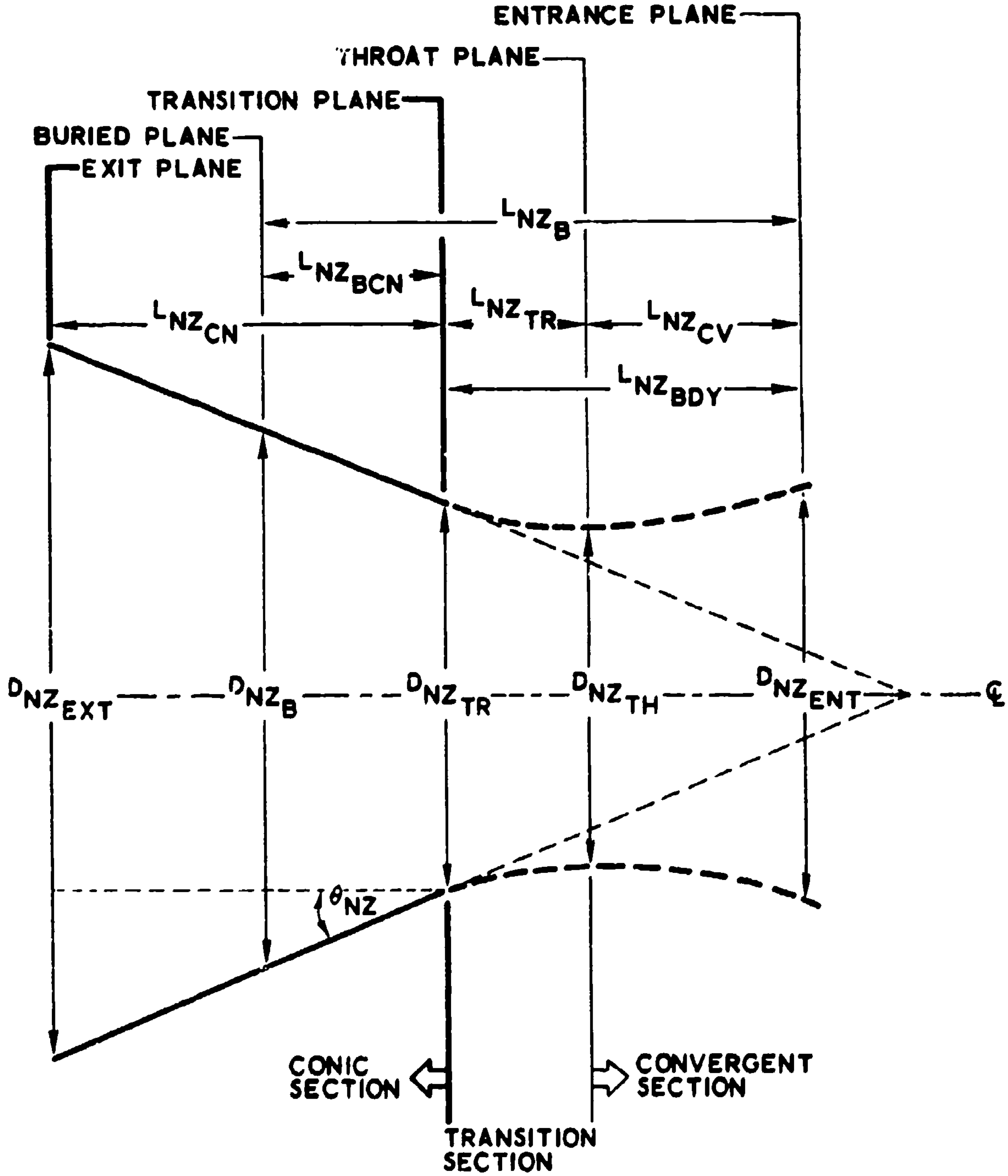

Fig. 170.1-5 Conical Nozzle, Conical Section

INPUT DATA, INTRA-MODEL:

The following data is input directly to this model by the program user. If a value is not input, the preset value is used.

Mnemonic	Symbol	Description; Ext. (Int.) Units	Preset
CNZ1	C_1	Proportionality factor relating convergent nozzle section length to nozzle throat diameter; N. D.	.4
CNZ2	C_2	Proportionality factor relating the radius of curvature of the convergent nozzle section contour to the nozzle throat diameter; N. D.	1
CNZ3	C_3	Proportionality factor relating the radius of curvature of the transition nozzle section contour to the nozzle throat diameter; N. D.	.2
KQDNZB	K_{QDB}	Associative quantity coefficient for QDNZB computation; N. D.	0
KQDNZEN	K_{QDEN}	Associative quantity coefficient for QDNZENT computation; N. D.	0
KQDNZEX	K_{QDEX}	Associative quantity coefficient for QDNZEXT computation; N. D.	0
KQDNZTH	K_{QDTH}	Associative quantity coefficient for QDNZTH computation; N. D.	0
KQLNZB	K_{QLB}	Associative quantity coefficient for QLNZB computation; N. D.	0
KQLNZ	K_{QL}	Associative quantity coefficient for QLNZ computation; N. D.	0

INPUT DATA, INTRA-MODEL (Cont.):

KLNZB	K_{LNZB}	Proportionality factor relating buried nozzle length to total nozzle length;		
		N. D.		0
NZHA	θ_{NZ}	Nozzle half angle;		
		deg	Figs. 2, 4, 5	0
RAEXTTH	ϵ_{NZ}	Nozzle expansion ratio at nozzle exit plane. Ratio of nozzle exit area to nozzle throat area;		
		N. D.		0

INPUT DATA, INTER-MODEL:

This model requires as input certain data which is usually output from a model of the specified model type. If the user has not specified such a source for this data, then it must be input directly with the intra-model input.

Mnemonic	Symbol	Description; Ext. (Int.) Units	Model Type
CVDELV	C*	Delivered characteristic velocity;	
		ft/sec	IBGAS
DWPPMT	$\dot{W}_{PP_{MT}}$	Propellent weight flow;	
		lb/sec	IBPERF
PCHAVG	P_{AVG}	Average chamber pressure;	
		PSIA	IBGAS

OUTPUT DATA:

The following data is output from this model. It is available for use as inter-model input to other models and to print, plot, and optimization routines.

Mnemonic	Symbol	Description; Ext. (Int.) Units	
ANZENT	$A_{NZ_{ENT}}$	Nozzle entrance area;	
		in^2	Eq. 13
ANZEXT	$A_{NZ_{EXT}}$	Nozzle exit area;	
		in^2	Eq. 15

OUTPUT DATA (Cont.):

Mnemonic	Symbol	Description; Ext. (Int.) Units		
ANZTH	$A_{NZ_{TH}}$	Nozzle throat area;		
		in^2		Eq. 1
ANZTR	$A_{NZ_{TR}}$	Nozzle transition area;		
		in^2		Eq. 14
DNZB	D_{NZ_B}	Buried nozzle diameter. Nozzle diameter measured at buried nozzle plane;		
		in	Figs. 3, 4, 5	Eqs. 27, 28, 29
DNZENT	$D_{NZ_{ENT}}$	Nozzle entrance diameter. Diameter of nozzle measured at nozzle entrance plane;		
		in	Fig. 3	Eq. 10
DNZEXT	$D_{NZ_{EXT}}$	Nozzle exit diameter. Diameter of nozzle measured at nozzle exit plane;		
		in	Fig. 5	Eq. 12
DNZTH	$D_{NZ_{TH}}$	Nozzle throat diameter. Diameter of nozzle measured at nozzle throat plane;		
		in	Fig. 2	Eq. 2
DNZTR	$D_{NZ_{TR}}$	Nozzle transition diameter. Diameter of nozzle measured at transition plane separating transition and conic sections;		
		in	Fig. 4	Eq. 11
KDNZENT	K_{DENT}	Proportionality factor relating nozzle entrance diameter to nozzle throat diameter;		
		N. D.		Eq. 3
KDNZTR	K_{DTR}	Proportionality factor relating nozzle transition diameter to nozzle throat diameter;		
		N. D.		Eq. 4
LNZ	L_{NZ}	Total nozzle length. Distance from nozzle entrance plane to nozzle exit plant;		
		in	Fig. 2	Eq. 21

OUTPUT DATA (Cont.):

Mnemonic	Symbol	Description; Ext. (Int.) Units			
LNZB	L_{NZ_B}	Buried nozzle section length. Distance from nozzle entrance plane to nozzle buried plane;	in	Fig. 2	Eq. 22
LNZBCN	$L_{NZ_{BCN}}$	Length buried in conic nozzle section. Distance from nozzle transition plane to nozzle buried plane. (Positive sense towards exit);	in	Fig. 5	Eq. 26
LNZBCV	$L_{NZ_{BCV}}$	Length buried in convergent nozzle section. Distance from nozzle throat plane to nozzle buried plane. (Positive sense towards entrance);	in	Fig. 3	Eq. 24
LNZBDY	$L_{NZ_{BDY}}$	Body nozzle section length. Distance from nozzle entrance plane to nozzle transition plane;	in	Fig. 2	Eq. 19
LNZBTR	$L_{NZ_{BTR}}$	Length buried in transition nozzle section. Distance from nozzle throat plane to nozzle buried plane. (Positive sense towards exit);	in		Eq. 25
LNZCN	$L_{NZ_{CN}}$	Conic nozzle section length. Distance from nozzle transition plane to nozzle exit plane;	in	Fig. 5	Eq. 18
LNZCV	$L_{NZ_{CV}}$	Convergent nozzle section length. Distance from nozzle entrance plane to nozzle throat plane;	in	Fig. 3	Eq. 16
LNZDV	$L_{NZ_{DV}}$	Divergent nozzle section length. Distance from nozzle throat plane to nozzle exit plane;	in	Fig. 2	Eq. 20

OUTPUT DATA (Cont.):

Mnemonic	Symbol	Description; Ext. (Int.) Units		
LNZP	L_{NZ_P}	Protruding nozzle section length. Distance from nozzle buried plane to nozzle exit plane;		
		in	Fig. 2	Eq. 23
LNZTR	$L_{NZ_{TR}}$	Transition nozzle section length. Distance from nozzle throat plane to nozzle transition plane;		
		in	Fig. 4	Eq. 17
QDNZB	Q_{DB}	Associative quantity, buried nozzle diameter. (See DNZB);		
		in		Eq. 30
QDNZENT	Q_{DENT}	Associative quantity, nozzle entrance diameter. (See DNZENT);		
		in		Eq. 31
QDNZEXT	Q_{DEXT}	Associative quantity, nozzle exit diameter. (See DNZEXT);		
		in		Eq. 32
QDNZTH	Q_{DTH}	Associative quantity, nozzle throat diameter. (See DNZTH);		
		in		Eq. 35
QLNZ	Q_L	Associative quantity, total nozzle length. (See LNZ);		
		in		Eq. 33
QLNZB	Q_{LB}	Associative quantity, buried nozzle length. (See LNZB);		
		in		Eq. 34
RATRTH	ϵ_{TR}	Expansion ratio at transition plane. Ratio of nozzle transition area to nozzle throat area;		
		N. D.		Eq. 6

OUTPUT DATA (Cont.):

Mnemonic	Symbol	Description; Ext. (Int.) Units	
RCNZCV	$R_{C_{CV}}$	Radius of curvature, convergent nozzle section contour;	
		in	Eq. 8
RCNZTR	$R_{C_{TR}}$	Radius of curvature, transition nozzle section contour;	
		in	Eq. 9
RDEXTTH	R_{DEXTTH}	Ratio, nozzle exit diameter to nozzle throat diameter;	
		N. D.	Eq. 7
RDTRTH	R_{DTRTH}	Ratio, nozzle transition diameter to nozzle throat diameter;	
		N. D.	Eq. 5
RLNZB	R_{LNZB}	Buried nozzle length ratio. Ratio of buried nozzle section length to total nozzle length;	
		N. D.	Eq. 23-a
RLNZP	R_{LNZP}	Protruding nozzle length ratio. Ratio of protruding nozzle section length to total nozzle length;	
		N. D.	Eq. 23-b

PRINT BLOCK KEY:

Nominally, only those lines with an asterisk to the left of the line number will be printed. By input, any of the lines given below may be printed or suppressed (see the section on output models for the details).

			NOZZLEG	NZGM1	NOZZLE GEOMETRY	
ANZENT	ANZEXT	ANZTH	*1	ANZTR	CNZ1	CNZ2
CNZ3	DNZB	DNZENT	*2	DNZEXT	DNZTH	DNZTR
KDNZENT	KDNZTR	KLNZB	*3	KQDNZB	KQDNZEN	KQDNZEX
KQDNZTH	KQLNZ	KQLNZB	*4	LNZ	LNZB	LNZBCN
LNZBCV	LNZBDY	LNZBTR	*5	LNZCN	LNZCV	LNZDV
LNZP	LNZTR	NZHA	*6	QDNZB	QDNZENT	QDNZEXT
QDNZTH	QLNZ	QLNZB	*7	RAEXTTH	RATRTH	RCNZCV
RCNZTR	RDEXTTH	RLNZB	*8	RLNZP	RDTRTH	
BPCN	BPCV	BPTR	*9	SINNZHA	COSNZHA	TANNZHA

180.1

MODEL TYPE: NOZZLEW (NOZZLE Weight)

MODEL NAME: NZWM1 (Single, Ablative, Parametric Scaling)

DESCRIPTION:

NZWM1 (NoZzle Weight Model number 1) utilizes parametric weight scaling equations to determine the weight of a solid rocket motor fixed or gimballed nozzle. A detailed description of both the equations and parametric scaling rationale may be found in reference 8.

The model is applicable for performance parameters within the following limits

15 < NZHA < 30 deg

300 < PCHAVG < 1000 psia

5 < RAEXTTH < 75

30 < TBPPMT < 140 sec

500 < WPPMT < 2,000,000 lb

where NZHA is associated with the NOZZLEG model type and the remaining quantities are defined in the Input Data, Inter-Model section below.

PROCEDURE:

Prior to entering NZWM1, the models specified by the IBGAS and IBPERF model types have evaluated the gas and performance properties of the propellent, and the model specified by the NOZZLEG model type evaluated the nozzle geometry. The nozzle weight penalty due to gimballed or other thrust vector control systems has been determined by the model specified for the TVCW model type.

The NZWM1 model is then executed and the nozzle weight is evaluated using a parametric weight scaling equation. The expended weights, due to ablation during thrusting, are also computed.

After leaving NZWM1, the remaining component weights of the motor are evaluated. The NZWM1 output data will then be used by the models specified by the SUBSTGW and PROPUL model types to evaluate the substage weights and propulsion characteristics.

EQUATIONS:

Total nozzle weight.

$$W_{NZ} = K_{WNZ}\, K_{TVNZ}\, C_1 \left[\frac{\left(W_{PP} C^*\right)^{C_2} \epsilon^{C_3}}{P_{AVG}^{C_4}\; T_B^{C_5}\; (\tan\theta)^{C_6}} \right]^{C_7} \qquad (1)$$

Total expended nozzle weight component.

$$W_{NZ_X} = K_{WNZX}\, C_8 \left(P_{AVG}\, T_B\right)^{C_9} W_{NZ} \qquad (2)$$

Expended (non-thrusting producing) nozzle weight component.

$$W_{NZ_{XI}} = K_{WNZXI}\, W_{NZ_X} \qquad (3)$$

Expended (thrust producing) nozzle weight component.

$$W_{NZ_{XT}} = 0 \qquad (4)$$

Total non-expended nozzle weight component.

$$W_{NZ_{NX}} = K_{WNZNX} \left(W_{NZ} - W_{NZ_X}\right) \qquad (5)$$

INPUT DATA, INTRA-MODEL:

The following data is input directly to this model by the program user. If a value is not input, the preset value is used.

Mnemonic	Symbol	Description; Ext. (Int.) Units	Preset
CNZW1	C_1	Scaling constant for WNZ computation; N. D.	0.0000772

INPUT DATA, INTRA-MODEL (Cont.):

Mnemonic	Symbol	Description; Ext. (Int.) Units	Preset
CNZW2	C_2	Scaling constant for WNZ computation; N. D.	1.2
CNZW3	C_3	Scaling constant for WNZ computation; N. D.	0.7
CNZW4	C_4	Scaling constant for WNZ computation; N. D.	0.8
CNZW5	C_5	Scaling constant for WNZ computation; N. D.	0.6
CNZW6	C_6	Scaling constant for WNZ computation; N. D.	0.4
CNZW7	C_7	Scaling constant for WNZ computation; N. D.	0.916
CNZW8	C_8	Scaling constant for WNZX computation; N. D.	0.00032
CNZW9	C_9	Scaling constant for WNZX computation; N. D.	0.5
KWNZ	K_{WNZ}	Proportionality factor for total nozzle weight; N. D.	1
KWNZNX	K_{WNZNX}	Proportionality factor for nozzle non-expended weight component; N. D.	1
KWNZX	K_{WNZX}	Proportionality factor for total expended nozzle weight component; N. D.	1
KWNZXI	K_{WNZXI}	Proportionality factor for non-thrust producing component of expended nozzle weight; N. D.	1

INPUT DATA, INTER-MODEL:

This model requires as input certain data which is usually output from a model of the specified model type. If the user has not specified such a source for this data, then it must be input directly with the intra-model input.

Mnemonic	Symbol	Description; Ext. (Int.) Units	Model Type
CVDELV	C^*	Delivered characteristic velocity; ft/sec	IBGAS
KTVNZ	K_{TVNZ}	Thrust vector control factor; N. D.	TVCW
PCHAVG	P_{AVG}	Average chamber pressure; psia	IBGAS
RAEXTTH	ϵ_{NZ}	Nozzle expansion ratio; N. D.	NOZZLEG
TANNZHA	$\tan(\theta)$	Tangent of nozzle half angle; N. D.	NOZZLEG
TBPPMT	T_B	Propellent burn time; sec	IBFERF
WPPMT	W_{PP}	Propellent weight; lb	PROPELW

OUTPUT DATA:

The following data is output from this model. It is available for use as inter-model input to other models and to print, plot, and optimization routines.

Mnemonic	Symbol	Description; Ext. (Int.) Units	
WNZ	W_{NZ}	Total nozzle weight; lb	Eq. 1

OUTPUT DATA (Cont.):

Mnemonic	Symbol	Description; Ext. (Int.) Units	
WNZNX	$W_{NZ_{NX}}$	Total non-expended nozzle weight component; lb	Eq. 5
WNZX	W_{NZ_X}	Total expended nozzle weight component; lb	Eq. 2
WNZXI	$W_{NZ_{XI}}$	Expended (non-thrust producing) nozzle weight component; lb	Eq. 3
WNZXT	$W_{NZ_{XT}}$	Expended (thrust-producing) nozzle weight component; lb	Eq. 4

PRINT BLOCK KEY:

Nominally, only those lines with an asterisk to the left of the line number will be printed. By input, any of the lines given below may be printed or suppressed (see the section on output models for the details).

```
                                  NOZZLEW    NZWM1      NOZZLE WEIGHT
WNZ       WNZNX       WNZX            *1     WNZXI      WNZXT
CNZW1     CNZW2       CNZW3           *2     CNZW4      CNZW5       CNZW6
CNZW7     CNZW8       CNZW9           *3     KWN2       KWNZNX      KWNZX
KWNZXI
```

190.1

MODEL TYPE: PAYLODG (PAYLOaD Geometry)

MODEL NAME: PAGM1 (Single, Simple Payload)

DESCRIPTION:

PAGM1 (PAyload Geometry Model number 1) evaluates the geometry for a simple single payload which may be defined in terms of its length and base diameter. See figure 1 and the figure associated with the model used as the top interstage (INTSTGG model type) for an appreciation of the pertinent geometry.

PROCEDURE:

Prior to entering PAGM1, all of the solid rocket motor substages have been sized.

PAGM1 then determines both the basic payload geometry and the payload requirements for interstage design.

After PAGM1 is executed, the interstages will be sized. The top interstage for the propulsion system will use PAGM1 output, together with the geometry of the top substage in the propulsion system, to determine its design requirements. After all of the interstages, stages, and the propulsion system have been sized, the payload geometry is used for sizing the payload section and shroud.

EQUATIONS:

Total payload length.

$$L_{PA} = L_{PA_{SF}} + L_{PA_B} + L_{PA_{SA}} \tag{1}$$

Payload cross-sectional area.

$$A_{PA} = \left(\frac{\pi}{4}\right) D^2_{PA_A} \tag{2}$$

EQUATIONS (Cont.):

Payload aft diameter for interstage attachment.

$$D_{SS_{ITA}} = D_{PA_A} \tag{3}$$

Length of interstage required for the payload.

$$L_{SS_{ITA}} = L_{PA_{SA}} \tag{4}$$

NOTE: The conical payload is for illustration only. The payload geometry is defined by the center line lengths and D_{PA_A}

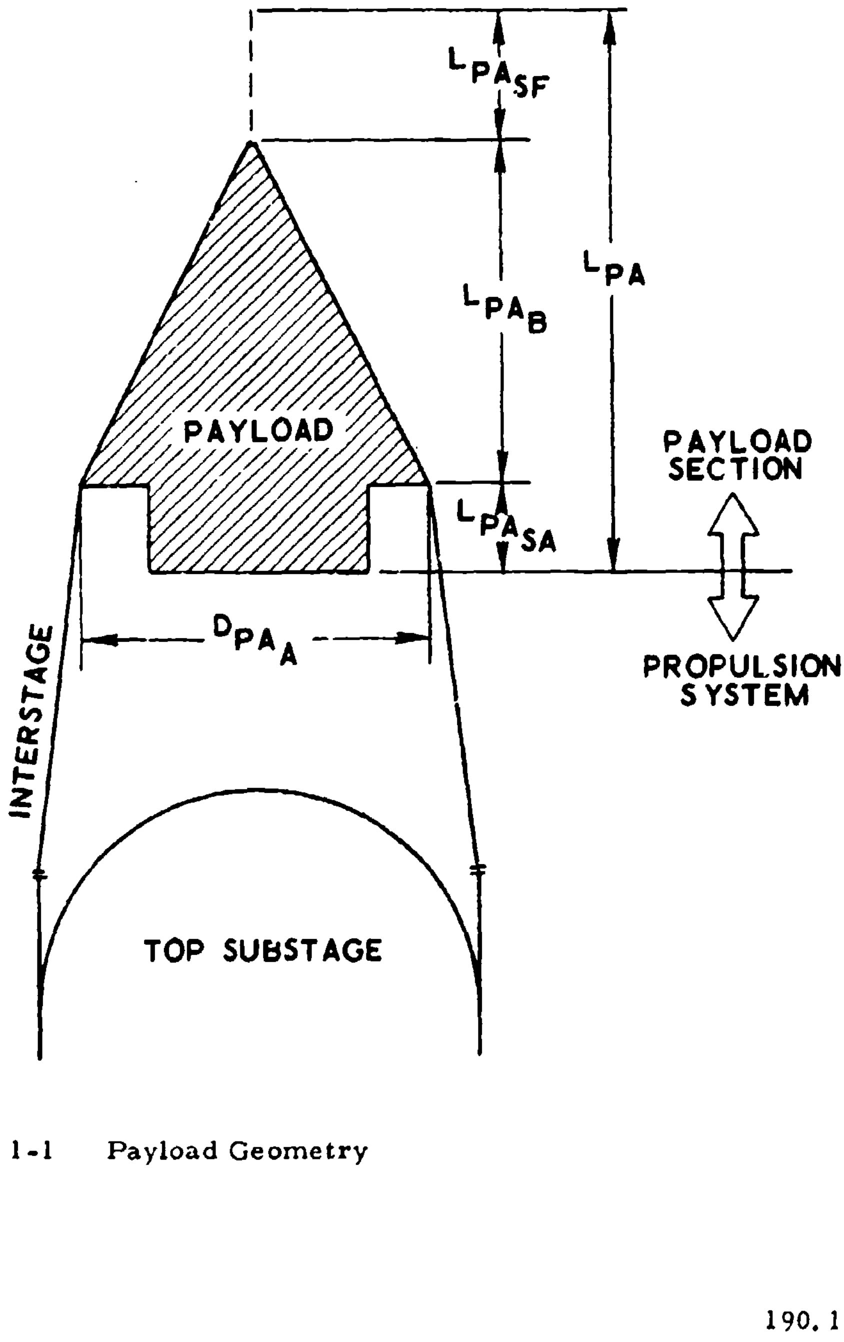

Fig. 190.1-1 Payload Geometry

INPUT DATA, INTRA-MODEL:

The following data is input to this model directly by the program user. If a value is not input, the preset value is used.

Mnemonic	Symbol	Description; Ext. (Int.) Units	Preset
DPAA	D_{PA_A}	Payload base (i.e., aft) diameter, required for defining the aft interstage attachment; in	0
LPAB	L_{PA_B}	Basic payload length component; in	0
LPASA	$L_{PA_{SA}}$	Payload aft spacing distance; in	0
LPASF	$L_{PA_{SF}}$	Payload forward spacing diatance; in	0

INPUT DATA, INTER-MODEL:

This model requires as input certain data which is usually output from a model of the specified model type. If the user has not specified such a source for this data, then it must be input directly with the intra-model input.

Mnemonic	Symbol	Description; Ext. (Int.) Units	Model Type
None			

OUTPUT DATA:

The following data is output from this model. It is available for use as inter-model input to other models and to print, plot, and optimization routines.

Mnemonic	Symbol	Description; Ext. (Int.) Units	
APA	A_{PA}	Payload cross-sectional area; in^2	Eq. 2

OUTPUT DATA (Cont.):

Mnemonic	Symbol	Description; Ext. (Int.) Units	
DSSITA	$D_{SS_{ITA}}$	Payload aft diameter for interstage attachment; in	Eq. 3
LPA	L_{PA}	Total payload length; in	Eq. 1
LSSITA	$L_{SS_{ITA}}$	Length of interstage required for the payload; in	Eq. 4

PRINT BLOCK KEY:

Nominally, only those lines with an asterisk to the left of the line number will be printed. By input, any of the lines given below may be printed or suppressed (see the section on output models for the details).

```
                                     PAYLODG    PAGM1    PAYLOAD GEOMETRY
APA        DPAA        DSSITA             *1    LPAB     LPASA          LPASF
LPA        LSSITA                         *2
```

200.1

MODEL TYPE: PAYLODW (PAYLOaD Weight)

MODEL NAME: PAWM1 (Direct Input)

DESCRIPTION:

PAWM1 (PAyload Weight Model number 1) is a simple payload weight model for which the payload weight is input directly by the program user.

Note that the payload weight does NOT normally include the weight of the shroud, payload adapter, etc.

PROCEDURE:

Prior to entering PAWM1, the substages have been sized and the model specified for the PAYLODG model type has evaluated the payload geometry.

PAWM1 then defines the payload weight.

After leaving PAWM1, the interstages, stages, and propulsion system are sized. The model specified for the PAYSECW model types then uses the payload weight, together with the shroud weight, etc., to determine the payload section weight.

EQUATIONS:

Total payload weight.

$$W_{PA} = K_{WPA} W_{PAYLOD} \tag{1}$$

Total non-expended payload weight component.

$$W_{PA_{NX}} = W_{PA} \tag{2}$$

Total expended payload weight component.

$$W_{PA_X} = 0 \tag{3}$$

EQUATIONS (Cont.):

Expended (thrust producing) payload weight component.

$$W_{PA_{XT}} = 0 \tag{4}$$

Expended (non-thrust producing) payload weight component.

$$W_{PA_{XI}} = 0 \tag{5}$$

INPUT DATA, INTRA-MODEL:

The following data is input to this model directly by the program user. If a value is not input, the preset value is used.

Mnemonic	Symbol	Description; Ext. (Int.) Units	Preset
KWPA	K_{WPA}	Coefficient for WPA computation; N. D.	1
WPAYLOD	W_{PAYLOD}	Payload weight input by user; lb	0

INPUT DATA, INTER-MODEL:

This model requires as input certain data which is usually output from a model of the specified model type. If the user has not specified such a source for this data, then it must be input directly with the intra-model input.

Mnemonic	Symbol	Description; Ext. (Int.) Units	Model Type

None

OUTPUT DATA:

The following data is output from this model. It is available for use as inter-model input to other models and to print, plot, and optimization routines.

OUTPUT DATA (Cont.):

Mnemonic	Symbol	Description; Ext. (Int.) Units	
WPA	W_{PA}	Total payload weight; lb	Eq. 1
WPANX	$W_{PA_{NX}}$	Total non-expended payload weight component; lb	Eq. 2
WPAX	W_{PA_X}	Total expended payload weight component; lb	Eq. 3
WPAXI	$W_{PA_{XI}}$	Expended (non-thrust producing) payload weight component; lb	Eq. 5
WPAXT	$W_{PA_{XT}}$	Expended (thrust producing) payload weight component; lb	Eq. 4

PRINT BLOCK KEY:

Nominally, only those lines with an asterisk to the left of the line number will be printed. By input, any of the lines given below may be printed or suppressed (see the section on output models for the details).

```
                                         PAYLODW    PAWM1      PAYLOAD WEIGHT
WPA       WPANX       WI·AX                   *1    WPAXI      WPAXT
KWPA      WPAYLOD                             *2
```

210.1

MODEL TYPE: PROPUL (PROPULsion Characteristics)

MODEL NAME: PCM1 (Constant Thrust, Single Engine)

DESCRIPTION:

PCM1 (Propulsion Characteristics Model number 1) evaluates the thrust and weight flow breakdown for a single constant thrust solid rocket engine. The engine is comprised of the following subsystems:

Motor

Nozzle

In addition to the thrust derived from the propellent, thrust components associated with the following subsystem expended weight components are evaluated.

Internal insulation

Thrust vector control

Nozzle

PROCEDURE:

Prior to executing PCM1, the model specified for the IBPERF model type has determined the propellent weight flow, burn time and specific impulse. The model specified for the NOZZLEG model type has determined the nozzle exit area and the models specified for the NOZZLEW and MOTORW model types have broken down the principle subsystem weight into expended components.

PCM1 is then executed and the expended subsystem weights are used to determine the inert and thrust producing weight flow components. These weight flow components are then used, together with the required specific impulses, to determine the vacuum thrust components. Finally, the vacuum thrust components are summed and the total engine vacuum thrust and sea-level thrust degradation are evaluated.

PROCEDURE (Cont.):

After PCM1 is executed, the remaining substages are sized and the propulsion characteristics for each engine within the vehicle are evaluated. After the entire vehicle is sized, the PCM1 output data is input to the applicable weight and propulsion model for the mission simulation. See REMARKS.

EQUATIONS:

Expended motor weight flow, excludes propellent.

$$\dot{W}_{MT_X} = \frac{W_{MT_X}}{T_B} \tag{1}$$

Expended (thrust producing) motor weight flow component, excludes propellent.

$$\dot{W}_{MT_{XT}} = \frac{W_{MT_{XT}}}{T_B} \tag{2}$$

Expended (non-thrust producing) motor weight flow component.

$$\dot{W}_{MT_{XI}} = \frac{W_{MT_{XI}}}{T_B} \tag{3}$$

Expended nozzle weight flow.

$$\dot{W}_{NZ_X} = \frac{W_{NZ_X}}{T_B} \tag{4}$$

Expended (thrust producing) nozzle weight flow component.

$$\dot{W}_{NZ_{XT}} = \frac{W_{NZ_{XT}}}{T_B} \tag{5}$$

Expended (non-thrust producing) nozzle weight flow component.

$$\dot{W}_{NZ_{XI}} = \frac{W_{NZ_{XI}}}{T_B} \tag{6}$$

EQUATIONS (Cont.):

Weight flow associated with expended (thrust producing) internal insulation.

$$\dot{W}_{IN_{XT}} = \frac{W_{IN_{XT}}}{T_B} \tag{7}$$

Weight flow associated with expended (thrust producing) thrust vector control system material.

$$\dot{W}_{TV_{XT}} = \frac{W_{TV_{XT}}}{T_B} \tag{8}$$

Thrust producing engine weight flow component. (Includes propellent);

$$\dot{W}_{EN_T} = K_{DWENT} (\dot{W}_{PP} + \dot{W}_{MT_{XT}} + \dot{W}_{NZ_{XT}}) \tag{9}$$

Inert (non-thrust producing) engine weight flow component.

$$W_{EN_I} = K_{DWENI} (\dot{W}_{MT_{XI}} + \dot{W}_{NZ_{XI}}) \tag{10}$$

Total engine weight flow.

$$\dot{W}_{EN} = K_{DWEN} (\dot{W}_{EN_T} + \dot{W}_{EN_I}) \tag{11}$$

Vacuum thrust component associated with the propellent.

$$F_{V_{PP}} = K_{FVPP} I_{SP_{VD}} \dot{W}_{PP} \tag{12}$$

Vacuum thrust component associated with expended (thrust producing) internal insulation.

$$F_{V_{IN}} = K_{FVIN} I_{SP_{IN}} \dot{W}_{IN_{XT}} \tag{13}$$

EQUATIONS (Cont.):

Vacuum thrust component associated with expended (thrust producing) thrust vector control material.

$$F_{V_{TV}} = K_{FVTV}\, I_{SP_{TV}}\, \dot{W}_{TV_{XT}} \tag{14}$$

Vacuum thrust component associated with expended (thrust producing) nozzle material.

$$F_{V_{NZ}} = K_{FVNZ}\, I_{SP_{NZ}}\, \dot{W}_{NZ_{XT}} \tag{15}$$

Engine vacuum thrust.

$$F_{V_{EN}} = K_{FVEN}\,(F_{V_{PP}} + F_{V_{IN}} + F_{V_{TV}} + F_{V_{NZ}}) \tag{16}$$

Engine thrust degradation due to atmospheric pressure.

$$\Delta F_{EN} = K_{DELFEN}\, C_1\, A_{NZ_{EXT}} \tag{17}$$

INPUT DATA, INTRA-MODEL:

The following data is input to this model directly by the program user. If a value is not input, the preset value is used.

Mnemonic	Symbol	Description; Ext. (Int.) Units	Preset
CPC1	C_1	Constant for DELFEN computation. Corresponds to atmospheric sea-level pressure; $lb/(in^2)$	14.695972
KDELFEN	K_{DELFEN}	Coefficient for DELFEN computation; N. D.	1
KDWEN	K_{DWEN}	Coefficient for DWEN computation; N. D.	1

INPUT DATA, INTRA-MODEL (Cont.):

Mnemonic	Symbol	Description; Ext. (Int.) Units	Preset
KDWENI	K_{DWENI}	Coefficient for DWENI computation; N. D.	1
KDWENT	K_{DWENT}	Coefficient for DWENT computation; N. D.	1
KFVEN	K_{FVEN}	Coefficient for FVEN computation; N. D	1
KFVIN	K_{FVIN}	Coefficient for FVIN computation; N. D.	1
KFVNZ	K_{FVNZ}	Coefficient for FVNZ computation; N. D.	1
KFVPP	K_{FVPP}	Coefficient for FVPP computation; N. D.	1
KFVTV	K_{FVTV}	Coefficient for FVTV computation; N. D.	1
ISPIN	$I_{SP_{IN}}$	Specific impulse of expended (thrust producing) internal insulation material; sec	0
ISPNZ	$I_{SP_{NZ}}$	Specific impulse of expended (thrust producing) nozzle material; sec	0
ISPTV	$I_{SP_{TV}}$	Specific impulse of expended (thrust producing) thrust vector control material; sec	0

INPUT DATA, INTER-MODEL:

This model requires as input certain data which is usually output from a model of the specified model type. If the user has not specified such a source for this data, then it must be input directly with the intra-model input.

Mnemonic	Symbol	Description; Ext. (Int.) Units	Model Type
ANZEXT	$A_{NZ_{EXT}}$	Nozzle exit area; in^2	NOZZLEG
DWPPMT	$\dot{W}_{PP_{MT}}$	Propellent weight flow; lb/sec	IBPERF
ISPVD	$I_{SP_{VD}}$	Vacuum delivered specific impulse; sec	IBPERF
TBPPMT	T_B	Propellent burn time; sec	IBPERF
WINXT	$W_{IN_{XT}}$	Expended (thrust producing) internal insulation weight component; lb	INTINSW
WMTX	W_{MT_X}	Total expended motor weight component; lb	MOTORW
WMTXI	$W_{MT_{XI}}$	Expended (non-thrust producing) motor weight component; lb	MOTORW
WMTXT	$W_{MT_{XT}}$	Expended (thrust producing) motor weight component; lb	MOTORW
WNZX	W_{NZ_X}	Total expended nozzle weight component; lb	NOZZLEW
WNZXI	$W_{NZ_{XI}}$	Expended (non-thrust producing) nozzle weight component; lb	NOZZLEW

INPUT DATA, INTER-MODEL (Cont.):

Mnemonic	Symbol	Description; Ext. (Int.) Units	Model Type
WNZXT	$W_{NZ_{XT}}$	Expended (thrust producing) nozzle weight component; lb	NOZZLEW
$W_{TV_{XT}}$	$W_{TV_{XT}}$	Expended (thrust producing) thrust vector control weight component; lb	TVCW

OUTPUT DATA:

The following data is output from this model. It is available for use as inter-model input to other models and to print, plot, and optimization routines.

Mnemonic	Symbol	Description; Ext. (Int.) Units	
DELFEN	ΔF_{EN}	Engine sea-level thrust degradation. DELFEN corresponds to DELF in the trajectory simulation models; lb	Eq. 17
DWEN	$\dot{W}_{EN}$	Total engine weight flow. Includes propellent, motor, and nozzle weight flow; lb/sec	Eq. 11
DWENI	$\dot{W}_{EN_I}$	Inert (non-thrust producing) engine weight flow component (includes motor and nozzle); lb/sec	Eq. 10
DWENT	$\dot{W}_{EN_T}$	Thrust producing engine weight flow component. (Includes propellent, motor, and nozzle.) DWENT corresponds to DWVAC in the trajectory simulation models; lb/sec	Eq. 9
DWINXT	$\dot{W}_{IN_{XT}}$	Motor weight flow associated with expended (thrust producing) internal insulation material; lb/sec	Eq. 7

OUTPUT DATA (Cont.):

Mnemonic	Symbol	Description; Ext. (Int.) Units	
DWMTX	$\dot{W}_{MT_X}$	Expended motor weight flow. Excludes propellent and nozzle;	
		lb/sec	Eq. 1
DWMTXI	$\dot{W}_{MT_{XI}}$	Expended (non-thrust producing) motor weight flow component, excludes nozzle;	
		lb/sec	Eq. 3
DWMTXT	$\dot{W}_{MT_{XT}}$	Expended (thrust producing) motor weight flow component. Excludes propellent and nozzle;	
		lb/sec	Eq. 2
DWNZX	$\dot{W}_{NZ_X}$	Expended nozzle weight flow;	
		lb/sec	Eq. 4
DWNZXI	$\dot{W}_{NZ_{XI}}$	Expended (non-thrust producing) nozzle weight flow component;	
		lb/sec	Eq. 6
DWNZXT	$\dot{W}_{NZ_{XT}}$	Expended (thrust producing) nozzle weight flow component;	
		lb/sec	Eq. 5
DWTVXT	$\dot{W}_{TV_{XT}}$	Motor weight flow associated with expended (thrust producing) thrust vector control system material;	
		lb/sec	Eq. 8
FVEN	$F_{V_{EN}}$	Total engine vacuum thrust. FVEN corresponds to FVAC in the trajectory simulation models;	
		lb	Eq. 16
FVIN	$F_{V_{IN}}$	Vacuum thrust component associated with the expended (thrust producing) internal insulation material;	
		lb	Eq. 13

OUTPUT DATA (Cont.):

Mnemonic	Symbol	Description; Ext. (Int.) Units
FVNZ	$F_{V_{NZ}}$	Vacuum thrust component associated with the expended (thrust producing) nozzle material. Note that this is not associated with the nozzle half angle divergence loss;
		lb Eq. 15
FVPP	$F_{V_{PP}}$	Vacuum thrust component associated with the propellent;
		lb
FVTV	$F_{V_{TV}}$	Vacuum thrust component associated with the expended (thrust producing) thrust vector control system material;
		lb Eq. 14

PRINT BLOCK KEY:

Nominally, only those lines with an asterisk to the left of the line number will be printed. By input, any of the lines given below may be printed or suppressed (see the section on output models for the details).

			PROFUL	PCM1	PROPULSION	CHARACTERISTICS
CPC1	DELFEN	DWEN	*1	DWENI	DWENT	DWINXT
DWMTX	DWMTXI	DWMTXT	*2	DWNZX	DWNZXI	DWNZXT
DWTVXT	FVEN	FVIN	*3	FVNZ	FVPP	FVTV
KDELFEN	KDWEN	KDWENI	*4	KDWENT	KFVEN	KFVIN
KFVNZ	KFVPF	KFVTV	*5	ISPIN	ISPNZ	
ISPTV			*6			

220.1

MODEL TYPE: PAYSECG (PAYload SECtion Geometry)

MODEL NAME: PLGM1 (Single Payload, No Shroud Geometry)

DESCRIPTION:

PLGM1 (PayLoad section Geometry Model number 1) evaluates the geometry for a simple payload section comprised of a single payload without shroud geometry. Although provision is made for defining a payload section length bias, Intra-Model Input is not normally required for this model. See figure 1 and the figures associated with the payload model utilized (PAYLODG model type) for an appreciation of the payload section geometry.

Note that this model is not applicable if a shroud geometry model (see SHROUDG model type) is utilized. However, this model may be used if a non-geometry dependent shroud weight model (see SHROUDW model type) is used.

PROCEDURE:

Prior to entering PLGM1, all vehicle subsystems within the propulsion system have been sized and the model specified for the PAYLODG model type has determined the payload geometry.

PLGM1 then uses the payload geometry to determine the payload section geometry.

After PLGM1 is executed, the payload section weight will be determined. The total vehicle geometry is then evaluated using the payload section geometry and propulsion system geometry.

EQUATIONS:

Payload section length. Figure 1

$$L_{PL} = L_{PA} + L_{PL_{SF}} \tag{1}$$

EQUATIONS (Cont.):

Payload section diameter. Figure 1

$$D_{PL} = D_{PA_A} \tag{2}$$

Payload section cross-sectional area.

$$A_{PL} = \left(\frac{\pi}{4}\right) D_{PL}^2 \tag{3}$$

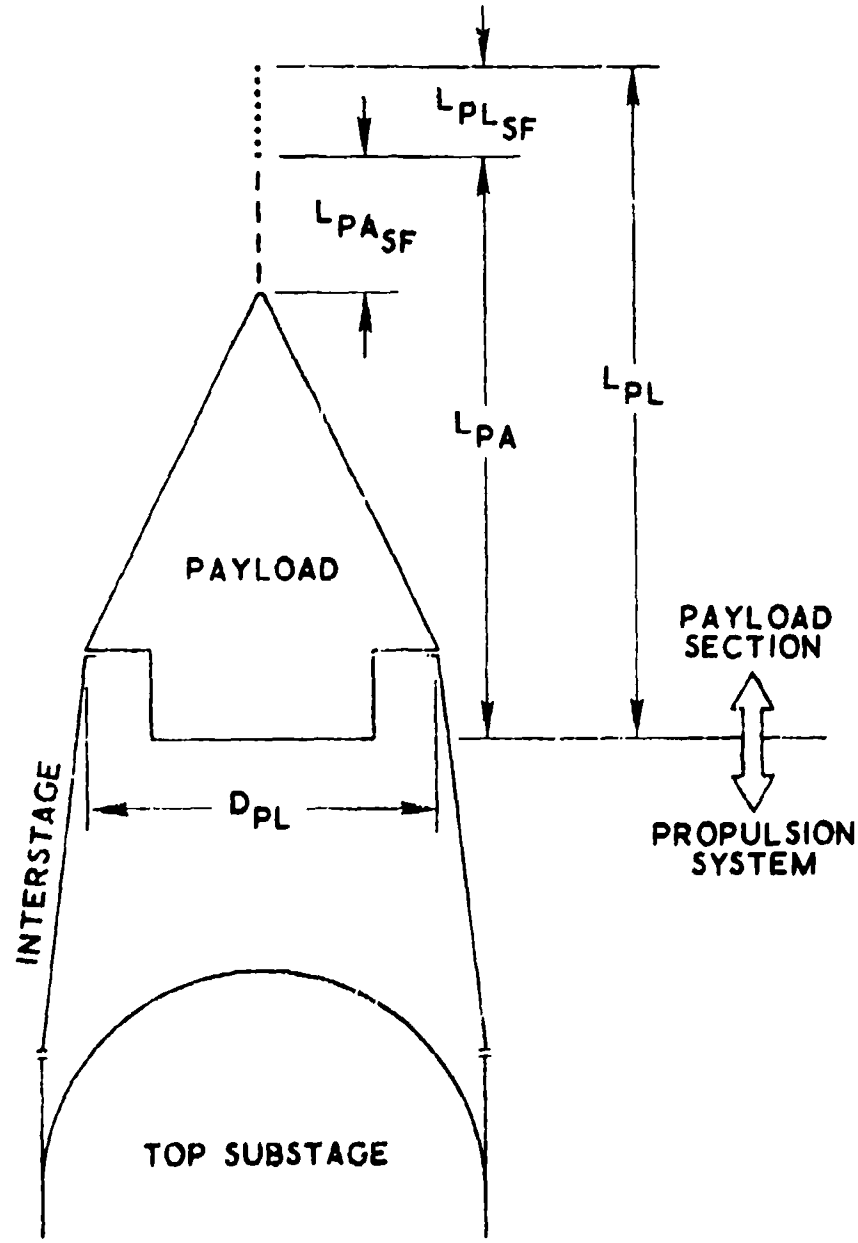

Fig. 220.1-1 Payload Section Geometry

INPUT DATA, INTRA-MODEL:

The following data is input to this model directly by the program user. If a value is not input, the preset value is used.

Mnemonic	Symbol	Description ; Ext. (Int.) Units		Preset
LPLSF	$L_{PL_{SF}}$	Payload section forward spacing distance; in	Fig. 1	0

INPUT DATA, INTER-MODEL:

This model requires as input certain data which is usually output from a model of the specified model type. If the user has not specified such a source for this data, then it must be input directly with the intra-model input.

Mnemonic	Symbol	Description; Ext. (Int.) Units		Model Type
DPAA	D_{PA_A}	Payload aft diameter; in		PAYLODG
LPA	L_{PA}	Total payload length; in	Fig. 1	PAYLODG

OUTPUT DATA:

The following data is output from this model. It is available for use as inter-model input to other models and to print, plot, and optimization routines.

Mnemonic	Symbol	Description; Ext. (Int.) Units	
APL	A_{PL}	Payload section cross-sectional area; in	Eq. 3
DPL	D_{PL}	Payload section diameter at interstage attachment; in	Eq. 2
LPL	L_{PL}	Payload section length; in	Eq. 1

PRINT BLOCK KEY:

Nominally, only those lines with an asterisk to the left of the line number will be printed. By input, any of the lines given below may be printed or suppressed (see the section on output models for the details).

```
                                   PAYSECG    PLGM1     PAYLOAD SECTION GEOMETRY
APL         DPL          LPL            *1    LPLSF
```

230.1

MODEL TYPE: PAYSECW (PAYload SECtion Weight)

MODEL NAME: PLWM1 (Single Payload, no Shroud)

DESCRIPTION:

PLWM1 (PayLoad section Weight Model number 1) is a weight synthesis model which evaluates the weight breakdown for a simple payload section comprised of a single payload without a shroud.

PROCEDURE:

Prior to entering PLWM1, all vehicle subsystems within the propulsion system have been sized and the model specified for the PAYLODW model type has evaluated the payload weight breakdown.

PLWM1 uses the payload weight breakdown to evaluate the payload section weight breakdown.

After PLWM1 is executed, the payload section weight breakdown, together with the propulsion system weight breakdown, will be utilized by the model specified for the VEHW model type to determine vehicle weight quantities.

EQUATIONS:

Total payload section weight.

$$W_{PL} = K_{WPL} W_{PA} \tag{1}$$

Total non-expended payload section weight component.

$$W_{PL_{NX}} = K_{WPLNX} W_{PA_{NX}} \tag{2}$$

Total expended payload section weight component.

$$W_{PL_X} = K_{WPLX} W_{PA_X} \tag{3}$$

EQUATIONS (Cont.):

Expended (non-thrust producing) payload section weight component.

$$W_{PL_{XI}} = K_{WPLXI} W_{PA_{XI}} \quad (4)$$

Expended (thrust producing) payload section weight component.

$$W_{PL_{XT}} = K_{WPLXT} W_{PA_{XT}} \quad (5)$$

INPUT DATA, INTRA-MODEL:

The following data is input to this model directly by the program user. If a value is not input, the preset value is used.

Mnemonic	Symbol	Description; Ext. (Int.) Units	Preset
KWPL	K_{WPL}	Coefficient for WPL computation; N. D.	1
KWPLNX	K_{WPLNX}	Coefficient for WPLNX computation; N. D	1
KWPLX	K_{WPLX}	Coefficient for WPLX computation; N. D.	1
KWPLXI	K_{WPLXI}	Coefficient for WPLXI computation; N. D.	1
KWPLXT	K_{WPLXT}	Coefficient for WPLXT computation; N. D.	1

INPUT DATA, INTER-MODEL:

This model requires as input certain data which is usually output from a model of the specified model type. If the user has not specified such a source for this data, then it must be input directly with the intra-model input.

INPUT DATA, INTER-MODEL (Cont.):

Mnemonic	Symbol	Description; Ext. (Int.) Units	Model Type
WPA	W_{PA}	Total payload weight; lb	PAYLODW
WPANX	$W_{PA_{NX}}$	Total non-expended payload weight component; lb	PAYLODW
WPAX	W_{PA_X}	Total expended payload weight component; lb	PAYLODW
WPAXI	$W_{PA_{XI}}$	Expended (non-thrust producing) payload weight component; lb	PAYLODW
WPAXT	$W_{PA_{XT}}$	Expended (thrust producing) payload weight component; lb	PAYLODW

OUTPUT DATA:

The following data is output from this model. It is available for use as inter-model input to other models and to print, plot, and optimization routines.

Mnemonic	Symbol	Description; Ext. (Int.) Units	
WPL	W_{PL}	Total payload section weight; lb	Eq. 1
WPLNX	$W_{PL_{NX}}$	Total non-expended payload section weight component; lb	Eq. 2
WPLX	W_{PL_X}	Total expended payload section weight component; lb	Eq. 3

OUTPUT DATA (Cont.):

Mnemonic	Symbol	Description; Ext. (Int.) Units	
WPLXI	$W_{PL_{XI}}$	Expended (non-thrust producing) payload section weight component;	
		lb	Eq. 4
WPLXT	$W_{PL_{XT}}$	Expended (thrust producing) payload section weight component;	
		lb	Eq. 5

PRINT BLOCK KEY:

Nominally, only those lines with an asterisk to the left of the line number will be printed. By input, any of the lines given below may be printed or suppressed (see the section on output models for the details).

			PAYSECW	PLWM1	PAYLOAD SECTION WEIGHT
WPL	WPLNX	WPLX	*1	WPLXI	WPLXT
KWPL	KWPLNX	KWPLX	*2	KWPLXI	KWPLXT

230.2

MODEL TYPE: PAYSECW (PAYload SECtion Weight)

MODEL NAME: PLWM2 (Single payload, shroud)

DESCRIPTION:

PLWM2 (PayLoad section Weight Model number 2) is a weight synthesis model which evaluates the payload section weight breakdown. The model is applicable for a payload section comprised of the following subsystem:

Payload

Shroud

PROCEDURE:

Prior to entering PLWM2, all vehicle subsystems within the propulsion system have been sized and the models specified for the PAYLODW and SHROUDW model types have evaluated the payload and shroud weight breakdown.

PLWM2 uses these payload and shroud weights to evaluate the payload section weight breakdown.

After PLWM2 is executed, the payload section weight breakdown, together with the propulsion system weight breakdown, will be utilized by the model specified for the VEHW model type to determine vehicle weight quantities.

EQUATIONS:

Total payload section weight.

$$W_{PL} = K_{WPL}\left(W_{PA} + W_{SH}\right) \tag{1}$$

Total non-expended payload section weight component.

$$W_{PL_{NX}} = K_{WPLNX}\left(W_{PA_{NX}} + W_{SH_{NX}}\right) \tag{2}$$

EQUATIONS (Cont.):

Total expended payload section weight component.

$$W_{PL_X} = K_{WPLX}\left(W_{PA_X} + W_{SH_X}\right) \tag{3}$$

Expended (non-thrust producing) payload section weight component.

$$W_{PL_{XI}} = K_{WPLXI}\left(W_{PA_{XI}} + W_{SH_{XI}}\right) \tag{4}$$

Expended (thrust producing) payload section weight component.

$$W_{PL_{XT}} = K_{WPLXT}\left(W_{PA_{XT}} + W_{SH_{XT}}\right) \tag{5}$$

INPUT DATA, INTRA-MODEL:

The following data is input to this model directly by the program user. If a value is not input, the preset value is used.

Mnemonic	Symbol	Description; Ext. (Int.) Units	Preset
KWPL	K_{WPL}	Coefficient for WPL computation; N. D.	1
KWPLNX	K_{WPLNX}	Coefficient for WPLNX computation; N. D.	1
KWPLX	K_{WPLX}	Coefficient for WPLX computation; N. D.	1
KWPLXI	K_{WPLXI}	Coefficient for WPLXI computation; N. D.	1
KWPLXT	K_{WPLXT}	Coefficient for WPLXT computation; N. D.	1

INPUT DATA, INTER-MODEL:

This model requires as input certain data which is usually output from a model of the specified model type. If the user has not specified such a source for this data, then it must be input directly with the intra-model input.

Mnemonic	Symbol	Description; Ext. (Int.) Units	Model Type
WPA	W_{PA}	Total payload weight; lb	PAYLODW
WPANX	$W_{PA_{NX}}$	Total non-expended payload weight component; lb	PAYLODW
WPAX	$W_{PA_{X}}$	Total expended payload weight component; lb	PAYLODW
WPAXI	$W_{PA_{XI}}$	Expended (non-thrust producing) payload weight component; lb	PAYLODW
WPAXT	$W_{PA_{XT}}$	Expended (thrust producing) payload weight component; lb	PAYLODW
WSH	W_{SH}	Total shroud weight; lb	SHROUDW
WSHNX	$W_{SH_{NX}}$	Total non-expended shroud weight component; lb	SHROUDW
WSHX	$W_{SH_{X}}$	Total expended shroud weight component; lb	SHROUDW
WSHXI	$W_{SH_{XI}}$	Expended (non-thrust producing) shroud weight component; lb	SHROUDW
WSHXT	$W_{SH_{XT}}$	Expended (thrust producing) shroud weight component; lb	SHROUDW

OUTPUT DATA:

The following data is output from this model. It is available for use as inter-model input to other models and to print, plot, and optimization routines.

Mnemonic	Symbol	Description; Ext. (Int.) Units	
WPL	W_{PL}	Total payload section weight. Includes payload and shroud; lb	Eq. 1
WPLNX	$W_{PL_{NX}}$	Total non-expended payload section weight component. Includes payload and shroud; lb	Eq. 2
WPLX	W_{PL_X}	Total expended payload section weight component. Includes payload and shroud; lb	Eq. 3
WPLXI	$W_{PL_{XI}}$	Expended (non-thrust producing) payload section weight component. Includes payload and shroud; lb	Eq. 4
WPLXT	$W_{PL_{XT}}$	Expended (thrust producing) payload section weight component. Includes payload and shroud; lb	Eq. 5

PRINT BLOCK KEY:

Nominally, only those lines with an asterisk to the left of the line number will be printed. By input, any of the lines given below may be printed or suppressed (see the section on output models for the details).

			PAYSECW	PLWM2	PAYLOAD SECTION WEIGHT
WPL	WPLNX	WPLX	*1	WPLXI	WPLXT
KWPL	KWPLNX	KWPLX	*2	KWPLXI	KWPLXT

240.1

MODEL TYPE: PROPELW (PROPELlent Weight)

MODEL NAME: PPWM1 (Direct input of propellent weights)

DESCRIPTION:

PPWM1 (ProPellent Weight Model number 1) determines the basic propellent properties (weight, volume, density) of a solid rocket motor for which the propellent weight is specified directly.

EQUATIONS:

Propellent volume.

$$V_{PP_{MT}} = \frac{W_{PP_{MT}}}{\rho_{PP_{MT}}} \tag{1}$$

INPUT DATA, INTRA-MODEL:

The following data is input directly to this model by the program user. If a value is not input, the preset value is used.

Mnemonic	Symbol	Description; Ext. (Int.) Units	Preset
RHOPPMT	$\rho_{PP_{MT}}$	Propellent density; lb/in^3	0
WPPMT	$W_{PP_{MT}}$	Propellent weight; lb	0

INPUT DATA, INTER-MODEL:

None

OUTPUT DATA:

The following data is output from this model. It is available for use as inter-model input to other models and to print, plot, and optimization routines.

Mnemonic	Symbol	Description; Ext. (Int.) Units
VPPMT	$V_{PP_{MT}}$	Propellent volume; in^3

PRINT BLOCK KEY:

Nominally, only those lines with an asterisk to the left of the line number will be printed. By input, any of the lines given below may be printed or suppressed (see the section on output models for the details).

```
                                    PROPELW    PPWM1       PROPELLENT WEIGHT
WPPMT      RHOPPMT      VPPMT           *1
```

250.1

MODEL TYPE: PROSYSG (PROpulsion SYStem Geometry)

MODEL NAME: PSGM1 (Sequential Stages)

DESCRIPTION:

PSGM1 (Propulsion System Geometry Model number 1) evaluates the geometry for a propulsion system comprised of sequential stages. See figure 1 for an illustration of the geometry associated with a typical propulsion system.

PROCEDURE:

Prior to entering PSGM1, all of the stages have been sized and the models specified for the STAGEG model types have determined the stage lengths for all stages comprising this propulsion system.

PSGM1 then sums these stage lengths and determines the total propulsion system length.

After PSGM1 has determined the propulsion system geometry, the propulsion system weight is evaluated. After all of the propulsion systems have been sized, the model specified for the VEHG model type will use the propulsion system geometry, together with the payload section geometry, to determine the total vehicle geometry. After the total vehicle geometry is evaluated, a final pass is made through all of the models and any remaining quantities dependent upon the total propulsion system length are evaluated.

EQUATIONS:

Total propulsion system length.

$$L_{PS} = \Sigma L_{SG} \qquad (1)$$

Where the summation includes all stages within the propulsion system.

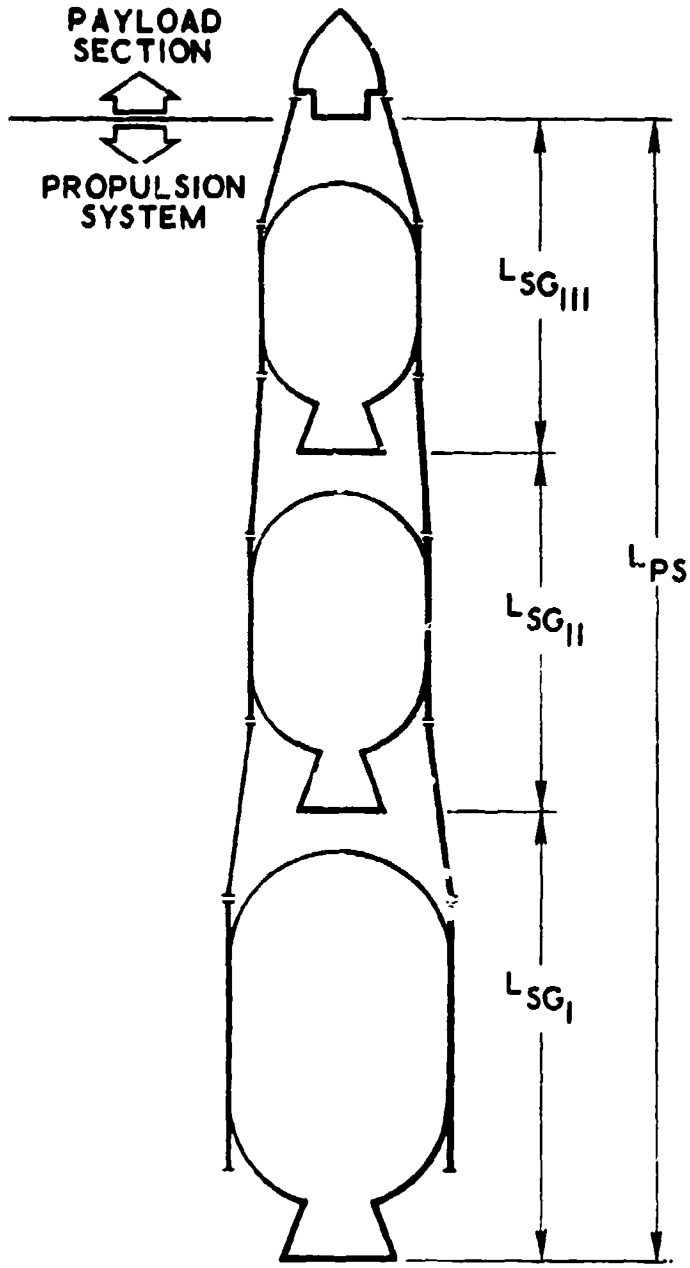

Fig. 250.1-1 Typical Three Stage Boost Vehicle

INPUT DATA, INTRA-MODEL:

The following data is input to this model directly by the program user. If a value is not input, the preset value is used.

Mnemonic	Symbol	Description; Ext. (Int.) Units	Preset
None			

INPUT DATA, INTER-MODEL:

This model requires as input certain data which is usually output from a model of the specified model type. If the user has not specified such a source for this data, then it must be input directly with the intra-model input.

Mnemonic	Symbol	Description; Ext. (Int.) Units	Model Type
LSG	L_{SG}	Stage length for each stage comprising the propulsion system; in	STAGEG

OUTPUT DATA

The following data is output from this model. It is available for use as inter-model input to other models and to print, plot, and optimization routines.

Mnemonic	Symbol	Description; Ext. (Int.) Units	
LPS	L_{PS}	Total propulsion system length; ft	Eq. 1

PRINT BLOCK KEY:

Nominally, only those lines with an asterisk to the left of the line number will be printed. By input, any of the lines given below may be printed or suppressed (see the section on output models for the details).

```
                              PROSYSG      PSGM1         PROPULSION SYSTEM GEOMETRY
LPS                                *1
```

260.1

MODEL TYPE: PROSYSW (PROpulsion SYStem Weight)

MODEL NAME: PSWM1 (Weight Synthesis)

DESCRIPTION:

PSWM1 (Propulsion System Weight Model number 1) is a weight synthesis model which evaluates the propulsion system weights. The propulsion system is comprised of the following subsystems.

Stages

PROCEDURE:

Prior to entering PSWM1, the models specified for the STAGEW model type have evaluated the stage weights and mass fractions which are not dependent upon the propulsion system or vehicle weights.

PSWM1 then uses the pertinent stage weight to determine the propulsion system weight quantities.

After leaving PSWM1, the total vehicle geometry and weights are evaluated. After the vehicle has been sized, the model specified for the STAGEW model type (and other major subsystem model types if required) is reentered and mass fractions dependent upon propulsion system quantities are evaluated.

EQUATIONS:

In the equations below, the summation includes all stages within the propulsion system.

Total propellent weight associated with the propulsion system.

$$W_{PP_{PS}} = \Sigma W_{PP_{SG}} \tag{1}$$

Total propulsion system weight.

$$W_{PS} = \Sigma W_{SG} \tag{2}$$

EQUATIONS (Cont.):

Total non-expended propulsion system weight component.

$$W_{PS_{NX}} = \Sigma\, W_{SG_{NX}} \qquad (3)$$

Total expended propulsion system weight component.

$$W_{PS_X} = \Sigma\, W_{SG_X} \qquad (4)$$

Expended (non-thrust producing) propulsion system weight component.

$$W_{PS_{XI}} = \Sigma\, W_{SG_{XI}} \qquad (5)$$

Expended (thrust producing) propulsion system weight component.

$$W_{PS_{XT}} = \Sigma\, W_{SG_{XT}} \qquad (6)$$

INPUT DATA, INTRA-MODEL:

The following data is input to this model directly by the program user. If a value is not input, the preset value is used.

Mnemonic	Symbol	Description; Ext. (Int.) Units	Preset
None			

INPUT DATA, INTER-MODEL:

This model requires as input certain data which is usually output from a model of the specified model type. If the user has not specified such a source for this data, then it must be input directly with the intra-model input.

Mnemonic	Symbol	Description; Ext. (Int.) Units	Model Type
WPPSG	$W_{PP_{SG}}$	Propellent weight for each stage comprising this propulsion system; lb	STAGEW

INPUT DATA, INTER-MODEL (Cont.):

Mnemonic	Symbol	Description; Ext. (Int.) Units	Model Type
WSG	W_{SG}	Total stage weight for each stage comprising this propulsion system; lb	STAGEW
WSGNX	$W_{SG_{NX}}$	Total non-expended stage weight component; lb	STAGEW
WSGX	W_{SG_X}	Total expended stage weight component; lb	STAGEW
WSGXI	$W_{SG_{XI}}$	Expended (non-thrust producing) stage weight component; lb	STAGEW
WSGXT	$W_{SG_{XT}}$	Expended (thrust producing) stage weight component; lb	STAGEW

OUTPUT DATA:

The following data is output from this model. It is available for use as inter-model input to other models and to print, plot, and optimization routines.

Mnemonic	Symbol	Description; Ext. (Int.) Units	
WPPPS	$W_{PP_{PS}}$	Total propellent weight associated with the propulsion system. Includes propellent weights of all stages comprising the propulsion system; lb	Eq. 1
WPS	W_{PS}	Total propulsion system weight. Includes propellent, non-expended and total expended weight components for all stages comprising the propulsion system; lb	Eq. 2

OUTPUT DATA (Cont.):

Mnemonic	Symbol	Description; Ext. (Int.) Units	
WPSNX	$W_{PS_{NX}}$	Total non-expended propulsion system weight component. Includes non-expended weight components for all stages comprising the propulsion system;	
		lb	Eq. 3
WPSX	W_{PS_X}	Total expended propulsion system weight component. Includes expended weight components for all stages comprising the propulsion system. Excludes propellent weight;	
		lb	Eq. 4
WPSXI	$W_{PS_{XI}}$	Expended (non-thrust producing) propulsion system weight component. Includes non-thrust producing weight components for all stages comprising the propulsion system;	
		lb	Eq. 5
WPSXT	$W_{PS_{XT}}$	Expended (thrust producing) propulsion system weight component. Includes thrust producing weight components for all stages comprising the propulsion system. Excludes propellent weights;	
		lb	Eq. 6

PRINT BLOCK KEY:

Nominally, only those lines with an asterisk to the left of the line number will be printed. By input, any of the lines given below may be printed or suppressed (see the section on output models for the details).

```
                                   PROSYSW    PSWM1       PROPULSION  SYSTEM WEIGHT
WPS        WPSNX        WPSX            *1    WPSXI       WPSXT          WPPPS
```

270.1

MODEL TYPE: STAGE (STAGE Geometry)

MODEL NAME: SGGM1 (Single Sequential Stage and Interstage)

DESCRIPTION:

SGGM1 (StaGe Geometry Model number 1) evaluates the geometry for a stage comprised of a single substage and interstage as illustrated in figure 1. By inputting coefficients and bias terms, considerable flexibility is provided for specifying the stage length, diameter, and cross-sectional area. However, since the Intra-Model Input Data is preset to the nominal stage configuration, user input data is not normally required for this model.

PROCEDURE:

Prior to entering SGGM1, the models specified for the SUBSTGG and INTSTGG model types have determined the final geometry for the substage and interstage.

SGGM1 (first entrance) then uses these primary component diameters and lengths to determine the overall stage geometry.

After leaving SGGM1, the weight for this particular stage is evaulated. After all the stages are sized, the models specified for the PROSYSG and VEHG model types will be executed and, utilizing the stage geometry together with their individual requirements, the overall propulsion system and vehicle is sized.

SGGM1 is then entered for the second time and stage fractions dependent upon propulsion system and vehicle quantities are evaluated.

EQUATIONS (FIRST ENTRANCE):

Stage length. Fig. 1

$$L_{SG} = K_{LSG1} L_{SS} + K_{LSG2} L_{IT_S} + K_{LSG3} \tag{1}$$

EQUATIONS (FIRST ENTRANCE) (Cont.):

Stage diameter.

$$D_{SG} = K_{DSG1} D_{SS} + K_{DSG2} D_{ITA} + K_{DSG3} D_{ITF} + K_{DSG4} \quad (2)$$

Stage cross-sectional area.

$$A_{SG} = K_{ASG1} A_{SS} + K_{ASG2} A_{ITA} + K_{ASG3} A_{ITF} + K_{ASG4} \quad (3)$$

Stage length to stage diameter ratio.

$$R_{LDSG} = \frac{L_{SG}}{D_{SG}} \quad (4)$$

EQUATIONS (SECOND ENTRANCE):

Propulsion system length to stage diameter ratio.

$$R_{LDPSSG} = \frac{L_{PS}}{D_{SG}} \quad (5)$$

Vehicle length to stage diameter ratio.

$$R_{LDVHSG} = \frac{L_{VH}}{D_{SG}} \quad (6)$$

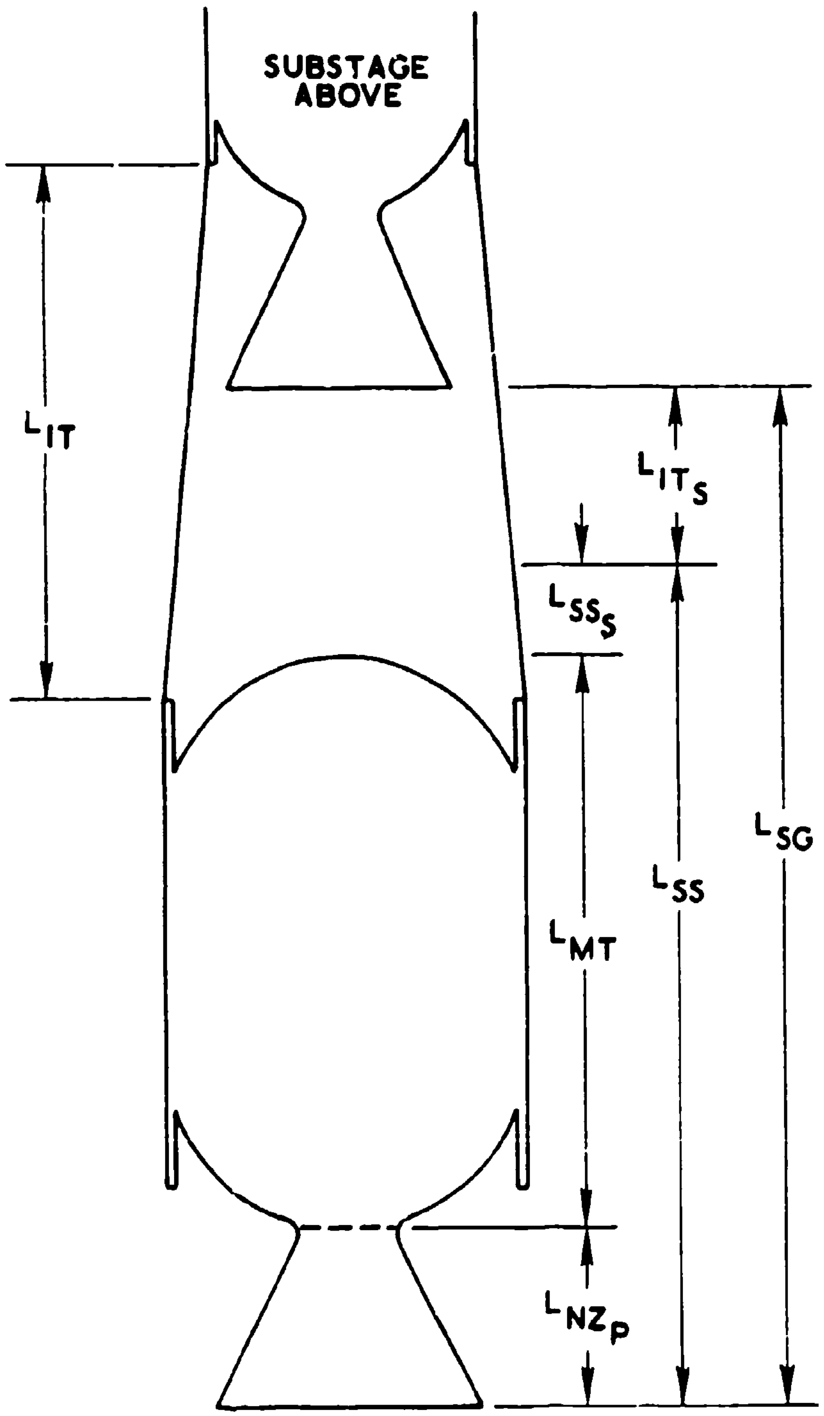

Fig. 270.1-1 Stage Geometry

INPUT DATA, INTRA-MODEL:

The following data is input to this model directly by the program user. If a value is not input, the preset value is used.

Mnemonic	Symbol	Description; Ext. (Int.) Units	Preset
KASG1	K_{ASG1}	Coefficient for stage area computation; N. D.	1
KASG2	K_{ASG2}	Coefficient for stage area computation; N. D.	0
KASG3	K_{ASG3}	Coefficient for stage area computation; N. D.	0
KASG4	K_{ASG4}	Bias for stage area computation; in^2	0
KDSG1	K_{DSG1}	Coefficient for stage diameter computation; N. D.	1
KDSG2	K_{DSG2}	Coefficient for stage diameter computation; N. D.	0
KDSG3	K_{DSG3}	Coefficient for stage diameter computation; N. D.	0
KDSG4	K_{DSG4}	Bias for stage diameter computation; in	0
KLSG1	K_{LSG1}	Coefficient for stage length computation; N. D.	1
KLSG2	K_{LSG2}	Coefficient for stage length computation; N. D.	1
KLSG3	K_{LSG3}	Bias for stage length computation; in	0

INPUT DATA, INTER-MODEL:

This model requires as input certain data which is usually output from a model of the specified model type. If the user has not specified such a source for this data, then it must be input directly with the intra-model input.

Mnemonic	Symbol	Description; Ext. (Int.) Units			Model Type
AITA	A_{IT_A}	Cross-sectional area, interstage aft base;			
		in^2			INTSTGG
AITF	A_{IT_F}	Cross-sectional area, interstage fore base;			
		in^2			INTSTGG
ASS	A_{SS}	Cross-sectional area, substage;			
		in^2			SUBSTGG
DITA	D_{IT_A}	Diameter, interstage aft base;			
		in			INTSTGG
DITF	D_{IT_F}	Diameter, interstage fore base;			
		in			INTSTGG
DSS	D_{SS}	Outside diameter, substage;			
		in			SUBSTGG
LITS	L_{IT_S}	Spacing distance associated with the interstage;			
		in		Fig. 1	INTSTGG
LPS	L_{PS}	Total propulsion system length;			
		in			PROSYSG
LSS	L_{SS}	Total substage length;			
		in		Fig. 1	SUBSTGG
LVH	L_{VH}	Total vehicle length;			
		in			VEHG

OUTPUT DATA:

The following data is output from this model. It is available for use as inter-model input to other models and to print, plot, and optimization routines.

Mnemonic	Symbol	Description; Ext. (Int.) Units		
ASG	A_{SG}	Stage cross-sectional area; in^2		Eq. 3
DSG	D_{SG}	Stage diameter; in		Eq. 2
LSG	L_{SG}	Stage length; in	Fig. 1	Eq. 1
RLDPSSG	R_{LDPSSG}	Propulsion system length to stage diameter ratio; N. D.		Eq. 5
RLDSG	R_{LDSG}	Stage length to stage diameter ratio; N. D.		Eq. 4
RLDVHSG	R_{LDVHSG}	Vehicle length to stage diameter ratio; N. D.		Eq. 6

PRINT BLOCK KEY:

Nominally, only those lines with an asterisk to the left of the line number will be printed. By input, any of the lines given below may be printed or suppressed (see the section on output models for the details).

			STAGEG	SGGM1	STAGE GEOMETRY	
ASG	DSG	KASG1	*1	KASG2	KASG3	KASG4
KDSG1	KDSG2	KDSG3	*2	KDSG4	KLSG1	KLSG2
KLSG3	LSG	RLDPSSG	*3	RLDSG	RLDVHSG	

280.1

MODEL TYPE: STAGEW (STAGE Weight)

MODEL NAME: SGWM1 (Single substage and interstage)

DESCRIPTION:

SGWM1 (StaGe Weight Model number 1) is a weight synthesis model which evaluates the stage weight breakdown and stage mass fractions for a stage having a single substage and interstage. The stage weight is comprised of the following subsystems:

Substage

Interstage

PROCEDURE:

Prior to entering SGWM1, the models specified by the SUBSTGW and INTSTGW model types have evaluated the substage and interstage weights. In addition to evaluating subcomponent weights peculiar to their particular requirements, they have defined a set of component weights in terms of expended or non-expended attributes.

Upon the first entrance to SGWM1, these expended and non-expended, substage and interstage, weight components are used in determining the stage weight breakdown. In addition, mass fractions which are not dependent upon propulsion system or vehicle quantities are evaluated.

The remainder of the stages are then sized and the models specified for the PROSYSW and VEHW model types will determine the propulsion system and vehicle weights.

After the entire vehicle has been sized, a second entrance is made to SGWM1 and the stage mass fractions which are dependent upon propulsion system and vehicle quantities are evaluated.

EQUATIONS (FIRST ENTRANCE):

Weight of propellent associated with this stage.

$$W_{PP_{SG}} = W_{PP_{SS}} \tag{1}$$

Total stage weight.

$$W_{SG} = K_{WSG} \left(W_{SS} + W_{IT}\right) \tag{2}$$

Total non-expended stage weight component.

$$W_{SG_{NX}} = K_{WSGNX} \left(W_{SS_{NX}} + W_{IT_{NX}}\right) \tag{3}$$

Total expended stage weight component.

$$W_{SG_X} = K_{WSGX} \left(W_{SS_X} + W_{IT_X}\right) \tag{4}$$

Expended (thrust producing) stage weight component.

$$W_{SG_{XT}} = K_{WSGXT} \left(W_{SS_{XT}} + W_{IT_{XT}}\right) \tag{5}$$

Expended (non-thrust producing) stage weight component.

$$W_{SG_{XI}} = K_{WSGXI} \left(W_{SS_{XI}} + W_{IT_{XI}}\right) \tag{6}$$

Total weight of stage expendables.

$$W_{SG_{XX}} = K_{WSGXX} \left(W_{PP_{SG}} + W_{SG_X}\right) \tag{7}$$

Total stage expended inert weight flow.

$$\dot{W}_{SG_I} = K_{DWSGI} \dot{W}_{EN_I} \tag{8}$$

Stage propellent mass fraction.

$$K_{SG_{PMF}} = \frac{W_{PP_{SG}}}{W_{SG}} \tag{9}$$

EQUATIONS (FIRST ENTRANCE)(Cont.):

Stage expended mass fraction.

$$K_{SG_{XMF}} = \frac{W_{SG_X}}{W_{SG}} \tag{10}$$

Stage structure mass fraction.

$$K_{SG_{SMF}} = \frac{W_{SG_{NX}}}{W_{SG}} \tag{11}$$

EQUATIONS (SECOND ENTRANCE):

Stage weight proportion

$$R_{WSGPS} = \frac{W_{SG}}{W_{PS}} \tag{12}$$

Stage propellent weight proportion.

$$R_{WPSGPS} = \frac{W_{PP_{SG}}}{W_{PP_{PS}}} \tag{13}$$

INPUT DATA, INTRA-MODEL:

The following data is input to this model directly by the program user. If a value is not input, the preset value is used.

Mnemonic	Symbol	Description; Ext. (Int.) Units	Preset
KDWSGI	K_{DWSGI}	Coefficient for DWSGI computation; N. D.	-1
KWSG	K_{WSG}	Proportionality factor for total stage weight; N. D.	1
KWSGNX	K_{WSGNX}	Proportionality factor for non-expended stage weight component; N. D.	1

INPUT DATA, INTRA-MODEL (Cont.):

Mnemonic	Symbol	Description: Ext. (Int.) Units	Preset
KWSGX	K_{WSGX}	Proportionality factor for total expended stage weight component; N. D.	1
KWSGXI	K_{WSGXI}	Proportionality factor for expended (non-thrust producing) stage weight component; N. D.	1
KWSGXT	K_{WSGXT}	Proportionality factor for expended (thrust producing) stage weight component; N. D.	1
KWSGXX	K_{WSGXX}	Coefficient for WSGXX computation; N. D.	1

INPUT DATA, INTER-MODEL:

This model requires as input certain data which is usually output from a model of the specified model type. If the user has not specified such a source for this data, then it must be input directly with the intra-model input.

Mnemonic	Symbol	Description; Ext. (Int.) Units	Model Type
DWENI	$\dot{W}_{EN_I}$	Inert engine weight flow; lb	PROPUL
WIT	W_{IT}	Total interstage weight; lb	INTSTGW
WITNX	$W_{IT_{NX}}$	Total non-expended interstage weight component; lb	INTSTGW
WITX	W_{IT_X}	Total expended interstage weight component; lb	INTSTGW

INPUT DATA, INTER-MODEL (Cont.):

Mnemonic	Symbol	Description; Ext. (Int.) Units	Model Type
WITXI	$W_{IT_{XI}}$	Expended (non-thrust producing) interstage weight component; lb	INTSTGW
WITXT	$W_{IT_{XT}}$	Expended (thrust producing) interstage weight component; lb	INTSTGW
WPPPS	$W_{PP_{PS}}$	Weight of propellent associated with the propulsion system; lb	PROSYSW
WPPSS	$W_{PP_{SS}}$	Weight of propellent associated with the substage; lb	SUBSTGW
WPS	W_{PS}	Total propulsion system weight; lb	PROSYSW
WSS	W_{SS}	Total substage weight. Includes propellent; lb	SUBSTGW
WSSNX	$W_{SS_{NX}}$	Total non-expended substage weight component; lb	SUBSTGW
WSSX	W_{SS_X}	Total expended substage weight component, does not include propellent; lb	SUBSTGW
WSSXI	$W_{SS_{XI}}$	Expended (non-thrust producing) substage weight component; lb	SUBSTGW
WSSXT	$W_{SS_{XT}}$	Expended (thrust producing) substage weight component, does not include propellent; lb	SUBSTGW

OUTPUT DATA:

The following data is output from this model. It is available for use as inter-model input to other models and to print, plot, and optimization routines.

Mnemonic	Symbol	Description; Ext. (Int.) Units	
DWSGI	$\dot{W}_{SG_I}$	Total stage expended inert weight flow. A negative value indicates weight loss from the stage (see KDWSGI). DWSGI corresponds to DWINERT in the trajectory simulation models; lb/sec	Eq. 8
KSGPMF	$K_{SG_{PMF}}$	Stage propellent mass fraction. Ratio of propellent weight to stage weight; N. D.	Eq. 9
KSGSMF	$K_{SG_{SMF}}$	Stage structure mass fraction. Ratio of non-expended stage weight to total stage weight; N. D.	Eq. 11
KSGXMF	$K_{SG_{XMF}}$	Stage expended mass fraction. Ratio of expended stage weight (excluding propellent) to total stage weight; N. D.	Eq. 10
RWSGPS	R_{WSGPS}	Stage weight proportion. Ratio of stage weight to propulsion system weight; N. D.	12
RWPSGPS	R_{WPSGPS}	Stage propellent weight proportion. Ratio of propellent weight associated with the stage to the propellent weight associated with the propulsion system; N. D.	Eq. 13
WPPSG	$W_{PP_{SG}}$	Weight of propellent associated with this stage; lb	Eq. 1
WSG	W_{SG}	Total stage weight. Includes substage and interstage; lb	Eq. 2

OUTPUT DATA (Cont.):

Mnemonic	Symbol	Description; Ext. (Int.) Units	
WSGNX	$W_{SG_{NX}}$	Total non-expended stage weight component. Includes substage and interstage. WSGNX corresponds to WTSTS in the trajectory simulation models;	
		lb	Eq. 3
WSGX	W_{SG_X}	Total expended stage weight component. Includes substage and interstage. Does not include propellent;	
		lb	Eq. 4
WSGXI	$W_{SG_{XI}}$	Expended (non-thrust producing) stage weight component. Includes substage and interstage;	
		lb	Eq. 6
WSGXT	$W_{SG_{XT}}$	Expended (thrust producing) stage weight component. Includes substage and interstage. Does not include propellent;	
		lb	Eq. 5
WSGXX	$W_{SG_{XX}}$	Total weight of stage expendables. Includes propellent, expended thrust producing, and expended non-thrust producing stage weight components. WSGXX corresponds to WTANK in the trajectory simulation models;	
		lb	Eq. 7

PRINT BLOCK KEY:

Nominally, only those lines with an asterisk to the left of the line number will be printed. By input, any of the lines given below may be printed or suppressed (see the section on output models for the details).

			STAGEW	SGWM1	STAGE WEIGHT	
WSG	WSGNX	WSGX	*1	WSGXI	WSGXT	WPPSG
KWSG	KWSGNX	KWSGX	*2	KWSGXI	KWSGXT	KWSGXX
KSGPMF	KSGSMF	KSGXMF	*3	DWSGI	KDWSGI	RWPSGPS

290.1

MODEL TYPE: SHROUDW (SHROUD Weight)

MODEL NAME: SHWM1 (Direct Input)

DESCRIPTION:

SHWM1 (SHroud Weight Model number 1) is a simple non-geometry dependent shroud weight model for which the shroud weight is input directly by the program user. It should be noted that shroud simulations will normally require a shroud weight model but not a shroud geometry model.

See the PAYSECW model type for payload section weight models which are applicable if this shroud weight model is used.

PROCEDURE:

Prior to executing SHWM1, all vehicle subsystems within the propulsion system have been sized and the model specified for the PAYLODW model type has evaluated the payload weight breakdown.

SHWM1 is then executed and the shroud weight is evaluated.

After SHWM1 is executed, the model specified for the PAYSECW model type will use the payload and shroud weights to evaluate the payload section weight breakdown.

EQUATIONS:

Total shroud weight.

$$W_{SH} = K_{WSH} W_{SHROUD} \qquad (1)$$

Total non-expended shroud weight component.

$$W_{SH_{NX}} = W_{SH} \qquad (2)$$

EQUATIONS (Cont.):

Total expended shroud weight component.

$$W_{SH_X} = 0 \tag{3}$$

Expended (non-thrust producing) shroud weight component.

$$W_{SH_{XI}} = 0 \tag{4}$$

Expended (thrust producing) shroud weight component.

$$W_{SH_{XT}} = 0 \tag{5}$$

INPUT DATA, INTRA-MODEL:

The following data is input to this model directly by the program user. If a value is not input, the preset value is used.

Mnemonic	Symbol	Description; Ext. (Int.) Units	Preset
KWSH	K_{WSH}	Coefficient for WSH computation; N. D.	1
WSHROUD	W_{SHROUD}	Shroud weight input by user; lb	0

INPUT DATA, INTER-MODEL:

This model requires as input certain data which is usually output from a model of the specified model type. If the user has not specified such a source for this data, then it must be input directly with the intra-model input.

Mnemonic	Symbol	Description; Ext. (Int.) Units	Model Type
None			

OUTPUT DATA:

The following data is output from this model. It is available for use as inter-model input to other models and to print, plot, and optimization routines.

Mnemonic	Symbol	Description; Ext. (Int.) Units	
WSH	W_{SH}	Total shroud weight; lb	Eq. 1
WSHNX	$W_{SH_{NX}}$	Total non-expended shroud weight component; lb	Eq. 2
WSHX	W_{SH_X}	Total expended shroud weight component; lb	Eq. 3
WSHXI	$W_{SH_{XI}}$	Expended (non-thrust producing) shroud weight component; lb	Eq. 4
WSHXT	$W_{SH_{XT}}$	Expended (thrust producing) shroud weight component; lb	Eq. 5

PRINT BLOCK KEY:

Nominally, only those lines with an asterisk to the left of the line number will be printed. By input, any of the lines given below may be printed or suppressed (see the section on output models for the details).

```
                                          SHROUDW    SHWM1      SHROUD WEIGHT
WSH        WSHNX        WSHX                   *1    WSHXI      WSHXT
KWSH       WSHROUD                             *2
```

300.1

MODEL TYPE: SUBSTGG (SUBSTaGe Geometry)

MODEL NAME: SSGM1 (Single Solid Rocket Motor)

DESCRIPTION:

SSGM1 (SubStage Geometry Model number 1) evaluates the geometry of a complete solid rocket motor substage, including the motor case, protruding nozzle and spacing required ahead of the forward closure for the igniter attachment, thrust termination, etc. Since this is the final geometry model executed in the substage geometry design, substage requirements for inter-stage design are also evaluated. See figure 1.

PROCEDURE:

Prior to entering SSGM1, the models specified for the CASEG, NOZZLEG and MOTORG model types have determined the final geometry for the case, nozzle and basic motor.

SSGM1 then uses these primary component diameters and lengths to determine the overall substage geometry, including interstage requirements.

After leaving SSGM1, the weight and propulsion models for this particular substage are sized. After all substages are sized, the interstage models will be executed and, utilizing the substage geometry data together with satisfying their individual requirements, the interstages are sized.

EQUATIONS:

Intersubstage spacing distance.

$$L_{SS_S} = K_{LS1} + K_{LS2} \, D_{CS_O} + L_{IT_{MT}} \tag{1}$$

Total substage length.

$$L_{SS} = L_{SS_S} + L_{MT} + L_{NZ_P} \tag{2}$$

EQUATIONS (Cont.):

Substage outside diameter.

$$D_{SS} = K_{D1} + K_{D2}\ D_{MT} \quad (3)$$

Substage cross sectional area.

$$A_{SS} = \left(\frac{\pi}{4}\right) D_{SS}^2 \quad (4)$$

Ratio, total substage length to case diameter.

$$R_{LDSSCS} = \frac{L_{SS}}{D_{CS_O}} \quad (5)$$

Substage diameter for forward interstage attachment.

$$D_{SS_{ITF}} = D_{SS} \quad (6)$$

Substage diameter for aft interstage attachment.

$$D_{SS_{ITA}} = D_{SS} \quad (7)$$

Length of interstage required (forward) for this substage.

$$L_{SS_{ITF}} = L_{MT_{CHF}} + L_{SS_S} - L_{MT_{SKF}} \quad (8)$$

Length of interstage required (aft) for this substage.

$$L_{SS_{ITA}} = L_{MT_{CHA}} + L_{NZ_P} - L_{MT_{SKA}} \quad (9)$$

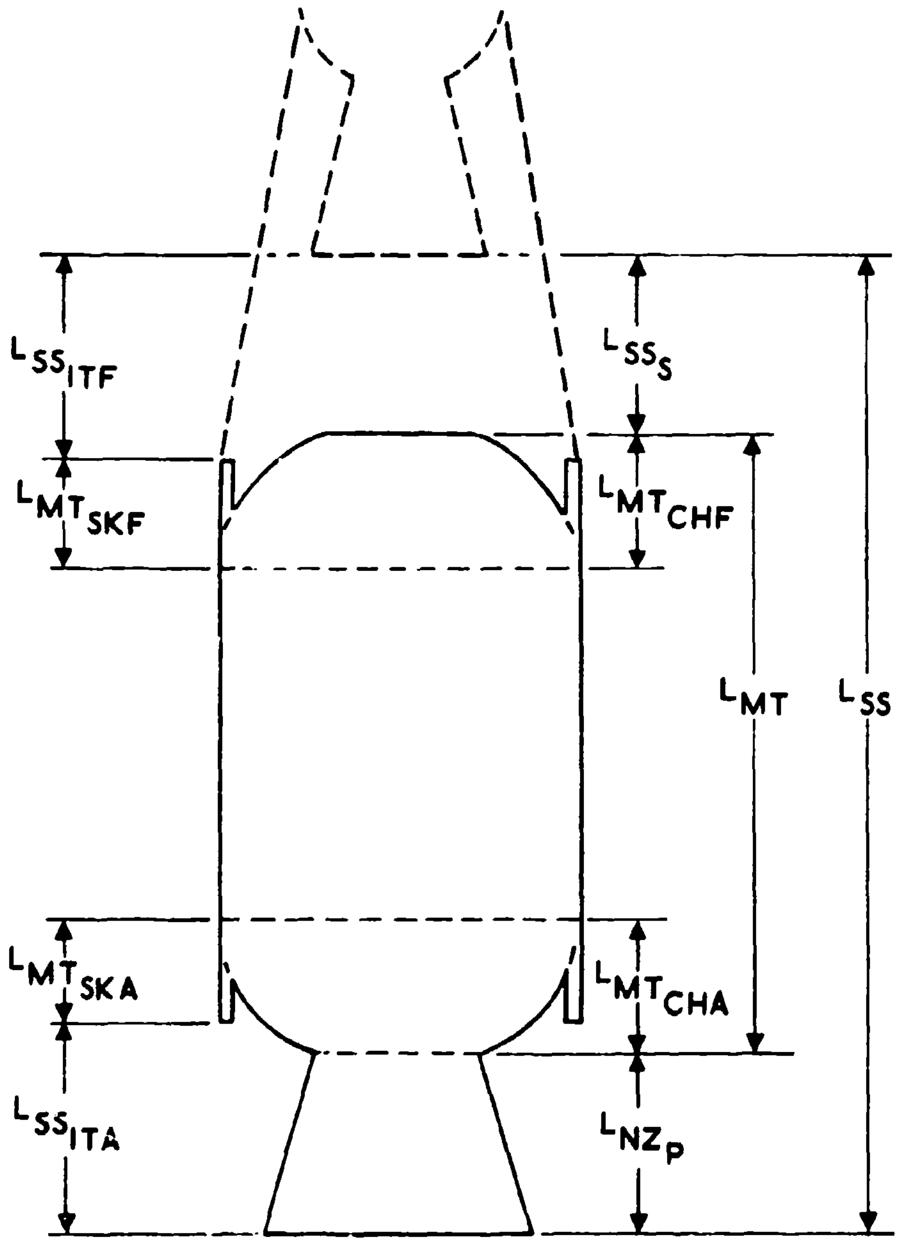

Fig. 300.1-1 Substage Geometry

INPUT DATA, INTRA-MODEL:

The following data is input to this model directly by the program user. If a value is not input, the preset value is used.

Mnemonic	Symbol	Description; Ext. (Int.) Units	Preset
KLSSS1	K_{LS1}	Bias for inter-substage spacing distance computation. Does not include thrust termination; in	0
KLSSS2	K_{LS2}	Proportionality factor relating a component of the inter-substage spacing distance to the outside case diameter. Does not include thrust termination; N. D.	0
KDSS1	K_{D1}	Bias for substage diameter computation; in	0
KDSS2	K_{D2}	Coefficient for substage diameter computation; in	1

INPUT DATA, INTER-MODEL:

This model requires as input certain data which is usually output from a model of the specified model type. If the user has not specified such a source for this data, then it must be input directly with the intra-model input.

Mnemonic	Symbol	Description; Ext. (Int.) Units	Model Type
DCSO	D_{CS_O}	Outside motor case diameter; in	CASEG
DMT	D_{MT}	Motor diameter; in	MOTORG
LMT	L_{MT}	Motor length; in	MOTORG

INPUT DATA, INTER-MODEL:

Mnemonic	Symbol	Description; Ext. (Int.) Units	Model Type
LMTCLA	$L_{MT_{CLA}}$	Length of motor aft closure; in	MOTORG
LMTCLF	$L_{MT_{CLF}}$	Length of motor forward closure; in	MOTORG
LMTSKA	$L_{MT_{SKA}}$	Length of motor aft skirt; in	MOTORG
LMTSKF	$L_{MT_{SKF}}$	Length of motor forward skirt; in	MOTORG
LNZP	L_{NZ_P}	Protruding nozzle length; in	NOZZLEG
LTTMT	$L_{TT_{MT}}$	Length, thrust termination; in	TTERMG

OUTPUT DATA:

The following data is output from this model. It is available for use as inter-model input to other models and to print, plot, and optimization routines.

Mnemonic	Symbol	Description; Ext. (Int.) Units	
ASS	A_{SS}	Substage cross sectional area; in	Eq. 4
DSS	D_{SS}	Substage outside diameter. May include raceways and other protrusions; in	Eq. 3
DSSITA	$D_{SS_{ITA}}$	Substage aft diameter for interstage attachment; in	Eq. 7

OUTPUT DATA:(Cont.):

Mnemonic	Symbol	Description; Ext. (Int.) Units	
DSSITF	$D_{SS_{ITF}}$	Substage forward diameter for interstage attachment;	
		in	Eq. 6
LSS	L_{SS}	Total substage length. Includes motor, protruding nozzle, and required spacing distance forward of the forward closure;	
		in	Eq. 2
LSSITA	$L_{SS_{ITA}}$	Length of interstage required (aft) for this substage;	
		in	Eq. 9
LSSITF	$L_{SS_{ITF}}$	Length of interstage required (forward) for this substage);	
		in	Eq. 8
LSSS	L_{SS_S}	Inter-substage spacing distance. Substage distance, measured along vehicle centerline, forward of fore motor closure. Used primarily for thrust termination equipment and any other spacing distance required between this substage and the nozzle of the substage forward of this substage;	
		in	Eq. 1
RLDSSCS	R_{LDSSCS}	Length to diameter ratio. Ratio of total substage length to outside case diameter;	
		N. D.	Eq. 5

PRINT BLOCK KEY:

Nominally, only those lines with an asterisk to the left of the line number will be printed. By input, any of the lines given below may be printed or suppressed (see the section on output models for the details).

```
                                      SUBSTGG   SSGM1    SUBSTAGE GEOMETRY
ASS        DSS        DSSITA              *1    DSSITF   KDSS1       KDSS2
KLSSS1     KLSSS2     LSS                 *2    LSSITA   LSSITF      LSSS
RLDSSCS                                   *3
```

310.1

MODEL TYPE: SUBSTGW (SUBSTaGe Weight)

MODEL NAME: SSWM1 (Weight Synthesis, Single Motor and Nozzle)

DESCRIPTION:

SSWM1 (Substage Weight Model number 1) is a weight synthesis model which evaluates the substage weight breakdown and substage mass fractions for a substage having a single solid rocket motor and nozzle. The substage weight is comprised of the following subsystems.

Motor

Nozzle

Note that the above subsystems do NOT include the interstage. See the STAGEW model for stage (substage plus interstage) weight quantities.

PROCEDURE:

Prior to entering SSWM1, the models specified by the NOZZLEW and MOTORW model types have evaluated the nozzle and motor weights. In addition to evaluating subcomponent weights peculiar to their particular requirements, they have defined a set of component weights in terms of expended or non-expended attributes.

These expended and non-expended motor and nozzle weights are input to SSWM1. The SSWM1 model will combine these quantities to determine the substage weight components and mass fractions.

After the SSWM1 model is executed, the interstage geometry and weights are determined. The model specified by the STAGEW model type will then use the substage and interstage quantities to determine the stage weights and mass fractions.

EQUATIONS:

Weight of propellent associated with the substage.

$$W_{PP_{SS}} = W_{PP_{MT}} \tag{1}$$

Total substage weight.

$$W_{SS} = K_{WSS} (W_{MT} + W_{NZ}) \tag{2}$$

Total non-expended substage weight component.

$$W_{SS_{NX}} = K_{WSSNX} (W_{MT_{NX}} + W_{NZ_{NX}}) \tag{3}$$

Total expended substage weight component (excluding propellent).

$$W_{SS_X} = K_{WSSX} (W_{MT_X} + W_{NZ_X}) \tag{4}$$

Expended (thrust producing) substage weight component (excluding propellent).

$$W_{SS_{XT}} = K_{WSSXT} (W_{MT_{XT}} + W_{NZ_{XT}}) \tag{5}$$

Expended (non-thrust producing) substage weight component.

$$W_{SS_{XI}} = K_{WSSXI} (W_{MT_{XI}} + W_{NZ_{XI}}) \tag{6}$$

Substage propellent mass fraction.

$$K_{SS_{PMF}} = \frac{W_{PP_{SS}}}{W_{SS}} \tag{7}$$

Substage expended mass fraction.

$$K_{SS_{XMF}} = \frac{W_{SS_X}}{W_{SS}} \tag{8}$$

Substage structure mass fraction.

$$K_{SS_{SMF}} = \frac{W_{SS_{NX}}}{W_{SS}} \tag{9}$$

INPUT DATA, INTRA-MODEL:

The following data is input to this model directly by the program user. If a value is not input, the preset value is used.

Mnemonic	Symbol	Description; Ext. (Int.) Units	Preset
KWSS	K_{WSS}	Proportionality factor for total substage weight; N. D.	1
KWSSNX	K_{WSSNX}	Proportionality factor for total non-expended substage weight component; N. D.	1
KWSSX	K_{WSSX}	Proportionality factor for total expended substage weight component; N. D.	1
KWSSXI	K_{WSSXI}	Proportionality factor for expended (non-thrust producing) substage weight component; N. D.	1
KWSSXT	K_{WSSXT}	Proportionality factor for expended (thrust producing) substage weight component; N. D.	1

INPUT DATA, INTER-MODEL:

This model requires as input certain data which is usually output from a model of the specified model type. If the user has not specified such a source for this data, then it must be input directly with the intra-model input.

Mnemonic	Symbol	Description; Ext. (Int.) Units	Model Type
WMT	W_{MT}	Motor weight, total; lb	MOTORW
WMTNX	$W_{MT_{NX}}$	Motor weight component, total non-expended; lb	MOTORW

INPUT DATA, INTER-MODEL (Cont.):

Mnemonic	Symbol	Description; Ext. (Int.) Units	Model Type
WMTX	W_{MT_X}	Motor weight component, total expended; lb	MOTORW
WMTXI	$W_{MT_{XI}}$	Motor weight component, expended, (non-thrust producing); lb	MOTORW
WMTXT	$W_{MT_{XT}}$	Motor weight component, expended, (thrust producing); lb	MOTORW
WNZ	W_{NZ}	Nozzle weight, total; lb	NOZZLEW
WNZNX	$W_{NZ_{NX}}$	Nozzle weight component, total non-expended; lb	NOZZLEW
WNZX	W_{NZ_X}	Nozzle weight component, total expended; lb	NOZZLEW
WNZXI	$W_{NZ_{XI}}$	Nozzle weight component, expended, (non-thrust producing); lb	NOZZLEW
WNZXT	$W_{NZ_{XT}}$	Nozzle weight component, expended, (thrust producing); lb	NOZZLEW
WPPMT	$W_{PP_{MT}}$	Propellent weight; lb	PROPELW

OUTPUT DATA:

The following data is output from this model. It is available for use as inter-model input to other models and to print, plot, and optimization routines.

Mnemonic	Symbol	Description; Ext. (Int.) Units	
KSSPMF	$K_{SS_{PMF}}$	Substage propellent mass fraction. Includes motor and nozzle;	
		N. D.	Eq. 7
KSSSMF	$K_{SS_{SMF}}$	Substage structure mass fraction. Includes motor and nozzle;	
		N. D.	Eq. 9
KSSXMF	$K_{SS_{XMF}}$	Substage expended mass fraction. Includes motor and nozzle;	
		N. D.	Eq. 8
WPPSS	$W_{PP_{SS}}$	Weight of propellent associated with the substage;	
		lb	Eq. 1
WSS	W_{SS}	Total substage weight. Includes motor and nozzle;	
		lb	Eq. 2
WSSNX	$W_{SS_{NX}}$	Total non-expended substage weight component. Includes motor and nozzle;	
		lb	Eq. 3
WSSX	W_{SS_X}	Total expended substage weight component. Includes motor and nozzle;	
		lb	Eq. 4
WSSXI	$W_{SS_{XI}}$	Expended (non-thrust producing) substage weight component. Includes motor and nozzle;	
		lb	Eq. 6
WSSXT	$W_{SS_{XT}}$	Expended (thrust producing) substage weight component. Includes motor and nozzle;	
		lb	Eq. 5

PRINT BLOCK KEY:

Nominally, only those lines with an asterisk to the left of the line number will be printed. By input, any of the lines given below may be printed or suppressed (see the section on output models for the details).

			SUBSTGW	SSWM1	SUBSTAGE WEIGHT	
WSS	WSSNX	WSSX	*1	WSSXI	WSSXT	WPPSS
KWSS	KWSSNX	KWSSX	*2	KWSSXI	KWSSXT	KSSPMF
KSSSMF	KSSXMF		*3			

320.1

MODEL TYPE: TTERMG (Thrust TERMination Geometry)

MODEL NAME: TTGM1 (Motor Centerline spacing Distance)

DESCRIPTION:

TTGM1 (Thrust Termination Geometry Model number 1) evaluates the spacing distance required, forward of the fore motor closure, for the thrust termination mechanism.

PROCEDURE:

Prior to executing TTGM1, the model specified for the CASEG model type has determined the case outside diameter.

TTGM1 then uses the case diameter to evaluate the spacing distance required for the thrust termination mechanism.

The thrust termination spacing distance will later be used by the model specified for the SUBSTGG model type to determine the required intersub-stage spacing distance.

EQUATIONS:

Thrust termination spacing length.

$$L_{TT_{MT}} = K_{LTTMT} \, C_1 \, D_{CS_O}$$

INPUT DATA, INTRA-MODEL:

The following data is input directly to this model by the program user. If a value is not input, the preset value is used.

INPUT DATA, INTRA-MODEL (Cont.):

Mnemonic	Symbol	Description; Ext. (Int.) Units	Preset
CTTG1	C_1	Constant for LTTMT computation; N. D.	0.01
KLTTMT	K_{LTTMT}	Coefficient for LTTMT computation; N. D.	1

INPUT DATA, INTER-MODEL:

This model requires as input certain data which is usually output from a model of the specified model type. If the user has not specified such a source for this data, then it must be input directly with the intra-model input.

Mnemonic	Symbol	Description; Ext. (Int.) Units	Model Type
DCSO	D_{CS_O}	Outside case diameter; in	CASEG

OUTPUT DATA:

The following data is output by this model. It is available for usage as inter-model input to other models and to print, plot, and optimization routines.

Mnemonic	Symbol	Description; Ext. (Int.) Units
LTTMT	$L_{TT_{MT}}$	Thrust termination spacing length. Distance measured along motor centerline forward of the fore motor closure, required for the thrust termination mechanism; in

PRINT BLOCK KEY:

Nominally, only those lines with an asterisk to the left of the line number will be printed. By input, any of the lines given below may be printed or suppressed (see the section on output models for the details).

```
                                        TTERMG      TTGM1        THRUST TERMINATION  OMETRY
CTTG1       KLTTMT        LTTMT            *1
```

330.1

MODEL TYPE: TTERMW (Thrust TERMination Weight)

MODEL NAME: TTWM1 (Parametric Scaling)

DESCRIPTION:

TTWM1 (Thrust Termination Weight Model number 1) utilizes a parametric scaling equation to determine the weight of the thrust termination mechanism for a solid rocket motor. See reference 8 for a description of the equation and parametric scaling rationale.

This model is applicable for performance parameters within the following limits (see Input Data, Inter-Model).

$$300 < \text{PCHAVG} < 1000 \text{ psia.}$$

$$40 < \text{TBPPMT} < 140 \text{ sec.}$$

$$3000 < \text{WPPMT} < 2{,}000{,}000 \text{ lb.}$$

PROCEDURE:

In addition to evaluating the thrust termination weight, the TTWM1 model determines the total weight breakdown in terms of expended and non-expended components.

These expended and non-expended component weights will later be used by the model specified for the MOTORW model type to determine the motor weights and mass fractions.

EQUATIONS:

Total thrust termination weight.

$$W_{TT} = K_{WTT}\, C_1 \left(\frac{W_{PP_{MT}}}{P_{AVG}\, T_B} \right)^{C_2} \tag{1}$$

EQUATIONS (Cont.):

Total non-expended thrust termination weight component.

$$W_{TT_{NX}} = K_{WTTNX} W_{TT} \tag{2}$$

Total expended thrust termination weight component.

$$W_{TT_X} = 0 \tag{3}$$

Expended (non-thrust producing) thrust termination weight.

$$W_{TT_{XI}} = 0 \tag{4}$$

Expended (thrust producing) thrust termination weight.

$$W_{TT_{XT}} = 0 \tag{5}$$

INPUT DATA, INTRA-MODEL:

The following data is input directly to this model by the program user. If a value is not input, the preset value is used.

Mnemonic	Symbol	Description; Ext. (Int.) Units	Preset
CTTW1	C_1	Scaling constant for WTT computation; N. D.	170
CTTW2	C_2	Scaling constant for WTT computation; N. D.	1.45
KWTT	K_{WTT}	Proportionality factor for thrust termination weight; N. D.	1
KWTTNX	K_{WTTNX}	Proportionality factor for non-expended thrust termination weight; N. D.	1

INPUT DATA, INTER-MODEL:

This model requires as input certain data which is usually output from a model of the specified model type. If the user has not specified such a source for this data, then it must be input directly with the intra-model input.

Mnemonic	Symbol	Description; Ext. (Int.) Units	Model Type
PCHAVG	P_{AVG}	Average chamber pressure; psia	IBGAS
TBPPMT	T_B	Propellent burn time; sec	IBPERF
WPPMT	$W_{PP_{MT}}$	Propellent weight; lb	PROPELW

OUTPUT DATA:

The following data is output from this model. It is available for use as inter-model input to other models and to print, plot, and optimization routines.

Mnemonic	Symbol	Description; Ext. (Int.) Units	
WTT	W_{TT}	Total thrust termination subsystem weight; lb	Eq. 1
WTTNX	$W_{TT_{NX}}$	Total non-expended thrust termination subsystem weight component; lb	Eq. 2
WTTX	W_{TT_X}	Total expended thrust termination subsystem weight component; lb	Eq. 3
WTTXI	$W_{TT_{XI}}$	Expended (non-thrust producing) thrust termination subsystem weight component; lb	Eq. 4
WTTXT	$W_{TT_{XT}}$	Expended (thrust producing) thrust termination subsystem weight component; lb	Eq. 5

PRINT BLOCK KEY:

Nominally, only those lines with an asterisk to the left of the line number will be printed. By input, any of the lines given below may be printed or suppressed (see the section on output models for the details).

```
                                        TTERMW   TTWM1     THRUST TERMINATION WEIGHT
WTT        WTTNX        WTTX                *1   WTTXI     WTTXT
CTTW1      CTTW2        KWTT                *2   KWTTNX
```

340.1

MODEL TYPE: TVCG (Thrust Vector Control Geometry)

MODEL NAME: TVGM1 (Gimballed nozzle)

DESCRIPTION:

TVGM1 (Thrust Vector Geometry Model number 1) evaluates the geometry required for the simulation of a gimballed nozzle. The gimbal point is located on the nozzle centerline and may be forward (see figure 1) or aft (see figure 2) of the nozzle throat plane.

PROCEDURE:

Prior to entering TVGM1, the model specified for the NOZZLEG model type has evaluated the nozzle geometry.

TVGM1 then uses this nozzle geometry to determine the gimballed nozzle envelope geometry.

EQUATIONS:

Gimballed nozzle length ratio. (Positive value if gimbal point is aft of nozzle throat plane.)

$$R_{LGB} = K_{RLGB1} + \frac{K_{RLGB2}}{\sqrt{\epsilon_{NZ}}} \tag{1}$$

Distance from nozzle throat plane to nozzle gimbal point. (Positive sense from nozzle throat plane towards nozzle exit plane.) (Figs. 1, 2)

$$L_{GB_{TH}} = R_{LGB} \, L_{NZ_{DV}} \tag{2}$$

EQUATIONS (Cont.):

Distance from nozzle gimbal point to nozzle exit plane. (Figs. 1, 2)

$$L_{GB_{EXT}} = L_{NZ_{DV}} - L_{GB_{TH}} \tag{3}$$

Nozzle gimbal envelope half angle for zero gimbal angle. (Figs. 1, 2)

$$\theta_{GB_2} = \arctan\left(\frac{D_{NZ_{EXT}}}{2L_{GB_{EXT}}}\right) \tag{4}$$

Nozzle gimbal envelope half angle. (Figs. 1, 2)

$$\theta_{GB_1} = \theta_{GB_2} + \theta_{GB} \tag{5}$$

Distance from nozzle gimbal point to edge of nozzle exit cone. (Figs. 1, 2)

$$L_{GB_{EDGE}} = \sqrt{\left(\frac{D_{NZ_{EXT}}}{2}\right)^2 + L^2_{GB_{EXT}}} \tag{6}$$

Diameter of gimballed nozzle envelope. (Figs. 1, 2)

$$D_{GB_{ENV}} = 2 \quad L_{GB_{EDGE}} \sin\left(\theta_{GB_1}\right) \tag{7}$$

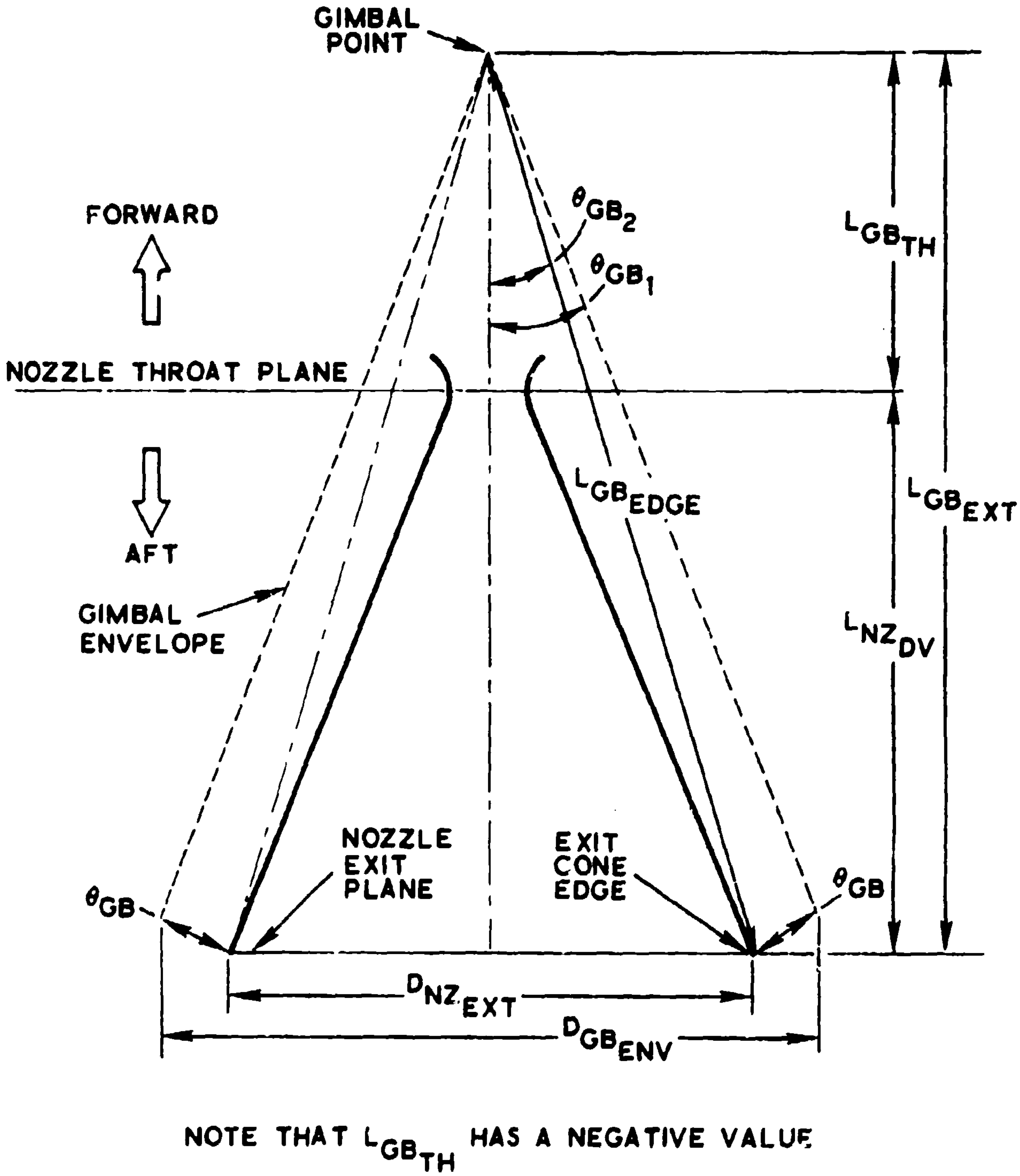

Fig. 340.1-1 Gimbal Point Forward of Nozzle Throat

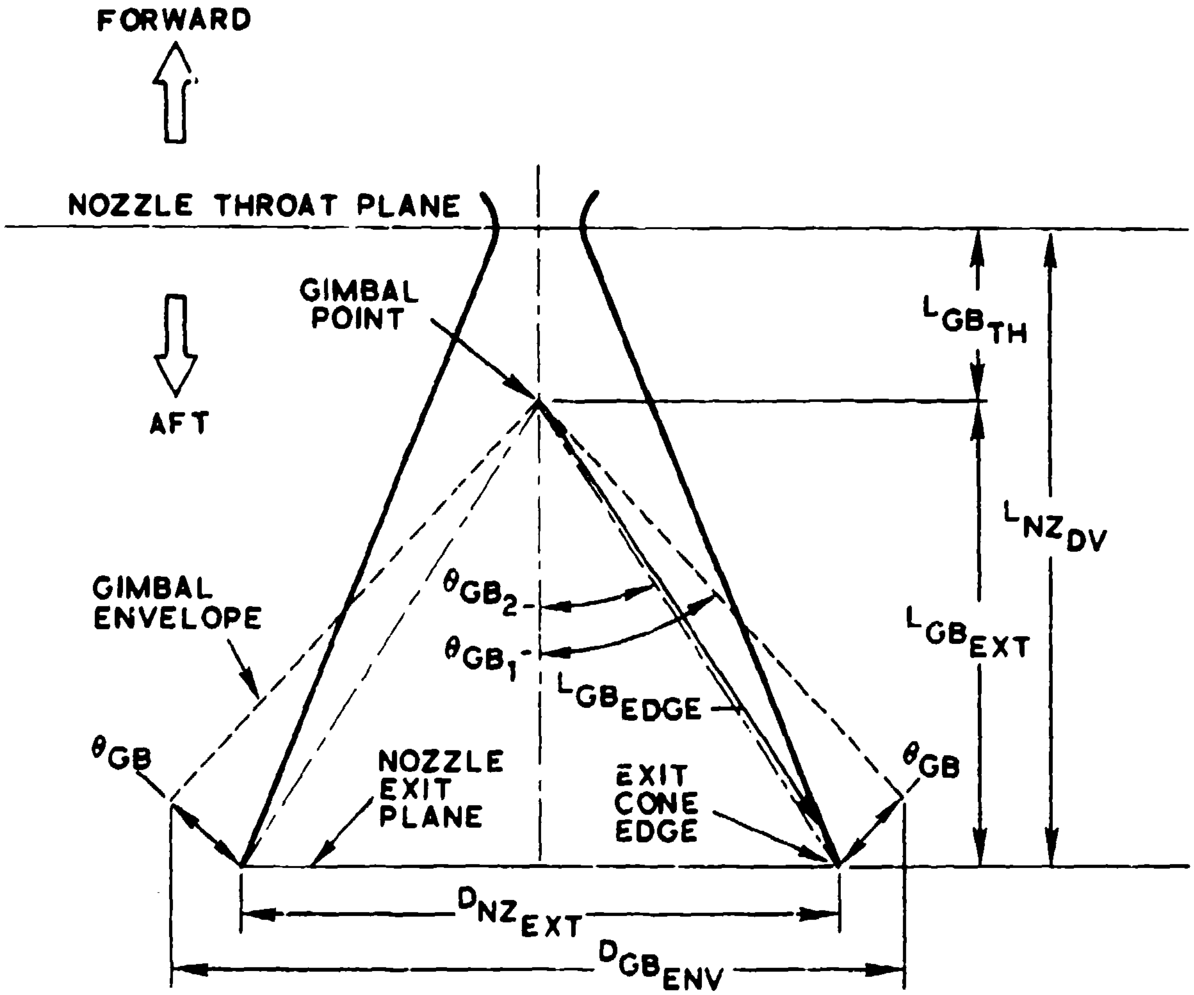

NOTE THAT $L_{GB_{TH}}$ HAS A POSITIVE VALUE

Fig. 340.1-2 Gimbal Point Aft of Nozzle Throat

INPUT DATA, INTRA-MODEL:

The following data is input directly to this model by the program user. If a value is not input, the preset value is used.

Mnemonic	Symbol	Description; Ext. (Int.) Units		Preset
KRLGB1	K_{RLGB1}	Bias for RLGB computation; N. D.		0
KRLGB2	K_{RLGB2}	Coefficient for RLGB computation; N. D.		0
GBANGLE	θ_{GB}	Nozzle gimbal angle; deg	Figs. 1, 2	0

INPUT DATA, INTER-MODEL:

This model requires as input certain data which is usually output from a model of the specified model type. If the user has not specified such a source for this data, then it must be input directly with the intra-model input.

Mnemonic	Symbol	Description; Ext. (Int.) Units		Model Type
DNZEXT	$D_{NZ_{EXT}}$	Nozzle exit diameter; in	Figs. 1, 2	NOZZLEG
LNZDV	$L_{NZ_{DV}}$	Divergent nozzle section length; in	Figs. 1, 2	NOZZLEG
RAEXTTH	ϵ_{NZ}	Nozzle expansion ratio at nozzle exit plane; N. D.		NOZZLEG

OUTPUT DATA:

The following data is output from this model. It is available for use as inter-model input to other models and to print, plot, and optimization routines.

Mnemonic	Symbol	Description; Ext. (Int.) Units		
DGBENV	$D_{GB_{ENV}}$	Diameter of gimballed nozzle envelope;		
		in	Figs. 1, 2	Eq. 7
GBENHA	θ_{GB_1}	Nozzle gimbal envelope half angle;		
		deg	Figs. 1, 2	Eq. 5
GBENHAZ	θ_{GB_2}	Nozzle gimbal envelope half angle for zero gimbal angle;		
		deg	Figs. 1, 2	Eq. 4
LGBEDGE	$L_{GB_{EDGE}}$	Distance from nozzle gimbal point to edge of nozzle exit cone;		
		in	Figs. 1, 2	Eq. 6
LGBEXT	$L_{GB_{EXT}}$	Distance from nozzle gimbal point to nozzle exit plane;		
		in	Figs. 1, 2	Eq. 3
LGBTH	$L_{GB_{TH}}$	Distance from nozzle throat plane to nozzle gimbal point. Measured on nozzle centerline, positive sense from nozzle throat plane towards nozzle exit plane;		
		in	Figs. 1, 2	Eq. 2
RLGB	R_{LGB}	Gimballed nozzle length ratio. Ratio of LGBTH to LNZDV. Positve sign indicates gimbal point is aft of nozzle throat plane;		
		N. D.	Figs. 1, 2	Eq. 1

PRINT BLOCK KEY:

Nominally, only those lines with an asterisk to the left of the line number will be printed. By input, any of the lines given below may be printed or suppressed (see the section on output models for the details).

```
                                    TVCG    TVGM1    THRUST VECTOR CONTROL GEOMETRY
GBANGLE    GBENHA    GBENHAZ         *1     KRLGB1     KRLGB2      LGBTH
LGBEDGE    DGBENV    LGBEXT          *2     RLGB
```

350.1

MODEL TYPE: TVCW (Thrust Vector Control Weight

MODEL NAME: TVWM1 (Gimballed nozzle or integral omnivector, statistical scaling)

DESCRIPTION:

TVWM1 (Thrust Vector control Weight Model number 1) utilizes a statistically derived equation to determine the weight of a gimballed nozzle thrust vector control system. In addition, a nozzle weight factor is determined for assessing the required nozzle weight penalty.

(See REMARKS for the simulation of an integral omnivector TVC system.) The subsystems considered within the TVC system weight are:

- Actuators
- Hydraulic pressurization system
- Plumbing
- Valves
- Roll control system

It should be noted that since the TVC weight equation is based upon a purely statistical analysis, the model is intended for usage only in total sizing and optimization studies. This model cannot be used for subsystem trade off studies. See reference 8 for a description of the equations and statistical scaling rationale.

This model is applicable for performance parameters within the following limits,

$15 < \text{NZHA} < 30$ deg

$300 < \text{PCHAVG} < 1000$ PSIA

$5 < \text{RAEXTTH} < 75$

$30 < \text{TBPPMT} < 140$ sec

$500 < \text{WPPMT} < 2{,}000{,}000$ lbs

where NZHA and RAEXTTH are associated with the NOZZLEG model type, PCHAVG is associated with the IBGAS model type, TBPPMT is associated with the IBPERF model type, and WPPMT is associated with the PROPELW model type.

PROCEDURE:

This is a two entrance model. Up on the first entrance to TVWM1, the nozzle weight penalty factor is evaluated. The model specified for the NOZZLEW model type is then executed to determine the nozzle weight.

TVWM1 is then entered for the second time, the TVC system weight is evaluated as a function of the nozzle weight, and the TVC system weight breakdown is determined.

EQUATIONS (FIRST ENTRANCE):

TVC nozzle weight penalty factor.

$$K_{TV_{NZ}} = \frac{C_1 \, K_{TVNZ1}}{\left(\epsilon_{NZ}\right)^{C_2}} + K_{TVNZ2} \tag{1}$$

EQUATIONS (SECOND ENTRANCE):

Total thrust vector control weight.

$$W_{TV} = K_{WTV} \, C_3 \left(W_{NZ}\right)^{C_4} \tag{2}$$

Total non-expended thrust vector control weight component.

$$W_{TV_{NX}} = W_{TV} \tag{3}$$

Total expended thrust vector control weight component.

$$W_{TV_X} = 0. \tag{4}$$

EQUATIONS (SECOND ENTRANCE) (Cont.):

Expended (non-thrust producing) thrust vector control weight component.

$$W_{TV_{XI}} = 0. \quad (5)$$

Expended (thrust producing) thrust vector control weight component.

$$W_{TV_{XT}} = 0. \quad (6)$$

INPUT DATA, INTRA-MODEL:

The following data is input directly to this model by the program user. If a value is not input, the preset value is used.

Mnemonic	Symbol	Description; Ext. (Int.) Units	Preset
CTVW1	C_1	Constant for KTVNZ computation; N. D.	2.1
CTVW2	C_2	Constant for KTVNZ computation; N. D.	0.116
CTVW3	C_3	Constant for WNZ computation; N. D.	2.7
CTVW4	C_4	Constant for WNZ computation; N. D.	0.604
KTVNZ1	K_{TVNZ1}	Coefficient for KTVNZ computation; N. D.	1
KTVNZ2	K_{TVNZ2}	Coefficient for KTVNZ computation; N. D.	0
KWTV	K_{WTV}	Coefficient for WTV computation; N. D.	1

INPUT DATA, INTER-MODEL:

This model requires as input certain data which is usually output from a model of the specified model type. If the user has not specified such a source for this data, then it must be input directly with the intra-model input.

INPUT DATA, INTER-MODEL:

Mnemonic	Symbol	Description; Ext. (Int.) Units	Model Type
RAEXTTH	ϵ_{NZ}	Nozzle expansion ratio at nozzle exit plane; N. D.	NOZZLEG
WNZ	W_{NZ}	Total nozzle weight. Includes weight penalty due to TVC requirements; lb	NOZZLEW

OUTPUT DATA:

The following data is output from this model. It is available for use as inter-model input to other models and to print, plot, and optimization routines.

Mnemonic	Symbol	Description; Ext. (Int.) Units	
KTVNZ	$K_{TV_{NZ}}$	Coefficient used by the nozzle weight model to assess a nozzle weight penalty to satisfy TVC system requirements; N. D.	Eq. 1
WTV	W_{TV}	Total thrust vector control weight; lb	Eq. 2
WTVNX	$W_{TV_{NX}}$	Total non-expended thrust vector control weight component; lb	Eq. 3
WTVX	$W_{TV_{X}}$	Total expended thrust vector control weight component; lb	Eq. 4
WTVXI	$W_{TV_{XI}}$	Expended (non-thrust producing) thrust vector control weight component; lb	Eq. 5
WTVXT	$W_{TV_{XT}}$	Expended (thrust producing) thrust vector control weight component; lb	Eq. 6

REMARKS:

This model is applicable for simulating an integral omnivector TVC system by inputting the following coefficients for the nozzle weight penalty factor.

KTVNZ1 = 0

KTVNZ2 = 1.05

PRINT BLOCK KEY:

Nominally, only those lines with an asterisk to the left of the line number will be printed. By input, any of the lines given below may be printed or suppressed (see the section on output models for the details).

			TVCW	TVWM1	THRUST VECTOR CONTROL WEIGHT
WTV	WTVNX	WTVX	*1	WTVXI	WTVXT
CTVW1	CTVW2	CTVW3	*2	CTVW4	
KTVNZ	KTVNZ1	KTVNZ2	*3	KWTV	

360.1

MODEL TYPE: VEHG (VEHicle Geometry)

MODEL NAME: VHGM1 (Single Propulsion System and Payload Section)

DESCRIPTION:

VHGM1 (VeHicle Geometry Model number 1) evaluates the geometry for a vehicle comprised of a single propulsion system and a single payload section. See figure 1 for an illustration of the geometry for a typical vehicle comprised of three stages, a payload and a shroud.

PROCEDURE:

Prior to entering VHGM1 all of the major vehicle subsystems have been sized and the models specified for the PROSYSG and PAYSECG model types have determined the pertinent propulsion system and payload section geometry.

VHGM1 is then executed and the vehicle geometry evaluated.

After VHGM1 is executed, the vehicle weight breakdown is evaluated by the model specified for the VEHW model type. The vehicle has then been completely sized. However, another pass will be made through all of the models to evaluate length and weight fractions dependent upon total vehicle geometry and weight quantities.

EQUATIONS:

Total vehicle length. Figure 1.

$$L_{VH} = L_{PS} + L_{PL} \tag{1}$$

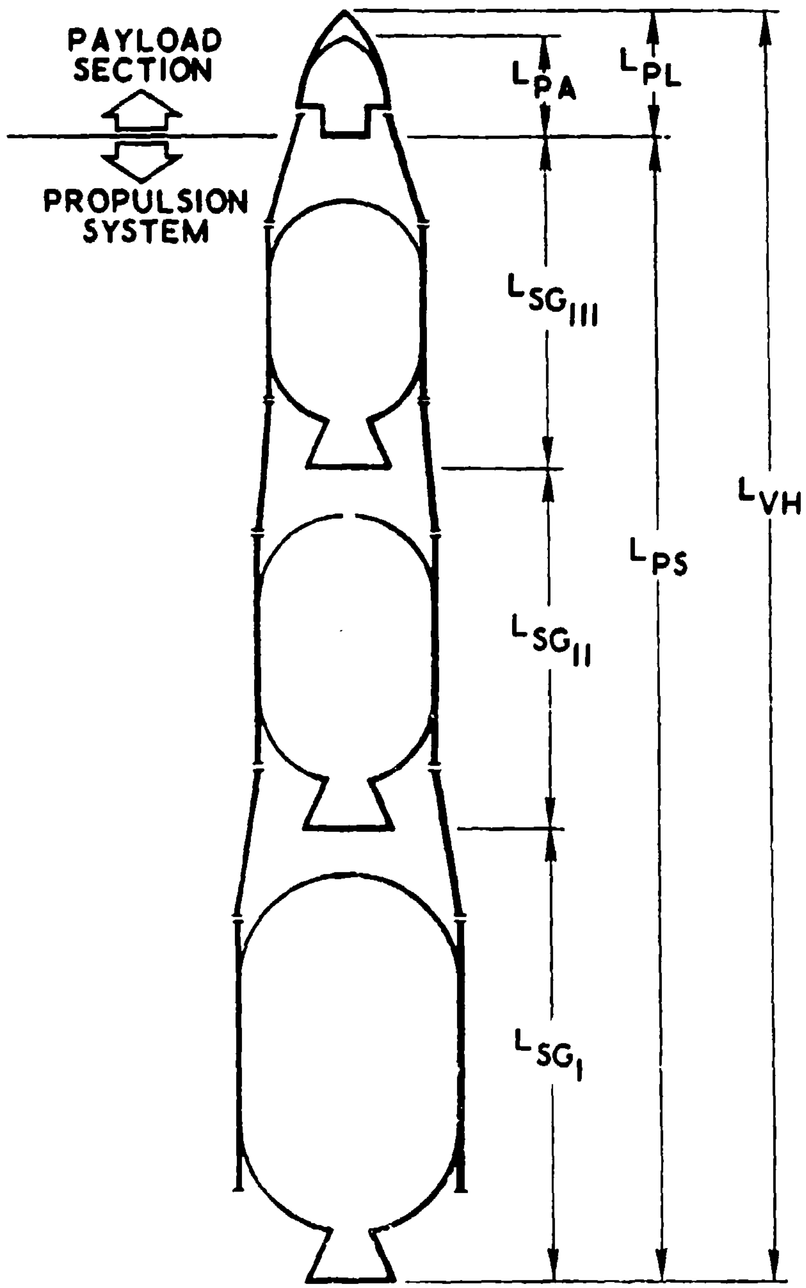

Fig. 360.1-1 Vehicle Geometry

INPUT DATA, INTRA-MODEL:

The following data is input to this model directly by the program user. If a value is not input, the preset value is used.

Mnemonic	Symbol	Description; Ext. (Int.) Units	Preset

None

INPUT DATA, INTER-MODEL:

This model requires as input certain data which is usually output from a model of the specified model type. If the user has not specified such a source for this data, then it must be input directly with the intra-model input.

Mnemonic	Symbol	Description; Ext. (Int.) Units		Model Type
LPL	L_{PL}	Total payload section length; in	Fig. 1	PAYSECG
LPS	L_{PS}	Total propulsion system length; in	Fig. 1	PROSYSG

OUTPUT DATA:

The following data is output from this model. It is available for use as inter-model input to other models and to print, plot, and optimization routines.

Mnemonic	Symbol	Description; Ext. (Int.) Units		
LVH	L_{VH}	Total vehicle length; in	Fig. 1	Eq. 1

PRINT BLOCK KEY:

Nominally, only those lines with an asterisk to the left of the line number will be printed. By input, any of the lines given below may be printed or suppressed (see the section on output models for the details).

```
LVH                                    VEHG     VHGM1        VEHICLE GEOMETRY
                                         *1
```

370.1

MODEL TYPE: VEHW (VEHicle Weight)

MODEL NAME: VHWM1 (Single Propulsion system and payload section.)

DESCRIPTION:

VHWM1 (VeHicle Weight Model number 1) is a weight synthesis model which evaluates the vehicle weight breakdown and mass fractions for a vehicle having a single propulsion system and a single payload section. The vehicle weight is comprised of the following subsystems:

Propulsion System

Payload Section

PROCEDURE:

Prior to entering VHWM1, the models specified for the PROSYSW and PAYSECW model type have evaluated the propulsion system and payload section weights. In addition to evaluating subcomponent weights peculiar to their particular requirements, they have defined a set of component weights in terms of expended or non-expended attributes.

VHWM1 then uses these expended and non-expended, propulsion system and payload section, weight components to determine the vehicle weight breakdown. In addition, the vehicle growth factor is evaluated.

After VHWM1 is executed, the vehicle has been completely sized. However, another pass will be made through all of the models to evaluate subsystem weight fractions dependent upon the vehicle weight breakdown.

EQUATIONS:

Total vehicle weight.

$$W_{VH} = K_{WVH}\left(W_{PS} + W_{PL}\right) \qquad (1)$$

EQUATIONS (Cont.):

Total non-expended vehicle weight component.

$$W_{VH_{NX}} = K_{WVHNX}\left(W_{PS_{NX}} + W_{PL_{NX}}\right) \quad (2)$$

Total expended vehicle weight component.

$$W_{VH_{X}} = K_{WVHX}\left(W_{PS_{X}} + W_{PL_{X}}\right) \quad (3)$$

Expended (non-thrust producing) vehicle weight component.

$$W_{VH_{XI}} = K_{WVHXI}\left(W_{PS_{XI}} + W_{PL_{XI}}\right) \quad (4)$$

Expended (thrust producing) vehicle weight component.

$$W_{VH_{XT}} = K_{WVHXT}\left(W_{PS_{XT}} + W_{PL_{XT}}\right) \quad (5)$$

Total propellent weight associated with the vehicle.

$$W_{PP_{VH}} = W_{PP_{PS}} \quad (6)$$

Vehicle growth factor.

$$K_{VH_{GF}} = \frac{W_{VH}}{W_{PA}} \quad (7)$$

INPUT DATA, INTRA-MODEL:

The following data is input to this model directly by the program user. If a value is not input, the preset value is used.

Mnemonic	Symbol	Description; Ext. (Int.) Units	Preset
KWVH	K_{WVH}	Coefficient for WVH computation; N. D.	1

INPUT DATA, INTRA-MODEL (Cont.):

Mnemonic	Symbol	Description; Ext. (Int.) Units	Preset
KWVHNX	K_{WVHNX}	Coefficient for WVHNX computation; N. D.	1
KWVHX	K_{WVHX}	Coefficient for WVHX computation; N. D.	1
KWVHXI	K_{WVHXI}	Coefficient for WVHXI computation; N. D.	1
KWVHXT	K_{WVHXT}	Coefficient for WVHXT computation; N. D.	1

INPUT DATA, INTER-MODEL:

This model requires as input certain data which is usually output from a model of the specified model type. If the user has not specified such a source for this data, then it must be input directly with the intra-model input.

Mnemonic	Symbol	Description; Ext. (Int.) Units	Model Type
WPA	W_{PA}	Total payload weight; lb	PAYLODW
WPL	W_{PL}	Total payload section weight; lb	PAYSECW
WPLNX	$W_{PL_{NX}}$	Total non-expended payload section weight component; lb	PAYSECW
WPLX	W_{PL_X}	Total expended payload section weight component; lb	PAYSECW

INPUT DATA, INTER-MODEL (Cont.):

Mnemonic	Symbol	Description; Ext. (Int.) Units	Model Type
WPLXI	$W_{PL_{XI}}$	Expended (non-thrust producing) payload section weight component; lb	PAYSECW
WPLXT	$W_{PL_{XT}}$	Expended (thrust producing) payload section weight component; lb	PAYSECW
WPPPS	$W_{PP_{PS}}$	Weight of propellent associated with the propulsion system; lb	PROSYSW
WPS	W_{PS}	Total propulsion system weight; lb	PROSYSW
WPSNX	$W_{PS_{NX}}$	Total non-expended propulsion system weight component; lb	PROSYSW
WPSX	$W_{PS_{X}}$	Total expended propulsion system weight component; lb	PROSYSW
WPSXI	$W_{PS_{XI}}$	Expended (non-thrust producing) propulsion system weight component; lb	PROSYSW
WPSXT	$W_{PS_{XT}}$	Expended (thrust producing) propulsion system weight component; lb	PROSYSW

OUTPUT DATA:

The following data is output from this model. It is available for use as inter-model input to other models and to print, plot, and optimization routines.

OUTPUT DATA (Cont.):

Mnemonic	Symbol	Description; Ext. (Int.) Units	
KVHGF	$K_{VH_{GF}}$	Vehicle growth factor. Ratio of total vehicle weight to payload weight;	
		N. D.	Eq. 7
WPPVH	$W_{PP_{VH}}$	Total propellent weight associated with the vehicle;	
		lb	Eq. 6
WVH	W_{VH}	Total vehicle weight;	
		lb	Eq. 1
WVHNX	$W_{VH_{NX}}$	Total non-expended vehicle weight component;	
		lb	Eq. 2
WVHX	W_{VH_X}	Total expended vehicle weight component;	
		lb	Eq. 3
WVHXI	$W_{VH_{XI}}$	Expended (non-thrust producing) vehicle weight component;	
		lb	Eq. 4
WVHXT	$W_{VH_{XT}}$	Expended (thrust producing) vehicle weight component;	
		lb	Eq. 5

PRINT BLOCK KEY:

Nominally, only those lines with an asterisk to the left of the line number will be printed. By input, any of the lines given below may be printed or suppressed (see the section on output models for the details).

			VEHW	VHWM1	VEHICLE WEIGHT	
WVH	WVHNX	WVHX	*1	WVHXI	WVHXT	WPPVH
KWVH	KWVHNX	KWVHX	*2	KWVHXI	KWVHXT	KVHGP